CRITICAL REVIEW OF GEOCHEMICAL PROCESSES AND GEOCHEMICAL MODELS ADAPTABLE FOR PREDICTION OF ACIDIC DRAINAGE FROM WASTE ROCK

MEND Project 1.42.1

**This work was done on behalf of MEND and sponsored by
Teck Corporation, and
the Ontario Ministry of Northern Development and Mines and
the Canada Centre for Mineral and Energy Technology (CANMET)
through the CANADA/Northern Ontario Development Agreement (NODA)**

April 1995

CRITICAL REVIEW OF GEOCHEMICAL PROCESSES AND GEOCHEMICAL MODELS ADAPTABLE FOR PREDICTION OF ACIDIC DRAINAGE FROM WASTE ROCK

E.H. Perkins, H.W. Nesbitt, W.D. Gunter,
L.C. St-Arnaud and J.R. Mycroft

submitted by

Noranda Technology Centre
Mineral Sciences Laboratory
Pointe-Claire, Québec

in collaboration with

Alberta Research Council
Resource Technology Department
Edmonton, Alberta

University of Western Ontario
Department of Earth Sciences
London, Ontario

to

Mine Environment Neutral Drainage (MEND) Program
Prediction Committee
March, 1995

EXECUTIVE SUMMARY

This report describes the geochemical processes occurring in acid-generating waste rock piles and evaluates available geochemical computer models with respect to their abilities to simulate the geochemical processes to predict the quality of acid rock drainage (ARD).

The geochemical processes which most control ARD quality are precipitation and dissolution, chemical diffusion, and surface reactions. Precipitation and dissolution control neutralization of acidic solutions and fixation of metals within solids. Chemical diffusion and surface reactions control the rates at which all precipitation and dissolution reactions occur. Quantitative reaction rates are required to accurately predict water quality from waste rock piles. Reaction rates determine which secondary minerals will form after dissolved ionic species and complexes are liberated in aqueous solutions in contact with the waste rock. Reaction rate equations need to incorporate the important influence of rate-modifying mechanisms such as bacterial catalysis. Galvanic effects may also have to be incorporated; however, insufficient data disallow a proper evaluation of their importance. Drying and wetting are the most important physical processes that affect water chemistry, by concentrating aqueous solutions to the point of precipitating solids and subsequently dissolving and removing these solids from solution contact. All processes mentioned above also occur during natural weathering of massive sulphide rock formations.

Field data required to describe geochemical processes in waste rock include detailed water analyses, rock mineralogy and trace element chemistry, exposed surface area, temperature, oxygen availability and water infiltration rates. Thermodynamic data are required to predict precipitation and dissolution reactions in waste rock. However, thermodynamic data for important secondary minerals in ARD are missing. Reaction rate equations and rate constants necessary to perform kinetic calculations are also insufficient. Data from laboratory and field tests can be used to compensate for the inadequacies of presently available geochemical databases.

Existing geochemical models are divided into five classes: equilibrium thermodynamic models, mass transfer models, coupled mass transport-mass transfer models, supporting models, and empirical and engineering models. Each class of geochemical models can be viewed as addressing a different type of ARD prediction objective. Equilibrium geochemical thermodynamic models address the identification of the soluble and mobile metal species and maximum metal concentrations. Mass transfer models more specifically address maximum metal concentrations and their evolution with time. Mass transfer-flow models address the prediction of concentration and load versus time. The engineering models are more directed towards examining decommissioning options. More developments are required in each model category to adequately achieve each prediction objective.

It is recommended to define thermodynamic equilibrium constants for important secondary minerals and to obtain kinetic rate data for dissolution and precipitation of important minerals. It is suggested that a model developed to predict water quality from waste rock piles should have a geochemical component that takes into account reaction kinetics. In the short term, model development efforts should be based on applications and improvements of some existing mass transfer models using data from well-defined laboratory and field test cases.

SOMMAIRE EXECUTIF

Ce rapport décrit les processus géochimiques qui surviennent dans les amas de roche stérile producteurs d'acide et évalue la capacité de modèles géochimiques disponibles pour simuler les processus géochimiques afin de prédire la qualité de l'eau de drainage acide.

Les processus géochimiques qui influencent le plus la qualité de l'eau de drainage sont la précipitation et la dissolution, la diffusion chimique et les réactions en surface. La précipitation et la dissolution contrôlent la neutralisation des solutions acides et la fixation des métaux dans les solides. La diffusion chimique et les réactions en surface déterminent les taux de précipitation et de dissolution. Une connaissance des cinétiques de réaction est nécessaire pour prédire avec précision la qualité de l'eau provenant des amas de roche stérile. Les cinétiques de réaction déterminent quels minéraux secondaires se forment après que les espèces et complexes ioniques dissous ont été libérés dans les solutions aqueuses en contact avec la roche stérile. Les équations de taux de réaction doivent incorporer l'influence importante des mécanismes modificateurs des taux de réaction, comme la catalyse bactérienne. Les effets galvaniques devraient peut-être aussi être incorporés, bien que le manque de données à ce sujet ne permet pas de faire une évaluation adéquate de leur importance. Le séchage et le mouillage sont les processus physiques qui affectent le plus la chimie de l'eau en concentrant les solutions aqueuses jusqu'à ce que les solides soient précipités, et ensuite en dissolvant et en éloignant ces solides de la solution aqueuse. Tous les processus mentionnés plus haut ont également lieu au cours de l'altération naturelle des formations de sulfures massifs.

Les données de terrain requises pour décrire les processus géochimiques dans la roche stérile comprennent les résultats d'analyses détaillées de l'eau et de la composition minéralogique, la superficie exposée, la température, l'apport d'oxygène et les taux d'infiltration d'eau. Des données thermodynamiques sont requises pour prédire les réactions de précipitation et de dissolution dans la roche stérile. Les données thermodynamiques relatives aux importants minéraux secondaires dans l'eau de drainage acide sont toutefois manquantes dans la documentation analysée. Les équations du taux de réaction èt les constantes cinétiques requises pour effectuer les calculs cinétiques sont également insuffisantes. Par contre, des données d'essais en laboratoire et sur le terrain peuvent être utilisées pour compenser les insuffisances des bases de données géochimiques disponibles présentement.

Les modèles géochimiques existants se répartissent en cinq catégories: les modèles thermodynamiques à l'équilibre, les modèles de transfert de masse, les modèles de transfert de masse-écoulement, les modèles de soutien, et les modèles empiriques et d'ingérierie. Chaque catégorie de modèle s'adresse à des objectifs de prédiction différents. Les modèles thermodynamiques à l'équilibre conviennent pour l'identification des espèces de métaux solubles et mobiles auxquelles on peut s'attendre dans l'eau de drainage acide. Les modèles de transfert de masse adressent la détermination de concentrations maximales de métaux et leur évolution avec le temps. Les modèles de transfert de masse-écoulement adressent la prédiction des concentrations et des charges en fonction du temps. Enfin, les modèles d'ingénierie géochimique conviennent le mieux pour examiner des options de désaffectation. Tous ces types de modèles nécessitent toutefois davantage de développement avant que chaque objectif de prévision puisse être réalisé adéquatement.

Il est recommandé de définir des constantes d'équilibre thermodynamique pour les minéraux secondaires importants, et d'obtenir des données sur les taux cinétiques pour la dissolution et la précipitation de minéraux importants. Il est également suggéré qu'un modèle de prévision de la qualité de l'eau provenant d'amas de roche stérile comporte une composante géochimique qui tienne compte de la cinétique des réactions. Dans l'immédiat, les efforts de développement de modèles devraient être faits à partir d'applications et d'améliorations de certains modèles de transfert de masse en utilisant des données provenant de cas de terrain et de laboratoire bien documentés.

TABLE OF CONTENTS

PART 2
REVIEW OF GEOCHEMICAL MODELS

TABLES

page #

FIGURES

page #

APPENDICES

1. INTRODUCTION

1.1 Objectives

The objectives of this report are (1) to describe the geochemical processes occurring in acid-generating waste rock piles and (2) to evaluate available geochemical computer models with respect to their abilities to describe the geochemical processes and their applicability to the prediction of water quality from waste rock piles. The report is a requirement of Supply and Services Canada contract 23440-3-9230/01-SQ between Noranda Technology Centre and Energy Mines and Resources, Canada. It is part of an effort to accomplish a main objective of the MEND program, which is "to provide a comprehensive, scientific, technical and economic basis to predict the long-term management requirements for reactive mine waste."

1.2 Background

Waste rock is produced in large quantities by mining and other earth-disturbing activities. A recent survey by MEND found approximately 350 million tonnes of acid-generating waste rock in Canada. Significant quantities of waste rock are also produced by large civil projects such as constructions of highways, railways, airports, and hydroelectric structures; some of these are acid-generating. However, the problem of acid rock drainage (ARD) generation is much more profound for mining industry than for civil engineering projects because mining occurs frequently in sulphide rock formations.

Waste rock volumes vary among mine sites, depending largely on the mining method. Waste rock is mostly piled above-surface during open pit mining, which is used when orebodies are shallow and massive. Typical stripping ratios (ratio of waste to ore) for open pit mining are near 3:1, but can reach larger values depending on orebody shape, orientation and wall stability. Ore properties are also critical factors: the mining of low-grade base metal orebodies, for example, is more amenable to open pit methods, because financial returns are more dependant on high production rates. Some waste rock is also produced from underground operations, but usually only at the early mine development stages.

Another mining practice that influences waste rock volumes is backfilling. At some operations, backfilling of waste rock significantly reduces the volumes of waste piled above the ground surface. The environmental impact of sulphidic waste rock placed underground is least if flooding occurs rapidly and groundwater flow is slow.

Sulphidic waste rock stored above ground oxidizes to produce acid and liberate metals, contaminating water contacting it. The higher spreading of the waste rock, the more severe the environmental impacts. At certain older Canadian mine sites, sulphidic waste spreads out over several kilometers as road construction material, requiring large-scale remediation efforts. ARD can also occur naturally on sulphidic rock outcrops.

Control and treatment of contaminated water require significant financial resources, enough to justify careful scientific analysis of the contaminant production. Typical objectives of these analyses are as follows:

- identification of soluble and mobile metal species
- determination of maximum metal concentrations
- determination of maximum metal loadings
- comparison of decommissioning options
- evaluation of the duration of dissolved metal production
- prediction of concentration and loadings versus time

These example objectives are stated in an increasing order of complexity. Similarly, analytical tools required to achieve these objectives also vary in complexity. These tools include a component addressing the geochemical processes occurring at the air-water-rock interfaces under dynamic environmental conditions.

MEND has identified the prediction of water quality from waste rock as an important priority for the mining industry. The needs and requirements for modelling development were discussed and reviewed during an international workshop MEND (1992). The workshop recommended conducting a review of available geochemical modelling tools adaptable to waste rock. A plan to develop a general physical and geochemical model for waste rock was also proposed. The workshop incorporated the review of existing geochemical models addressing the prediction of acid generation from waste rock by Nicholson (1992). This review stated that although existing models address many geochemical processes occurring in waste rock, these models do not incorporate important details of chemical feedback mechanisms that would allow them to predict metal release rates.

1.3 Organization of the report

The report is divided in two parts corresponding to objectives (1) and (2) stated earlier. Geochemical processes are critically reviewed in Part 1 and geochemical models are evaluated in Part 2. Part 1 begins with a description of the physical settings in which geochemical processes occur (Section 3). Mechanisms underlying acid generation, acid neutralization, secondary mineral precipitation, and evolution of aqueous solution composition are then addressed (Section 4). Geochemical processes responsible for chemical alterations of waste rock are identified and ranked in Section 5. Geochemical reactions and geochemical processes are discussed quantitatively in Section 6, leading to the list of model input parameters in Section 7.

Specific geochemical models are described and evaluated in Part 2 following their classification in Section 9. Test cases were run for different classes of models and the results are presented along with descriptions of individual models in Sections 10 to 14. Summary and conclusions are given in Section 15.

Fundamental information from recent geochemical literature is included in appendices. Appendix A provides references to thermodynamic and kinetic properties of minerals, particularly carbonate and silicate minerals, commonly found in waste rock piles. Appendix B is a critical review of fundamental literature related to the kinetics of leaching of sulphide and oxide minerals. Information on support and availability of each model reviewed in Part 2 is included in Appendix F. A complete list of references is in Appendix G.

PART 1

REVIEW OF GEOCHEMICAL PROCESSES

2. PREVIOUS WORK

Documented descriptions of geochemical processes in waste rock piles are not commonly found. However, Morin et al. (1991) recently reviewed the geochemical literature and collected case studies of observations of chemical reactions in rock piles. On internal reactions occurring in waste rock piles, the review concluded that the present state of knowledge of acid generation is limited by the lack of consideration of stoichiometry and rates of reactions. Otwinoski (1994) performed a quantitative review of chemical processes involved in the production of acid mine drainage from the oxidation of pyrite, and provided descriptions of several interactions which could occur between chemical processes. SRK (1993) reviewed oxidation and contaminant release processes from waste piles, and proposed a framework for incorporating these processes in a comprehensive model, which would include laboratory column tests to determine effective chemical parameters. Extensive efforts on monitoring and predicting reactions in waste rock piles have been done in Australia, focusing on monitoring and modelling gas transfer processes. Ritchie (1994) recently summarized the experience gained, and pointed out that the chemical environment of waste rock piles is not well understood.

Recent MEND studies, such as the one by Choquette et.al (1994), include detailed geochemical field measurements in waste rock piles. Other recent studies, such as Yanful and Payant (1993), document the geochemistry of waste rock leachates from laboratory column experiments. However, the most detailed information on geochemical processes in sulphide mineral environments are in mine tailings studies such as Blowes and Jambor (1990), and Dubrovsky et al. (1984). Mine tailings are usually better documented than waste rock piles because solid and water samples are obtained much easier in tailings than in waste rock. Especially applicable to waste rock environments are studies describing geochemical processes in the unsaturated zone of tailings, some of which may have mineralogical features which are very similar to waste rock. Other pertinent information are found in fundamental geochemical studies of sulphide oxidation and acid mine waters such as Nordstrom et al., 1979a and Nordstrom, 1982. The soil physics literature also contains a significant amount of interesting information on geochemical processes in unsaturated soils (for example, Ghildyal and Tripathi, 1987).

Even if tailings and soils can be considered, in some respects, good chemical analogues to rock piles, they are however poor physical analogues due to large differences in porosity and permeability. This limitation could be compensated by information from literature on the weathering of ore bodies and development of gossans, as reviewed by Day and Cowdery (1990). These authors have suggested that the study of undisturbed weathered rock could provide new data on minerals and rock types active in acid generation, on pH buffering levels, and for identifying mobile metal species.

However, the applicability of the gossan literature to waste rock piles is limited by the lack of documentation on the time of occurrence of weathering events and the absence of a water quality database. Nickel at al. (1977) and Alpers and Brimhall (1989) are good examples of studies on the weathering of gossans. Jambor (1994) recently discussed limits of the use of information derived from gossans in the interpretation of the geochemical evolution of tailings. Boyle (1994) emphasized that there is only limited understanding of natural sulphide oxidation as it occurs in gossans, and that more studies would be needed to apply knowledge from gossan oxidation to make predictions of dissolved metal mobility.

The present document takes into account all applicable sources of information mentioned above, without duplicating previous review efforts. This is achieved by identifying geochemical processes within the context of the most current state of knowledge in the field of aqueous geochemistry. The review does not attempt to list all chemical reactions which could be found in waste rock piles. It rather identifies the geochemical processes by which the chemical reactions occur. The emphasis of the review is on processes which should be incorporated into predictive models to be applied to the myriad of mineral assemblages found in waste rock piles, and to evaluate processes which mostly affect individual minerals and elements.

3. PHYSICAL SETTING

Waste rock piles are typically composed of silt, sand, gravel, cobble and boulder-sized detritus. Like soils, they are porous media and, typically, both are undersaturated in the sense that pore spaces (interstices) are occupied, at least in part, by a gas phase. A liquid phase may be present, but it does not permanently fill the pores. There may be, however, perched water tables, as evidenced by seeps bleeding along the slopes of some waste rock piles (Morin et al., 1991).

Waste rock piles are wetted and dried intermittently by infiltration of rainwater and by seasonal runoff (e.g. melt waters). The typically coarse nature of the rock piles results in a high percentage of large pores (macropores) and correspondingly low percentage of very small pores, leading to high permeabilities. These properties result in predictable stages during the wetting and drying of waste rock, which give rise to, and may control, the nature of geochemical processes operative in waste rock piles.

The cycle followed during wetting and drying is summarized in Fig. 1. It begins with macropores temporarily saturated, and ends with dry macropores containing precipitated, soluble salts. The four sequential stages are infiltration, drainage, evaporation and air-oxidation. The stages develop sequentially, with minor to extensive overlap of stages. Real wetting and drying cycles are repeated and interrupted continually by renewed infiltration of rainwater and seasonal runoff. The time required to complete the entire cycle is dependent upon porosity, permeability, and other physical and climatic parameters.

The interaction between wetting and drying and geochemical processes are further illustrated. During saturation, solutes are acquired by reaction with solids of the waste rock. (Fig. 1a). After infiltration, waters of macropores are subsequently drained (Fig. 1b). During the drainage stage, acquired solutes are transported to water tables (perched or permanent), and to drainage ditches and ponds. Air is introduced (via suction) into the macropores as drainage proceeds (Fig. 1b), and with introduction of air, evaporation of undrained water commences (Fig. 1c). As drainage continues, evaporation becomes an increasingly important drying process, and may become dominant. The relative importance of drainage and evaporation during drying is determined by the physical properties of the waste rock pile, which include hydraulic conductivity, suction potential, and a chemical potential gradient between water in the pores and water in the atmosphere (Ghildyal and Tripathi, 1987).

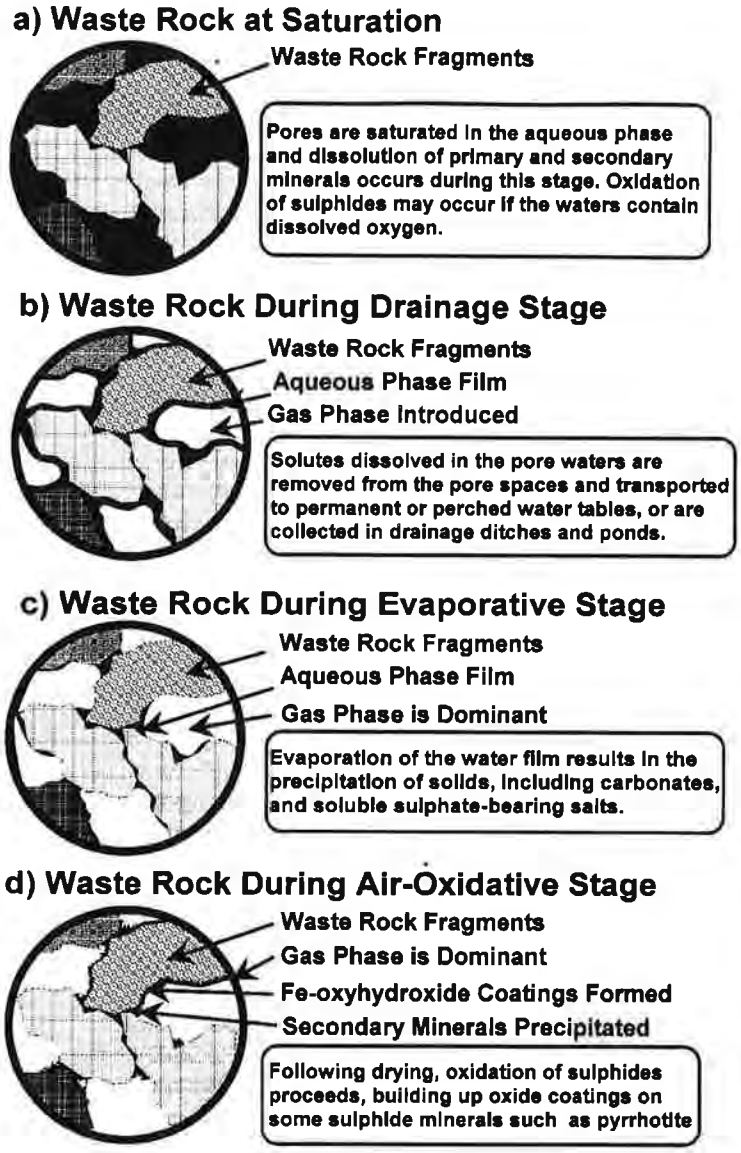

Figure 1. Stages of the Wetting and Drying Cycle

Evaporative drying of pore solutions results in precipitation of a suite of secondary minerals, the compositions of which are dependent upon the composition of the pore solutions being evaporated (Fig 1d). Nordstrom (1982) and Nordstrom et al. (1979) emphasize that, in the unsaturated zone where air-evaporation is prevalent, **Fe-sulphate salts** are the most abundant secondary products found on surfaces of rocks containing sulphides. Jambor (1986) observes melanterite, Fe-oxyhydroxides and jarosite, for example, in the unsaturated zone of the Waite Amulet tailings. These secondary minerals are certain to be present in waste rock piles where evaporative drying occurs. These minerals may also dissolve during a subsequent infiltration event. Dissolution

of the Fe-SO_4 salts in infiltration waters of waste rock piles may have a dramatic effect on water quality and is one of the geochemical processes addressed in this review.

Atmospheric gases introduced into waste rock piles include molecular oxygen (Ritchie, 1994b), which may remain in the gas phase or dissolve in undrained waters of the waste rock pile. These oxidized solutions (liquid or gas) promote oxidation of sulphide minerals.

The important link between the physical and chemical processes in waste rock piles is very evident. A thorough waste rock pile model would have to incorporate both physical and chemical processes. However, physical processes are not within the scope of this review; practical boundaries between physical and chemical processes are discussed further in Section 4.

4. CHEMICAL REACTIONS IN MINE WASTES

4.1 Acid Generation

4.1.1 General Description

Oxidation of sulphide minerals results in production of sulphuric acid (Ahmad, 1974), as indicated by reaction of pyrite with oxygen:

$$FeS_2 + 7/2O_2 + H_2O \rightarrow Fe^{2+} + 2H^+ + 2SO_4^{2-} \quad (1)$$

Reaction (1) proceeds at intermediate oxidation potentials where sulphate ion is the dominant sulphur species and Fe^{2+}-species are dominant over Fe^{3+} aqueous species. Where oxidation potentials are sufficiently high, aqueous Fe^{2+} is oxidized to Fe^{3+} according to:

$$2Fe^{2+} + 1/2O_2 + 2H^+ \rightarrow 2Fe^{3+} + H_2O, \quad (2)$$

and if the pH of the solution is sufficiently high, Fe(III)-oxyhydroxides such as ferrihydrite [$Fe(OH)_3$] may precipitate:

$$Fe^{3+} + 3H_2O \rightarrow Fe(OH)_3 + 3H^+ \quad (3)$$

The sum of reactions (1), (2) and (3) (the overall reaction) is:

$$FeS_2 + 15/4O_2 + 7/2H_2O \rightarrow Fe(OH)_3 + 2H_2SO_4 \quad (4)$$

The stoichiometry of reactions (1) and (4) provides the means to predict the amount of acid produced through oxidation of one mole (120 g) of pyrite. The compositions of sulphide minerals vary considerably; consequently, an accurate calculation of the amount of acid generated from a given mass of waste rock requires a knowledge of the sulphide mineralogy and proportions in the waste rock. Reactions similar to (4) can be written for each mineral to determine the moles of acid produced per mole of the specific sulphide mineral oxidized. The reaction for pyrrhotite (FeS used as a proxy) is:

$$FeS + 9/4O_2 + 5/2H_2O \rightarrow Fe(OH)_3 + H_2SO_4 \quad (5)$$

which demonstrates that half as much acid is produced per mole of pyrrhotite as per mole of pyrite.

4.1.2 Acid-Generating Potential of Sulphides

Consideration of the total mass of each acid generator (e.g. each sulphide mineral) in the waste, combined with the stoichiometry of the associated acid-generating reaction, yields the **maximum acid-generating potential** of the waste. The **real acid-generating potential** will be over

estimated if correction is not made for sulphides permanently isolated from oxidizing agents. Some sulphides may be completely encased in comparatively unreactive minerals such as quartz, hence unavailable to react with solutions. This aspect is important in waste rock containing coarse materials. Other sulphides may be situated below perched and permanent water tables or associated with near-stagnant portions of flow regimes. These sulphides may not be oxidized because oxidizing agents of the fluids, once consumed, are not replenished at a rate sufficient to produce measurable amounts of acid.

Many waste sites are heterogeneous in a stratigraphic sense, resulting from deposition of successive horizons of wastes. Ideally, the evaluation of real acid-generating potential at these heterogeneous sites has to be evaluated by subdividing the pile in sub-sections of similar properties; the potential for each sub-section is calculated, and all results are then integrated to obtain an accurate estimate of the acid-generating potential for the entire pile.

4.1.3 Rates of Acid-Generation

Acid generating potential of wastes provides no insight into the rate at which acid is produced, hence it provides no indication of the acid content of a litre of solution emanating from waste. This is vital if there is to be accurate prediction of acid mine drainage. Prediction of the acid content of mine drainage can be achieved based on the concept of "**limiting constituents**". If, as suggested by Nicholson (1990) and references therein, supply of oxygen limits the amount of pyrite oxidized (hence acid generated) by reaction (4), then O_2 is referred to as the "limiting constituent". On the assumption that all steps in the reaction are rapid compared with the rate of supply of oxygen, then all oxygen dissolved in a litre of solution will be consumed and an equivalent amount of sulphuric acid will be produced according to the stoichiometry of the appropriate reaction. If pyrrhotite is oxidized, reaction (5) is applied to calculate sulphuric acid production. The amount of acid generated is predictable from the amount of the limiting constituent (O_2) present in a litre of solution. The assumption inherent in this calculation is that reaction rates are rapid compared with supply of oxidant. Assumptions included in the calculation are:

(1) that the oxidizing solution contacts a sufficiently large amount of sulphide to consume all oxygen;
(2) that all Fe released to solution is precipitated as ferrihydrite (which implies a rapid rate of precipitation of $Fe(OH)_3$).
(3) that the mineral dissolves congruently, releasing both Fe and S in precisely the proportions present in the mineral.

The prediction of acid generation, based on the limiting constituents concept, is incorrect if any one of the assumptions mentioned above is invalid (Morin, 1990). If pyrrhotite, for example, dissolved incongruently, with Fe being preferentially leached, and sulphur accumulating as native sulphur at the mineral surface, the amount of acid predicted to form from reaction (5) would be greatly overestimated. Pyrrhotite does, in fact, dissolve incongruently (Pratt et al., 1994a). Alternatively, if only half of the Fe released to solution were precipitated (slow precipitation rate)

then only half the acid would be produced, the other half of the sulphate generated being balanced by aqueous Fe^{2+} rather than hydrogen ions. Alternatives to the limiting constituents calculation are discussed at the end of this section.

4.2 Neutralization of Acids

4.2.1 General Description

Acids generated by oxidative dissolution of sulphides may be neutralized by reaction with other minerals which act as solid bases. This is apparent from the chemistry of waste rock leachates such as those reported by Yanful and Payant (1993) in the study of Stratmat waste rock. Leachate compositions were dominanted by Fe^{3+} and SO_4, but there was substantial Mg, Fe^{2+} and Al in the leachates. This suggests that substantial amounts of Mg- and Al-bearing minerals were leached. The only Mg-bearing minerals of the Stratmat waste rock were dolomite and Mg-chlorite, with the latter being approximately 20 times more abundant than dolomite. The most likely source of Mg and Al would be Mg-chlorite. Certainly albite has provided little Al to solution because Na is reported only at one-hundredth the concentration of Mg in the leachates. Similarly, dissolution of dolomite [$CaMg(CO_3)_2$] should yield equal amounts of Ca and Mg to leachates during its dissolution (or 825 mg/L Ca for each 500 mg/L of Mg). The Ca content of the Stratmat leachates demonstrates clearly that little dolomite has dissolved, hence most of the Mg is derived from the only other mineralogical source Mg-chlorite. Data from the Stratmat leachates is presented and further discussed in Section 10 of this report.

The solid bases of most mine wastes are carbonate, oxyhydroxide and Al-silicate minerals. The neutralizing potential of these minerals is determined by a number of factors, some of the more important of which are now discussed.

4.2.2 Neutralizing Potential of Minerals

Acids may be neutralized in mine wastes through dissolution of minerals such as calcite. The neutralization reaction can be written as:

$$2CaCO_3 + H_2SO_4 \rightarrow 2Ca^{2+} + 2HCO_3^- + SO_4^{2-}, \quad (9)$$

where two moles of calcite neutralize one mole of sulphuric acid and produce Ca-HCO_3-SO_4 dissolved salts. Other carbonates such as dolomite and siderite have the same **potential** to neutralize acids. Continued reaction causes the solute concentrations to increase, which may lead to precipitation secondary phases such as of gypsum ($CaSO_4 \cdot H_2O$), anhydrite ($CaSO_4$) and/or basanite ($CaSO_4 \cdot 1/2H_2O$).

Oxides, oxyhydroxides and hydroxides of Al, Fe and of most other transition metals can neutralize acids. Goethite and gibbsite are used as examples:

$$2Fe(OH)_3 + 3H_2SO_4 \rightarrow 2Fe^{3+} + 3SO_4^{2-} + 9/2H_2O \quad (10)$$

$$2Al(OH)_3 + 3H_2SO_4 \rightarrow 2Al^{3+} + 3SO_4^{2-} + 6H_2O. \quad (11)$$

Continued neutralization of acid by gibbsite and ferrihydrite increases concentrations of Al^{3+}, Fe^{3+} and sulphate in solution, and may lead to precipitation of phases such as jarosite and alunite.

Al-silicates are common in mine wastes and have the potential to neutralize acids. The albite component of plagioclase is here considered:

$$NaAlSi_3O_8 + 2H_2SO_4 \rightarrow Na^+ + Al^{3+} + 3SiO_2(aq) + 2SO_4^{2-} + 2H_2O. \quad (12)$$

A similar reaction can be written for the anorthite component of plagioclase:

$$CaAl_2Si_2O_8 + 4H_2SO_4 \rightarrow Ca^{2+} + 2Al^{3+} + 2SiO_2(aq) + 4SO_4^{2-} + 4H_2O \quad (13)$$

The albite and anorthite components of plagioclase neutralize 2 and 4 moles of sulphuric acid per mole of solid dissolved, and complete dissolution yields Na- Ca-Al-sulphate dissolved salts. K-feldspar (microcline, orthoclase, sanidine) has the same potential as albite to neutralize acids (reaction 12). Chlorite is common in mineral deposits and has a high potential to neutralize acids:

$$Mg_5Al_2Si_3O_{10}(OH)_8 + 8H_2SO_4 \rightarrow 5Mg^{2+} + 2Al^{3+} + 3SiO_2(aq) + 8SO_4^{2-} + 12H_2O \quad (14)$$

Other phyllosilicates such as biotite, muscovite and clay minerals also neutralize acids. Acids may be neutralized through dissolution of kaolinite according to:

$$2Al_2Si_2O_5(OH)_4 + 3H_2SO_4 \rightarrow 2Al^{3+} + 2SiO_2(aq) + 3SO_4^{2-} + 5H_2O \quad (15)$$

Continued dissolution of these phases increases the solute content of solutions, which may lead to precipitation of other secondary clay minerals.

Reactions (9) to (15) have been written so that the mineral dissolves completely in solution, and written this way, the stoichiometry of the reactions provide the **maximum neutralization potential** of the mineral. Maximum neutralizing potential is seldom realized because mineral dissolution generally is accompanied by precipitation of secondary phases. The nature of the precipitated phases is dependent upon the composition, abundance and chemical properties of the solution, including pH, Eh and the concentrations of solutes. For example, reactions (12) and (13) are only valid for the pH range of roughly 2 to 4. Precipitation of secondary phases reduces the neutralizing potential of minerals, and inclusion of the secondary phases in neutralization reactions permits evaluation of the **net acid production** of wastes. It is demonstrated in the following section that the nature of secondary phases formed can be predicted a priori, only by consideration of both thermodynamic and kinetic considerations. The requisite rate laws for precipitation generally have not been elucidated. There are, however, some secondary products that commonly form in mine

wastes. These are included in reactions presented subsequently, to illustrate the effects of their formation on net acid production. The secondary minerals used in the following reactions are common in waste rock and tailings, but these are not the only important secondary phases to form.

Neutralization of sulphuric acid by calcite dissolution (reaction 9) increases the pH of the resulting solution, and also releases bicarbonate to solution. Continued dissolution of calcite may result in saturation and precipitation of siderite ($FeCO_3$), if there is sufficient Fe^{2+} in solution. The consequence is production of hydrogen ions:

$$Fe^{2+} + HCO_3^- \rightarrow FeCO_3(s) + H^+ \qquad (16)$$

Just as dissolution of calcite neutralizes acid in reaction (9) by consuming hydrogen ions, reaction (16) demonstrates that precipitation of carbonate minerals (siderite here) produces acid (liberates hydrogen ions to solution); consequently, precipitation of siderite counteracts the neutralizing effect of calcite dissolution. Blowes and Ptacek (1994) recently provided a general discussion of acid-neutralization reactions in mine tailings based on extensive field studies, and discuss the influence of secondary siderite on pH. Generally, precipitation of secondary minerals, including carbonates, oxyhydroxides and clay minerals, produces acid, which can have a major effect net acid production. Formation of these secondary minerals should be included in net acid production, as now discussed.

4.3 **Net Acid Production**

4.3.1 General Description

Net acid production is estimated by conventional acid mine drainage prediction techniques which include static and kinetic tests (Ferguson, 1985). Acid-base accounting (Smith and Sobek, 1978; Sencindiver, 1981) is the most commonly used static method. By this method, the acid-generating potential is calculated from either total sulphur analysis or from pyritic sulphur analysis. Neutralization potential is obtained by adding a known amount of HCl and titrating with standardized NaOH to pH 7. Acid-generating potential is then compared to neutralization potential to indicate net neutralization (or net acid production) potential. This approach and others similar approaches are known to be quite inaccurate in predicting net acid production potential (Coastech, 1989). More accuracy would be possible if prediction methods would account for the mineralogy of the waste, noting particularly the nature of the acid-generators (sulphides primarily) and solid bases (carbonate, oxyhydroxide and silicate minerals). The nature of the precipitates should also be considered, as should the rates (and mechanisms) by which minerals dissolve and precipitate, over time, during weathering of the mine wastes. Arguments leading to this conclusion follow.

4.3.2 Precipitation of Secondary Minerals

If calcite dissolution is accompanied by siderite precipitation, the neutralizing potential of calcite is diminished. The acid-base reaction involving pyrite and calcite are apparent by combining reactions (1) and (9):

$$FeS_2 + 7/2O_2 + H_2O + 2CaCO_3 \rightarrow Fe^{2+} + 2Ca^{2+} + 2HCO_3^- + 2SO_4^{2-}. \quad (17)$$

If siderite is included as a secondary product (reaction 16) then:

$$FeS_2 + 7/2O_2 + 2H_2O + 3CaCO_3 \rightarrow FeCO_3 + 3Ca^{2+} + 2HCO_3^- + 2SO_4^{2-}. \quad (18)$$

Comparison of reactions (17) and (18) demonstrates that, theoretically, precipitation of siderite increases by 50 percent the amount of calcite needed to neutralize the sulphuric acid generated by oxidative dissolution of pyrite. If instead of siderite, ferrihydrite ($Fe(OH)_3$) precipitates, the reaction is:

$$FeS_2 + 9/2O_2 + 2H_2O + 4CaCO_3 \rightarrow Fe(OH)_3 + 4Ca^{2+} + 4HCO_3^- + 2SO_4^{2-}, \quad (19)$$

and comparison with reaction (17) demonstrates a 100 percent increase in the amount of calcite needed to neutralize the acid. Reactions (17), (18) and (19) show that the nature of the secondary mineral formed influences substantially net acid production. This point is emphasized in the following generality: **the extent to which minerals neutralize acids cannot be predicted without knowing which secondary minerals form.**

Note that as reactions (18) and (19) proceed to the right, Ca^{2+} and SO_4^{2-} build up in solution and gypsum may eventually precipitate. Precipitation of the salt does not affect net acid production.

The type of reaction that occurs during precipitation of secondary phases is important. There are two general types of reaction, one affects the concentration of hydrogen ions in solution and are referred to as hydrolysis reactions. The other, precipitation of salts, has no affect on H^+. Reaction (16), where siderite is precipitated, is an hydrolysis reaction; hydrogen ion concentration of solution is affected by the reaction, as it is in the precipitation of other carbonates in acidic and near-neutral solutions. Precipitation of a salt, such as gypsum or NaCl, does not consume or produce H^+.

Precipitation of secondary clay minerals, such as gibbsite, kaolinite, halloysite, illite and smectites, affects the neutralizing potential of Al- silicates, and net acid production. Introduction of kaolinite as a secondary product after albite yields:

$$NaAlSi_3O_8 + 1/2H_2SO_4 + 1/2H_2O \rightarrow 1/2Al_2Si_2O_5(OH)_4 + 2SiO_2(aq) + Na^+ + 1/2SO_4^{2-} \quad (20)$$

Comparison of reactions (12) and (20) demonstrates that precipitation of kaolinite reduces the neutralization potential of albite by 75 percent. The **neutralization potential** of Al-silicate minerals is determined by the type of secondary product formed, and inclusion of Al-silicates in net acid production requires knowledge of the secondary minerals produced in mine wastes.

4.3.3 Net Acid Production and Mass Balances

Mass balance or "limiting constituent" calculations can be used to determine net acid production. The concept is applied by writing a reaction involving the mineral(s) producing acid, the mineral(s) neutralizing the acid (through dissolution), and the secondary phase(s) formed. As an example, consider oxidative dissolution of pyrite in the presence of calcite and in highly oxidizing, near-neutral solution, where ferrihydrite precipitates. Assuming sufficient calcite to neutralize all acid produced, reaction (19) provides the pertinent stoichiometry and mass balances required for calculation of net acid production. Four moles of calcite are required to neutralize the acid generated by oxidation of one mole of pyrite. If, however, siderite is precipitated as the secondary mineral, then the pertinent reaction is (18), and only three moles of calcite are required to neutralize the acid produced by oxidation of one mole of pyrite. It is apparent from this abbreviated treatment that net acid production requires knowledge of the secondary phase during oxidation of sulphide minerals. The secondary phases precipitated depend on the mineralogy of the wastes, and on the temperature, Eh, pH and solute contents of solutions associated with the wastes.

Few generalizations can be made about the types of secondary products formed in rock wastes; consequently a procedure more sophisticated than the limiting constituent approach is desirable for detailed net acid production calculations.

4.3.4 Net Acid Production and Chemical Kinetics

The acid generated per litre of solution, and the amount neutralized, depends on the rates at which acid-generating and acid-neutralizing minerals dissolve, and the rates at which secondary phases form. Chemical kinetics theory can be used to calculate reaction rates. Although the approach is fundamentally sound, application of absolute kinetics requires a large amount of information, including rate equations for all solids dissolved and precipitated. Kinetic data for dissolution of common minerals are available but there are few kinetic data for precipitation of secondary products. The dearth of kinetic data is an impediment to application of kinetic calculations, but this is an active research area in geochemistry. Reasonable kinetic models should be available in a few years.

Appendix A provides reference to the available thermodynamic and kinetics properties of a suite of minerals commonly found in waste rock piles, particularly sulphides, sulphates, iron hydroxides, carbonate and silicate minerals. Appendix B includes a review of the rate equations for leaching, and specifies the conditions under which the equations are applicable. The minerals emphasized are pyrite, pyrrhotite, arsenopyrite, goethite, magnetite and hematite, although other minerals are included. Where there is appropriate information, the mechanisms of mineral weathering are summarized. Appendix B also compares inorganic and biological rates of mineral leaching, and supplies rate equations and real and apparent rate constants from which modellers can determine the conditions under which inorganic and biological leaching are dominant. Information, where lacking, is noted. Appendix B is, therefore, the basis for quantitative modelling. Without these data, and particularly the relative rates of leaching of the sulphide minerals, quantitative geochemical modelling of waste rock piles would have limited usefulness for prediction.

4.3.5 Net Acid Production and Local Equilibrium Thermodynamics

Predictions of net acid production and the formation of secondary minerals can be made with reasonable accuracy using "reaction path" calculations. These calculations can be considered as a simplification of chemical kinetic calculations. They follow the disappearance of reactants and the appearance of products as the reaction progresses by invoking the concept of local equilibrium between the solution and secondary mineral products (Helgeson et al., 1969).

The theory and application of reaction path calculations are well documented (Helgeson et al., 1969; 1970). Reaction path calculations allow for the dissolution of one or more solids in an aqueous solution of specified composition by numerically titrating the solids in one aliquot per time step. The driving force for reaction is disequilibrium between the initial solution and the solids. The compositional evolution of the solution is calculated as the solid dissolves as a function of relative time. Precipitation of secondary phases is allowed as they become saturated in the evolving solution, and the effects of precipitation on solution composition are determined. The calculations include speciation of all solutes during evolution of the solution, and evaluation of the amounts of solids dissolved and precipitated during the course of the reaction. Redox reactions are included so that oxidative dissolution of minerals such as pyrite, pyrrhotite and arsenopyrite can be taken into account.

A variant of reaction path calculations is to incorporate kinetic rate laws where available. Dissolution rates of many minerals are known from experiment or from controlled field studies; consequently, time to dissolve minerals can be incorporated into reaction path calculations as the monitor of reaction progress (Helgeson, 1970). Since rates of precipitation of many solids are unknown, the reaction path procedure of allowing precipitation upon achieving saturation with respect to secondary solids is the only practical approach available to incorporate precipitation. Fortunately, many of the important secondary minerals of mine wastes precipitate readily so that there may be no great error introduced by assuming that these precipitates form once saturation is exceeded.

The next section of the report (Section 5) discusses geochemical processes with special emphasis on reaction rates and the fundamental mechanisms which influence them. Section 6 provides pertinent examples of reaction path calculations, whereby reaction progress is monitored by the amount of a mineral dissolved (i.e. relative time). Section 6 also provides examples where dissolution kinetic rate laws are incorporated into the reaction path calculations.

5. GEOCHEMICAL PROCESSES

5.1 General Description

Table 1 provides a list of geochemical processes, and classifies geochemical processes into mass transfer processes involving minerals in waste rock and the rate-determining processes which control the path of these reactions. Mass transfer processes include the different important reactions discussed in the previous section such as sulphide mineral oxidation (equation 1), dissolution of calcite (equation 9) and alumino-silicate dissolution (equations 12 through 15).

It is difficult to clearly separate geochemical processes from physical processes because they are so closely linked together in nature. For example, mixing of waters and gases (i.e. fluid mixing) in waste rock piles is a physical process, and has relevance to geochemical processes in that the new solution compositions may be supersaturated or undersaturated with respect to solid phases as a result of mixing. Of primary concern are these reactions which occur as a result of new solution compositions, whether a product of mixing, gas introduction/removal, or other processes. The physical conditions giving rise to solution compositions are of secondary interest in the present review. Efficiency of mixing, time required for mixing, flushing rates and other aspects, although important for calculating chemical loading rates from waste rock piles, are not required to understand geochemical processes, and therefore not considered in detail herein.

Table 1. Classification of geochemical processes

Mass-transfer processes	**Rate-controlling processes**	**Rate-modifying factors**
DISSOLUTION / PRECIPITATION	DIFFUSION	CATALYSIS
by: acid-base reactions	- macroscopic	bacterial
hydrolysis	- microscopic	galvanic
redox reactions	- atomic-scale	abiotic
co-precipitation	NUCLEATION	TEMPERATURE
gas release/capture		
Wetting-drying	SURFACE REACTION	PRESSURE
	ADSORPTION/	SURFACE AREA
ION EXCHANGE / SORPTION	DESORPTION	
RADIOACTIVE DECAY		

Geochemical reactions in the unsaturated zone occur primarily at the interfaces between solids, gases and aqueous solutions; the rates at which these reactions occur are controlled by the transport (or trapping) of constituents to and across the interfaces. Rate controlling mechanisms are fundamentally important because they determine the rate at which the mass transfer processes proceed. The present section of the review will address geochemical processes following the classification in Table 1.

5.2 **Precipitation and Dissolution**

5.2.1 Mechanisms and Rate-Controlling Steps

As seen in Section 3, dissolution of silicate minerals contributes to neutralization of acids. Conversely, precipitation of oxyhydroxides and clay minerals produces acidity, which may lower water quality. Dissolution and precipitation affect substantially the primary minerals of waste rock piles. Sulphide minerals undergo oxidative dissolution in O_2-bearing aqueous solutions (M^{c}Kibben and Barnes, 1986), as do other minerals containing metals in reduced states (e.g. Fe(II)-silicates, carbonates and oxyhydroxides), thus increasing the heavy metal and sulphate content of drainage waters. Dissolution and precipitation are major geochemical processes affecting the mineralogy of waste rock piles and drainage water compositions and are therefore emphasized throughout this review.

Dissolution of solids takes place in a series of steps, summarized in Table 2. The sequence of steps includes adsorption/desorption, diffusion, and surface chemical reactions. The controlling process (the slowest process in the sequence) is determined by the properties and compositions of both the minerals and the solutions involved in the reactions, and just as these properties change over time, so may the processes controlling dissolution, precipitation, hence acid generation, neutralization, heavy metal contents and total dissolved solids in waters draining waste rock piles.

Table 2. Sequence of steps in solid dissolution reactions

1	Diffusion of solutes from bulk solution to the mineral surface, across a stagnant solution layer.
2	Adsorption of solute onto the mineral surface.
3	Transport of reactants to reactive sites via surface, lattice or dislocation (short-circuit) diffusion.
4	Surface chemical reaction
5	Diffusion of reaction products from the reactive sites to the surface of the solid.
6	Desorption of product from the surface.
7	Diffusion of product through the stagnant layer to bulk solution.

Any one of the above steps may limit the rate of dissolution or precipitation, but the three most common rate-controlling steps are diffusion through the stagnant water layer[1] (step 1), diffusion on surfaces or through the solid (step 2), and rate of reaction at solid surface sites (step 4). Berner (1981) discusses these mechanisms and points out that minerals with low solubility, such as Al-silicates, are controlled by reaction at mineral surfaces (step 4 of preceding list). Minerals with high solubility products, however, are typically controlled by diffusion (transport limited dissolution rate; steps 1, 3, 5 and/or 7). Table 3 illustrates the relationship between solubility and mechanism controlling dissolution rate (Berner, 1981).

Precipitation involves the added, initial step of nucleation, but subsequent growth of precipitates includes sorption, diffusion and surface reaction. Rates of reactions may be altered by electromotive forces generated by galvanic cells (see section 5.5), but dissolution and precipitation also are controlled by diffusion, surface reaction and sorption processes.

[1]The thickness of the stagnant layer is typically 30 μm in natural environments (Plummer, 1972).

Table 3. Dissolution rate-controlling mechanism for various substances - arranged in order of solubilities in pure water (After Berner, 1981)

SUBSTANCE	SOLUBILITY mole per litre	DISSOLUTION RATE CONTROL
$Ca_5(PO_4)_3OH$	2×10^{-8}	Surface Reaction
$KAlSi_3O_8$	3×10^{-7}	Surface Reaction
$NaAlSi3O_8$	6×10^{-7}	Surface Reaction
$BaSO_4$	1×10^{-5}	Surface Reaction
AgCl	1×10^{-5}	Diffusion
$SrCO_3$	3×10^{-5}	Surface Reaction
$CaCO_3$	6×10^{-5}	Mixed
Ag_2CrO_4	1×10^{-4}	Surface Reaction
$PbSO_4$	1×10^{-4}	Mixed
$Ba(IO_3)_2$	8×10^{-4}	Diffusion
$SrSO_4$	9×10^{-4}	Surface Reaction
Opaline SiO_2	2×10^{-3}	Surface Reaction
$CaSO_4 \cdot 2H_2O$	5×10^{-3}	Diffusion
$Na_2SO_4 \cdot 10H_2O$	2×10^{-1}	Diffusion
$MgSO_4 \cdot 7H_2O$	3×10^{0}	Diffusion
$Na_2CO_3 \cdot 10H_2O$	3×10^{0}	Diffusion
KCl	4×10^{0}	Diffusion
NaCl	5×10^{0}	Diffusion
$MgCl_2 \cdot 6H_2O$	5×10^{0}	Diffusion

5.2.2 Influence of Wet-Dry Cycling

The wetting and drying cycle is the major influence on the geochemical processes occurring within unsaturated waste rock piles. Repeated infiltration, drainage, evaporative drying and air-oxidation of the pile results in dissolution and precipitation of minerals. During dry periods, minerals in waste rock react with the gaseous phase occupying pores and interstices. In the absence of a bulk aqueous phase, gas-solid reactions produce a variety of secondary minerals, some of them very soluble salts (Nordstrom et al., 1979; Nordstrom, 1982; Steger, 1982; Buckley and Woods, 1985a,b; Pratt et al., 1994a).

The non-volatile phases accumulate on waste rock surfaces until dissolved in rainwater or runoff infiltrating through the rock pile. During infiltration, soluble salts and other solids are dissolved in solution. The subsequent evaporative stage of the cycle (Fig. 1) is particularly important. During evaporation, Fe and SO_4 along with other solutes, are concentrated, and minerals are precipitated as

the residual waters of the piles become more concentrated. Comparatively insoluble constituents such as Fe and Al oxyhydroxides, carbonates, jarosite ($KFe_3(SO_4)_2(OH)_6$), and its aluminous analogues may precipitate. Continued evaporation will lead to precipitation of highly soluble Fe and Mg sulphate minerals including melanterite ($FeSO_4 \cdot 7H_2O$), copiapite ($Fe^{2+}Fe_4^{3+}(SO_4)_6(OH)_2 \cdot 20H_2O$) and coquimbite ($Fe_2(SO_4)_3 \cdot 9H_2O$) and their dehydration products. Epsomite ($MgSO_4 \cdot 7H_2O$) and its dehydration products may also precipitate. These salts will dissolve rapidly during infiltration, producing solutions rich in Fe, Mg and SO_4 (Nordstrom 1982).

5.3 **Diffusion**

5.3.1 Macroscopic Diffusion

Diffusion occurs on many scales in waste rock piles (Fig. 2). Oxidation of sulphides decreases the partial pressure of oxygen within the pile, creating a partial pressure gradient between the interior of the pile and the atmosphere. Oxygen consequently diffuses from the surrounding atmosphere into the rock pile, thus replenishing oxygen and promoting additional oxidation of sulphides. Oxygen is replenished by physical processes as well. Macroscopic diffusion is an important process affecting waste rock piles. The interested reader is directed to comprehensive reviews by Ritchie (1994a,b,c) and Morin et al. (1991). A thorough, quantitative treatment of these processes is given by Ghildyal and Tripathi (1987).

5.3.2 Microscopic Diffusion

Soluble salts dissolve so rapidly when contacted by solutions that transport of solutes away from the dissolving mineral surface limits the rate of dissolution. The rate-limiting step is diffusion of solutes through a thin film of stagnant water, separating the mineral surface from bulk solution (Fig. 2). The thickness of the stagnant water layer is typically 10^{-2} to 10^{-4} cm thick, depending upon the amount of agitation and convection in the bulk solution. Sulphate salts are likely to precipitate during evaporation of pore waters. Subsequent infiltration of rainwater into the waste rock pile will result in rapid dissolution of the highly soluble sulphate salts, and according to the arguments of Berner (1981), diffusion will limit the rate of dissolution. Microscopic diffusion therefore is an important process of waste rock piles.

5.3.3 Atomic-scale Diffusion

Atomic-scale diffusion occurs in solids containing an abundance of vacancies (Fig. 2), dislocations and line defects. It also occurs along boundaries separating mineral grains (Kittel, 1956; Weertman and Weertman, 1965; Shewmon, 1963). Dislocations and grain boundaries are particularly important in that they provide avenues along which waters and gases penetrate rocks (Meunier and Velde, 1976). Grain boundary diffusion must influence, and may well control, redox reactions and leaching rates in waste rock piles, but its importance has not been established.

Lattice diffusion (Fig. 2) can affect substantially the weathering of minerals (Shewmon, 1963). Pyrrhotite is non-stoichiometric, typically of composition Fe_7S_8, and is composed of two Fe(III) ions and five Fe(II) ions per unit formula (Pratt et al., 1994a). For every two Fe(III) ions present on the cationic lattice, there is also one vacancy present (to maintain charge balance within the mineral). The lattice substitution can be portrayed as:

$$3Fe^{2+} = 2Fe^{3+} + 1 \text{ vacancy.}$$

In pyrrhotite, Fe can diffuse through the lattice by "jumping" from one vacancy to another (Fig. 2). Upon exposure to air, Fe(II) is oxidized to Fe(III) at the mineral surface. A chemical potential gradient in Fe(II) is established between the interior of the grain and the oxidized surface. In response, Fe diffuses from the interior to the surface where it forms Fe(III)-- oxyhydroxides (Pratt et al., 1994a); consequently, oxidation of pyrrhotite is initially controlled by diffusion of Fe through the lattice, via vacancies.

By contrast with pyrrhotite, natural pyrite is close to stoichiometric composition (FeS_2). Vacancies are not abundant and diffusion of Fe to the oxidized surface has not been observed (Buckley and Woods, 1985a,b). We cite the pyrite and pyrrhotite examples to emphasize that crystallographic and compositional properties of minerals, including sulphides, have substantial effect on reactivity. Reviews by Ribbe (1974) and Vaughan and Craig (1978) are recommended for additional information on thecrystallographic and mineralogical properties of sulphides

5.3.4 Diffusion-Controlled Reactions

All constituents leached from minerals by aqueous solution must diffuse through a stagnant layer of water adhered to the surfaces of the minerals before entering bulk solution. Existence of such stagnant layers are exemplified by Nocol (1988) which showed that iron hydroxide coatings form when the pH of the microenvironment surrounding the sulphide particles is greater than 3.5. Consequently there is the potential for diffusive transport to determine the dissolution rate of all minerals. Berner (1981) suggests that the dissolution rates of minerals with high solubility products are controlled by diffusion of reaction products through the stagnant water layer. Gypsum dissolution rate, for example, is predicted, and observed, to be controlled by this mechanism.

Diffusion of constituents through the mineral being leached may control the rate of dissolution. Diffusion of Fe through pyrrhotite initially controls the oxidation rate of this mineral in air and in dilute sulphuric acid solutions (Pratt et al., 1994a, 1994b). There is no evidence, however, that solid-state diffusion of Fe affects the rate of oxidation of pyrite in air (Nesbitt and Muir, 1994), and pyrite dissolution is controlled by surface reactions (M^{c}Kibben and Barnes, 1986). Pyrrhotite is non-stoichiometric and contains large numbers of vacancies, which promote solid state diffusion. Pyrite contains a small number of vacancies, hence diffusion is unimportant, and other processes control its oxidation rate.

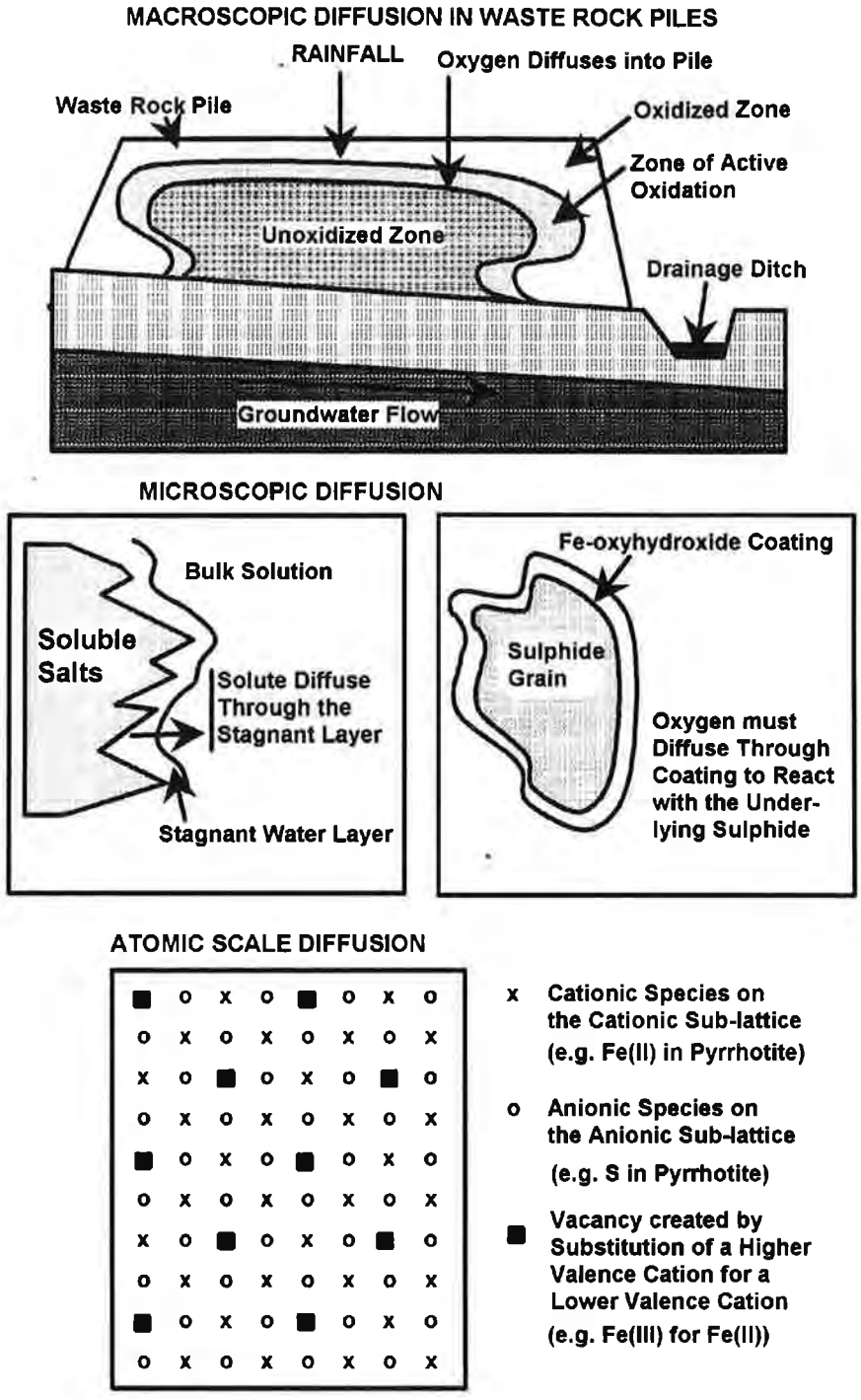

Figure 2. Diffusion in Waste Rock Piles

Fe-oxyhydroxide (ferrihydrite) and other coatings commonly form on sulphide minerals in mine tailings (Blowes et al., 1992; Jambor, 1987). As the crusts thicken, the time required for constituents to diffuse through the coating becomes greater, and reactions which were initially surface-reaction controlled may, after time, become controlled by diffusion through the secondary coating. Rates of reaction then would be dependent both on the diffusion coefficient of species through the coating and on the thickness of the coating. Fe-oxyhydroxide coatings on sulphide minerals may control release rates of acid to solution, particularly after reaction has proceeded sufficiently to build up thick coatings on minerals. The coating, however, must envelop the entire mineral surface and it must remain intact if diffusion is to become rate limiting. The situation is likely in mine tailings. It is much less likely in waste rock piles where they are dried, shrink and expose the underlying minerals.

5.3.5 Air-Oxidation and Spalling in Wastes

Air-oxidation of sulphide minerals produces Fe(III)-oxyhydroxides at the surface of pyrrhotite (Pratt et al., 1994a; Nesbitt and Muir, 1994). These coatings are a few Ångströms to tens of microns thick. When this occurs, either oxidants must diffuse through these coating to oxidize underlying sulphides, or Fe of pyrrhotite diffuses from the interior of the mineral to the surface where it reacts with oxygen (oxidant) to form the oxyhydroxides (Pratt et al., 1994a). Hence, reaction rates necessarily decrease as the thickness of the coatings increase (Fig. 2). Removal of the Fe from the interior results in build-up of a residue of sulphur as disulphide and polysulphide (Pratt et al., 1994a). Dehydration of the oxyhydroxides causes shrinkage, curling and spalling of the Fe(III)-oxyhydroxides from the surface of pyrrhotite, exposing the sulphur-rich residual layer (Pratt et al., 1994b). Spalling is promoted by the distinctly different bonding characteristics of the Fe(III)-oxyhydroxide layer, which has a significant ionic component, and the S-rich layer, which is dominantly covalent. The interface between the two layers is weak, and the oxyhydroxide layer is easily spalled during wetting and drying cycles (Pratt et al., 1994b).

Pyrite may respond similarly to pyrrhotite with regards to spalling. Fresh pyrite is two parts sulphur, and displays more covalent character than fresh pyrrhotite. Fe(III)-oxyhydroxides formed at pyrite surfaces probably are not bonded strongly to the surfaces and spalling is possible. The process may be common at other sulphide mineral surfaces as well, but documentation is required. If it is prevalent, it has significant implications for water quality, particularly suspended particulate load, and also for release of heavy metals such as Zn and Pb to solution. Also, the coating of mineral surfaces can be very dependent on field micro-environmental conditions. For example, a study by Norecol (1988) on the Cinola gold project showed that, if local pH was above 3.5, the Fe-oxyhydroxides would coat the sulphides, but at pH less than 3.5, the Fe-oxyhydroxides were detached from the sulphides and were deposited on carbonate rocks.

5.4 **Reactions at Mineral Surfaces**

5.4.1 Abiotic Reactions - Surface Complexation

Silicates are a major component of waste rock piles and Berner and Holdren (1977) demonstrated conclusively that the rate of dissolution of feldspar minerals during weathering is controlled by reactions occurring at the surfaces of these minerals (Table 3). Berner and Schott (1982) extended these findings to include pyroxenes and amphiboles, as well as sparingly soluble oxides and sulphides such as hematite and pyrite (Berner, 1981). It is therefore apparent that all processes affecting the surfaces of these minerals necessarily affect their rates of dissolution. This fact has received recognition in the geochemical literature over the past 10 to 15 years, culminating in numerous recent reviews emphasizing the importance of surface processes, and particularly the importance of surface complexes (Davis and Kent, 1990; Wollast and Stumm, 1990; Herring and Stumm, 1990).

Stumm and co-workers (Stumm and Wollast, 1990) demonstrate that Fe and Al oxide dissolution rates are controlled by surface chemical reactions, and that the nature of the complex-forming ligand determines the rate at which the metal is detached from the surface. Rate studies of M^{c}Kibben and Barnes (1986) indicate that surface reactions control the rate of dissolution of pyrite. Rates of dissolution of other sparingly soluble sulphides may be controlled by surface reactions as well. The mechanisms by which surface reactions occur are active fields of research in geochemistry and represent an important process in waste rock piles. Coordination chemistry of surfaces, and surface complexation theory, have been summarized recently (Stumm and Wollast, 1990). Their review, and studies included therein, provide detailed chemical background into coordination chemistry and complexation theory.

Surface complexes form by reaction of one or more aqueous species with a metal, hydroxyl (OH^-) or oxide (O^{2-}) species exposed at, but attached to, mineral surfaces. Formation of surface complexes weakens bonds between the metal, hydroxyl or oxide species and the solid, thus promoting dissolution. The effect of surface complexes depends upon temperature, pH, Eh, the concentration of complexing agents in solution, the chemical properties of the mineral surface, and upon the strength of the surface complex formed. The field is an exceptionally active area of research today (Schindler, 1990).

Modelling of dissolution of solids, using the concept of surface complexation, has increased dramatically in aqueous geochemistry. There are few sophisticated applications to mine wastes, hence there is potential for great strides in understanding through application of the concept. There are, however, obstacles to its application, the most important of which is the amount of data required to develop quantitative models applicable to mineral surfaces in complex settings such as waste rock piles. New surface analytical techniques permit rapid collection of these data so that inclusion of surface complexation theory into geochemical modelling of geological systems should develop rapidly.

5.4.2 Biological Processes

Nordstrom (1982) provides an excellent review of microbial oxidation. The importance of *thiobacillus* is emphasized, noting that *Thiobacillus ferrooxidans* are implicated as a catalyst in the production of acid drainage waters. The bacteria provide a means to rapidly oxidize $Fe^{2+}(aq)$ to Fe^{3+} which, in turn, promotes oxidative dissolution of pyrite. However, biological processes are here discussed only in so far as they are related to geochemical processes. The interested reader is directed to Appendix B of this review, and to the review of Nordstrom (1982, and references therein).

As the pH of waters of the unsaturated and saturated zones approaches 4, bacterial action typically increases, enhancing the rate of oxidative dissolution of pyrite. Oxidative dissolution of pyrite and/or pyrrhotite (alone, or in the presence of solid bases such as Al-silicate or carbonate minerals), yield solution pH values close to or above four. The pH of solutions flushing through the unsaturated zone (some of which may collect in perched or permanently saturated zones) display pH values less than four as a result of dissolution of melanterite; consequently there may be a close relationship to the amount of melanterite, or other sulphate salts and solid acids, present in the undersaturated zone and bacterial activity.

Although biological processes are not geochemical processes, they can be viewed as mediators of chemical reactions, increasing the rate of reaction where conditions permit. From the perspective of geochemical processes they can be considered akin to catalysts. Rate equations for dissolution can be modified to incorporate a term for each bacterium that affects a reaction rate. The term should include the "concentration" of the specific bacterium, the concentration of constituents that both promote and inhibit bacterial activity, and a rate constant reflecting the catalytic effect of the bacterium. The overall rate equation includes a term for each bacterium affecting the rate of reaction (e.g. rate of dissolution of pyrite). The effects of biological activity can be included in geochemical modelling codes and should be included where prediction of water quality is required.

5.5 **Galvanic Reactions**

Galvanic effects (also referred to as self-potential phenomenon) have been invoked to explain the alteration zones observed in sulphide-rich and oxide-rich ore deposits (Thornber, 1982). In these deposits, the process operates on the scale of the ore body, provided there is good (electrical) connection between surface outcrops and subsurface portions of the ore body. The galvanic process can also occur on the scale of the hand sample, and on microscopic scale, provided two different sulphide or oxide minerals are in contact, and in contact with an aqueous solution (Fig. 3). These reactions are independent of the amount of oxygen (or other oxidant) dissolved in solution as one mineral acts as oxidant while the other acts as reductant.

Rock waste piles include varied and complex mineral assemblages of sulphide and oxide minerals. Contact between different semi-conductors produces an electrochemical potential, and the presence of the aqueous solution completes the circuit (Fig. 3). The cells will therefore operate during the

infiltration and drainage stages of the wetting and drying cycle, or wherever a film of water covers the surface of the aggregate.

The reaction products of galvanic reactions are generally different from reaction products formed by oxidative dissolution of individual sulphide or oxide minerals. Pyrite and pyrrhotite are used as examples to emphasize this aspect. Dissolution of pyrite and pyrrhotite by O_2-saturated solutions causes Fe(II) of pyrite to be oxidized and produce Fe(III)-oxyhydroxides, Fe(III) sulphates and/or Fe^{3+}(aq) species (Nesbitt and Muir, 1994; Buckley and Woods, 1985a,b; M^{c}Kibben and Barnes, 1986). Disulphide of pyrite and monosulphide of pyrrhotite will be oxidized to one or more of polysulphides, native sulphur, thiosulphate or sulphate (Buckley and Woods, 1985a,b; Mycroft et al., 1990; Nesbitt and Muir, 1994). All products formed by oxidative dissolution of these minerals display higher oxidation states than observed in the mineral being oxidized. The products of the pyrite-pyrrhotite galvanic reaction (in presence of solution) have been identified in a study by Nakazawa and Iwasaki (1985) and are discussed in the following paragraphs.

Nakazawa and Iwasaki (1985) identified the reaction products of the pyrite-pyrrhotite galvanic cell using Auger and XPS spectroscopy. The S2p spectrum of the galvanically reacted pyrrhotite surface indicates the presence of disulphide and polysulphides, not present in the unreacted pyrrhotite surface. By contrast, comparison of the S2p spectrum of unreacted and galvanically reacted pyrite, indicates the accumulation of monosulphide at the pyrite surface. Apparently, some disulphide of pyrite is reduced to monosulphide during galvanic reaction with pyrrhotite and some monosulphide of pyrrhotite is oxidized to disulphide and polysulphide. Fe2p XPS spectra reveal the presence Fe(III)-oxyhydroxides on the surfaces of both minerals, suggesting that Fe(II) of both sulphides is oxidized to Fe(III) during the reaction.

The production of monosulphide from pyrite occurs as a result of the galvanic process; it is not produced by oxidative dissolution of pyrite in O_2-bearing solutions (Buckley and Woods, 1985a,b; Nesbitt and Muir, 1994). The presence of monosulphide clearly demonstrates that galvanic reactions produce reaction products different from oxidative dissolution of the minerals.

Galvanic cells involving other sulphides have been studied (Majima, 1969), but since the intent of this review is to document the processes occurring within rock wastes, the pyrite-pyrrhotite couple is sufficient to illustrate galvanic reactions. There are likely to be many local galvanic cells set up within a rock waste pile, each the result of separate sulphide-sulphide, sulphide-oxide and oxide-oxide mineral assemblages. Competition among the localized cells is likely in the saturated zones as a result of communication via the aqueous phase. The competition complicates the process. The rates of reaction and the types of secondary products formed may depend upon the ease of communication among the various galvanic cells operating in the saturated zone.

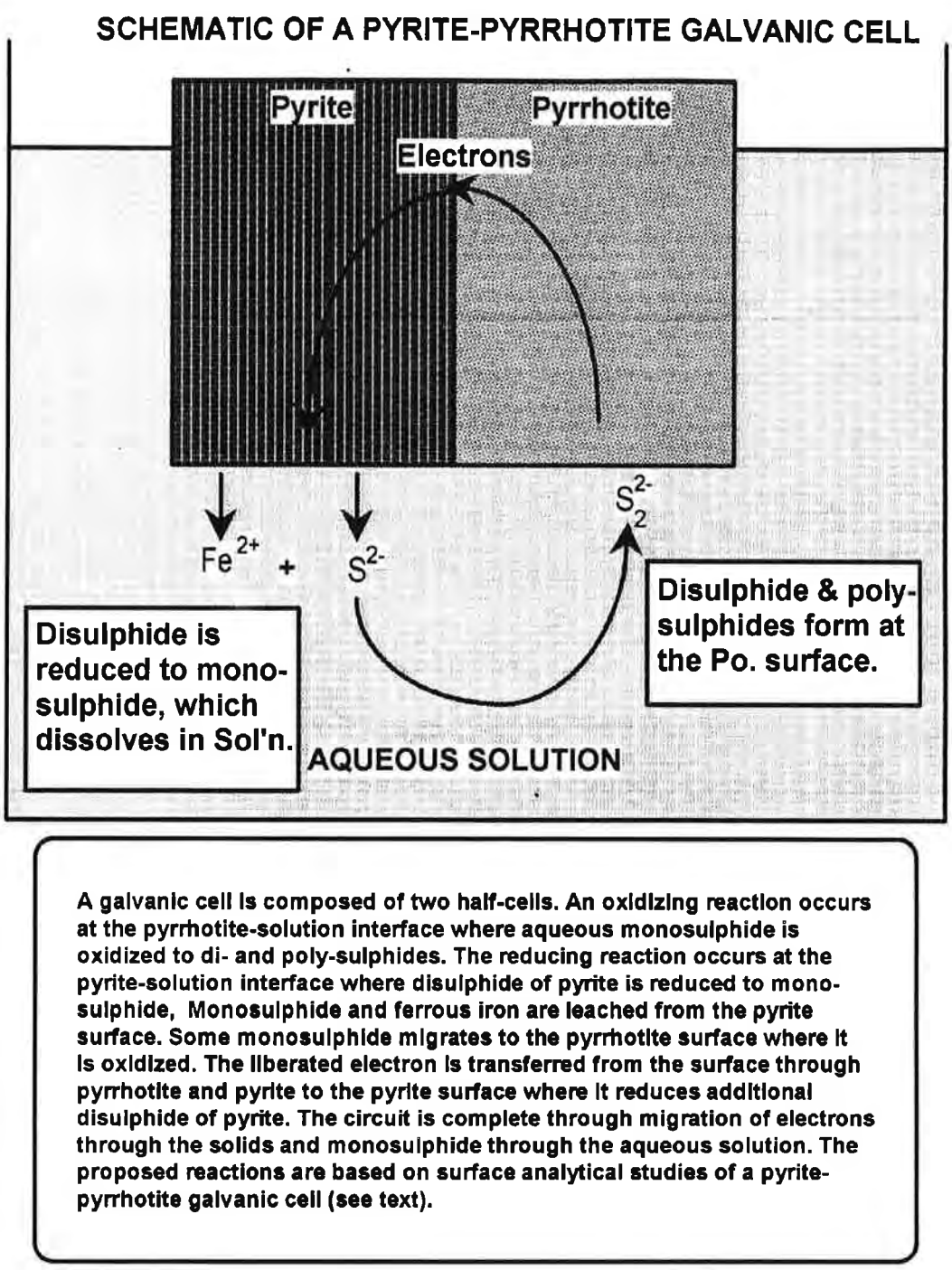

A galvanic cell is composed of two half-cells. An oxidizing reaction occurs at the pyrrhotite-solution interface where aqueous monosulphide is oxidized to di- and poly-sulphides. The reducing reaction occurs at the pyrite-solution interface where disulphide of pyrite is reduced to mono-sulphide, Monosulphide and ferrous iron are leached from the pyrite surface. Some monosulphide migrates to the pyrrhotite surface where it is oxidized. The liberated electron is transferred from the surface through pyrrhotite and pyrite to the pyrite surface where it reduces additional disulphide of pyrite. The circuit is complete through migration of electrons through the solids and monosulphide through the aqueous solution. The proposed reactions are based on surface analytical studies of a pyrite-pyrrhotite galvanic cell (see text).

Figure 3. Pyrite-pyrrhotite Galvanic Cell with Proposed Reactions

Two properties of waste rock piles minimize the effects of galvanic processes compared to natural gossans. Firstly, as most piles are unsaturated, the "electrical circuit" is open and galvanic reactions cannot occur. Secondly, waste rock piles are aggregates, with few good contacts between individual rock fragments, thus preventing development of galvanic cells on the scale of the entire waste rock pile. However, galvanic micro-environments may develop within individual rock fragments containing sulphides and oxides.

Micro-environments created by galvanic cells may have Eh and pH conditions substantially different from surrounding environments. For example, even where oxidizing conditions prevail, a pyrite and pyrrhotite galvanic cell may create a micro-environment where the Eh is sufficiently low, that $H_2S(aq)$ and HS^- may dominate over SO_4^{2-}. Transition metal species such as Zn^{2+} or Pb^{2+}, if present in the associated solution, may precipitate as a result of high concentrations of H_2S or HS^-. Once the cell ceases to function, oxidizing conditions may return to the micro-environment, leading to dissolution of the precipitated sulphides. The galvanic process may therefore yield low Zn^{2+} and Pb^{2+} concentrations while the cells function, but rapid increase in metal contents of drainage may follow when galvanic cells cease to function.

In summary, there is extensive discussion in the literature on the large-scale occurrence of galvanic processes (Thornber, 1975a, 1975b; Majima, 1969; Hiskey and Wadsworth, 1975; Mizoguchi and Habashi, 1983; Nakazawa and Iwasaki, 1985; Kwong, 1993). Galvanic processes probably occur at smaller scales in waste rock piles, but insufficient data exists to evaluate the importance of this mechanism. As the reaction products formed through oxidative dissolution of each mineral are generally different from those produced by galvanic processes, understanding of both processes may be important to properly interpret the secondary reaction products of waste rock piles. Electrochemical measurements could probably be performed to quantify galvanic processes. Techniques used for measuring electrochemical potential of mineral flotation solutions (Pillai and Bockris, 1984) may be of use. At the large-scale, field work recently proposed to MEND might yield more information on the practical use of measuring self-potential in waste rock piles.

5.6 **Exchange, Sorption and Other Processes**

Ion exchange and sorption capacities of solids depend on the surface area contacted by solution and on the electrostatic properties of the solid surface. Clay minerals and zeolites display large exchange and sorption capacities per unit mass of solid, and where these minerals are found in quantity, cation exchange and sorption may control the proportions of metals dissolved in solutions (Renick, 1924; Foster, 1950; Nesbitt and Cramer, 1993). Similarly, colloids and very fine-grained solids, such as Fe and Mn oxyhydroxides, display exceptionally large surface areas relative to mass, and may have a significant effect on cation and anion proportions of associated solutions. Organic matter is also known to be an excellent medium for sorption of dissolved metals.

As cation and anion exchange reactions proceed, charge balance is maintained, both in solution and on the exchange substrate; consequently, exchange cannot affect the total equivalents of species dissolved in solution (an equivalent = moles of species "i" per litre of solution multiplied by the charge

on "i"). In other words, cation and anion exchange cannot lead to substantial increase in the total dissolved solids (TDS) of solutions. · Sorption reactions are similarly restricted in their capability to substantially modify the TDS of aqueous solutions. Sorption reactions can proceed only so far as charge balance is maintained at the interface between solid and solution and in the bulk solution. As a result, extensive desorption of cations cannot occur without an equivalent amount of anions being added to bulk solution, or without the pH of the solution increasing (increase in OH^-) to offset the addition of cations to solution. In fact, ion exchange and sorption reactions are highly pH-dependent. Sulphate desorption from goethite, for example, must be balanced by an equivalent increase in a cation or a decrease in pH. Blowes and Cherry (1986) demonstrated that SO_4 increases in tailings pore water are offset largely by increase in aqueous Fe(II).

The mechanism through which water quality can be affected by ion exchange and sorption is the tendency of some ionic species to exchange or adsorb on solid surfaces more than others. Tendencies to exchange or adsorb depend on several ionic properties such as charge and hydrated radius. If exchanges occur between metal ions of different toxicity, the overall water quality could be affected. If desorption of a toxic metal is couterbalanced by an increase in non-toxic anions such as sulphate of chloride, the resulting water quality will decrease. The attenuation of metal concentations in waters in contact with soils with high ion exchange capacities has been extensively documented in field studies done around landfill sites, such as Yanful et al (1988). For waste rock, most piles initially contain solids with low exchange capacity and low surface/mass ratio. The bulk of trace and major metals and non-metals are therefore unlikely to be controlled by ion exchange or sorption. However, as the waste rock oxidizes, sorption of metals is more likely to occur on the surface of clayey minerals produced from the alteration of alumino-silicate rock, and on the surface of secondary oxide and hydroxide precipitates. In many field studies, adsorption and co-precipitation are found to be the only mechanism for the attenuation of mobile metal species such as Zn and Ni.

Co-precipitation occurs when metals released from primary minerals are incorporated into structural sites of minerals such as goethite ($FeO(OH)$) or ferrihydrite ($Fe(OH)_3$) as solid solutions. Alternatively, metals may be adsorbed onto mineral surfaces and subsequently covered, or "encased", by precipitating minerals. Co-precipitation has been found to control the concentrations of several metals in acid mine water (Blowes and Jambor 1990). After co-precipitation, metals can remain "encased" until the overlying precipitate is dissolved. Metals and non-metals adsorbed and subsequently "encased" may be incorporated, during aging, into the structure of the mineral onto which it was initially adsorbed. Whether "encased", included into separate mineral phases, or incorporated into solid solutions, co-precipitated metals and non-metals (trace and major) will be released primarily through dissolution rather than desorption reactions. Dissolution is therefore the major process affecting co-precipitated metal and non-metal release to solution.

Sorption on organic matter was discussed above as mechanism which could possibly reduce the concentration of aqueous species. Other processes could also occur if organic matter is present. For example, the production of organic acids from the oxidation of the organic matter by heterotrophic bacteria could potentially decrease pH and accelerate sulphide oxidation. Another scenario that could occur is the complexation of metals and a subsequent increase in metal mobility. In general however, unless organic matter is deliberately placed within waste rock piles, organic matter accumulation is small and its effects are limited. Yanful and Payant (1993) hypothesized that an observed acceleration of sulphide oxidation was due to the presence of organic acids, but subsequent testing refuted the hypothesis. Tassé et al (1994) discuss the complexation of metals by organic molecules in the context of a tailings site covered with wood-chips.

Exchange of non-volatile cation and anion species cannot occur between the gaseous phase and solids. Most transition metals and constituents of the group Vb and VIb elements of the Periodic Table (including sulphur) are non-volatile, hence gas-solid exchange is one of the least important processes affecting acidic drainage waters of waste rock piles.

5.7 **Summary**

The most important geochemical processes in waste rock piles are dissolution and precipitation. Four classes of mineral-fluid reactions are identified as contributing to acid and metal release and consumption:

- Oxidation of sulphides releasing acid, major and trace metals and sulphate.
- Precipitation of oxyhydroxides releasing acid and consuming major and trace metals.
- Dissolution/precipitation of sulfate minerals mediating the dissolved metal concentrations as well as TDS.
- Dissolution of oxyhydroxides, carbonates and silicates consuming acid.

Co-precipitation can also provide a major control on trace metal concentrations. Ion exchange and sorption only have a secondary effect.

6. QUANTITATIVE EVALUATION OF PROCESSES AND REACTIONS

6.1 General Description

Geochemical processes affecting waste rock piles differ depending upon whether an aqueous or a gaseous solution contacts solids of the waste. The non-volatility of most common species necessitates that reaction products accumulate at the surface of waste rock being weathered during reaction with the gas phase. The presence of an aqueous solution, however, permits removal of constituents from the reacting surface by dissolution and subsequent transport away from the site of reaction. An example of this difference is the accumulation of the soluble salt, melanterite ($FeSO_4 \cdot 7H_2O$), at the surface of Fe-sulphide minerals oxidized by reaction with atmospheric oxygen (Nordstrom, 1982). These salts may well determine the quality of waters flushed through the unsaturated zones during periodic rainfall events, or during seasonal runoff, as shown in this section.

6.2 Oxidation of Sulphide Minerals

6.2.1 Conceptual Aspects

Buckley and Woods (1985a,b), using X-ray Photoelectron Spectroscopy (XPS), identified an Fe-sulphate reaction product on the surface of pyrite oxidized in air for 14 days, and melanterite ($FeSO_4 \cdot 7H_2O$) was found in unsaturated zones of tailings (Blowes et al., 1992; Jambor, 1987; Nordstrom et al., 1979a; Nordstrom, 1982). The overall stoichiometry of the reaction, where pyrite is oxidized by air to produce melanterite, is:

$$FeS_2 + 7/2O_2 + 8H_2O \rightarrow FeSO_4 \cdot 7H_2O + H_2SO_4 \qquad (21)$$

Although Buckley and Woods (1985a,b) detected the Fe-sulphates, they did not (and could not) identify the acid, although it can exist as a solid in exceptionally low humidity environments. Sulphuric acid can exist in solid form as rhomboclase ($HFe(SO_4)_2 \cdot 3H_2O$), and has been recently observed at Iron Mountain, Ca. (Alpers and Nordstrom, 1991). It may also form in rock wastes during extreme drying. Partially oxidized sulphur species, such as native sulphur or polysulphides, may also form during air-oxidation of pyrite (Pratt et al., 1994a; Mycroft et al., 1990). These studies demonstrate that soluble salts form during air oxidation of common sulphide minerals. The presence of salts in unsaturated zones is of fundamental importance because their dissolution may lead to more acidic drainage than would occur in their absence. A reaction likely to occur during flushing is dissolution of melanterite:

$$Fe(SO_4) \cdot 7H_2O + 1/4O_2 \rightarrow Fe(OH)_3 + H_2SO_4 + 4.5H_2O, \qquad (22)$$

where the salt rapidly dissolves in aqueous solution. Oxidizing solutions which dissolve melanterite may precipitate ferrihydrite, goethite or hematite and produce acidity (sulphuric acid) as shown by reaction (22). Dilute solutions of pH between 3 and 4 can be realized by this process, as demonstrated subsequently.

Other transition metal sulphate salts are likely to form in the unsaturated zone of rock wastes, and like melanterite, the salts generally are soluble. They dissolve rapidly on contact with aqueous solutions, and periodic flushing may lead to elevated heavy metal concentrations in mine drainage. Their dissolution may also contribute to acidic drainage by promoting precipitation of oxyhydroxides and carbonates by reactions such as:

$$2CuSO_4 + CO_2 + 3H_2O \rightarrow Cu_2CO_3(OH)_2 + 2H_2SO_4 \quad (23)$$

where copper sulphate salts form through air-oxidation of Cu-bearing sulphides. Similar reactions involving oxidative dissolution of zinc and lead sulphides may lead to precipitation of cerussite ($PbCO_3$), smithsonite ($ZnCO_3$) and/or oxyhydroxides of these metals. Regardless of where the minerals precipitate, acidity in the form of sulphuric acid will be generated.

6.2.2 Quantitative Aspects

The geochemical processes introduced above can be investigated quantitatively using **reaction path** calculations. As an example of this type of calculation, the amount of acidity generated by oxidative dissolution of pyrite can be calculated, and compared with the amount generated by dissolution of melanterite (and precipitation of ferrihydrite) in waste rock piles. We emphasize that reaction path calculations represents a broad class of geochemical modelling, and a variety of computer codes are available to carry out the calculations. The various codes are discussed in the second part of the review.

The concept behind reaction path modelling has been explained previously, but additional detail is required. Reaction path modelling often uses a chemical frame of reference rather a spatial or temporal frame of reference. Reactions associated with oxidative dissolution of pyrite, for example, can be related directly to the amount of pyrite dissolved, using a chemical framework rather than real time or spatial framework. However, if the rate of pyrite dissolution is known, then a real time framework can be substituted in place of the chemical framework (i.e. absolute time is substituted for relative time). The advantage of this approach is that the complexity of chemical reactions can be investigated without large amounts of hydrological/hydrogeological data. Throughout the calculations, all concentrations of aqueous species and amounts of solids dissolved or precipitated are normalized to 1000 g of solvent (H_2O), or alternatively, 1 litre of solution, since all solutions considered here are dilute.

6.3 Oxygenated Rainwater-Sulphide Mineral Reactions

The first reaction path calculation simulates reaction between oxygenated rainwater and pyrite. The calculation provides a baseline against which to evaluate the effects of other reactions that may occur within waste rock piles. The two reactants, rainwater and pyrite, are considered to react as rainwater is flushed through the waste.

The rainwater composition used is representative of precipitation from northern Saskatchewan, where anthropogenic inputs are minimal (Cramer and Smellie, 1994). Rainwater composition can vary widely among different geographical locations across Canada, depending on the vicinity of a location to industrial centres and the direction of provailing atmospheric currents which can carry atmospheric pollutants such as SO_2 and Nox. The pH of this particular rainwater was determined by assuming that atmospheric CO_2 has dissolved in the rainwater to saturation levels, resulting in a pH of 5.67. The amount of oxygen dissolved in rainwater is approximately $8.5x10^{-5}$ M/L at 25°C. With this amount of dissolved oxygen available, a **limiting constituent** calculation requires $4.9x10^{-5}$ M/L of hydrogen ions to be produced through oxidative dissolution of pyrite (reaction 4). The pH of the resulting solution is approximately 4.3 once all oxygen is consumed. Results of the **reaction path** calculation are now considered.

Table 4. Chemical composition of Saskatchewan rainwater

Element	Concentration
K^+	0.5 mg/L
Na^+	0.4 mg/L
Mg^{2+}	0.1 mg/L
Ca^{2+}	0.8 mg/L
Cl^-	0.7 mg/L
SO_4^{2-}	0.8 mg/L
$SiO_{2\,(aq)}$	0.15 mg/L
$O_{2\,(diss)}$	$8.5x10^{-5}$ M/L
pH	5.67

The Saskatchewan rainwater is initially undersaturated with respect to all minerals. As shown in Fig. 4, dissolution of 2.7 mg of pyrite (per litre of solution) decreases the pH to approximately 4.05 while total dissolved sulphur and iron, S(Tot) and Fe(Tot), increase to approximately 1.6 mg/L and 0.54 mg/L respectively. After oxidative dissolution of only $7.5x10^{-6}$ g of pyrite, ferrihydrite saturation is achieved (Fig. 4), and continued pyrite dissolution results in precipitation of approximately 2.0 mg of the hydroxide at the pH minimum. The partial pressure of dissolved oxygen is initially representative of water saturated in atmospheric oxygen ($8.5x10^{-5}$ M/L), but at the pH minimum, most of the dissolved oxygen is consumed and continued pyrite dissolution decreases the partial pressure to approximately 10^{-70} (atm.) at pyrite saturation. The decrease in P_{O2} causes the solution to become undersaturated in ferrihydrite and in response, reductive dissolution of the solid releases Fe to solution, and causes pH to increase.

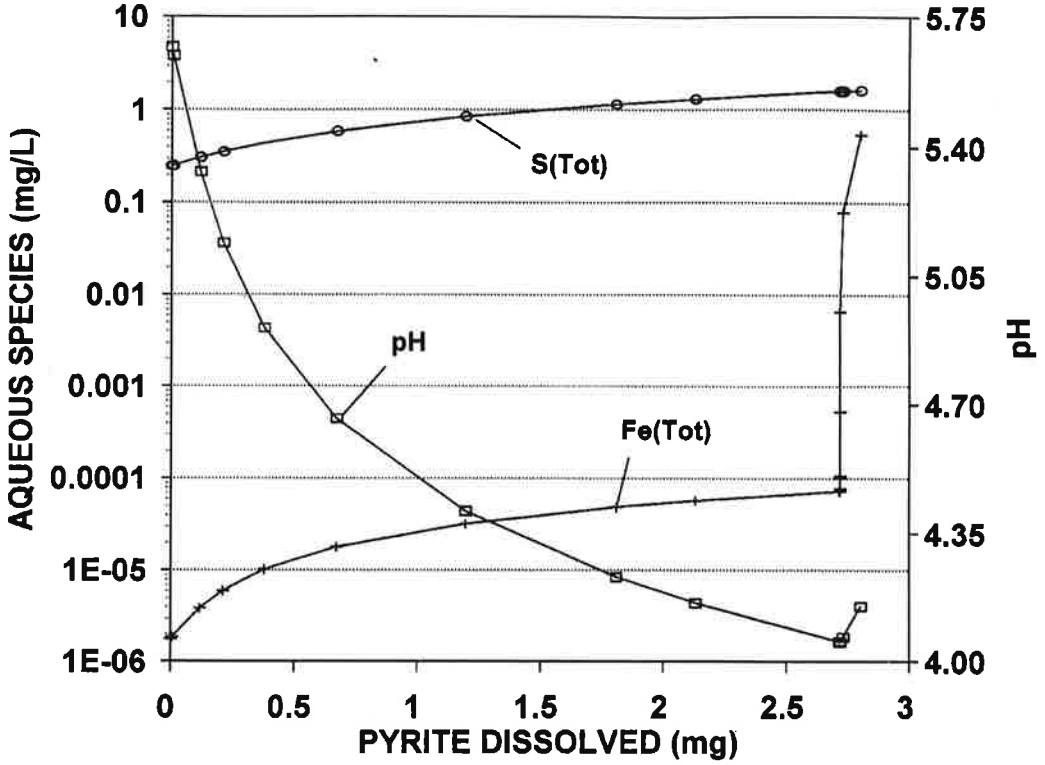

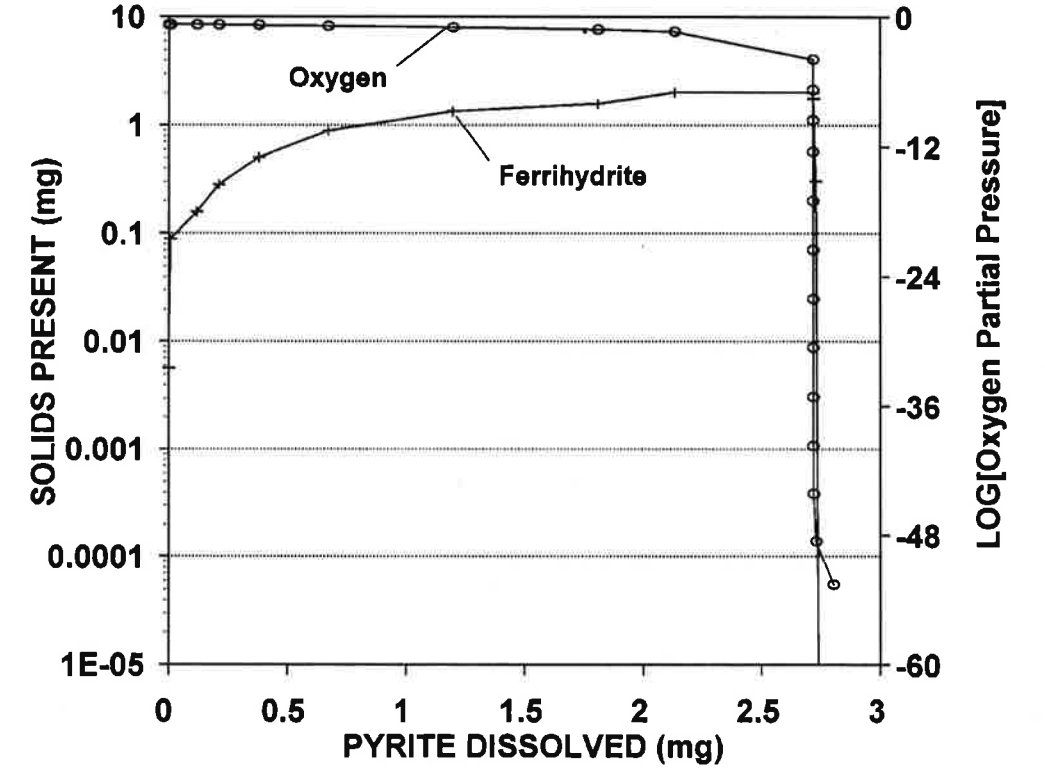

Figure 4. Changes to Solutes, Solids and Gases during Pyrite Dissolution

Rainwater flushed through the unsaturated zone may contact only limited amounts of pyrite; consequently, each volume of rainwater migrating through the zone may dissolve significantly less pyrite than was dissolved in the reaction path calculation. By plotting the reaction path results in chemical space (i.e. the amount of pyrite dissolved as the X-axis of Fig. 4), the consequences of dissolving a smaller amount of pyrite are apparent (Fig. 4). If, for example, just 1 mg of pyrite were dissolved, the pH would be approximately 4.5, Fe(Tot) and S(Tot) would be, respectively, $3x10^{-5}$ mg/L and 0.8 mg/L (2.4 mg/L if represented as SO_4). Approximately 1 mg of ferrihydrite would have formed and the solution would still be close to saturation in O_2. The **reaction path** calculations provide quantitative chemical information, independent of spatial co-ordinates, because the results are related directly to the important reactant species, pyrite. The chemical co-ordinate could equally well have been the dissolved oxygen content of the reacting solution.

Distribution of the major aqueous Fe species, as a function of pyrite dissolution, is illustrated in Fig. 5. These illustrate the changing chemistry of the solution during oxidative dissolution of pyrite. The abrupt increase in Fe(Tot) of Fig. 5 coincides with the onset of reductive dissolution of ferrihydrite. As demonstrated by Fig. 5, the reaction path calculations provide quantitative data on evolution of the solution during reaction. The calculations also provide the mass of minerals dissolved and precipitated as the reaction proceeds.

The basis for the local equilibrium concept, hence reaction path modelling, is that secondary minerals precipitate once saturation is achieved, and equilibrium between the secondary product (e.g. ferrihydrite) and solution is maintained so long as there is sufficient solid present to maintain saturation. For these calculations we consider ferrihydrite to form once saturation is achieved. Other phases such as goethite, FeO(OH), may precipitate in place of ferrihydrite, or there may be no precipitation of Fe(III)-oxyhydroxides. These possibilities all can be modelled.

6.4 Dissolution of Melanterite and Pyrite

Air-oxidation of pyrite occurs in the unsaturated zone, and as discussed previously, oxidized phases such as melanterite are likely to form (reaction 21). The following reaction path calculation considers reaction of both pyrite and melanterite with rainwater saturated in atmospheric oxygen and carbon dioxide. The Saskatchewan rainwater composition, used for previous calculations (Fig. 4), is used here. The solution is considered to react with an excess of pyrite and 100 mg of melanterite ($FeSO_4 \cdot 7H_2O$). Melanterite is soluble and dissolves rapidly in solution; consequently its rate of dissolution is arbitrarily considered to be ten times more rapid than the rate of oxidative dissolution of pyrite. The results of this reaction path calculation are illustrated in Fig. 6.

Comparison of the reaction path results summarized in Figs. 4 and 6 demonstrate that addition of melanterite, as a reactant, has substantial effect on solution composition. Total dissolved sulphur is more abundant, total dissolved Fe is greater, pH is appreciably lower, and the amount of ferrihydrite precipitated is greater (Fig. 6). Dissolution of melanterite supplies Fe to

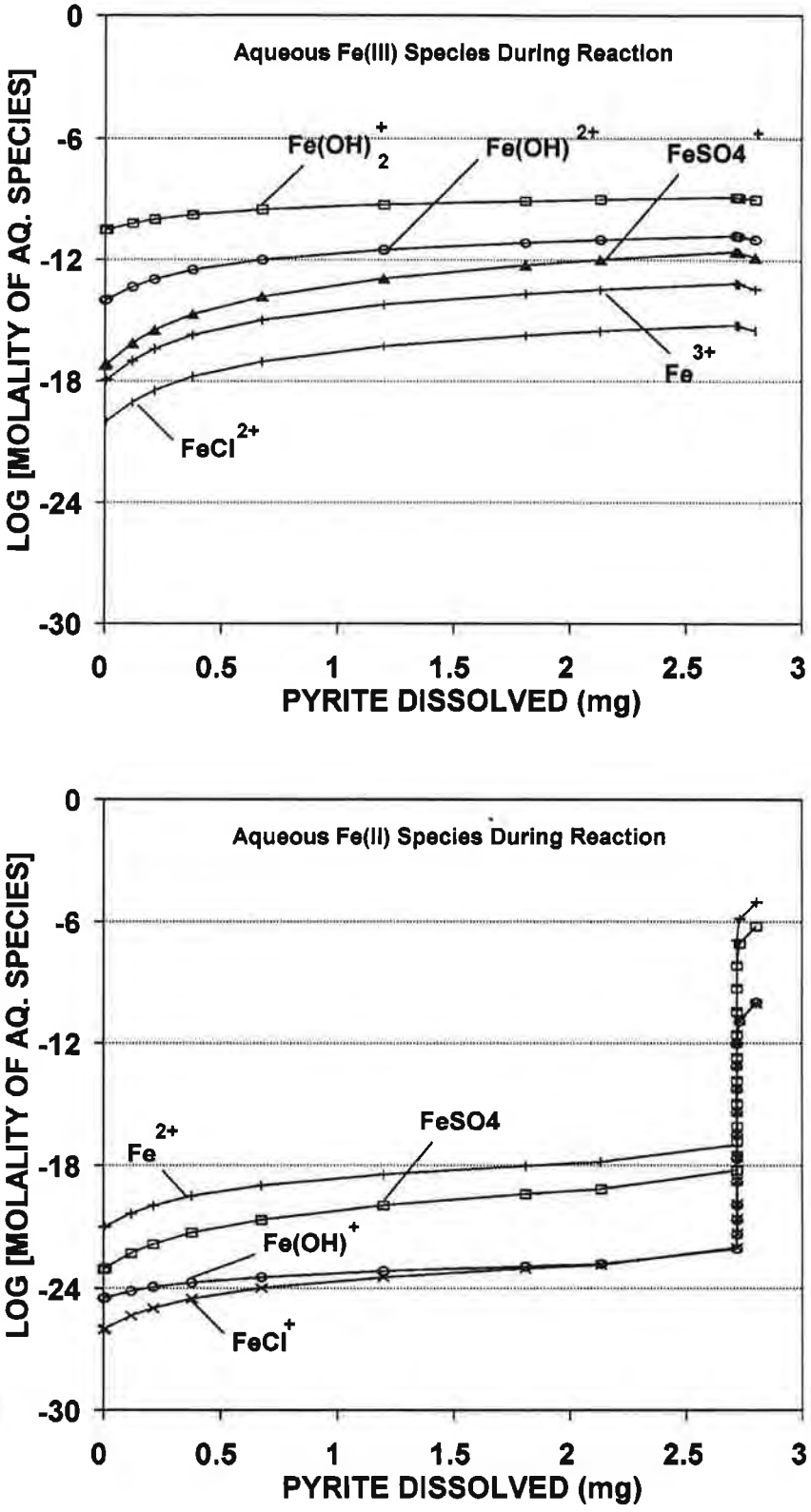

Figure 5. Changes to Aqueous Fe Species during Pyrite Dissolution

solution in addition to that supplied by oxidative dissolution of pyrite. As a result, greater amounts of ferrihydrite are precipitated and more acidity is produced (reaction 21, Fig. 6). Similar results are obtained if goethite precipitates in place of ferrihydrite. The pH is not only lower than for the air-oxidized pyrite calculation (Fig. 4), but it decreases more rapidly with respect to the amount of pyrite dissolved. As shown by Fig. 4, the pH of the solution is approximately 4.5 after dissolution of 1 mg of pyrite. With melanterite added as a reactant (Fig. 6), the pH is approximately 3.7, after dissolution of 1 mg of pyrite.

Ferrihydrite precipitates as melanterite is dissolved (Fig. 6), but at the point where approximately 1.6 mg of pyrite has dissolved, the amount of ferrihydrite present reaches a maximum, then decreases with continued reaction. Oxygen is effectively consumed at the maximum in precipitated ferrihydrite. Beyond the maximum, ferrihydrite undergoes reductive dissolution, as the system is driven towards progressively more reducing conditions by dissolution of melanterite and pyrite. The increase in pH, after the pH minimum, is a response to reductive dissolution of ferrihydrite. The dramatic increase in Fe(Tot) results from reductive dissolution of ferrihydrite and continued dissolution of melanterite and pyrite.

It is apparent from the calculations summarized in Figs. 4 and 6 that the nature and abundance of secondary reaction products, here melanterite and ferrihydrite, have a fundamentally important effect on acidity of solution, and well may be considered a major control on pH of solutions percolating through the unsaturated zone of waste rock piles. The calculation also demonstrates that there is little likelihood to predict accurately acid mine drainage properties without being able to predict the secondary mineral assemblages formed in rock wastes.

The above calculations of net acid production applicable only for the conditions stipulated. The calculations can be extended to include a wide range of reactant and product minerals. This type of predictive net acid production may be useful to predict AMD, provided that care is taken to properly constrain the initial conditions. However, the intent here is to identify the geochemical processes that may affect rock wastes and emphasis on applications to net acid production are not pursued.

6.5 Other Minerals

Pyrite is the only primary mineral considered in the previous calculations. Effects of other minerals such as other sulphides, carbonates and silicates also can be considered by including them as reactants in the reaction path calculations. However, only a few illuminating examples are presented here; it is impractical to address the multitude of possible assemblages that may exist in waste rock piles.

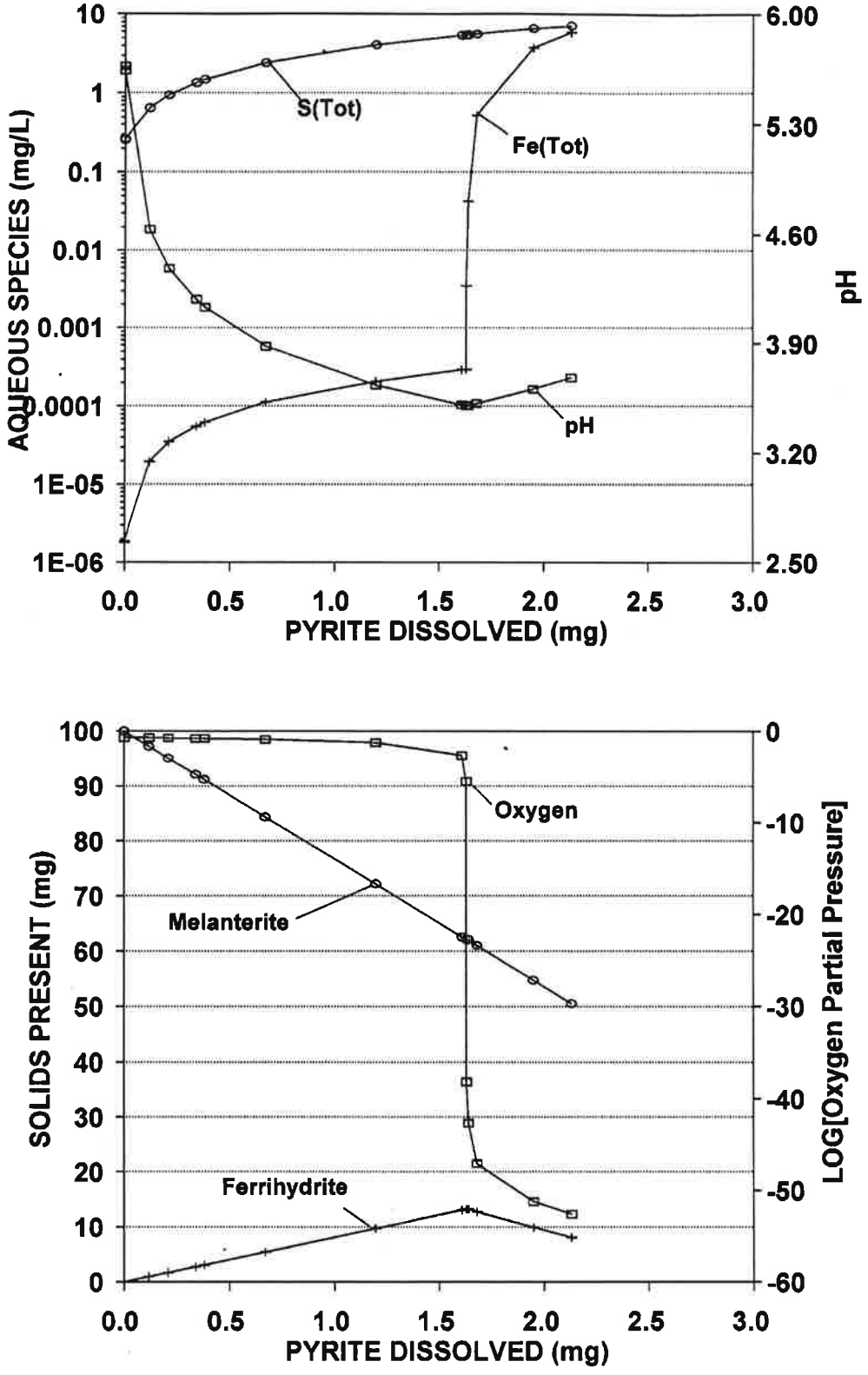

Figure 6. Changes to Constituents during Pyrite & Melanterite Dissolution

6.5.1 Pyrrhotite

Pyrrhotite is a common mineral of waste rock and a calculation is performed assuming that pyrite, pyrrhotite and melanterite are present in the ratio 60:10:1. As well, pyrrhotite is considered to dissolve twice as fast as pyrite and melanterite 10 times more rapidly than pyrite. These minerals are reacted with the O_2-saturated rainwater used in previous calculations and the results are shown in Fig. 7.

Fe(T), S(T) and pH are similar to those obtained for melanterite plus pyrite dissolution (Fig. 6), demonstrating that inclusion of pyrrhotite as reactant, alters the resulting solutions minimally (compare Figs. 6 and 7). The explanation is that melanterite, with its rapid dissolution rate dominates dissolved Fe(Tot), S(Tot), pH and P_{O2} .

The reaction path calculation involving pyrrhotite may not reflect natural processes as closely as does the pyrite-melanterite calculation (Fig. 6) because the alteration products of pyrrhotite are more complex and the process of alteration is different (Pratt et al., 1994a).

6.5.2 Arsenopyrite

The secondary oxidation products of arsenopyrite have been studied by Buckley and Walker (1988), Richardson and Vaughan (1989) and Nesbitt et al. (1993). Buckley and Walker (1988) argue that arsenic is oxidized more rapidly than Fe(II) of arsenopyrite, and that sulphur is not affected by oxidation during 7 days of air-oxidation. They suggest.that Fe(III)-oxides, Fe(III) arsenites or Fe(III) arsenates form. Nesbitt et al. (1993) observe Fe(III), As(III), As(V) and an abundance of OH^- relative to O^{2-} on arsenopyrite surface oxidized in air for 25 hours. The data suggest that Fe(III)-oxides, Fe(III)-arsenites, Fe(III)-arsenates, as well as H_3AsO_3 and H_3AsO_4 form on the surfaces of air-oxidized arsenopyrite. Scorodite ($FeAsO_4 \cdot 7H_2O$) is a secondary product of oxidized mine wastes containing arsenopyrite (Dove and Rimstidt, 1985). Dissolution of these Fe-As-bearing salts may generate As-bearing acids in arsenopyrite-bearing wastes during infiltration:

$$FeAsO_4 \cdot 7H_2O \rightarrow Fe(OH)_3 + H_3AsO_4 + 4H_2O \qquad (24)$$

Field studies and laboratory studies of oxidation of arsenopyrite are required to properly model oxidative dissolution of arsenopyrite. There are few kinetics data available for arsenopyrite (Appendix B) and the dissolution mechanism is uncertain. Furthermore, uncertainty of the thermodynamic data for scorodite, and some of the arsenic aqueous species, precludes meaningful reaction path calculations of oxidative dissolution of arsenopyrite.

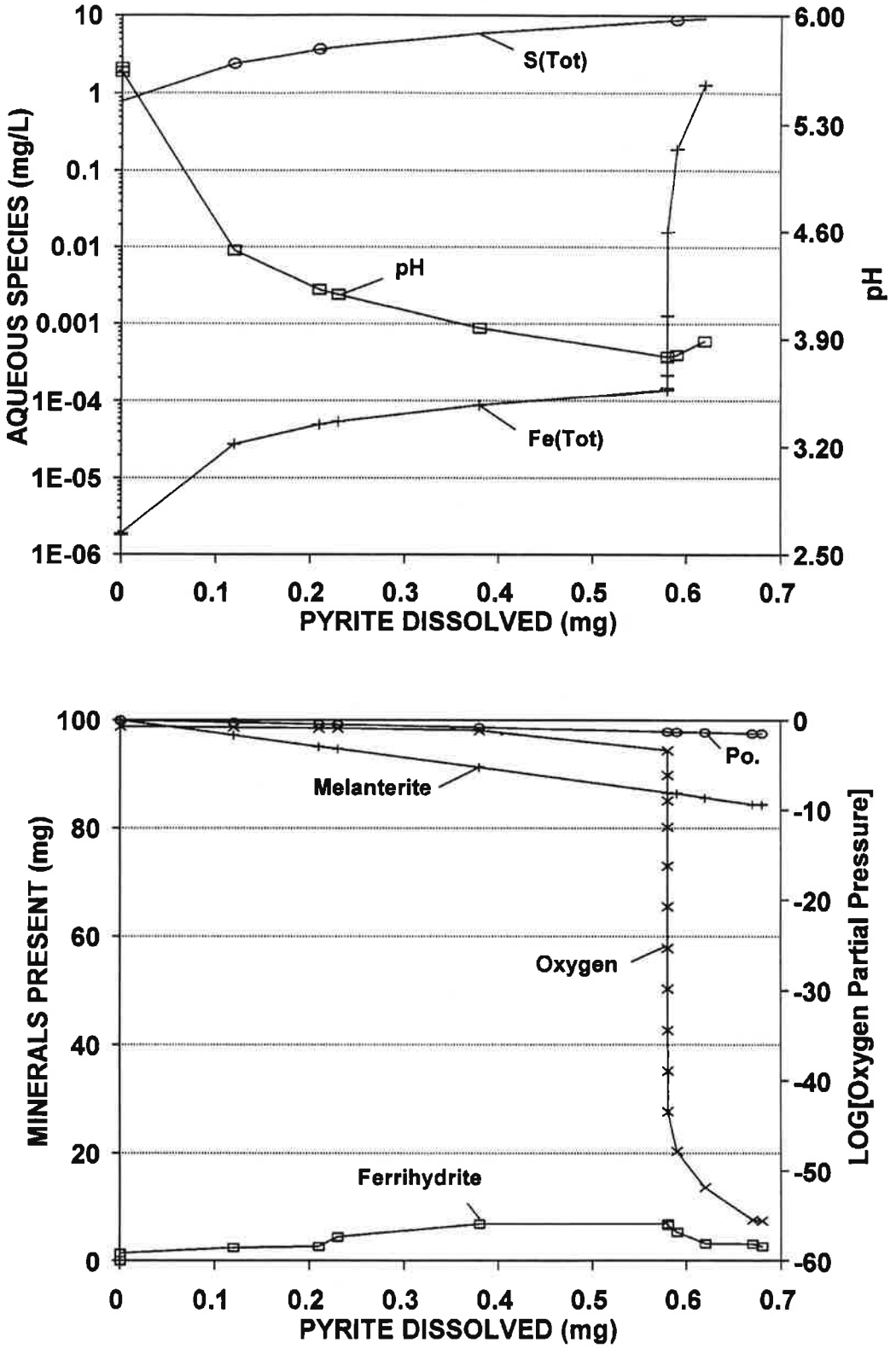

Figure 7. Changes to Constituents during Py., Po. & Melanterite Dissolution

6.5.3 Other Sulphides

A wide range of sulphide minerals, including galena, sphalerite and chalcopyrite, occur in waste rock and may contribute to acidic drainage, as well as to elevated heavy metals contents of drainage. A few generalizations about the behaviour of sulphide minerals can be made.

Berner argues that dissolution of highly insoluble minerals are controlled by surface reaction processes (Table 3). Rates of dissolution of sulphides such as arsenopyrite, galena and sphalerite, which are sparingly soluble in reducing conditions, should be controlled by surface reaction processes, as is pyrite (M^{c}Kibben and Barnes, 1986). Rate of oxidation of sulphides that display significant non-stoichiometry, and contain appreciable vacancies, may be controlled by diffusion through the bulk mineral, as is the oxidation of pyrrhotite (Pratt et al., 1994a). Rates of dissolution of soluble sulphide minerals and sulphosalts probably will be controlled by diffusion of solutes through the stagnant water layer. These generalizations should be verified for individual minerals.

6.5.4 Feldspars

Surface analytical studies demonstrate that an amorphous siliceous layer forms on feldspar surfaces leached by mineral acids (Casey et al., 1988; Muir et al., 1988, 1990; Nesbitt et al., 1991; Muir and Nesbitt, 1991, 1992). Nesbitt et al. (1991) demonstrate that addition of 1 mg/L of alkali, alkaline earth and Al-bearing salts to the acidic leaching solutions decreases the thickness of the leached layer to less than 70 Å. These findings confirm the XPS surface studies of Petrovic et al. (1976) who note that leached layers on feldspar were less than 10-20 Å thick. With no substantial leached layer to control reaction rates (via diffusion), dissolution of feldspars is surface-reaction controlled (Berner and Holdren, 1977; Berner, 1978; Holdren and Berner, 1979; Berner and Holdren, 1979), as predicted from is low solubility (Table 3, Berner, 1981).

Surface reactions are complex and rates of dissolution may vary greatly depending upon the nature of the dissolved species present in solution. Recognition that feldspar dissolution rates are controlled by surface reactions has lead to the study of the effects of various aqueous species on feldspar dissolution rates (Murphy and Helgeson, 1987; Amrhein and Suarez, 1988; Blum and Lasaga, 1988). The comparatively new field of "surface complexation theory" has grown rapidly in recognition of the fundamentally important role that aqueous species have on rates of dissolution (see reviews by Davis and Kent, 1990 and Stumm and Wollast, 1990).

Plagioclase and K-feldspar (microcline and orthoclase) are common in waste rock and their presence can have significant effect on water quality. They do not react with air as do sulphide minerals because feldspars contain no elements that undergo redox reactions in natural settings. As a result, they are reactive towards aqueous solutions only, in which they may dissolve slowly. The rates of feldspar dissolution are known, although rates of precipitation are unknown (Appendix A). Their effect is primarily to neutralize dissolved acids, as indicated by reactions (12), (13) and (20).

The plagioclase solid solution series ranges from albite to anorthite composition and the reactivity of the mineral varies depending upon composition (Casey et al., 1991). Albite, the sodic component of the series, is used in the following reaction path calculation.

The reaction considered is dissolution of pyrite and albite in Saskatchewan rainwater saturated in atmospheric oxygen and carbon dioxide. It is therefore identical to the reaction shown in Fig. 4. except that albite has been included as a reactant. The rates at which feldspars dissolve are dependent to great extent upon the pH of the leachant (Murphy and Helgeson, 1987; Stillings et al., 1992). Compared with most sulphides, the rates are slow (Casey et al., 1992; McKibben and Barnes, 1986), hence albite is considered to react with solution at the same rates as pyrite in the following calculation. The results are illustrated in Fig. 8.

The results of including albite as a reactant with pyrite are emphasized by comparing Figs. 4 and 8. The amount of pyrite dissolved in both calculations is similar as is total dissolved sulphur[S(Tot)] in both runs. The pH of the solution is greater where albite is present as a reactant (pH $\approx$ 4.43 compared with pH $\approx$ 4.05 in Fig. 4). Total dissolved iron is appreciably lower and the amount of ferrihydrite precipitated is greater in the calculation where albite is present as a reactant. The differences, pH, Fe(Tot) and amount of ferrihydrite precipitated, result primarily from neutralization of sulphuric acid by dissolution of albite (reaction 12). In response to albite dissolution, Al(aq) and SiO_2(aq) increase in solution leading to precipitation of gibbsite, followed by precipitation of kaolinite. Precipitation of these secondary Al-bearing phases counters the acid neutralization effects of albite dissolution (compare reaction 12 with 20).

The combined effects of albite dissolution and precipitation of secondary Al-bearing phases is insufficient to neutralize all the acid generated by oxidative dissolution of pyrite. Only if there were a large amount of albite present (large surface area exposed to solutions) or if the reaction rate of albite were significantly greater than that of pyrite could all the acid produced be neutralized by albite dissolution. These calculations demonstrate clearly that accurate prediction of the neutralizing effects of albite (and other Al-silicates) in rock wastes can be evaluated accurately only if the amounts of Al-silicate minerals present in the waste are known, and if the dissolution rates are known.

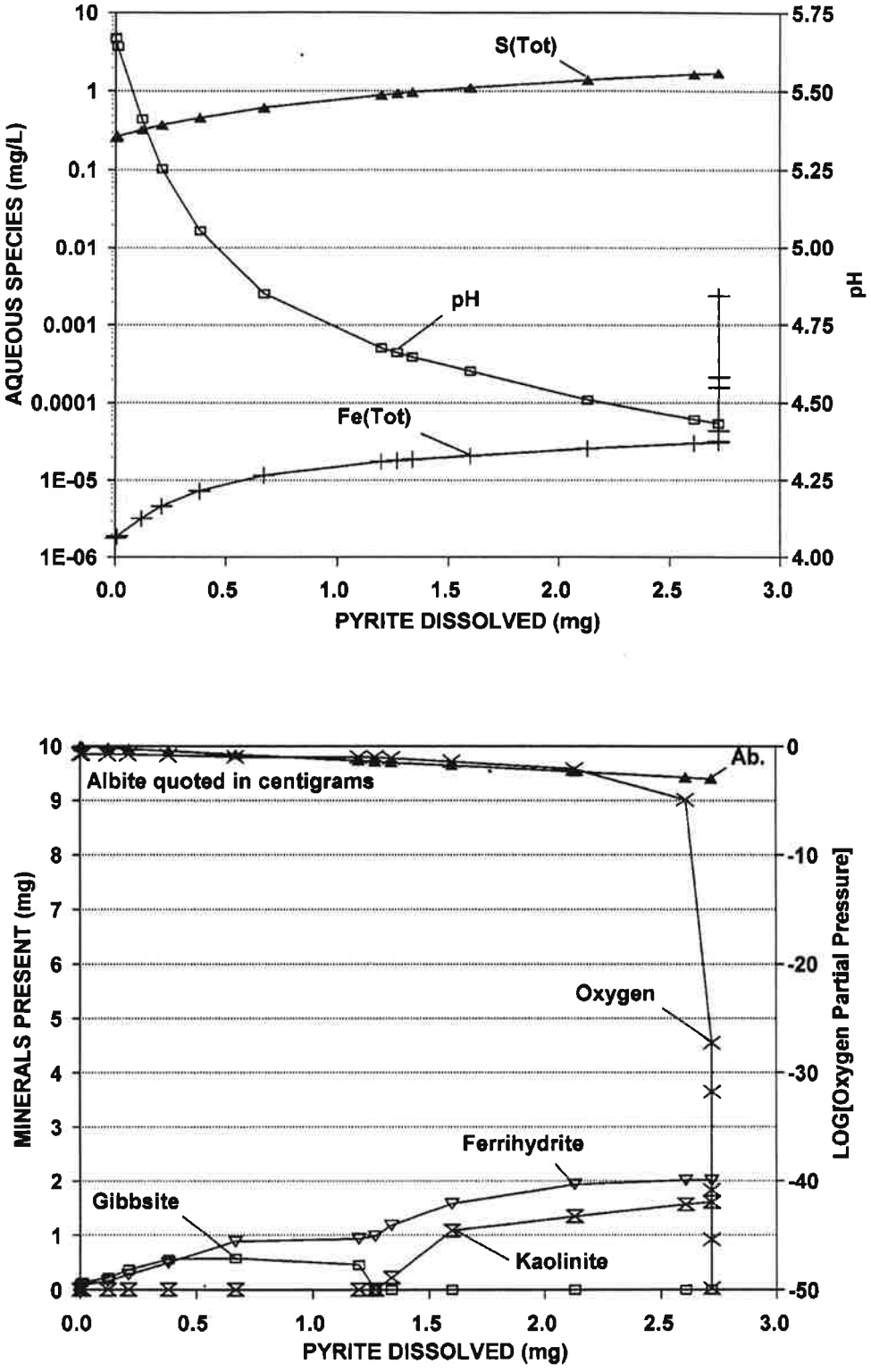

Figure 8. Changes to Constituents during Pyrite and Albite Dissolution

6.5.5 Other Silicate Minerals

Like albite, dissolution of most common Al- silicate minerals are controlled by surface reactions, and as for feldspars (Amrhein and Suarez, 1988), surface complexation is critical to their dissolution rate. Mafic and clay mineral dissolution rates may be greater than dissolution rates of feldspars, and they may be more effective neutralizing agents than the feldspars. As well, mafic minerals such as pyroxenes, amphiboles and biotite, contain trace metals which may be released to solution during dissolution, thus contributing to the heavy metal content of waters draining waste rock piles. References to data for Al-silicates are presented in Appendix A.

6.5.6 Calcite

Berner (1978) demonstrates that calcite dissolution is diffusion-controlled in solutions of pH less than four, but surface reaction-controlled in solutions of pH six and greater. Talman et al. (1990) incorporate calcite reaction kinetics in acidic, near-neutral and basic solutions into one rate equation, and from it the rate of calcite dissolution can be calculated for any pH condition. Rate equations for calcite and pyrite indicate that in oxidizing, acidic to near-neutral solutions, calcite dissolution is more rapid than oxidative dissolution of pyrite (Talman et al., 1990; M^{c}Kibben and Barnes, 1986), and a reaction path calculation is performed where calcite dissolves twice as fast as pyrite in Saskatchewan rainwater, saturated in both O_2 and CO_2. The results are shown in Fig. 9.

Comparison of these results with those shown in Fig. 4 (where only pyrite dissolves) demonstrates the dramatic effect of calcite on solution pH. Whereas a minimum pH of 4.1 is achieved in Fig. 4, the minimum is 5.4 in Fig. 9. The dissolution rate of calcite increases substantially with decreased pH; consequently, more rapid dissolution of calcite may lead to pH values greater than the value of 5.4 obtained by this reaction path calculation.

The total dissolved sulphur [S(Tot)] for both runs is similar but the Fe(Tot) is appreciably lower where calcite dissolves (compare Fig. 9 with Fig. 4). Other aspects of the two calculations are similar. The calculations demonstrate the dramatic effect that calcite has on drainage from mine wastes.

6.5.7 Other Carbonate Minerals

Dolomite ($CaMgCO_3$) is a common carbonate mineral. It generally is much less reactive than calcite and its dissolution reaction kinetics are more uncertain (Garrels et al., 1960). Like the feldspar minerals, dolomite is a base (solid) and has potential to neutralize acids, but a low dissolution rate impedes its effectiveness to neutralize acids.

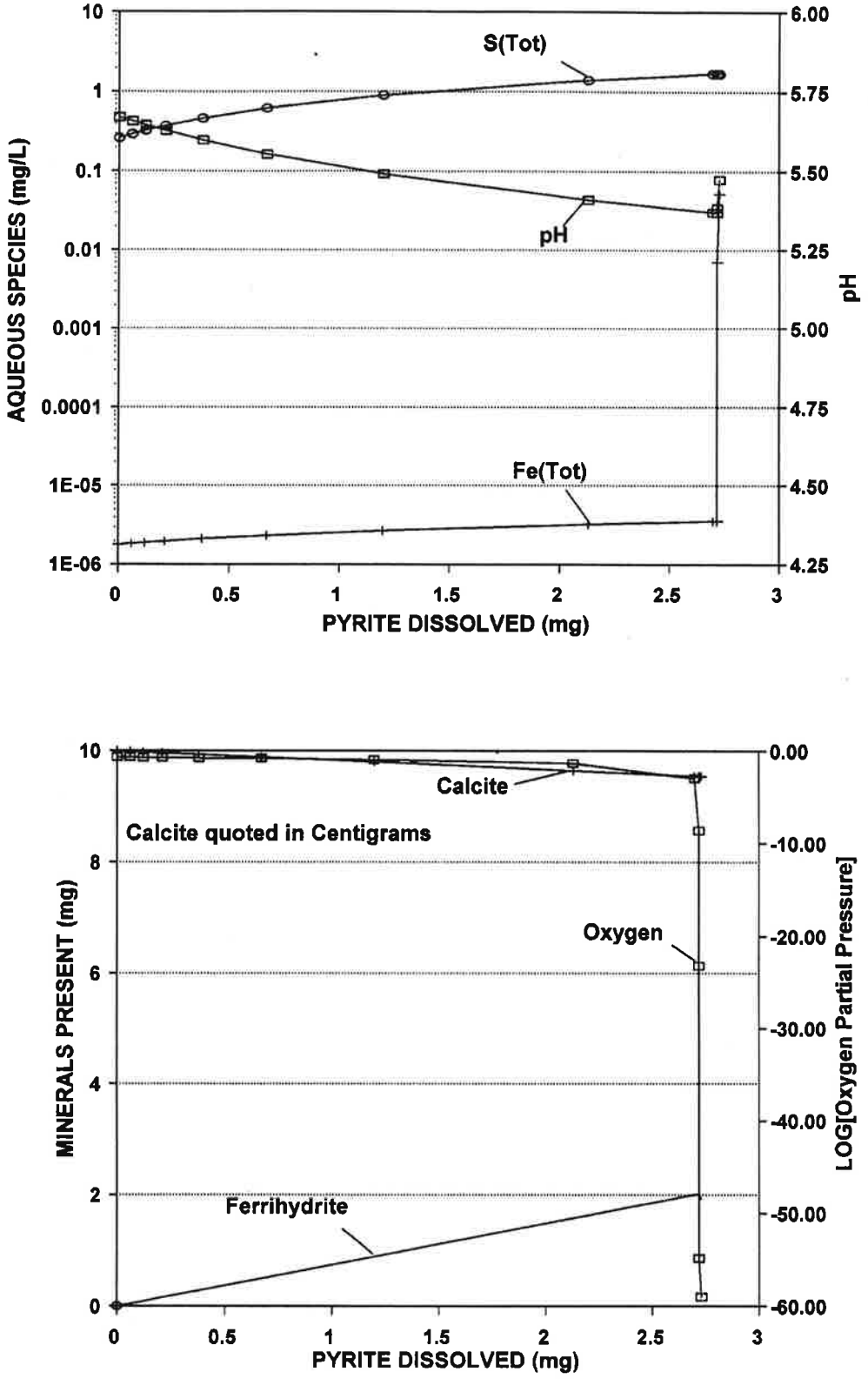

Figure 9. Changes to Constituents during Pyrite and Calcite Dissolution

Siderite ($FeCO_3$) is another carbonate mineral common in some waste rock piles. It contains Fe in the reduced state. Its dissolution, while neutralizing acid, also consumes oxidants such as oxygen. Its solubility has been investigated recently (Bruno et al., 1992) and kinetics of siderite dissolution are now being studied by the same group. Fe(III)-oxyhydroxides are likely to precipitate at the solution-siderite interface where the effective pH may remain high due to dissolution of the carbonate. Precipitation may produce an oxyhydroxide coating, and the effectiveness of siderite to neutralize acids may therefore be limited by its isolation from solution. Study of siderite dissolution characteristics in mine wastes is required to better understand its role in neutralization of acids.

6.5.8 Oxide and Hydroxide Minerals

Oxides, hydroxides and carbonates of many transition metals, such those of Mn, Zn, Pb Cu, are often found in mine wastes. Some of these minerals may be important at certain mine waste sites while inconsequential at others. Because of their specificity to mine sites, their abundance (hence importance) must be evaluated at individual mine sites from knowledge of regional and local geology, mineralogy, climatology, and so on, although detailed information about individual waste rock piles may be unnecessary. The following discussion concentrates on the metal oxides and hydroxides more important to acid generation from waste rock piles: those of Fe, Al and Mn.

Oxides and hydroxide minerals are involved in several important geochemical processes: acid generation, pH buffering, and redox buffering. Precipitation of Fe^{3+} and Al^{3+} released from sulfide and silicate weathering as hydroxides or oxyhydroxides contributes to acid generation from waste rock piles. Precipitation of Fe^{3+} and Al^{3+} on carbonate minerals can reduce or curtail these minerals' availability to neutralizing acid, as observed at several Canadian sites. Precipitation of Fe^{3+} and Al^{3} on the surfaces of actively oxidizing sulphide particles is less likely, since at the low pH characteristic of the microenvironment of such oxidizing sulphide particles, Fe^{3+} and Al^{3+} are usually soluble.

Oxides and hydroxides of Fe^{3+} and Al^{3+} can, on the other hand, provide buffering capacity to prevent pH from dropping infinitely. If severe sulphide oxidation occurs in a waste dump, the pH of the drainage tends to drop significantly below neutral levels once carbonate minerals are depleted or become unavailable. The pH decrease is resisted by the dissolution of iron and aluminum hydroxides, because these dissolution reactions are acid-consuming. The drainage pH is buffered at around pH 4.5 before aluminum hydroxide is exhausted and at around pH 3.0 before ferric hydroxide is depleted. The buffering hydroxides may be secondary minerals precipitated during early stages of acid generation, or they may be a part of the original mineralogy. It is only after the buffering capacity of these ferric and aluminum hydroxides is depleted that the drainage pH can drop well below pH 2.5. It should be noted that, although the dissolution of iron and aluminum hydroxides buffers the pH, it does not reduce the total acidity of the drainage.

The presence of iron hydroxide and manganese oxide can buffer the redox potential at the groundwater table/waste rock interface if it exists. Because of limited oxygen supply and organic decomposition, the ground water within a waste rock dump tends to become reducing. The reduction of Fe^{3+} (as ferric hydroxide) to soluble Fe^{2+} and of Mn^{4+} (as MnO_2 particles) to soluble Mn^{2+} will resist

the decrease of redox potential, maintaining the Eh at specific levels until the oxidized species are exhausted. This generates two adverse environmental effects: First, the dissolution of $Fe(OH)_3$ and MnO_2 may release all the trace metals which had co-precipitated with them, degrading the groundwater quality. The trace metal-scavenging ability of $Fe(OH)_3$ and MnO_2 have been well documented. Second, the buffering of redox potential by $Fe(OH)_3$ and MnO_2 will maintain the Eh well above the range where sulphate reducing bacteria can thrive, deterring the potential benefits arising from sulphate reduction.

6.6 Reaction Progress, Reaction Rate and Hydrogeology

Changes to solution composition shown in Figs. 4-9 are plotted as a function of the amount of pyrite dissolved. The amount of pyrite dissolved, however, can be related directly to time, provided an appropriate rate equation is available for pyrite dissolution. Once changes to solution composition are correlated with time rather than amount of pyrite dissolved, the reaction path calculations can be correlated directly with hydrogeological models (through time). The correlation will be accurate wherever pyrite is available to react, and provided that the amount of secondary products formed are not sufficient to significantly alter the porosity and permeability of the rock waste. Conversion from "pyrite dissolved" co-ordinates (Fig. 4) to time is performed as follows.

M^{c}Kibben and Barnes (1986) give rate laws in moderately acidic solutions (Appendix B), which are closest to the conditions for which the reaction path calculations were performed. We emphasize, however, that there are no detailed rate studies that provide a rate equation applicable to the entire range of conditions covered by the reaction path results.

The conversion to time (in days), using the rate equations of M^{c}Kibben and Barnes, is illustrated in Fig. 10. This figure is entirely analogous to Fig. 4 except that the amount of "time" required to dissolve pyrite has been plotted on abscissa in place of "pyrite dissolved". The conversion requires the concentrations of H^+, Fe^{3+} and dissolved oxygen in solution during each stage of the reaction. Fortunately, the reaction path calculation provides these data, and the changing concentrations of these species are included in the calculation of time.

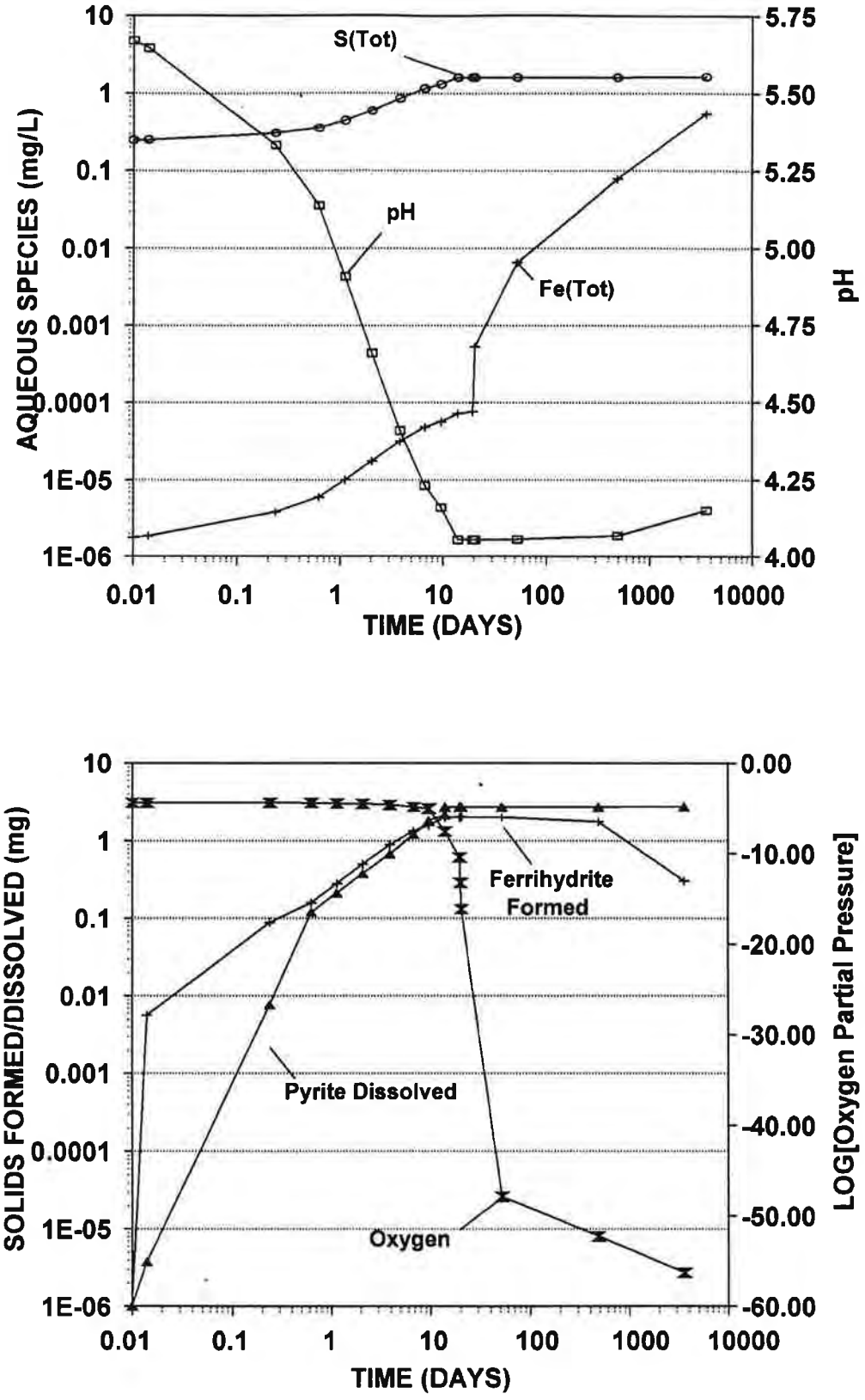

Figure 10. The Data of Fig. 4. shown as a Function of Time.

As shown on Fig. 10, the amount of pyrite dissolved (with respect to time) follows three approximately straight-line segments. These segments correspond to distinct processes controlling rate of dissolution. The initial, steep trend (from zero time to 0.7 days) is controlled by the amount of dissolved oxygen in solution. As the reaction proceeds, H^+ increases in solution. Since the rate of dissolution of pyrite is inversely proportional to $\sqrt{H^+}$, as H^+ increases in solution between 0.7 days and 11 days, the pyrite dissolution rate decreases. Once pH reaches a minimum and is maintained at approximately 4.05, the rate of dissolution is effectively constant, yielding the last, "flat" segment of the pyrite dissolution curve (between 11 and 3000 days). These calculations demonstrate clearly that dissolved oxygen and pH have the greatest control on pyrite dissolution for this particular reaction path calculation.

The time conversion was performed assuming that one litre of Saskatchewan rainwater saturated in atmospheric oxygen and carbon dioxide reacted with pyrite with a surface area of 1 cm^2. The actual mass of pyrite depends on its grain size. Here we consider dissolution of only 3 mg of pyrite.

Conversion to time co-ordinate permits linkage of reaction path calculations with hydrogeological modelling. Time-travel curves obtained from hydrological calculations, coupled with these reaction path calculations, permits accurate estimation of the location (along flow paths) where the bulk of the pyrite is dissolved, the location where pH reaches critical values (with regards to bacterial activity) and where waters are finally depleted of their dissolved oxygen. These aspects are all vital to accurate prediction of acid mine drainage.

7. MODEL INPUT PARAMETERS

7.1 Field and Laboratory Data

7.1.1 Water Chemistry

Geochemical models use water chemistry data to yield information on which of all the possible reactions have occurred. The chemical composition of water in contact with solids also provides a target or endpoint that some geochemical models try to reach. Because of this, the chemical analyses must be sufficiently accurate to exclude the possibility of missing constituents. Generally, this is not so for ARD analyses. Morin (1991), in a study using duplicate water samples and different commercial laboratories, has shown the poor precision of chemical analyses of acid mine drainage. More care must be taken in the planning, execution and evaluation of the water analyses than has been done in the past. Charge balance can be used to detect the possibility of missing constituents, but can only identify major missing components. Trace constituents will not affect the charge balance significantly, but can significantly affect reactions with the solids and gases.

Water chemistry analyses to be used for geochemical modelling should include acidity and alkalinity, pH, metals (Cu, Fe, Zn, Pb, Mn, Cd ...) and sulphate (SO_4) concentrations, major cations (Ca, Mg, K, Na, ...), other anions (Cl, S ...), Eh and a redox pair (Fe(II)/Fe(III)). Commonly missing from acid mine water analyses are total inorganic carbon (TIC) and dissolved silica (SiO_2); these are indicators of the activities of mineral families, such as carbonates and aluminosilicates, which are important in neutralizing acids formed by oxidation of sulphide minerals.

Water samples to be analyzed should always be filtered. The filtering of iron-rich waters can influence the water analysis. Laxer and Chandler (1982) have shown that Fe(III) colloids will pass through 0.45 micron filter paper, thus contributing to the "dissolved" iron. They recommend using a filter finer than 0.1 micron to prevent this.

7.1.2 Mineralogy

Knowledge of the mineralogy in a waste rock pile is essential to geochemical predictions. It has been established, both experimentally and from field observation, that different sulphide minerals have different rates of dissolution (Kwong, 1993; Rimstidt et al., 1994). Equally important are mineral phases that can neutralize the produced acid (Blowes and Ptacek, 1994). The most important acid-consuming minerals are the common carbonate minerals (calcite, dolomite and siderite). Silicate minerals are less important because of their slower reaction rates.

Primary sulphide minerals often contain impurities released to the environment when the sulphide minerals are oxidized. For example, Jambor (1994) lists sphalerite a source of Cd, pyrite and pyrrhotite as sources of Ni and Co, and magnetite for Cr. Consequently, knowledge of trace element mineralogy is necessary to accurately predict metal releases to acid mine drainage.

As emphasized earlier in this report, formation of secondary minerals is also important in geochemical predictions. Several of these secondary minerals have been found in tailings (Alpers et

al., 1994; Jambor, 1994) and we would expect them to also form in waste rock. Secondary minerals can control the trace metal levels in the aqueous phase, can contribute to neutralization, can promote co-precipitation and adsorption, and can control the TDS levels by precipitation and redissolution. Determination of which secondary mineral phases are present is very useful, but not always feasible in waste rock due to the small occurrence of these minerals relative to primary minerals and to their amorphous characteristics. Secondary mineralogy should only be determined as much as practically possible. Lack of data can be compensated by assumptions from the interpretation of water chemistry measurements, from data obtained on other typical field sites, or from geochemical predictions based on primary mineralogical data.

7.1.3 Exposed Surface Area and Grain Contact

Surface area is one of the most difficult parameters to estimate. Methods of measurement range from sieve analysis to nitrogen adsorption (i.e. BET). Surface area estimates can vary by a factor of one hundred among different methods (White and Peterson, 1990). The problem is partly one of scale due to surface roughness and the difficulty in differentiating the surfaces of adjacent minerals. As specific surface area is considered directly proportional to rates of reaction per unit mass, incorrect assumptions about specific surface area can have devastating effects on the estimation of acid generation rates.

Ion exchange and sorption also depend on specific surface area. As discussed earlier in this report, it is considered less important in waste rock piles as it is overshadowed by the large amount of mineral dissolution, precipitation, and co-precipitation. Exposed surface area and grain contacts are also important to quantify galvanic effects, which depend on sulphide mineral pairs being in intimate contact. Whether it is an important rate mechanism in waste rock piles has not been investigated.

7.1.4 Temperature

Sulphide oxidation is an exothermic process and, depending upon the reaction rate, can heat up the surrounding material. Temperature must be specified to make any thermodynamic calculations. Fortunately, some measurements of temperature distributions in rock piles exist and many computer programs to estimate the temperature variation in a rock pile have been developed (for example, Pantelis and Ritchie, 1991a). For practical geochemical modelling, the extreme temperature limits for waste rock piles are 0°C and 100 C, the freezing and boiling points of water, respectively, at atmospheric pressure. At these temperatures, an error of 5°C should not result in significant variations in the geochemical modelling calculations. However, we recommend that modellers do a temperature sensitivity analysis for their specific problems, particularly where the potential of bacterial catalysis exists.

7.1.5 Oxygen Availability

The availability of oxygen is critical to acid generation in waste rock dumps. The supply of oxygen to the interior of a pile is mostly through gaseous diffusion and advection. Gaseous advection in waste rock piles can occur by three mechanisms: wind advection, thermal advection and barometric pumping (Morin et al., 1991). For geochemical modelling, a means is needed to couple the physical

transport of oxygen to the aqueous oxidation site. Once the rate of supply of oxygen is determined, it is input into the rate equation for sulphide oxidation.

Oxygen availability may limit the rate of sulphide oxidation in waste rock dumps, as summarized by Ritchie (1994). However, oxygen availability does not influence precipitation and dissolution, the process that most directly influences dissolved metal production.

7.1.6 Water Availability

As shown in the above discussion, two-phase flow is important in waste rock piles. Perhaps even more important is the large vadose zone that exists partly because of the large size of the particles making up the pile, creating a dual permeability network concentrating flow in channels of high hydraulic conductivity and around any finer grained matrix of low hydraulic conductivity. This has been represented conceptually by Broughton and Robertson (1991) as "flow path reactors" and "local reactors", and is referred to as "channelling" and "stratification" in the MEND review by Morin et al. (1991).

In addition to the importance of the buffering of the water by oxygen, the water-rock or water-mineral ratio is important. In the unsaturated zone this ratio changes continually, ranging from near-saturation during flushing events caused by rainstorms to near residual water content during dryer periods between rain events when evaporation occurs. The water content of the waste rock pile is an important physical modelling component which must be linked to the geochemistry. In the saturated zone, oxidation and evaporation events disappear, but neutralization processes can continue. There, the rate of flow must be linked to the rate of geochemical processes taking place to properly evaluate the extent of neutralization before the water escapes from the waste rock pile.

The water balance is very important, and all physical processes which control the entry of water to a pile must be accounted for reliable prediction of water quality. Physical processes are excluded from the scope of this review. The following statement is useful to differentiate geochemical processes from physical processes: *geochemistry concerns the reactions between gases, water and minerals, while physics concerns the supply, mixing, and outflow of the gases, water and minerals.*

7.1.7 Waste Rock Pile Structure and Composition

The waste rock pile structure has a major impact on the flow paths which influence the location of major acid generation sites within the pile. The waste rock pile structure is controlled by the construction method and the waste rock size. Formation of secondary structures due to physical faulting or geochemical formation of a hardpan layer (e.g. such as at the Heath Steele Mines; Boorman and Watson, 1976) can alter the hydraulic conductivity of the pile by forming conduits for, or barriers to, flow. Transport of fine particles by migrating water may also be important in altering hydraulic conductivity.

The composition of waste rock dumps depends on the mining sequence. For example, at the south dump at Mine Doyon, Gélinas et al. (1991) found that different portions of the dump were dominated by distinct rock types. They report a global composition of the dump of approximately 50%

sericite schists, 25% silica volcanoclastics and 25% intermediate igneous rocks. Both the structure and the composition of a dump need to be known for proper, comprehensive modelling.

7.1.8 Laboratory Prediction Tests

A number of laboratory procedures have been used to simulate the production of ARD, and have been described in detail by a number of authors (Broughton and Robertson, 1991; Coastech Research Inc., 1989). "Static" tests are used to estimate the total capacity of a sample to generate acid, assuming total reaction of oxidizing and neutralizing minerals. "Kinetic" tests include shake flask extractions, humidity cells and column tests or lysimeters. Kinetic data have been used two different ways. The first approach is exemplified by Chapman et al. (1993), who predicted metal releases using empirical equations fitted to the laboratory kinetic data. The second approach is to use the laboratory kinetic data to validate geochemical models developed from thermodynamic principles. The first approach ignores the differences between the laboratory and field conditions and is therefore very site and condition-specific. We therefore recommend the second approach, of which a specific example is presented in Section 10.2.

7.2 **Thermodynamic Data**

7.2.1 Equilibrium Thermodynamic Data

Accurate thermodynamic data are essential to adequately model geochemical processes. This data is used to estimate the activity coefficients of individual species in solution and the saturation state of minerals with respect to the aqueous phase. The thermodynamic data used by most modelling programs consists of a set of equilibrium constants, which describe the equilibrium between a phase or component (i.e. mineral, aqueous species or complex, or gas) and a set of aqueous components. Equilibrium constants vary with temperature and pressure. Some programs use, instead of equilibrium constants, a database of free energy, enthalpy of formation, third law entropy, heat capacity, and volume.

There is a lack of thermodynamic data for some important secondary phases which are known to form in the unsaturated zones mine wastes, including such minerals as alunogen, and most Fe(III)-bearing sulphate salts, including copiapite and rhomboclase. Some of these minerals may have substantial impact on water quality. Appendix A lists these minerals and some of the other minerals for which thermodynamic data are lacking.

Two different conventions are presently used to estimate the activity coefficients of aqueous species: the ion association method (see review of Johnson and Pytkowiez, 1979) and the specific ion interaction method (see review of Pitzer, 1979). The ion association method considers ion pairs and complexes as distinct entities in solution. In the thermodynamic database using this method, free energies or equilibrium constants are tabulated for the formation of these aqueous complexes or ion pairs. The activity coefficients for ion pairs and complexes are estimated using the Davies or the Extended Debye-Huckel equations. In the Pitzer or specific interaction method, there are no ion pairs or complexes; all dissolved components are assumed to be fully dissociated. The ionic interactions are factored into the activity coefficients of the ions. Obviously, the activity coefficients calculated from

the two methods will differ; so will the molalities and the ionic strengths. However the activities of the ions will be the same. To avoid confusion, the Pitzer molalities and activity coefficients are referred to as "stoichiometric" or "total" whereas "individual" or "true" is used for the ion association method. The thermodynamic database for the Pitzer approach is based on measurement of interaction coefficients for various electrolytes. Tabulated in the database are interaction coefficients for each doublet (i.e. cation-anion pair, cation-cation pair, anion-anion pair), triplet (i.e. cation-cation-anion, cation-anion-anion) and neutral combination (i.e. neutral-anion, neutral-cation). The two methods are not mutually exclusive. The Pitzer approach is considered to give a more accurate representation of the thermodynamic properties of solutions with ionic strengths greater than 1; in other cases, the best representation is given by a combination of interaction coefficients and association coefficients. Unfortunately, Pitzer parameters only exist for the more simple electrolytes and, at this stage, are not completely available for the compositions of the brines associated with ARD.

A good thermodynamic database should be internally consistent. Unfortunately, this is not always the case. Data is often extracted from the literature without regard for accuracy, and questionable extrapolations or estimations are sometimes used. In some cases, critical phases or aqueous species are ignored. Comments on database qualities are provided in Part 2 of this report.

7.2.2 Kinetic Data

The equilibrium condition represents an extreme which geochemical reactions are moving towards (Brantly, 1992). It is generally agreed (Lasaga, 1981, 1984; Lasaga et al., 1994) that the rate of a reaction depends on how far the reactant concentrations are from equilibrium. This is often quantitatively expressed by the saturation index (SI), which is defined as the log of the ratio of the ion activity product (IAP) of the reaction to the equilibrium constant. The SI equals 0 at equilibrium, is greater than zero for supersaturation and less than zero for undersaturation. Thus for a simple zeroth order reaction where the rate of the surface reaction is the rate controlling factor (as opposed to diffusion in the aqueous phase), the rate (R) can be expressed as the product of the rate constant (k), SI and the surface area (A) of the reacting phases:

$$R = kA\,(1 - 10^{SI})$$

For higher order reactions, the rate is also dependent on the thermodynamic concentrations or activities of certain rate determining ions (oxygen in the case of pyrite oxidation). Often, there is a choice of several pathways or combinations of "elementary" reactions to approach equilibrium. The total rate is the sum of all the "elementary" reactions leading to this final state. Again in the case of pyrite oxidation, this could be the combination of oxygen and Fe(III):

$$R = A\,(1 - 10^{SI})\,(k_{O2}a_{O2} + k_{Fe(III)}a_{Fe(III)})$$

The activities of O_2 and Fe(III) may be raised to a certain power whose value is usually determined by experiment. Otwinowski (1994) provides a more detailed discussion and summary of past research on the kinetics of the oxidation of pyrite.

Equations like the one presented above form the basis for reaction path or mass transfer modelling. The input parameters needed are the rate constant, k, and the surface area, A. Besides these

variables whose values must be determined, the effect of inhibitors and accelerators (i.e. catalysts) have to be considered. Generally the effect of inhibitors on the rate law can be approximated by multiplying the rate term by some function of their concentration to reduce the rate appropriately. This is the approach used by Sverdrup and Warfvinge (1993). A catalyst could be treated exactly the same way. As stated earlier in this report, the most important catalyst for the oxidation of sulphide minerals is probably bacteria. Also, galvanic effects may turn out to be important rate accelerators as more information becomes available.

There are tabulations of rate constants, the most complete being those of Sverdrup (1990) and Fleer and Johnston (1986). However, both these tabulations concentrate on silicate and carbonate minerals. Sverdrup and Warfvinge (1988) have classified minerals into five groups based on their dissolution kinetics in a normal weathering environment. The most rapidly dissolving group (with rate constants between 10^{-5} to 10^{-8} moles/m^{2}s) are the carbonate minerals (i.e. calcite, aragonite, dolomite, magnesite and brucite). The silicates are split into three weathering groups: fast, with rate constants between 10^{-9} to $10^{-10.5}$ moles/m^{2}s (i.e. anorthite, nepheline, jadeite, leucite, spodumene, pyroxenes such as forsterite, diopside, wollastonite, hedenbergite, bronzite, amphiboles such as hornblende and glaucophane, chlorites, garnets and epidotes), intermediate, with rate constants between $10^{-10.5}$ to 10^{-12} moles/m^{2}s (i.e. pyroxenes such as enstatite, hypersthene, and augite, amphiboles such as tremolite, actinolite and anthophyllite, and serpentines such as chrysotile and talc) and slow, with rate constants between 10^{-12} to 10^{-13} moles/m^{2}s (i.e. feldspars such as albite, orthoclase, and plagioclase, clay minerals like gibbsite and kaolinite, and micas such as muscovite and biotite). The "non-reactive" or "inert" group, with the smallest rate constants (10^{-14} to 10^{-16} moles/m^{2}s), contains quartz, rutile and zircon. These data illustrate well the rapid neutralization of ARD by carbonates and the slow reactions with basic silicate minerals.

Under the extremely acid environment of a waste rock dump, most of the rates of the mineral-fluid reactions would be much faster than the above tabulated rates. Silicate reactions become more important over long time frames during which a waste rock dump can produce ARD. As mentioned in Part 1, kinetic data for some important minerals are presently unavailable. A partial list of these minerals is tabulated in Appendix A, and discussions on the validity of currently available kinetic data are included in the literature review of Appendix B.

7.3 **Discussion**

7.3.1 Alkalinity and acidity

Alkalinity and acidity measurements consist of acid or base titrations to fixed pH values and are difficult to interpret, as their use entails a number of assumptions which are not always valid. For example, in many natural systems, the dissolved carbonate species (CO_3^{--}, HCO_3^- and H_2CO_3) and their complexes are main contributors to alkalinity and acidity through the equilibria:

$$CO_3^{--} + H^+ \quad <--> \quad HCO_3^- + H^+ \quad <--> \quad H_2CO_3$$

For this reason, many people treat alkalinity as a direct measurement of total dissolved carbonate. However, this may be inappropriate if there is not sufficient dissolved CO_2 in the fluid or

if the pH is low. In addition, both acid and base titrations include the effects of other dissolved constituents. For example, in very acidic systems with high sulphate concentrations, the equilibrium

$$SO_4^{--} + H^+ \quad <--> \quad HSO_4^-$$

can significantly affect the titration, and must be included as well. Similar effects can occur due to the presence, among others, of boron, silica, phosphate, ammonia, organic acids, and to a lesser extent, base metal ions. If these other components affecting alkalinity are present in significant amounts it becomes impossible to extract carbonate values. Alternatively, in acid waters where the alkalinity is small or zero, most or all of the carbonate will be present as dissolved CO_2 or H_2CO_3 which would not be detected by an alkalinity measurement.

The theoretical background for the treatment of alkalinity and acidity of fluids has been discussed by many authors (for example; Stumm and Morgan, 1981) and the effects documented for a number of systems (for example; Carothers and Kharaka, 1978). Many geochemical modelling programs allow alkalinity to be input as part of the fluid analysis. However, many have deliberately avoided the use of alkalinity and acidity because of the number of required assumptions and the resulting numerical problems. These problems can be avoided by the use of total inorganic carbon (TIC) measurements.

7.3.2 Bacterial Catalysis

Studies (for example Nicholson, 1994) have shown the importance of bacteria in enhancing the oxidation rate by one to two orders of magnitude at low pH and intermediate temperatures. It is difficult to characterize their activity in a waste rock pile, although it has been done in a few cases such as at the White dump at the Rum Jungle Minesite in Australia (Harries and Ritchie, 1982 & 1983b) and at the South dump at Mine Doyon in Canada (Guay, 1994) where T. ferrooxidans was found to dominate.

The aerobic bacterial oxidation of iron depends on a number of factors: temperature, pH, CO_2, O_2, ionic strength and Fe(II) concentrations, surface area and population density. Microbial catalysis under optimum laboratory conditions has been found to speed up the aerobic oxidation of pyrite by a factor of 300, the aerobic oxidation of ferrous iron by over a million, and the anaerobic oxidation of pyrite by a factor of two (Otwinowski, 1994). The effect of bacteria on ARD must be included in geochemical modelling. It can be directly integrated into the abiotic rate law as a catalytic effect or it can simply be considered another reaction pathway and its rate law summed to the overall rate law.

7.3.3 Aqueous Redox Equilibrium

One commom assumption is that water is in internal redox equilibrium, and that a measurement of the redox potential (Eh) or a statement of redox conditions (e.g. fixed oxygen pressure) adequately describes the equilibrium between the various redox couples. This assumption has been documented to be very poor for most natural systems (for example, see Thorstenson, 1984), and there is no reason to presume that it is any better for systems perturbed by man. Nordstrom et al. (1979a) found that careful independent measurements of Eh in acid mine waters were in agreement with calculated Eh

values based on the measured concentration of dissolved Fe(II) and Fe(III). Although the soluble iron was found to control the measured redox potential, Nordstrom et al. found that it was out of equilibrium with dissolved oxygen. Consequently, if there are multiple redox pairs in a water and knowledge of them is important, there is no alternative but to measure each redox couple independently. If this is not possible, then some assumptions must be made as to the state of equilibrium between redox couples.

Proper Eh measurements are difficult to make and interpret. In reducing environments, the platinum electrode can be poisoned by foreign ions such as sulphide, while in highly oxygenated environments the platinum surface can act as an oxide electrode that responds to pH (Whitfield, 1974). To further complicate the problem of making an accurate measurement, redox species can be present in concentrations too low to give an adequate electrode response. The alternative measurement, chemical analysis of the concentrations of a redox pair, is not simple. Preservation of the sample is necessary to ensure that oxidation does not take place before chemical analysis. Morin (1987) discusses the errors occurring when reduced, high iron groundwaters are collected but not preserved. The Fe(II) oxidizes to Fe(III) and precipitates as $Fe(OH)_3$. Chemical analysis of the water will indicate low dissolved iron dominated by Fe(III).

The best method to measure redox potential depends on the specific solution conditions. , Eh measurements must be relied upon under certain conditions such as where one of the two ions of the redox pair is below detection limit. Redox potential measurements should always be documented in detail so that eventual users or modellers can interpret them properly.

Another complication in modelling redox reactions is the rate dependency of the aerobic oxidation of ferrous iron. In geochemical modelling, it is assumed that the approach to homogeneous equilibria in the aqueous phase is extremely rapid compared to heterogeneous equilibria. As a first step in any mass transfer calculation, a distribution of species in the aqueous phase is calculated assuming equilibrium. If redox is not at equilibrium, the calculation is not unique. For example, the saturation index (SI) of a redox mineral will be different depending on what species is used to define the equilibrium constant. To illustrate this, consider the following two pyrite dissolution reactions:

$$FeS_2 + 7/2O_2 + H_2O \rightarrow Fe^{2+} + 2SO_4^{2-} + 2H^+$$

$$FeS_2 + 15/4O_2 + 1/2H_2O \rightarrow Fe^{3+} + 2SO_4^{2-} + H^+$$

If iron is in redox equilibrium, the SI's calculated using either reaction would be identical because the reaction between Fe(II) and Fe(III) is in equilibrium with the O_2-H_2O couple; if iron is not in redox equilibrium, the SI's would be different. This could lead to the apparent contradiction that the SI value calculated based on pyrite dissolution to Fe(II) predicts supersaturation, while the SI value calculated based on pyrite dissolution to Fe(III) predicts undersaturation. This means that pyrite is both precipitating and dissolving at the same time. This can be handled in modelling through the appropriate rate equations for the two "elementary" reactions. However, the standard SI analysis for a mineral is done assuming homogeneous equilibrium, which is not correct when the redox couple pertinent to that mineral is out of equilibrium. To our knowledge, this point has been ignored in the literature.

7.3.4 Surface Area

The contribution of surface area to the reaction rates is difficult to estimate. In the final analysis, "reactive" surface area is often used as an adjustable parameter in absolute rate modelling of geochemical processes (see for example Stromberg and Banwart, 1994). The surface area is not constant but changes as minerals precipitate or dissolve. In addition, one needs to know the surface area in contact with the aqueous phase. Surfaces can be coated with reaction products; incongruent reactions can result in a leached layer. Reactions involving primary minerals may become diffusion-limited or completely shut down. Kinetic models such as the "shrinking core" model for pyrite (see Nicholson, 1994; Ritchie 1994a & c) take this into account. However, assumptions of a uniform leached layer or product layer coating a reacting mineral are often not justified. Pratt et al. (1994b) has shown that reaction products coating sulphide mineral surfaces show mudcracks and spall off, providing continuous channels to the sulphide mineral surface. "Reactive surface" may not correlate with measured surface. Structural defects on the atomic scale such as stacking faults are often not known, and their effect is hidden in the surface area term. Anbeek (1993), based on laboratory measurements of steady state dissolution rates, has shown that weathered grains (free from any surface coatings) dissolve much more slowly than grains which have freshly fractured surfaces prepared by grinding. This comparison was for grains of identical size and BET surface areas. He proposes that weathering creates non-reactive surface sites versus reactive surface sites created by grinding. Stromberg and Banwart (1994) found the BET surface area to be independent of grain size for grain sizes above 10 microns, presumably due to the sensitivity of the measurement to inner pore surfaces. White and Peterson (1990), in a compilation of data, conclude that "reactive" surface areas are one to three orders of magnitude less than the BET surface area, and are attributed to the reaction site density and dislocation density on a mineral surface. However, for reactions where transport of ions through the aqueous phase to and from the surface is rate limiting, "reactive" surface area is not important. The rate law equations based on the rate of surface reaction will overestimate the rate of reaction; rate laws based on diffusion will have to be applied.

7.3.5 Decommissioning Options

Decommissioning options comprise physical and geochemical means to limit or mitigate ARD. They can be broadly classified as isolation, in-situ remediation, and capture and treatment. Isolation would include, for example, moving the waste rock into a water body (water cover). In-situ remediation would include options such as dry covers or limestone addition. Treatment would include alkalinity addition to the toe waters, and treatment using wetlands.

Generally, the nature of the decommissioning option will dictate the long-term physical conditions in the waste rock pile. For example, the application of a water cover will create a saturated, low flow physical environment; a dry cover will create unsaturated, low flow conditions; neutralization will tend to promote variably saturated, high-flow environments. Models must be capable of simulating the geochemical processes which could occur under all the physical environments described above.

8. SUMMARY OF PART 1

1) Acid generation cannot be predicted accurately without knowing which secondary minerals form. Prediction of secondary mineral formation requires consideration of reaction rates. Reaction rates (kinetics) are therefore required for accurate water quality predictions of water quality from waste rock piles.

2) Reaction rate equations and rate constants necessary to perform kinetic calculations are insufficient at present. Reaction path calculations based on relative time frames can provide limited help in overcoming the present data deficiencies.

3) The most important geochemical processes controlling rates of acid generation and water quality from sulphidic waste rock piles are precipitation and dissolution, chemical diffusion, and surface reactions.

4) The following points can be concluded on dissolution and precipitation:

   a) dissolution of carbonate minerals is rapid and thus provides readily-available neutralization of acidic solutions

   b) dissolution of Al-silicates can neutralize acidic waters if the time of contact of the water with the minerals is long; where permeabilities are high and residence times are short, Al-silicates are unlikely to neutralize large amounts of acid.

   c) Dissolution and precipitation are much more important controls on drainage water quality than are ion exchange or adsorption/desorption processes.

5) Diffusion is a rate-limiting process

   a) at the macroscopic scale: diffusion of O_2 into waste rock piles is an important control on oxidation of sulphides.

   b) at the microscopic scale: diffusion through a stagnant water layer adhering to mineral surfaces can control dissolution rates

   c) at the atomic scale: diffusion of species such as the Fe(III) ion through pyrrhotite, and possibly other non-stoichiometric minerals, is the rate limiting step in the initial stages of air-oxidation.

6) Reaction rates can also be controlled by processes occurring at the surfaces of minerals, such as surface complexation. For example, surface reactions control the rate of dissolution of sulphides, oxides and Al-silicate minerals.

7) Co-precipitation is a process controlling the concentrations of several metals in acid mine water. By this process, metals released from primary minerals may be incorporated into

structural sites of secondary minerals. They are subsequently "encased" and unavailable for subsequent desorption or exchange, and may only be released through dissolution.

8) Bacterial activity can greatly accelerate sulphide oxidation rates and therefore is an important rate-modifying process

9) Wetting and drying are important physical processes that affect water chemistry, as exemplified by the following facts:

   a) In aerated portions of waste rock piles, iron sulphate salts are likely to precipitate and accumulate during the drying cycle. Subsequent infiltration results in rapid dissolution of these salts, precipitation of Fe-oxyhydroxides and decrease in pH.

   b) Evaporative drying of unsaturated waste rock piles causes hydrous secondary iron minerals to coat sulphide mineral surfaces. These minerals dehydrate, crack and spall from the drying surfaces. The effect is to expose the sulphide surfaces to atmospheric gases including O_2, which results in renewed oxidation of the sulphides.

10) Galvanic reactions may be an important rate-modifying process for oxidation of sulphides. Unfortunately, insufficient data disallow a proper evaluation of the importance of this process.

11) Geochemical processes occurring in waste rock bear some similarity with processes which occur in the unsaturated zone of tailings deposits. However, the reactions occurring in waste rock piles are more influenced by the presence of oxygen and by wetting and drying cycles than those in tailings.

12) Field data are required to describe geochemical processes in waste rock include detailed water analyses and mineralogy, exposed surface area, temperature, oxygen availability and water infiltration. Water analyses should include measurements of total inorganic carbon (TIC) and dissolved silica to provide a good description of major acid-neutralizing reactions. A definition of reactive surface area is also required to define rates of reactions; this parameter is very difficult to measure, but should nevertheless be estimated as accurately as possible.

13) Equilibrium thermodynamic databases are required to predict precipitation and dissolution reactions in waste rock. Some thermodynamic data for important secondary minerals in ARD are missing. Kinetic data are required to predict reaction rates, but kinetic databases have serious deficiencies. More research should be conducted to obtain kinetic rate data; inhibitive and catalytic effects should be included in kinetic rate equations. Column tests and other bulk laboratory and field tests should be used to compensate for the inadequacies of presently available geochemical databases.

PART 2

REVIEW OF GEOCHEMICAL MODELS

9. CLASSIFICATION OF MODELS

A very limited number of modelling programs have been specifically designed to model the acid waste water problem. However, there exists a number of "general" geochemical modelling programs which may be suitable for the purpose. The programs can be loosely divided into five categories: equilibrium models, mass transfer models, coupled mass transfer-flow models, "supporting" models and "empirical and engineering" models.

Equilibrium thermodynamic models are static models of an aqueous solution. They are used to estimate the concentrations and activities of all the important aqueous species in a specific water and to calculate the saturation indices for various minerals. Many of the programs that fall into this category have considerable freedom in input, allowing various corrections to be made for poor or incomplete water analyses, modifying the water chemistry as a result of a user defined reaction path or process, or allowing constraints such as a gas partial pressure or the presence of a solid phase to control the water chemistry. Programs in this category are listed in Figure 11, and are reviewed in Section 10. Their strength is based upon their rigorous treatment of the aqueous phase and their ability to modify the fluid composition based upon a user-specified process.

Mass transfer models are dynamic models which allow the reactions in a closed system between a fluid and a rock to be calculated. Initially, all or some of the minerals in the rock are not in equilibrium with the fluid. As these "reactant" minerals dissolve into the fluid, the fluid composition changes and secondary (product) minerals may precipitate from or dissolve into the fluid. The amount of the product minerals will change as a function of time. The identity of product minerals will potentially change as new product minerals are formed, and others may be completely destroyed. Mass transfer models are also known as reaction path models. Figure 11 lists programs falling into this category and detailed descriptions are done in Section 11.

Coupled mass transfer-flow models are open-system versions of mass transfer programs, or mass transfer programs which have been expanded to include flow. These programs are complex and are aimed at simulating a wide variety of geochemical processes. However, there is rarely enough data to allow the accurate modelling of complex natural systems. The complexity of the programming has severely limited the number of "general" programs in this area, as most of those available are suited only for a specific type of problem. Coupled mass transfer-flow models are also known as mass transfer-mass transport models. They are listed in Figure 11 and described in Section 12.

"Support" models include all of the supporting programs, those programs which calculate and display intensive variable diagrams, which calculate or fit thermodynamic databases, or which calculate any of the needed thermodynamic or physical-chemical properties. Programs in this category can also have a phenomenological component, such as nanograms (Figure 11). This class of geochemical

programs is reviewed in Section 13. However, the review only includes coupled phenomenological and thermodynamic models and those which generate information needed specifically for one of the geochemical models described in one of the previous sections. The phenomenological models that have been designed specifically for ARD are grouped with the "empirical and engineering" models in Section 14.

"Empirical and engineering" computer models specific to acid mine drainage have been developed and used (Figure 11). These models do not perform general geochemical calculations, but rather limit the number of geochemical and physical processes as much as possible without losing the capability of simulating the bulk geochemical and physical behaviour of the mine dump.

The next part of this report reviews geochemical models according to the sequence and classification of Figure 11. The capabilities of thermodynamic equilibrium and mass transfer models are evaluated using two test cases. The first test case was selected from the Mine Doyon field site (Choquette et. al, 1993); the second test case was taken from column data produced by the controlled leach of waste rock from the Stratmat waste rock pile (Yanful and Payant, 1993). The capabilities of each reviewed model to simulate the different geochemical processes discussed in Part 1 are tabulated in Section 16, along with summary tables on the applicability of each class of models.

The classification and evaluation procedures followed in Part 2 are inspired by other model reviews and compilations which have appeared in the literature. Early reviews include those by Nordstrom et. al (1979b) on thermodynamic equilibrium models and by EPRI (1984) on solute transport models. Other reviews were done by Grove and Stollenwerk (1987) and Engesgaard and Christensen (1988). Yeh and Tripathi (1989) performed a critical review of the approaches used for transport modelling, and Mangold and Tsang (1991) thoroughly listed and reviewed groundwater flow and solute transport models. A recent review of geochemical models was done by Alpers and Nordstrom (1994). The present review does not list, describe or evaluate as many models as some of the previous generic reviews. In contrast to those previous efforts, the present review is more focussed on geochemical components, covers a broader spectrum of model categories, and concentrates on a more specific prediction problem.

Class 1: Equilibrium Geochemical Thermodynamic Models

EQ3 (T. Wolery, LLNL)	MULTEQ (EPRI)
PHREEQE (USGS)	PHRQPITZ (USGS)
WATEQ4F - (USGS)	ESP (OLI systems)
MINTEQA2 (EPA)	ECHEM (EPA)
SOLVEQ (M. Reed, U. Oregon)	SOLMINEQ.88 (USGS-ARC)
GEOCHEM (G. Sposito, U. California)	PATHARC (E.H. Perkins, ARC)

Class 2: Geochemical Mass Transfer Models

PATHARC (E.H. Perkins, ARC)	CHILLER (M. Reed, U. Oregon)
EQ6 (T. Wolery, LLNL)	REACT (C. Bethke, U. Illinois)
STEADYQL	

Class 3: Coupled Geochemical Mass Transfer - Flow Models

PHREEQM (USGS)	FMT (C. Novak, Sandia)
REACTRAN (C. Moore)	KGe0Flow (D. Sevougian, Battelle)
CIRF.A (P. Ortoleva)	1DREACT (C. Steefel, Battelle)
MPATH (P. Lichtner)	FCT (C. Steefel, Battelle)
Unnamed (W. White, USBM)	MINTRAN (Waterloo)

Class 4: Supporting Geochemical Models

Ge0-Calc (T.H. Brown, UBC)	TACT, ACT2(C. Bethke, U. Illinois)
SUPCRIT (Helgeson, U. Berkeley)	Ge0-Tab (T.H. Brown, UBC)
BALANCE (USGS)	NETPATH (USGS)
RXN (C. Bethke, U. Illinois)	BOUNDS (D. Kerrick, Penn. State U.)

Class 5: Empirical and Engineering Models

WATAIL (R. Nicholson, U. Waterloo)	RATAP (CANMET)
Q-ROCK (SRK)	ACIDROCK (Scharer, U. Waterloo)
FIDHELM (ANSTO)	Unnamed (K. Morin)

Figure 11. Classification of Geochemical Models

10. EQUILIBRIUM GEOCHEMICAL THERMODYNAMIC MODELS

10.1 Background

Equilibrium geochemical thermodynamic models are the most widely used of any of the geochemical computer models. These models have their origins in the pioneering work of Garrels and Thompson (1962) on the speciation of ions in a natural water using the ion association approach. Common to all the models is the ability to make such equilibrium speciation calculations for a large range of water compositions. From the estimates of the mixing properties of the aqueous phase, the saturation states of several minerals and gases are calculated. Besides these basic calculations, each model has some simple mass transfer options and most have a temperature capability. The primary purpose of equilibrium models is to thermodynamically calculate the activity coefficients of the aqueous components to estimate mineral saturations, quantified as saturation indices (SI). Detailed explanations of the methods and assumptions associated with thermodynamic equilibrium calculations are available from several sources, including Stumm and Morgan (1981).

Differences between equilibrium models may be due to two factors: (1) the level of completeness and accuracy of the thermodynamic database; (2) the accuracy of the method of solution for the speciation of the water. The thermodynamic databases include both standard state and mixing (solute-solvent interaction) properties. The standard state properties are easily compared. Mixing properties are handled by an activity coefficient model. As discussed in Section 7.2.1, two activity coefficient models are in standard use for modelling waters and are, in order of complexity, the ion association and the Pitzer method. Nearly all geochemical codes use the ion association method based either on the Davies equation or the Extended Debye-Hückel equation. However the Pitzer model is the best for activity coefficients in brines. Unfortunately, Pitzer parameters only exist for the more simple electrolytes and, at this stage, are not completely available for the compositions of the brines associated with ARD. The second effect that can influence the results of equilibrium models, the precision of the method of solution, is a minor problem with the fast speed and large memories of modern computers. However, when incorporating multiple speciation calculations in a mass transfer or mass transport problem, streamlining calculation procedures may end up sacrificing precision.

10.2 Specific Models

10.2.1 EQ3

EQ3 (Wolery, 1992a & b; Daveler and Wolery, 1992) is the equilibrium geochemical thermodynamic computer code most widely used by agencies investigating nuclear waste disposal in the US. In addition, it has been used by many different authors for projects such as ore deposition and subsequent alteration, diagenetic/basin modelling, chemical modelling at mid-ocean ridges, etc. One strength of EQ3 is the high degree of flexibility in dealing with various model input parameters. Parameters such as pH, pHCl, Eh, pe, oxygen fugacity, or analytical data for each component of a redox can be specified. EQ3 is supplied with five different thermodynamic databases: a composite database for general use based on Extended Debye-Hückel formulation, a data set based upon

SUPCRT92, one based upon the Data Bank of the Nuclear Energy Agency of the European Community, one based upon the Pitzer formulation, and one based upon the modified Pitzer formulation of Harvie, Møller and Weare. EQ3 is used as a pre-processor for EQ6, a mass transfer geochemical computer code. Williams-Jones et. al (1993) used EQ3 to interpret waste rock leach column data, and the results are reported in Yanful and Payant (1993).

10.2.2 SOLMINEQ.88 PC/SHELL

SOLMINEQ.88pc/shell is a personal computer version of SOLMINEQ.88, an equilibrium geochemical thermodynamic modelling computer code (Kharaka et al., 1988). It has a user-friendly interface for program data input and for rapid examination of program output. The program has many useful options to modify or correct possible incorrect water analyses. The largest user group of SOLMINEQ.88 pc/shell is oil companies, whom typically use the program to examine deep formation waters and production waters. Several SOLMINEQ.88 options have been developed with this group in mind, and include boiling, fluid mixing, ion exchange, and a limited mass transfer function. SOLMINEQ.88 pc/shell is currently supported by the Alberta Research Council, Alberta, Canada.

10.2.3 PHREEQE and PHRQPITZ

PHREEQE and the Pitzer version, PHRQPITZ, are widely used equilibrium geochemical thermodynamic modelling codes. The user base is widespread, in part because PHREEQE (Parkhurst et al., 1990) is taught as part of two courses offered at the National Training Centre of the USGS. PHRQPITZ (Plummer et al., 1988) uses the complex Pitzer formulation for activity coefficients while PHREEQE uses ion pairing and the Extended Debye-Hückel equation. The weakness in PHRQPITZ is the lack of Pitzer coefficients for several ions, particularly the iron species and complexes; although this is slowly being rectified (Reardon and Beckie, 1986). Besides the normal functions, PHREEQE calculates molalities and activities of aqueous species as a function of either mixing fluids, titration of minerals into solution (irreversible reaction), and temperature changes. An interactive input preparation program (PHRQINPT) has been bundled with PHREEQE to aid in the preparation of an input file. PHREEQE has been incorporated into several transport codes. Alpers and Nordstrom (1991) applied PHREEQE and PHRQPITZ to an acid mine water study at Iron Mountain, California.

10.2.4 MINTEQA2

MINTEQA2 (Allison et al., 1991) is an equilibrium geochemical thermodynamic modelling code supported by the Environmental Research Laboratory, US Environmental Protection Agency. Of all of the codes currently examined, MINTEQA2 (version 3.11) has the greatest flexibility in modelling surface reactions. It includes seven different options (the activity K_d model, the activity Langmuir model, the activity Freundlich model, the ion exchange model, the constant capacitance model, the triple layer model and the diffuse layer model) for surfaces, with up to five different surfaces, each of which may have two different sites. MINTEQA2 has a limited mass transfer capability that allows calculation of the change in the composition of the aqueous phase by mineral equilibration. To aid in the preparation of an input file, an interactive input preparation program (PRODEFA2) has

been bundled with MINTEQA2. Al et. al (1994) present a recent application of MINTEQA2 in a geochemical study of the Kidd Creek tailings impoundment. The use of MINTEQA2 may be mandatory for certain projects examined by USEPA.

10.2.5 WATEQ4F

WATEQ4F, and the UNIX version WQ4F (Ball and Nordstrom, 1991), is the most recent version of WATEQ, developed by the US Geological Survey. WATEQ4F is an equilibrium geochemical thermodynamics code which has several trace elements and the corresponding aqueous species and complexes in its database. As in EQ3, redox couples may be independently specified and are not required to be in equilibrium with each other. An input preparation program (WQ4FINPT) has been bundled with WATEQ4F to aid in the preparation of an input file. WATEQF has recently been applied by Wicks and Groves (1993) to study rates of calcite dissolution in acid mine drainage.

10.2.6 SOLVEQ

SOLVEQ is a PC program developed in the mid-1970's (Reed, 1982; Reed and Spycher, 1984; Spycher and Reed, 1988, 1990a) at the University of Oregon for calculating the distribution of aqueous species and mineral saturation indices in natural waters. In addition to homogenous equilibria, the current version of SOLVEQ calculates partial heterogenous equilibria, wherein equilibration of a given water with specified minerals or gas fugacities can be forced. SOLVEQ has been used frequently for modelling of hydrothermal waters where the temperatures are variable. The program GEOCAL, which prompts the user by asking questions, is used to prepare input files for SOLVEQ. SOLVEQ is used as a preprocessor for CHILLER, a mass transfer geochemical modelling code.

10.2.7 PATHARC

PATHARC is a mass transfer geochemical modelling computer code that has capabilities for calculating reactions as a function of time in addition to the calculation of the equilibrium state. It has been included in this section as it calculates much of the same information as the above codes, and can be used as an equilibrium geochemical thermodynamics code if specified to take zero time steps. PATHARC is designed to run on a personal computer and have a user friendly interface. It is available from the Alberta Research Council, Alberta, Canada. PATHARC is described more fully in the next section on mass transfer models.

10.3 **Equilibrium Thermodynamic Modelling of Mine Doyon Waters**

Rather than examine the raw thermodynamic databases in detail for the ARD problems, we take the approach of Nordstrom et al. (1979b), who used speciation calculations on river and sea water to compare geochemical codes. We have examined an ARD brackish case (water BH-91-01-SOIL) and a brine case (water BH-91-06-ROCK) from Mine Doyon with the equilibrium thermodynamic codes provided in seven geochemical models. In all but one of the cases we used the ion association method

with the Extended Debye-Hückel for activity coefficient corrections and compared these calculations with those predicted using the Pitzer model option in EQ3NR. A detailed description of the chemical data used in the modelling is given in Appendix C.

Before modelling, the sulphate values for the two water analyses were corrected to achieve a 1% charge balance for SOLMINEQ and the Eh was calculated from the iron redox couple. The values for sulphate ranged from 2819 to 3159 mg/L and from 123,894 to 143,450 mg/L, and the Eh from .205 to .570 volts and from .375 to .629 volts in the brackish and brine waters respectively.

The results for each water are presented in Tables 5 and 6. The first three columns in each table (from left to right) identify the species (only the "free" ion species are given for each element) and the analyzed amount of each in mg/L and molality. The remaining columns are the molality of the species calculated by each of the geochemical models. These should be equal to or less than the analyzed values due to the effect of speciation. Other information (charge balance, ionic strength, activity of water, ferrous/ferric activity ratio) is given at the base of the table.

The results in Table 5 (the "brackish" water) show considerable similarity between the calculated results from all of the various models. The Pitzer version of EQ3 is not considered in Table 5 because "individual" and "total" molalities are not comparable . The differences are clearly the results of slightly different thermodynamic databases, with slightly different properties for various species and with some species missing from various databases. The most significant differences between each computer model for major species in the brackish water is the iron(III) and aluminum molalities which vary by 100% between models. Other free ion molalities vary by as much as 50%. For the minor species the copper, lead and zinc values calculated by EQ3 are extremely high and very similar to the analytical values probably because of lack of copper, lead and zinc complexes in the EQ3 database.

The results for the brine are given in Table 6. The Pitzer version of EQ3 is not considered in Table 6 because "individual" and "total" molalities are not comparable . Once again, the results for the models using the ion association method with the Extended Debye-Hückel activity coefficient equation are similar but with larger differences resulting from differences between databases due to the increased ionic strength of the brine. Here the maximum variation in the calculated values of the aluminum molalities is a factor of 8 but only 3 if the prediction of WATEQ4F is not considered. A factor of 3 would be more in line with the Fe (III) variation. Generally the higher the valence of the ion, the larger the uncertainty. Again, the minor species values (i.e. copper, lead and zinc) calculated by EQ3 are extremely high and very similar to the analytical values due to the lack of copper, lead and zinc complexes in the EQ3 database. The results for both ARD water analyses using geochemical models with Extended Debye-Hückel activity coefficient estimates appear to be consistent with the largest differences occurring in predicted aluminum and iron(III) molalities.

Table 5. Analytical and calculated aqueous speciation for a brackish water at 25°C from drill hole BH9101SOIL from the Mine Doyon dump.

Species	An. mg/L	An.Molal	Ver=1994	2.1/1992	Jan/1993	3.11/91	1994	Oct/1991	7.1/1992		7.1/1992
A.R.D.	BRACKISH	Code =>	SOLMINEQ	WATEQ4F	PHREEQE	MINTEQA2	PATH.ARC	SOLVEQ	EQ3NR/dh		EQ3NR/p
Na+	22	.958E-03	.861E-03	.920E-03	.923E-03	.922E-03	.861E-03	.919E-03	.910E-03		N/C
K+	21	.533E-03	.505E-03	.509E-03	.510E-03	.505E-03	.521E-03	.503E-03	.503E-03		N/C
Ca++	288	.720E-02	.443E-02	.428E-02	.430E-02	.424E-02	.461E-02	.419E-02	.497E-02		N/C
Mg++	357	.147E-01	.791E-02	.804E-02	.808E-02	.903E-02	.731E-02	.788E-02	.745E-02		N/C
Mn++	25	.456E-03	.290E-03	.288E-03	.282E-03	.284E-03	.286E-03	.281E-03	.257E-03		N/C
Fe++	445	.798E-02	.433E-02	.306E-02	.289E-02	.299E-02	.422E-02	.522E-02	.318E-02		N/C
Fe+++	55	.987E-03	.391E-05	.395E-05	.264E-05	.262E-05	.389E-05	.559E-05	.296E-05		N/C
Al+++	19	.705E-03	.167E-03	.108E-03	.145E-03	.152E-03	.205E-03	.161E-03	.113E-03		N/C
SiO2	26	.433E-03	.433E-03	.433E-03	.433E-03	.433E-03	.433E-03	.433E-03	.433E-03		N/C
Cu++	0.3	.473E-05	.304E-05	.284E-05	.277E-05	.282E-05	.297E-05	.275E-05	.471E-05		N/C
Pb++	0.27	.131E-05	.494E-06	.477E-06	.480E-06	.452E-06	.473E-06	.128E-05	.130E-05		N/C
Zn++	1	.153E-04	.101E-04	.808E-05	.858E-05	.802E-05	.120E-05	.888E-05	.153E-04		N/C
Cor SO4	3159	.329E-01	.186E-01	.205E-01	.206E-01	.215E-01	.185E-01	.187E-01	.209E-01		N/C
^Charge	+11%		+0.4%	-3%	N/A	-3%	0.0%	0.0%	-5%		N/C
Ionic	Strength		.0746	.0780	.0784	.0825	.0735	.0745	.0786		N/C
TDS	10060		4419	4406	N/A	N/A	N/A	N/A	N/A		N/A
aH2O	N/A		.9991	.9991	.9991	N/A	N/A	.9992	.9992		.9992
pH	4.69		4.69	4.69	4.69	4.69	4.69	4.69	4.69		4.69
Eh volt	.205		.570	.570	.570	.570	.570	.570	.570		N/A
Log.	aFe2/3		3.375	3.386	3.375	3.396	3.355	3.371	3.375		N/A

* Other analytical data: conductivity = 3953uS; acidity 1439mg/L $CaCO_2$; SO_4 = 2819 mg/L.

** Abbrevations: N/A = not available; N/C = not comparable

Table 6. Analytical and calculated aqueous speciation for a brine at 25°C from drill hole BH9106ROCK from the Mine Doyon south dump.

A.R.D.	BRINE	Code	SOLMINEQ	WATEQ4F	PHREEQE	MINTEQA2	PATH.ARC	SOLVEQ	EQ3NR/dh		EQ3NR/p
Species	An. mg/L	An.Molal	1994	2.1/1992	Jan/1993	3.11/91	1994	Oct/1991	7.1/1992		7.1/1992
Na+	18	.832E-03	.522E-03	.726E-03	.720E-03	.694E-03	.450E-03	.663E-03	.655E-03		N/C
K+	0.31	.843E-05	.651E-05	.724E-05	.724E-05	.709E-05	.671E-05	.623E-05	.658E-05		N/C
Ca++	528	.140E-01	.742E-02	.602E-02	.572E-02	.563E-02	.633E-02	.420E-02	.666E-02		N/C
Mg++	9626	.421E+00	.164E+00	.147E+00	.134E+00	.157E+00	.110E+00	.106E+00	.104E+00		N/C
Mn++	456	.882E-02	.488E-02	.265E-02	.488E-02	.543E-02	.385E-02	.287E-02	.303E-02		N/C
Fe++	19788	.377E+00	.171E+00	.980E-01	.203E+00	.234E+00	.129E+00	.101E+00	.212E+00		N/C
Fe+++	6477	.123E+00	.221E-02	.900E-03	.261E-02	.293E-02	.149E-02	.158E-02	.271E-02		N/C
Al+++	9610	.379E+00	.209E-01	.610E-02	.350E-01	.317E-01	.522E-01	.143E-01	.206E-01		N/C
SiO2	208	.368E-02	.368E-02	.368E-02	.368E-02	.368E-02	.368E-02	.367E-02	.365E-02		N/C
Cu++	76	.127E-02	.710E-03	.346E-03	.660E-03	.747E-03	.557E-03	.385E-03	.126E-02		N/C
Pb++	1.8	.934E-05	.344E-05	.794E-06	.549E-06	.882E-06	.249E-05	.932E-05	.928E-05		N/C
Zn++	48	.781E-03	.453E-03	.124E-03	.420E-03	.332E-03	.296E-04	.226E-03	.776E-03		N/C
Cor SO4	143450	.159E+01	.341E+00	.284E+00	.319E+00	.384E+00	.537E+00	.215E+00	.320E+00		N/C
^Charge	+16%		+0.1%	+3%	+1%	0%	0%	0.0%	-6%		N/C
Ionic	Strength		1.740	1.324	1.756	1.981	2.063	1.224	1.598		N/C
TDS	200530		190287	168261	N/A	N/A	N/A	N/A	N/A		N/A
aH2O	N/A		.9711	.9728	.9716	N/A	.9663	.9658	.9721		1.0003
pH	2.37		2.37	2.37	2.37	2.37	2.37	2.37	2.37		2.37
Eh volt	.375		.629	.629	.629	.629	.629	.629	.629		N/A
Log.	aFe2/3		2.378	2.389	2.380	2.392	2.414	2.379	2.378		N/A

* Other analytical data: conductivity = 43766 uS; acidity 122134 mg/L $CaCO_2$; SO_4 = 123894 mg/L.
** Abbrevations: N/A = not available; N/C = not comparable

The SIs (saturation indices) for selected minerals pertinent to ARD have been recorded in Table 7 for the brackish water and in Table 8 for the brine. Even if thermodynamic data for the carbonate minerals are present in all the equilibrium models, SIs for carbonate minerals such as calcite, dolomite and siderite could not be calculated because the Mine Doyon water analyses do not contain any TIC analyses. In the field, observed CO_2 degassing is probably generated by carbonate mineral dissolution. If no TIC analyses are available, rates of carbonate dissolution may not be modelled accurately. We also point out that neutralization by silicate mineral reactions are equally important over the long term, and that it is equally important that both dissolved aluminum and silica be analyzed in acid mine waters. Carbonate mineral neutralization reactions were discussed earlier in Section 4.2, and modelling of these reactions is further carried out in Section 11.

Modelling inaccuracies can also appear for the sulphide minerals because of the lack of sulphide analyses. Here though, the concentration of sulphide can be calculated through the sulphate analyses if the sulphide/sulphate is assumed to be in equilibrium with the ferrous/ferric redox couple. The high Ehs of our waters would cause the equilibrium dissolved sulphide values to be very low. Since the sulphide/sulfate couple is not expected to be in equilibrium with the iron redox couple, the concentration of sulphide ions may be significant. For example, the copper sulphide, covellite, is known to precipitate in the tailings waste environment (Alpers et al., 1994; Jambor, 1994).

One other element that is often not analyzed in ARD waters is silica. Without dissolved silica, the saturations of the silica minerals cannot be calculated. Fortunately, silica values were measured for the Mine Doyon waters. For the brackish water, muscovite and kaolinite are supersaturated while chlorite, anorthite and amorphous silica are undersaturated. In the brine, both kaolinite and muscovite would dissolve; amorphous silica would be the only precipitating silicate among the tabulated silicate minerals.

The potassium sulphate phases jarosite and alunite are more highly supersaturated in the brackish water. This is due to the low potassium in the brine and the low pH. The metal oxides and hydroxides, amorphous ferric hydroxide, amorphous aluminum hydroxide, goethite, boehmite and maghemite are all supersaturated in the brackish water and become less supersaturated or undersaturated in the brine. The high positive SIs for goethite may partially be a result of iron colloids being included in the chemical analysis for dissolved iron.

The SIs of the simple sulphate minerals gypsum, melanterite, epsonite, anglesite, chalcanthite and zincosite increase in the brine. In fact, both gypsum and anglesite are predicted to precipitate from the brine. Based on field observations in tailings, the secondary mineral alunogen would also be expected to precipitate from the brine (Blowes and Ptacek, 1994). However, this cannot be tested with the current programs because none of their databases contain thermodynamic data for alunogen (reflected by the blank spaces in Tables 7 and 8).

As can be seen by the remaining blank spaces in the two tables (indicated by N/A), not all the codes contain thermodynamic data for the same minerals. However, all the codes provide simple means to add additional thermodynamic data for minerals. This may not be the case for aqueous species, especially when reactions between the aqueous species are encoded directly into the program code rather than being fully described in the database.

Table 7. Saturation indices from a Mine Doyon ARD brackish water at (BH9101SOIL- 24/4/91) at 25°C for common ARD reactive minerals.

A.R.D. Brackish Code	SOLMINEQ	WATEQ4F	PHREEQE	MINTEQA2	PATH.ARC	SOLVEQ	EQ3NR/dh		EQ3NR/p
Mineral [Formula]	1994	2.1/1992	Jan/1993	3.11/91	1994	Oct/1991	7.1/1992		7.1/1992
Gypsum [CaSO4.2H2O]	-0.25	-0.25	-0.25	+0.02	N/A	-0.39	-0.28		-0.38
Melanterite [FeSO4.7H20]	N/A	-2.79	-2.78	-2.53	-0.23	N/A	-2.61		-2.32
Epsonite [MgSO4.7H2O]	N/A	-2.40	N/A	-2.35	N/A	N/A	-2.59		-2.52
Anglesite [PbSO4]	-1.04	-1.01	-1.01	-1.07	-1.09	-0.52	-0.52		-0.65
Chalcanthite [CuSO4.5H2O]	N/A	-5.39	N/A	-5.38	-5.46	N/A	-5.17		-5.40
Zincosite [ZnSO4]	-11.03	-10.58	N/A	-10.58	N/A	N/A	N/A		N/A
Alunogen [Al2(SO4)3.18H2O]	N/A	N/A	N/A	N/A	N/A	N/A	N/A		N/A
Alunite [KAl3(SO4)2.(OH)6]	+9.84	+7.40	+8.35	+8.28	N/A	+6.21	+9.45		+10.30
Jarosite [KFe3(SO4)2(OH)6	N/A	+10.90	+10.94	+16.45	N/A	N/A	+11.17		N/A
Amorphous [Fe(OH)3]	+3.20	+2.88	+2.89	+2.88	+4.56	N/A	+2.16		N/A
Goethite [FeO(OH)]	+7.49	+8.77	+8.79	+7.27	+9.68	N/A	+7.28		N/A
Amorphous [Al(OH)3]	+2.05	-1.59	-1.27	N/A	N/A	N/A	N/A		N/A
Boehmite [AlO(OH)]	+2.65	+0.63	N/A	+0.96	+0.83	-0.09	+0.96		+1.24
Maghemite [Fe2O3]	+9.54	+9.16	N/A	+9.16	N/A	N/A	N/A		N/A
Amorphous [SiO2]	-0.57	-0.64	-0.64	-0.34	-0.64	-0.65	-0.65		N/A
Kaolinite [Al2Si2O5(OH)4]	+6.42	+4.28	+4.91	+6.64	+6.71	+4.85	+6.96		N/A
Chlorite [Mg5Al2Si3O10(OH)8]	-24.40	-25.41	-24.76	N/A	-26.91	-28.49	-22.29		N/A
Muscovite [KAl3Si3O10(OH)2]	+7.39	+6.16	+7.11	+6.84	+7.35	+5.14	+8.35		N/A
Anorthite [CaAl2Si2O8)	-6.51	-7.27	-6.63	-6.42	N/A	-8.15	-6.11		N/A

* Abbreviations: N/A = not available

Table 8. Saturation indices from a Mine Doyon ARD brine (BH9106ROCK- 24/4/91) at 25°for common ARD reactive minerals.

A.R.D. BRINE Code	SOLMINEQ	WATEQ4F	PHREEQE	MINTEQA2	PATH.ARC	SOLVEQ	EQ3NR/dh		EQ3NR/p
Mineral [Formula]	1994	2.1/1992	Jan/1993	3.11/91	1994	Oct/1991	7.1/1992		7.1/1992
Gypsum [CaSO4.2H2O]	+0.39	+0.27	+0.33	+0.62	N/A	+0.09	+0.21		-0.54
Melanterite [FeSO4.7H20]	N/A	-0.63	-0.74	-0.58	+1.71	N/A	-0.49		-1.72
Epsonite [MgSO4.7H2O]	N/A	-0.74	N/A	-0.65	N/A	N/A	-1.03		-1.36
Anglesite [PbSO4]	+0.22	-0.63	+0.02	+0.01	+0.05	+0.84	+0.65		-0.95
Chalcanthite [CuSO4.5H2O]	N/A	-2.63	N/A	-2.86	-2.71	N/A	-2.41		-3.40
Zincosite [ZnSO4]	-8.94	-8.66	N/A	-8.75	N/A	N/A	N/A		N/A
Alunogen [Al2(SO4)3.18H2O]	N/A	N/A	N/A	N/A	N/A	N/A	N/A		N/A
Alunite [KAl3(SO4)2.(OH)6]	+0.22	-1.30	-0.76	-1.25	N/A	-3.65	+0.32		-5.18
Jarosite [KFe3(SO4)2(OH)6	N/A	+4.01	+3.67	+9.10	N/A	N/A	+4.14		N/A
Amorphous [Fe(OH)3]	-1.52	-1.49	-1.64	-1.63	-0.37	N/A	-2.31		N/A
Goethite [FeO(OH)]	+2.78	+4.41	+4.26	+2.78	+4.76	N/A	+2.83		N/A
Amorphous [Al(OH)3]	-3.32	-6.57	-6.42	N/A	N/A	N/A	N/A		N/A
Boehmite [AlO(OH)]	-2.71	-4.34	N/A	-4.26	-4.27	-5.55	-4.19		-5.42
Maghemite [Fe2O3]	+0.14	+0.44	N/A	+0.20	N/A	N/A	N/A		N/A
Amorphous [SiO2]	+0.52	+0.43	+0.48	+0.83	+0.31	+0.28	+0.28		N/A
Kaolinite [Al2Si2O5(OH)4]	-2.12	-3.52	-3.13	-1.51	-1.60	-4.23	-1.51		N/A
Chlorite [Mg5Al2Si3O10(OH)8]	-49.61	-49.78	-49.14	N/A	-52.91	-55.53	-48.32		N/A
Muscovite [KAl3Si3O10(OH)2]	-9.73	-9.82	-9.24	-9.68	-9.44	-12.77	N/A		N/A
Anorthite [CaAl2Si2O8)	-19.77	-19.76	-19.71	-19.13	N/A	-22.12	-19.37		N/A

* Abbreviations: N/A = not available

The larger discrepancies in calculated SIs for the same mineral in Table 7 or 8 can be due to a number of reasons: differences in the stoichiometry for the same mineral, differences in the thermodynamic data for the mineral, differences in the thermodynamic data for the aqueous species and different methods for calculating the mixing properties of the aqueous phase. Remembering that SI is logarithmic, differences in the thermodynamic data for the aqueous species cannot explain all of the larger discrepancies in the SIs. The aqueous data for the free ions contained in Tables 5 and 6 show much smaller variations than those recorded in Tables 7 and 8. This suggests that the thermodynamic databases for the minerals contain significant differences. This is particularly evident for melanterite and the iron and aluminum hydroxides. Statistical analyses of the SI results of tables 7 and 8 are included in Appendix D.

Differences in the thermodynamic data used for the minerals can constitute a large source of error. Solid solution are not well represented, if at all. In low temperature environments, precipitating solids are often amorphous or poorly crystalline. Consequently, one "phase" may have a range of free energies depending on the degree of crystallinity. Generally, the more amorphous the phase, the greater its solubility. We suspect that the degree of crystallinity and the consequent different solubilities for the same mineral account for the larger discrepancies in the SIs in Tables 7 and 8.

The SI for a mineral does not depend on the aqueous species used to write the dissolution reaction for the mineral from which the SI is calculated. The reason for this is because the aqueous species are all related to each other through homogeneous equilibria (except as noted earlier for redox equilibria). As long as the reaction is chemically balanced, the SI of a certain mineral for a specific water will be constant no matter what chemical species are chosen to write the dissolution reaction. However, the SI does depend on the stoichiometry of the mineral. For example, the SI for calcite written as $Ca_2(CO_3)_2$ or two units of $CaCO_3$ would be twice that compared to the SI for calcite where the dissolution reaction was written using one unit of $CaCO_3$. This could be avoided by following the suggestion of Nordstrom (1995) of normalizing the SI by dividing by the total number of ions (or elements) in the mineral formula. This presently is not done. Consequently whenever the unnormalized SI of a mineral predicted by two codes is found to be consistently different by an integer number, an integer difference in the mineral formula stoichiometry used in the two databases should be suspected to be the cause of this difference. This observation also points out the danger of comparing SIs of different minerals calculated by the same program. A mineral with the largest SI does not necessarily precipitate faster than a mineral with a lower SI. The final point is that the SI of a mineral must go to zero at equilibrium, regardless of how many formula units are used.

Finally, the activity coefficient calculation method should only be used over the concentration range it is valid for. The ion association model should not be used at high concentrations (i.e. above ionic strengths of 0.1 to 1) while the specific ion interaction model can be used at all ionic strengths. The two models should give similar results below an ionic strength of 0.1. Therefore, both the Pitzer model and the Extended Debye-Hückel should apply to the brackish water. Comparison of the results from EQ3NR contained in Table 7 illustrates this. Generally, there is good agreement between the SI predictions of the Pitzer and the Extended Debye-Hückel calculations. This is not the case for the brine, as seen in Table 8. The difference between the two is generally greater than one and is particularly high

for alunite, one of the more complex phases for which there is enough Pitzer coefficients available to calculate its SI.

10.4 **Discussion**

There is no doubt that the Pitzer formulation can give a better thermodynamic representation of concentrated solutions or brines. Steady progress is being made in this direction, as seen in the work of Ptacek and Blowes (1994), where PHRQPITZ has been used to examine acid mine waters. However the thermodynamic data for the interaction coefficients needed for the Pitzer approach are incomplete. Not all waters can be modelled using the Pitzer method for activity coefficient estimation. The lack of data for Fe(III) for the Pitzer formulation poses a problem. In contrast, the thermodynamic data for the ion association method is quite complete. One method would be to use the Pitzer formulation for brine systems where Fe(II) dominates and in brine systems where Fe(III) dominates use the Extended Debye-Hückle or ion association model until Pitzer coefficients become available for Fe(III). This is exactly the approach used by Alpers and Nordstrom (1991). Although we can model the dilute waters of ARD quite well using an Extended Debye-Hückel approach, the complete thermodynamic properties of ARD brines are poorly defined. Large errors can be expected in modelling ARD brines due to the paucity of thermodynamic data for brines. However the geochemical codes can still be used for sensitivity analyses of brines to evaluate different pathways in ARD.

New programs are continuously being written for special applications or to consider unusual conditions (for example, WHAM by Tipping, 1994). Older codes are continuously being abandoned or heavily modified. Programs such as BAL, DISTRB, DIST, SPEC, BOIL and REACTION are just a few examples from the past. Sometimes they are rewritten and re-issued, sometimes they are just rediscovered by a new set of users.

Commercial software programs are evolving to the point where dedicated programs may not be necessary to make many of these calculations. An example is the program SPECIATE (Nesbitt et al, 1992), which can be used to calculate the distribution of species for over 40 elements at up to 150°C. It was written as a set of macros in Quattro Pro©, a spreadsheet supported and marketed by Borland. Macro programs such as these are not as fast and powerful as most of those discussed above. However, the ease of modification, the advanced plotting capabilities and the links to databases can make them interesting alternatives, especially for problems with unusual constraints.

10.5 **Summary**

- All of the examined models can estimate saturation indices (SIs). Agreement between ion pairing-based models is fair (within 25%), with the largest differences occurring for the high TDS water. Differences are attributed to differences in the thermodynamic databases. The largest differences in SI (i.e. greater than a factor of 2) result from the uncertainty in the thermodynamic properties of the poorly crystalline or amorphous solids, or the lack of thermodynamic data for the stability of one or several aqueous complexes.

- The most important task to be completed in the future for the equilibrium thermodynamic models for application to ARD is to improve their thermodynamic databases. None of the programs had thermodynamic data for all primary and secondary minerals likely to be encountered in weathering waste rock. For example, thermodynamic data for phases such as alunogen must be collected by experiment or estimated and added to the mineral databases.

- The stability of the carbonate minerals could not be calculated because the waters were not chemically analyzed for TIC. In order to determine the stability of the basic buffering minerals, TIC and dissolved silica must be part of the chemical analysis.

- Distribution of species calculations, such as undertaken by the equilibrium programs described above, is a mature technology. The SI predictions of the equilibrium models are for the most part similar. Any of the major programs can be successfully used to examine typical ARD problems, thus the choice of one program over another rests on the exact nature of the extended problem, availability of the programs and personal preference.

- WATEQ4F has the most complete mineral thermodynamic database pertinent to acid mine drainage. SOLMINEQ.88 pc/shell is most user-friendly thermodynamic equilibrium program. MINTEQA2 has the most complete ion exchange and adsorption capabilities, and is supported and approved by the USEPA; use of this program may be mandatory for projects examined by EPA. Previous and current versions of MINTEQA2 and PHREEQE are the most often applied to ARD problems.

- Large differences exist between ion association- and Pitzer-based models for prediction of mineral SIs in very high ionic strength waters. However, the Pitzer formulation, which is more accurate, suffers from paucity of data for the iron aqueous species. The Pitzer formulation is incorporated in the models PHRQPITZ and EQ3.

11. GEOCHEMICAL MASS TRANSFER MODELS

11.1 Background

Mass transfer geochemical modelling is the calculation of the various states (distribution of mass between the phases and species) that a "closed" chemical system undergoes as it proceeds towards thermodynamic equilibrium. Such "reaction path" calculations were pioneered by Garrels and Mackenzie (1967) and first solved using sophisticated computer models by Helgeson et al. (1969, 1970).

In the simplest sense, the initial system is composed of two or more subsystems, each of which are in internal thermodynamic equilibrium. One of the subsystems consists of the aqueous fluid, and any solids (or gases) in equilibrium with the fluid, while all other phases present are assigned to the other subsystems. Once the initial state of each subsystem is determined, a small amount of mass from each of the other subsystems is allowed to enter the fluid system, and the change in the amount and composition of each solid phase and the change in concentration of each aqueous species determined. The rate of interaction can be defined by the user (relative rates) or by using the kinetic rate laws and constants determined for each phase through experimentation. As the reactants (other subsystems) dissolve into the fluid, the existing equilibrium phases may dissolve or precipitate and new phases may appear. The process continues either to user-specified limits or until total equilibrium has been reached.

The restriction of a "closed" system can be lifted by defining the rate at which mass is added to the main subsystem or removed from it. For example, evaporation removes mass. Energy in the form of heat can also be added or removed. There are numerous other variations which can be included.

A simple example would be a system comprised of three subsystems: two piles of salt (one $CaCl_2$ and the other NaCl), and a beaker of hot water. A small amount of each salt would be added to the beaker based upon a rate equation, and the change in the fluid composition determined. Both salts would be added until the fluid is saturated with the first one, probably $CaCl_2$. At which point, the $CaCl_2$ subsystem would be included with the water subsystem as an equilibrium phase. NaCl would continue to be added to the fluid and the changes in the fluid composition monitored until all of the NaCl was used up or the fluid was saturated with NaCl. It is worth noting that the addition of NaCl would cause some minor precipitation of $CaCl_2$. In this example, the mass transfer model would determine the change with time of the mass of each salt and of the aqueous concentration of Ca, Na and Cl. A more complex example would be very similar to the one above, except for much more extensive bookkeeping due to the possible appearance or disappearance of many more solids, and due to the presence of many more aqueous species and complexes.

11.2 **Specific Models**

11.2.1 EQ6

EQ6 (Wolery, 1992a; Wolery and Daveler, 1992; Wolery et al., 1990; Delaney et al., 1986, Delaney and Wolery, 1984) is a reaction path model supplied as part of the EQ3/6 software package. It is the most widely used mass transfer package in North America for three main reasons: first, it is a powerful and comprehensive model; second, it has been well tested by a large number of users; third, it has excellent documentation published by Lawrence Livermore National Laboratory. Its main disadvantage is that it is complex and not easily mastered by the casual or untrained user. A PC version is being prepared, but at present it needs to be run on a workstation or larger computer.

EQ6 uses problem data prepared by EQ3 to define the initial solution composition, a set of user-specified input parameters to specify the solid phases and temperature changes, and the appropriate thermodynamic database (one of the five supplied with the EQ3/6 package). The user can specify a titration model, fluid mixing, reaction in a closed system, reactions in some simple open systems, and heating/cooling processes. Rate laws for dissolution and growth kinetics are included, but relative rate laws can also be specified. A gas buffer can be applied to the system. One powerful option in EQ6 is the ability to model solid solution in minerals.

In addition to the normal problem specification, the user has a wide range of options to control convergence, printing, numerical methods for solution, overriding of database information and a variety of other parameters. The program output consists of a detailed printout, a restart file to continue the run, and several terse output files which can be parsed for plotting or summarizing purposes.

11.2.2 CHILLER

CHILLER (Reed, 1992; Reed and Spycher, 1984, Spycher and Reed, 1988, 1990b) is a reaction path model which was originally developed to model the geochemistry of hydrothermal ore genesis, particularly in the presence of a gas phase (epithermal deposits). CHILLER has been improved over the years and includes provision for reaction of a fluid with solid phases, and mixing of fluids of different temperatures. CHILLER includes provision for gas non-ideality and for non-ideal solid solutions of solid phases. In addition to the normal output file, CHILLER writes restart information and plot information to separate output files. CHILLER is strongest for the handling of processes involving gases. It handles evaporation, isothermal and isobaric boiling, boiling following a preset temperature/pressure path, boiling with an enthalpy constraint and condensation. CHILLER uses the ion association method, incorporating the Extended Debye-Hückel equation, to estimate activity coefficients of aqueous species. CHILLER is a compact program and runs easily on a PC. An accompanying program, MINPLOT, is used to plot the generated data.

A disadvantage of the CHILLER model is the need for user-specified "relative" rate laws to define the rates at which mineral reactants are added to the fluid. Besides the need to decide on the rates, the user has to specify a fixed step size for reactant addition. In problems where the rate of

reactant addition changes significantly with time, the program may have to be stopped to change the step size, then restarted. This may have to be repeated several times in order to obtain a complete run. If the specified step size is too large, the program may not converge or it might miss some small events. Like EQ6, CHILLER has a number of options, including convergence value modifiers to overcome convergence problems in difficult simulations.

11.2.3 PATHARC

PATHARC is a reaction path model with provision for fluid mixing at a user specified rate and evaporation. PATHARC uses kinetic rate laws for dissolution and precipitation kinetics. A gas buffer can be specified to constrain the process being modelled. Output includes detailed text of the chemistry and reactions and files containing plot information. Activity coefficients of aqueous species are calculated by PATHARC using the ion association method and the Extended Debye-Hückel equation. If the user specifies that no times steps be taken, then PATHARC essentially becomes an equilibrium geochemical thermodynamic model, similar to the equilibrium models discussed previously.

The strength of PATHARC is that the current version has been incorporated in a user-friendly, windowing, menu-driven PC environment. The user can prepare detailed plots on the screen and print them on a range of supported printers, including colour lasers, by selecting one or more screen options with a mouse. Currently supported plots include: the mass (or the change in mass or the volume %) of any number of solid phases as a function of time or log time, or as a function of the mass, change in mass or volume % of any solid; the molality (or log activity) of any number of aqueous species or complex as a function of time, log time or the molality (or log activity) of any species or complex. Similar plot capabilities also exist for gases.

PATHARC follows reaction paths by integrating derivatives with respect to time, a different numerical methodology than the other models. This has certain accuracy and speed advantages under most circumstances. Unfortunately, it can lead to very small step sizes and long runs under other circumstances. When numerical drift exceeds a specified level, PATHARC uses similar numerical methodology to CHILLER and EQ6 to reduce the drift. Like EQ6, it adjusts step sizes according to process occurrance and to user-specified constraints.

Two restrictions of PATHARC are that it is restricted to modelling iso-thermal processes and that it does not include provision for solid solution mineral phases in the program structure. Another restriction of PATHARC is that the users are not allowed to change internal convergence parameters.

11.2.4 REACT

REACT (Benthke, 1992) calculates the mass transfer which occurs between a fluid and a set of minerals, either isothermally or along a temperature path. The mineral reactions can be arbitrary or specified with a simple rate law. Alternatively, the user can specify that the system will evolve from one condition to another, for example move from pH=5 to pH=6.5. If no steps are specified, REACT runs as an equilibrium geochemical thermodynamics model, similar to that described in the previous section. REACT allows fluid mixing using the "flush" model, buffered components, and flow-through modelling

where minerals are prevented from dissolving once they precipitate. REACT can use a number of databases, including those based upon an Extended Debye-Hückel activity coefficient model, a Pitzer activity coefficient model and the model of Harvie, Möller and Weare. Another option is the ability to trace the equilibrium fractionation of the stable isotopes over the course of a reaction path.

The output from REACT can be read by a plotting program called GTPLOT, and displayed on the screen. Almost all system variables can be plotted on the ordinate axis while the abscissa can be selected from one of about 15 system variables. A useful feature is the ability to graphically and automatically display and update the REACT output as it is calculated. Although REACT and GTPLOT run on UNIX workstations under the Motif graphical interface, provision has been made to display the output on a variety of output devices, including ASCII terminals and a variety of printers.

11.2.5 STEADYQL

STEADYQL (Furrer et. al, 1989; 1990) is a mass transfer program that has been specifically designed to model reactions in soil horizons, and thus specifically includes flux into and out of the volume. STEADYQL assumes there are three classes of reactions: equilibrium (fast), kinetically controlled (slow), and buffered (fixed for the run). STEADYQL also includes provision for degassing, ion exchange and adsorption. The user specifies all reactions, equilibria and kinetic constants, therefore allowing enough flexibility to add dissolved or solid constituents. However, since the number of reactions has to be fixed by the user, this model is less general than some others. The model also assumes that all reactions will go to steady state, which is generally not the case in waste rock piles.

In a recent paper, Strömberg and Banwart (1994) used column tests to develop a specific set of input parameters to apply STEADYQL to a waste rock pile at the Aitik copper mine in Sweden. This recent effort represents significant progress in waste rock geochemical modelling. Relevant conclusions include (1) the relative weathering rate of minerals taken from the literature are correct for ARD, (2) iron oxidizing bacteria are important, (3) BET measurements of surface area in the lab are two orders of magnitude too high compared to reactive surface area, and (4) the silicate minerals are the most significant control on neutralization of acidity at this site. These conclusions are in agreement with those stated in Part 1 of the present report.

11.3 **Mass Transfer Modelling of the Stratmat Column Experiments**

The test data set for mass transfer models was taken from the recent lysimeter study on waste rock from the Stratmat property (Yanful and Payant, 1993). Potentially acid-generating samples from the Stratmat site were used in lysimeter tests to evaluate cover strategies. Here we examine the data from the leaching of three control columns. The mineralogy of the waste rock used in the experiments is presented in Table 9, and the chemistry of the leachate is presented in Table 10.

Each experiment was run in triplicate, and subjected to cycles of eight weeks of wet conditions and eight weeks of dry conditions for a period of approximately three years. The wet periods were physically simulated by doubling the average weekly rainfall for the year and adding this amount of distilled water (650 ml) weekly to the columns. One of the uncertainties from the Stratmat column

experiments is whether the oxygen supply becomes depleted in the columns between aqueous flushes. Therefore, two extremes of oxygen entry were considered for the mass transfer modelling of the Stratmat column experiments. In one case, the minimum oxygen available for reaction was assumed to be that of oxygen saturated in water with no addition by diffusion once the water enters the column. For the other case, the maximum oxygen available for reaction was assumed to be one mole per kilogram of water. This quantity was based on the total pore volume of the column assuming that the air present is replaced once by advection during one leach cycle. The first scenario will be referred to as "unbuffered" O_2 and the second as "buffered" O_2.

For each mass transfer run, the mineralogy (Table 9) was allowed to react with rain water. The change in water composition with time was calculated by each model and the results were plotted against time, or, when relative rates of reaction were used, against the amount of minerals added. The results were compared to the water chemistry measured in the laboratory (Table 10) for validation.

Table 9. Average mineralogy of Stratmat waste rock samples used in lysimeter tests

Minerals	S.G. (g/cc)	Weight %	Volume %
Quartz	2.65	35.0	40.07
Muscovite	2.82	30.0	32.27
Albite	2.63	5.0	5.77
Fe-Chlorite	3.3	6.0	5.51
Mg-Chlorite	2.6	3.0	3.50
Dolomite	2.86	0.2	0.21
Siderite	3.5	0.3	0.26
Rhodochrosite	3.7	0.1	0.08
Pyrite	5.00	20.	12.14
Sphalerite	4.1	0.1	0.07
Chalcopyrite	4.2	0.1	0.07
Galena	7.5	0.1	0.04
TOTALS	Av. SG=3.22	99.9	99.99

Note: Although siderite and rhodochrosite were not specifically identified, microprobe analyses by McGill University indicate the presence of ankerite and high amounts of manganese in the dolomite.

Table 10. Leachate from NTC indoor ARD STRATMAT column leaching experiments, 29/09/93

A.R.D.	Ctrl#1	Ctrl#2	Ctrl#3
Specie	mg/L	mg/L	mg/L
Na	6.1	6.1	6.1
K	<5.0	<5.0	<5.0
Ca	105.	147.	138.
Mg	456	597	532
Mn	36	59	41
Fe++	430	440	490
Fe+++	3370	3160	3510
Al	470	577	543
SiO2	86	97	110
Cu	7.4	10.9	11.8
Pb	<.25	<.25	<.25
Zn	81	339	66
As	17.5	19.5	26.8
Cd	0.33	0.82	0.43
Co	0.39	0.48	0.43
Cr	<.03	<.03	<.03
Ni	0.16	0.20	0.16
Sb	2.67	2.60	2.47
Se	0.81	0.94	1.13
Te	0.60	0.58	0.64
Tl	<.25	<.25	<.25
SO4	13603	15251	15011
Cl	N/A	N/A	7.4
HPO4	N/A	N/A	<.10
NO3	N/A	N/A	<.05
^Chg	N/A	N/A	N/A
TDS	N/A	N/A	N/A
Acidty	10136	10558	10664
pH@25C	2.29	2.28	2.25
Eh	N/A	N/A	N/A

* N/A = not available

Numerically, it is very difficult to follow a reaction path over an extremely large change in a small component. The transition between oxidizing to reducing conditions, which can be called the oxygen "cliff", is the most common case. The activity of dissolved oxygen changes from near atmospheric conditions to values in the order to 10^{-50} over very small changes in the other components. Reaction step size has to be very small at this point and consequently, the simulations can take a very long time to complete, or even fail under these conditions. A massive amount of programming is required for geochemical codes to handle these sharp fronts. The problems are the worse in dilute solutions when no phases are present to buffer the conditions.

Three mass transfer models were tested: CHILLER, PATHARC and EQ6. During the "oxygen cliff" conditions, PATHARC and EQ6, take very small steps and large amounts of computer time. The step size may become small enough that these programs stop, necessitating a restart run with slightly modified parameters. In CHILLER, the user defines the titration increment step sizes to get past the front.

The amount of program output for this class of models is very large thus, for reasons of brevity, the results were only presented in graphical format. Both CHILLER and PATH.ARC have graphical output routines distributed with them; however, EQ6 does not. A statistical analysis of the mass transfer modelling results is done in Appendix D. A typical portion of an EQ6 output has been included in Appendix E.

11.3.1 CHILLER

The minerals were allowed to dissolve in the proportions present in the Stratmat column (Table 9) because kinetic rates of mineral dissolution and precipitation can not be specified in this model. The two cases modelled are presented in Figures 12 ("unbuffered case" i.e water saturated with oxygen at 25°C) and Figure 13 ("buffered case" i.e water buffered with one mole of atmospheric oxygen). The rates used are the default relative rates, and the results are plotted against the amount of minerals added, labelled "grams of minerals titrated". The thermodynamic database used with CHILLER is incomplete with respect to waste rock minerals. This affects the identity and sequence of secondary minerals forming as a result of sulphide reactions. A low temperature database is also available for CHILLER but was not accessible in time to use for the calculations carried out here.

The reactions are driven by the oxidation of the sulphide minerals, which lowers the pH (Figure 12a [unbuffered] and 13a [buffered]) and causes hematite (Figures 12b and 13b) to precipitate. The minerals appear in the order: hematite, followed by gibbsite, which is replaced by kaolinite and then followed by quartz. This set of minerals continue to form until the activity of oxygen drops from saturation with the atmosphere to a molality below 10^{-50} (Figures 12c and 13c; it appears as 10^{-50} on the figures as the plot program supplied with CHILLER defaults to this value). At this point the sulphide minerals rapidly become saturated, the pH starts to rise and total dissolved iron rises rapidly (Figure 13e) due to the dissolution of hematite (caused by the rapid decrease in oxygen partial pressure):

$$Fe_2O_3 + 4H^+ \rightarrow 2Fe^{++} + 0.5O_2 + 2H_2O$$

As pH steadily increases, pyrite starts to precipitate and hematite reprecipitates (Figures 12b and 13b) and steadily increases in amount. The excess oxygen necessary for formation of hematite is provided by the reduction of sulphate:

$$15Fe^{++} + 2SO_4^{=} + 13H_2O \rightarrow FeS_2 + 7Fe_2O_3 + 26H^+$$

The excess H^+ is consumed by the continued buffering action from the congruent solution of the carbonate minerals and the incongruent dissolution of the silicate minerals which continue forming kaolinite and quartz. The difference between the unbuffered and the buffered oxygen case is that the excess oxygen in the buffered case allows the sulphate (Figures 12d and 13h) to build up high enough in solution so that anglesite and alunite precipitate (Figure 13d).

As expected, the pH reached a minimum at which point the dissolved oxygen was rapidly depleted and the Fe(II)/Fe(III) ratios reversed to Fe(II) being dominant. This oxygen "cliff" (Figures 12c and 13c) occurs when 0.04 grams of rock have reacted (i.e. rock "titrated") for the unbuffered and 156 grams for the buffered case. Only for the buffered case does the pH reach the value observed in the Stratmat control experiment (pH=2.2, Table 10). The concentration of total iron (Figure 13e) is also similar to the experimental values observed in the Stratmat control experiment, but only when dissolved Fe(II) is the dominant species (Figure 13f). Most of the Fe(III) has precipitated as hematite (Figure 13 b and g). The model does not match the Fe(III) values observed in the experiments, probably because hematite is much more stable than ferrihydrite.

Even though ferrihydrite is more soluble in these environments, it nucleates first (Nordstrom et al., 1979a) and can slowly dehydrate to form goethite and hematite (Nordstrom, 1982). Morin et al. (1988) also consider ferrihydrite as the most likely iron oxy-hydroxide to precipitate in the Nordic Main tailings area, although in some cases they feel goethite may precipitate first. If the dissolved Fe(III) is controlled by the precipitation of ferrihydrite, then the dissolved Fe(III) could build up higher in the aqueous phase before saturation is reached. Another possibility is that the sample was improperly preserved and some of the Fe(II) oxidized to Fe(III) before the chemical analysis was made. The dissolved sodium, potassium, aluminum and copper predicted by the model are significantly higher than the experiment. Lead, zinc, manganese, calcium and magnesium are in reasonable agreement.

The absence of rate laws in CHILLER may explain some of the disagreement. As stated before, in nature the carbonates are fast acting compared to the silicates. The only sources of aluminum, potassium and sodium are the silicate minerals. They were actually titrated into the solution faster than the carbonates because of their much greater abundance and therefore the aqueous phase would be expected to see an accelerated rise of the alkalies and aluminum over that expected if kinetic rates

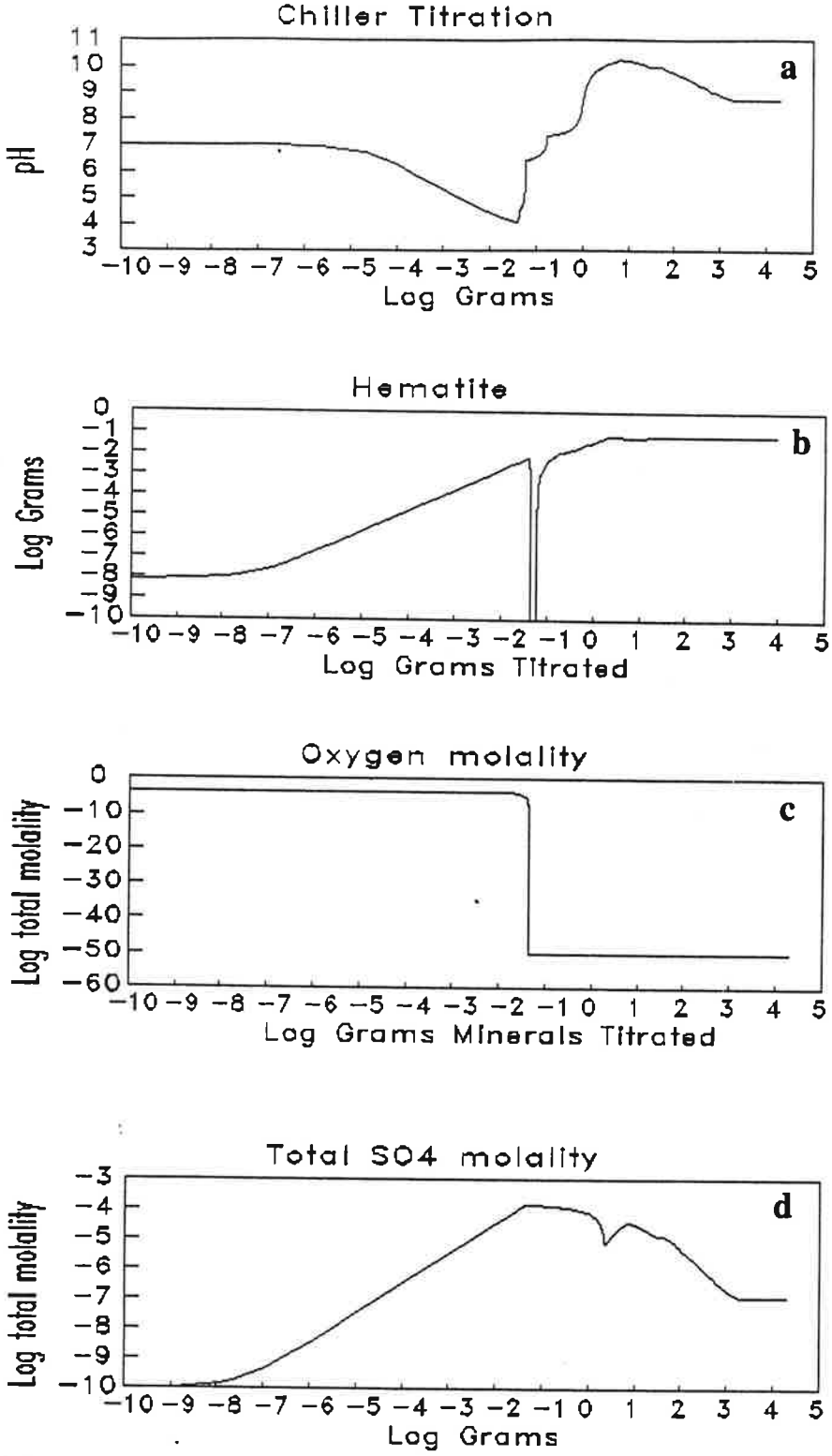

Figure 12. **CHILLER results, oxygen saturated in water, no excess oxygen (unbuffered case)**

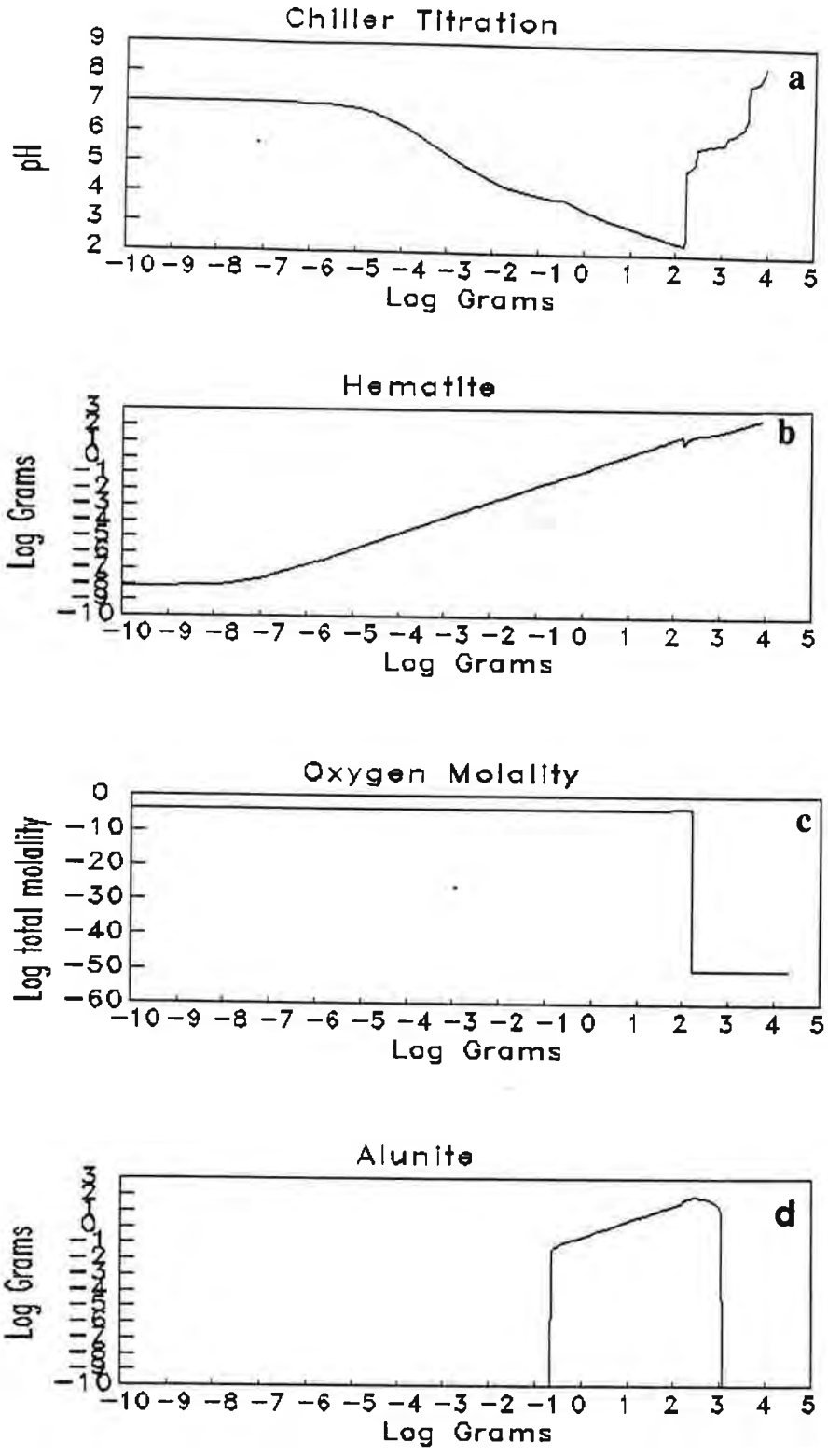

Figure 13. **CHILLER results, oxygen saturated in water, 1 mole of excess oxygen (buffered case).**

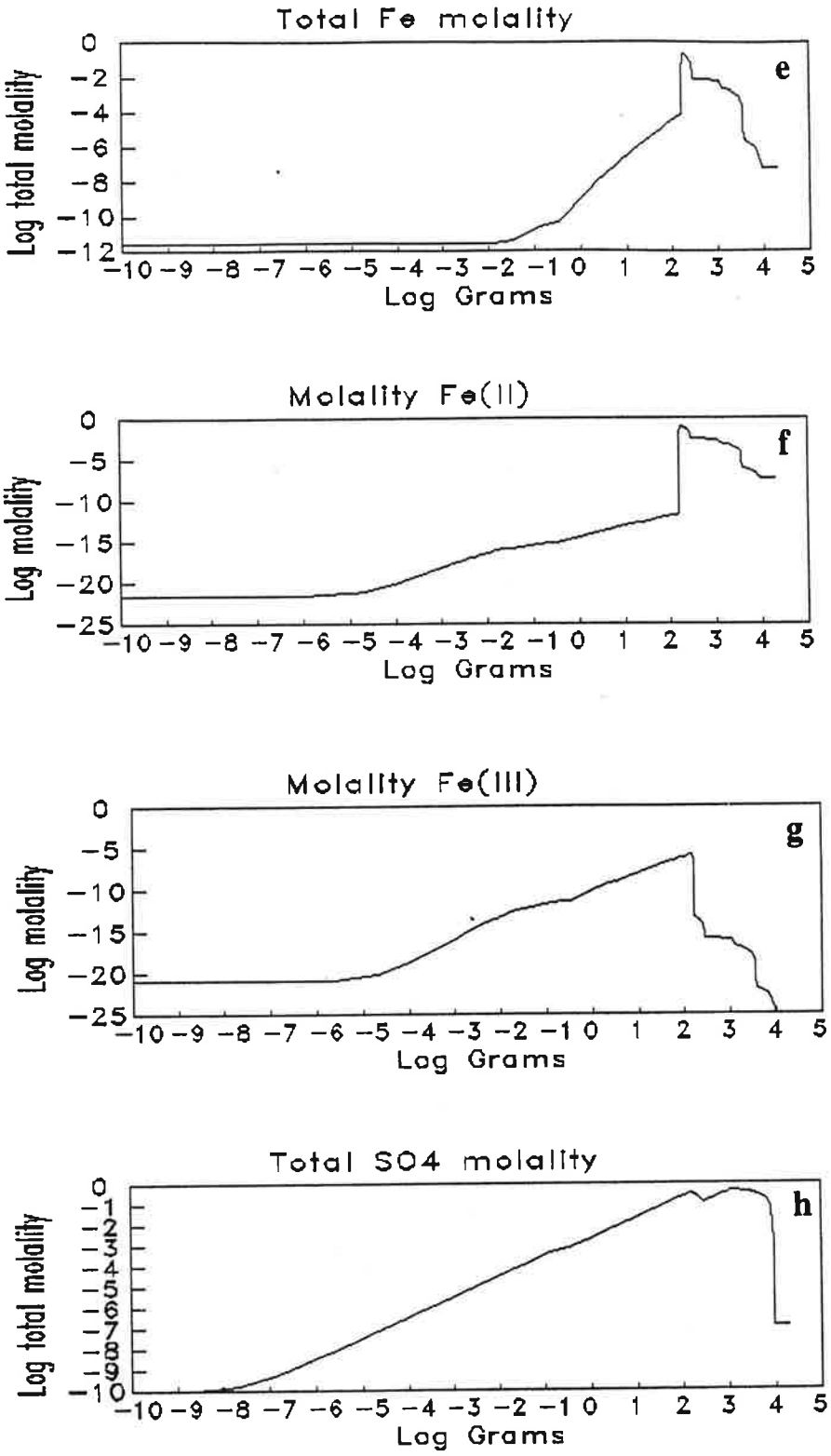

Figure 13 (cont'd). **CHILLER results, oxygen saturated in water, 1 mole of excess oxygen (buffered case)**

were used. This buildup could be reduced by artificially reducing the relative rates of the silicates to the carbonates. However since kinetic rate laws cannot be used in CHILLER at this time, the relative rates are only fitted parameters. Another possibility is that the thermodynamics of the controlling mineral phases are incorrect, but this is unlikely. It is possible that the thermodynamics of the aqueous complexes are in error; that is the aluminum complexes are too stable relative to aluminum. In Table 6, where the results of equilibrium geochemical thermodynamic models were compared using a brine, the SOLVEQ model, which has a database common to that of CHILLER, predicted the lowest value for the concentration of the free aluminum ion of the seven models tested, which would result in the highest value for total soluble aluminum from the dissolution of aluminous phases.

11.3.2 PATHARC

As in the CHILLER simulations, the Stratmat column mineralogy and fluid composition, with one mole of oxygen as an initial reactant, were used. However the PATHARC run only simulated an oxidizing environment; the simulation was not run long enough to reach a reducing environment. The volume fraction of each mineral in the column was used to specify the initial grain size and surface areas. No further attempt was made to obtain better values. The main thermodynamic database for PATHARC can include elementary rate equations for dissolution and precipitation kinetics, thus rate information was specified for the appropriate phases which were identified in the Stratmat column experiments. The rates specified were functions of pH, Fe(III), O_2, CO_2, OH, and/or a constant. If no rate data existed, equilibrium was allowed to control the formation of new phases.

The simulation was stopped after one mole of oxygen had reacted, which was predicted to take 4 1/2 years (Figure 4). The maximum rate of change occurred within the first year. This is shown clearly by the pH versus log time (Figure 4a) and the pH versus time (Figure 4b), where the pH rapidly dropped from 7 to approximately 4.5, held constant for several months, then dropped to the mid 2 range, where it remained constant for the rest of the run. This pH value is consistent with the pH in Table 10. At the time the simulations terminated, the predicted levels of magnesium and sodium were approximately one-third of the experimental values, while the predicted levels of calcium and aluminum were much lower. The lower values of magnesium and calcium were due to the predicted precipitation of anhydrite and antigorite, phases without rate terms in the thermodynamic data base. The only solid sources of sodium and aluminum in the reactant phases are the silicate minerals. Therefore, the sodium and aluminum concentrations in the water must be directly related to the congruent or incongruent dissolution of the silicate minerals.

The aqueous cation components complex significantly with sulphate, and under high sulphate loads their solubility will be dominated by sulphate complexes (see aluminum, iron and sodium on Figures 4c, 4d and 4e). Thus as sulphate levels rise further, more cations will be present in solution.

Figure 4f shows the effects of the difference in reaction rates on the change of mass of some of the phases from the simulation. The carbonates (only siderite is shown on this Figure; see also Figure 4h) react the quickest. Pyrite dominates because of the rapid reaction rates and the large mass present. Anhydrite precipitates thus buffering the calcium in solution (also shown in Figure 4g). The change in

the silicates (illustrated here by chamosite) can not be seen because the rates of silicate mineral dissolution are much slower than for sulphide and carbonate minerals.

Figure 4h shows one of the significant effects of buffering acid production through reaction with carbonate minerals, carbon dioxide gas production. The amount of carbonate minerals present (dolomite, rhodochrosite and siderite) decrease rapidly to zero over a few months. As this occurs, ferrihydrite precipitates (Figure 4g) and the amount of inorganic carbon in solution increases until carbon dioxide gas is released from the water to the atmosphere. In this simulation, almost 0.1 moles of carbon dioxide gas was released as a result of the carbonate minerals buffering the pyrite dissolution.

The effects of buffering of the carbonate minerals can be clearly seen in Figures 4b and h. The dissolution of siderite, dolomite and rhodochrosite buffer the solution at a pH of approximately 4.5 until the rate of pyrite dissolution (Figure 4f) and ferrihydrite precipitation (Figure 4g) starts to dominate the pH control. The pH then falls in two steps to 3.4 and 2.6. At a pH of 3.4, all the siderite and rhodochrosite have been consumed and at a pH of 2.6, the dolomite has completely reacted out. At this point, ferrihydrite redissolves and buffers the pH at 2.6 for a period of 4 years, after which it disappears (Figure 4g); the pH would then be expected to drop further, but the run was stopped at this point.

As mentioned previously, CHILLER was run from oxidizing to reducing conditions while PATHARC was only run under oxidizing conditions. The differences between the PATHARC simulation and the CHILLER simulation in the oxidizing region are a mostly result of PATHARC using rate laws to control dissolution and precipitation, while CHILLER uses arbitrarily specified rates. Differences in the thermodynamic data base of each program also modify some of the details of the calculated reactions, but this is not as significant as the omission of "kinetic" rate laws in CHILLER. It is important to note that even if there are some differences, the basic processes in both simulations are similar: the drop in pH expected from the dissolution of pyrite is countered by the dissolution of the carbonate minerals such as calcite and siderite, then hydroxide minerals such as ferrihydrite. The dissolution of the silicate minerals is important because it provides long-term buffering and provides alkali metals and Al into solution which later form secondary minerals.

The differences between the PATHARC simulation and the actual Stratmat leach data can be explained in part by the precipitation of anhydrite and antigorite. These were treated as phases without kinetic data, thus they precipitated much too rapidly and limited the amount of magnesium and calcium. On the other hand, PATHARC predicted too high Fe(III) and SO_4 concentrations which can be attributed to the lack of an Fe(III)-SO_4 mineral phase in the thermodynamic database. For example precipitation of jarosite could control the levels of soluble Fe(III) and SO_4 in the solution, but this phase was not present in the PATHARC database. Another difference between the simulation and the experiments is the difference in the elapsed time. Reaction rates, hence elapsed times, are directly proportional to surface area which is one of the hardest parameters to estimate. No attempt was made to optimize this parameter in the PATHARC input.

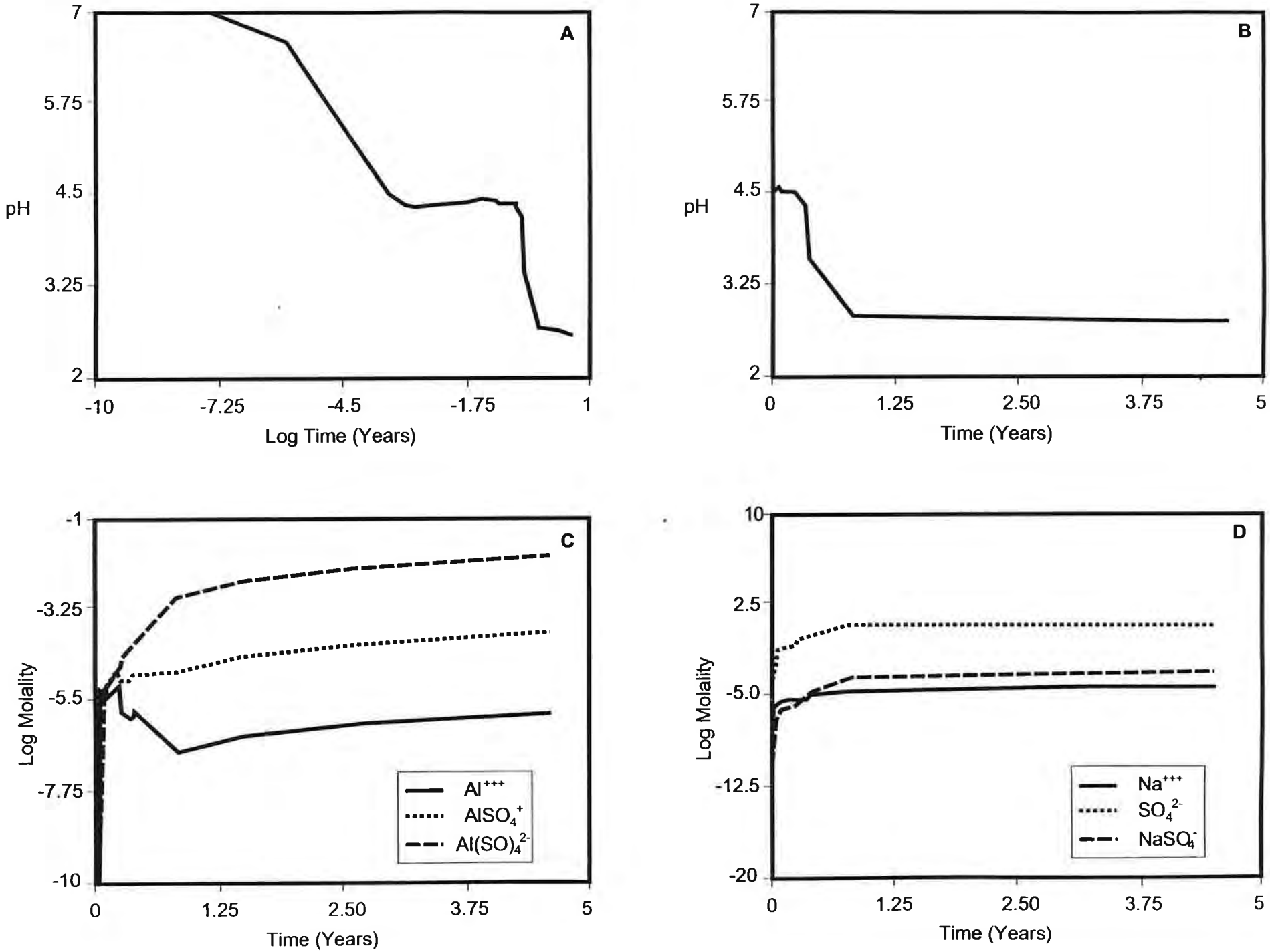

Figure 14. PATHARC results

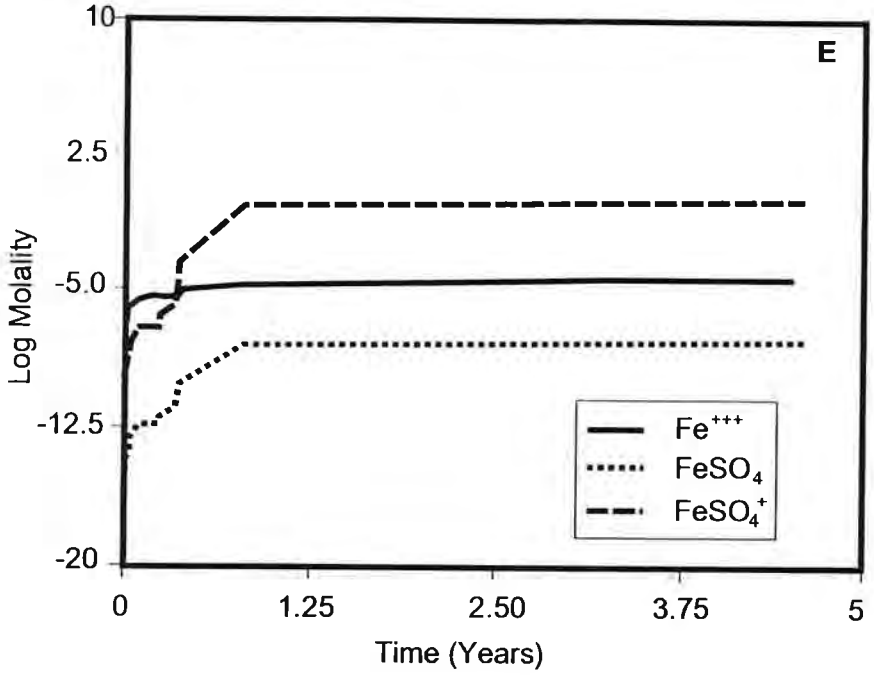

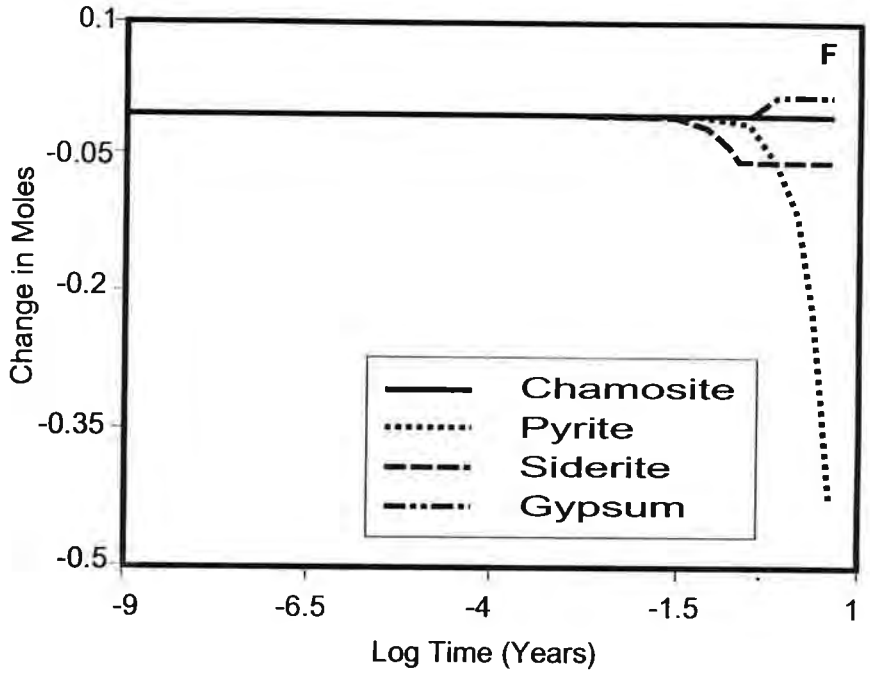

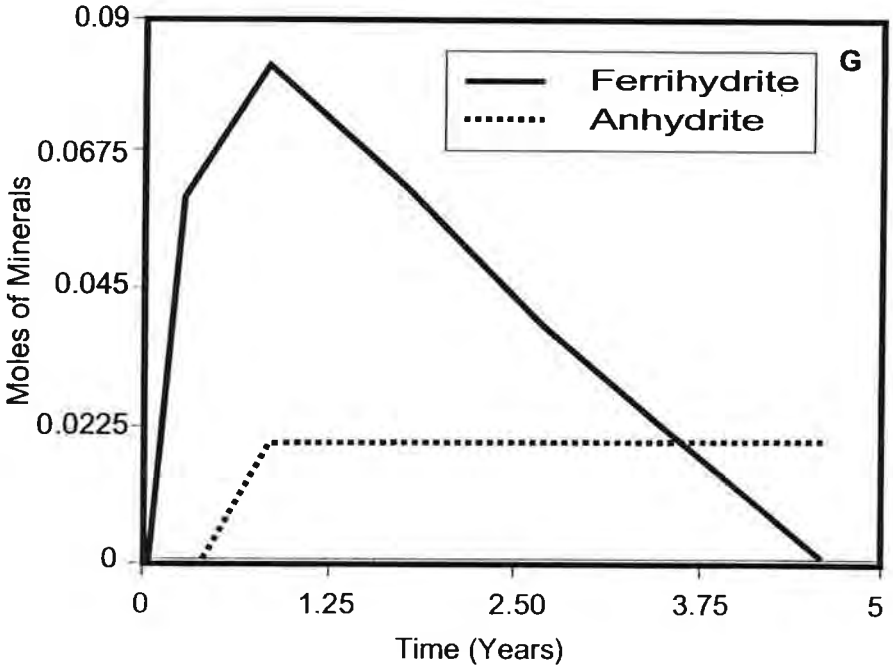

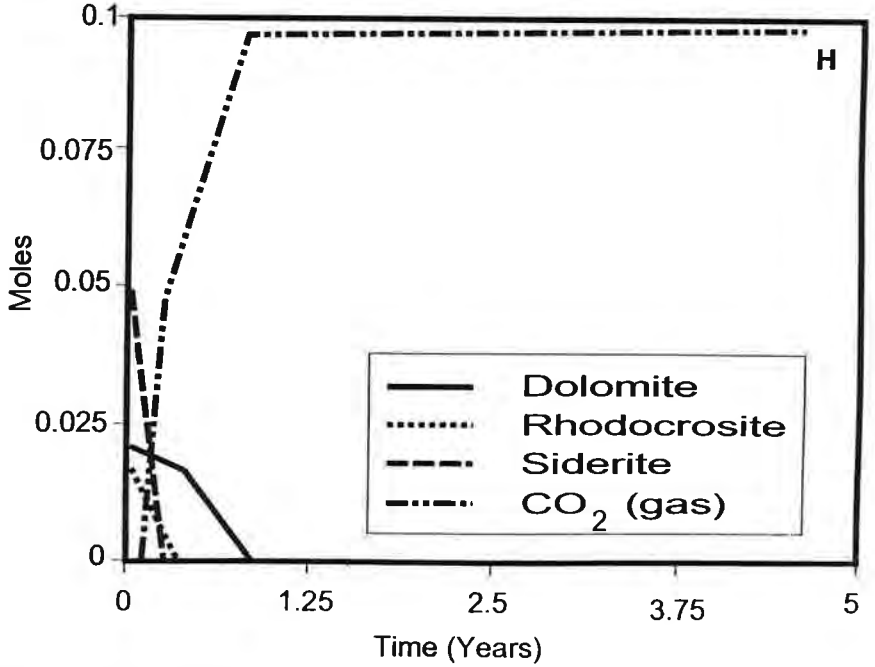

Figure 14 (cont'd). PATHARC results

11.3.3 EQ6

EQ6 was used to simulate the reactions occurring in a rock pile, with results similar to the simulations of CHILLER and PATH.ARC. The output was written to a series of files, and a representative portion of the output has been included in Appendix E.

The conditions simulated used an initial set of reactants based on the Stratmat column mineralogy (as was used for CHILLER and PATHARC; Table 9) which reacted with an initial fluid (rainwater) at a fixed oxygen fugacity (partial pressure). Approximately 3.2 days after the reactions have begun, the fluid has dissolved some of the initial phases, and has come to equilibrium with the following pure minerals; ordered dolomite, kaolinite, pyrolusite and quartz. The fluid has also come to equilibrium and begun precipitating a clay mineral, a divalent smectite with 12 end members, described by the calcium, magnesium, potassium and sodium end-members of beidellite, montmorillonite and nontraonite. The pH has not shifted significantly at this point as it is being buffered by the carbonate and to a lesser extent by the silicate reactions.

As time progresses, the carbonate minerals disappear and the sulphide reactions overpower the slower reacting silicate buffering phases, and the system quickly becomes more acidic with much higher sulphate levels, very similar to the simulations previously discussed. The temporal differences between the EQ6 runs and the PATH.ARC runs are a direct result of slightly different kinetic parameters being used and different mineralogies in the database, while the slightly different intermediate mineralogy predicted by EQ6, PATH.ARC and CHILLER is a direct result of differences in the thermodynamic databases used in the simulations.

11.4 **Discussion**

The graphical output of the mass transfer models clearly illustrate the interdependence of reactions occurring in waste rock. These graphs, as well as the text output from EQ6 in Appendix E, also show the complexity of the calculations.

CHILLER, PATHARC and EQ6 can all simulate evaporation which is an important process in the unsaturated zone of waste rock piles. However in the simulations presented here, only oxidation, dissolution and precipitation were modelled; the effect of evaporation was not modelled. Evaporation would provide a concentration increase and would result in the precipitation of more sulphate minerals. This would be followed by a dilution event as more water was added to the column and the sulphate minerals would dissolve. This cycling of the secondary sulphate precipitates would control the TDS of the waters during flushing events. Obviously, to decide on a unique path for these events is difficult unless one knows the rate of evaporation followed by the rate of mixing of the water upon addition of the next increment of water. However, these events do occur at regular intervals in the column and would have been responsible for additional evolution in the water composition. This would also add to the differences between the measured water chemistry and that modelled by simply adding oxygen. The fact that the simple mass transfer calculations were able to evolve a fresh water into a

contaminated water that was similar to a water that was produced in a column experiment provides hope that more complex mass transfer calculations could lead to a relatively accurate simulation, providing that the physics of the column experiment were modelled in detail.

As was mentioned in the section on the equilibrium geochemical thermodynamic models, modern software programs are advancing to the point that dedicated programs may not be necessary to make many of these calculations. A recent example is Steinmann et al (1994) who prepared a simple mass transfer program using a commercial spreadsheet program, and a more complicated mass transfer program using Mathematica©. They compared the results to ones from MPATH (discussed in the next section) and concluded that they were reasonable. They also concluded that simpler programs illustrate the basic principles of mass transfer and are suitable for teaching. These simple models should be used only for cases where their assumptions are fully verified by field and experimental observations.

11.5 **Summary**

- Mass transfer models can be used to perform modelling of fluid-rock interactions in waste rock while taking into account reaction kinetics. However, other than a few applications such as those in this report and the application of STEADYQL, none have been used.

- STEADYQL has recently been applied to examine water-rock interactions at the Aitik waste rock pile in Sweden. This recent effort represents progress in waste rock geochemical modelling because it is the first kinetic modelling application to an ARD field situation. More applications of mass-transfer models to ARD problems should be done.

- EQ6 is the best documented mass transfer program. Five different thermodynamic databases are provided, including a Pitzer database. It is the only mass transfer program to include solid solution for minerals.

- PATHARC runs on a personal computer, and is the most user-friendly mass-transfer program due to its windowing interface for user input and graphical examination of output. It includes multi kinetic terms for dissolution and precipitation, but can only handle iso-thermal iso-baric problems.

- CHILLER is best for handling gas equilibrium, boiling or condensation. It runs on a personal computer. User must specify relative rates of reaction for each phase as kinetics are not included in the program. The program uses a user-specified, fixed step size which may necessitate a number of runs to completely model a process.

- REACT is user-friendly, and includes provision for a number of databases, including a Pitzer database. REACT takes advantage of the Motif graphical interface on UNIX workstations to provide a well integrated environment for modelling.
- The mass-transfer models which should be most considered for application to ARD prediction problems are EQ6, for completeness, and PATHARC, for PC-based efficiency.

12. COUPLED GEOCHEMICAL MASS TRANSFER - FLOW MODELS

12.1 Background

There are many problems with the coupling of flow, mass transport and mass transfer, the most serious being the relative time scales of the processes. Equilibrium in a fluid for many aqueous species occurs in milliseconds, while reactions between solids and fluids can take 100 to 200 times longer. Fluid flow, heat transport and solute transport have their own characteristic times. Each process has their own characteristic representative volume as well. Numerical techniques have been, and continue to be, developed to address this serious problem. Nevertheless, the definitive work is yet to be written.

Two other practical difficulties with coupled models are:

- Software limitations: for example, EQ3/6 consists approximately 60,000 lines of Fortran code. To program and couple equivalent capabilities with a flow/transport computer code is a massive undertaking.

- Hardware limitations: some closed system mass transfer calculations can last for tens of hours of computing time on a workstation. Computing resources required to repeat these calculations for any significant number of grid blocks are too large for most users.

The traditional approach to solving this problem, generally taken by people with a background in groundwater hydrology or reservoir modelling, has been to develop or take an existing 2-D or 3-D fluid flow code and to include transport equations for one or more components. The components are often inert or react with the solid matrix through a simple distribution coefficient (or K_d). In recent years, these models have been extended by the needs of the oil industry to predict thermal-enhanced oil recovery (or similar processes) or by groups concerned with the need to predict the fate of subsurface contaminants. In some models, the complexity of the reaction terms and the number of components have increased, while in other models, the ability to deal with thermal events (temperatures up to 350°C) and flashing/condensation has been included.

An alternative approach has been taken by those with a background in geochemistry. These individuals concentrate their efforts in describing the geochemical reactions that occur between the fluid and the formation, and only the minimum necessary effort to provide fluid flow, heat flow and solute transport. The geochemical portions of these codes are essentially open system versions of the mass-transfer models described in the previous section of this report. The methods used to couple the flow and transport equations to the geochemical equations vary from model to model, and primarily depend upon the class of problem that the author intended to address.

12.2 **Specific Models**

12.2.1 REACTRAN

REACTRAN simulates one-dimensional flow of an aqueous solution through a reactive porous medium and predicts the temporal and spatial distribution of aqueous species and minerals a system. The conceptual model and theoretical background to REACTRAN is described by Ortoleva et. al (1987). REACTRAN divides all chemical reactions into two classes, depending upon their rate of reaction. Those that are fast compared to the time step used to model the process are treated as equilibrium reactions, while those that have a similar or longer time scale use specific rate equations.

As part of the input for REACTRAN, the user specifies the initial mineralogy, the initial fluid chemistry and the temperature gradient along the flow path. The user also specifies all possible reactions, both for the aqueous species and solid phases and, if appropriate, their rate constants. The program begins by initially calculating the flow field. The transport of the dissolved species by advection, diffusion and dispersion is calculated. The amount of material entering the fluid through rate controlled mineral dissolution is also included. At the end of each step, the fluid and the equilibrium phases are brought into internal equilibrium. All non-equilibrium phases are checked to see if they have been completely dissolved or come to equilibrium with the fluid. If the porosity and permeability have changed significantly, then the flow velocities are updated. The next time step is taken and the process is repeated.

In addition to numerous modelling studies of natural systems, REACTRAN has been used to model core flood experiments for the oil industry (Haskin et. al, 1989).

12.2.2 CIRF.A

CIRF.A simulates the two-dimensional flow of an aqueous solution through a reactive porous medium and predicts the temporal and spatial distribution of aqueous species and minerals. The numerical methods used in CIRF.A are in a continuous state of expansion and development by the authors.

CIRF.A includes the Debye-Hückel activity model for aqueous species and complexes, temperature and pressure corrections for the thermodynamic properties, multiple rate laws per solid phase and a nucleation threshold for precipitation. The Fair-Hatch equation is used to describe the relationship between porosity and permeability. The thermodynamic properties and related constants are maintained in a database. The CIRF.A package includes several programs to manage and update the thermodynamic database, extract geometric information about the lithological units from maps, and a list-directed program to build the input files. The output from CIRF.A (mineralogy, porosity, fluid composition, etc) can be displayed using MOVIE.NET, which is dependent upon AVS graphics software.

CIRF.A and REACTRAN have been used to describe geochemical systems that have (1) very sharp, transient, compositional gradients caused by reaction fronts and (2) a strong interaction between fluid flow, solute transport and reactions. These systems are characterized by narrow reaction fronts, reaction fingering and the development of seals (zones of low permeability/porosity). These reaction fronts have a relatively small spatial extent compared to the overall dimensions of the processes being modelled and can lead to very severe numerical problems. CIRF.A specifically addresses these problems through the use of robust solvers and moving adaptive gridding. Because of this, the authors claim that millimetre-thick reaction fronts can be resolved in processes with dimensions in the order of one hundred meters or more.

CIRF.A has been used to simulate a number of problems in the oil industry, including dolomitization, creation of pressure seals in sandstones, acid stimulation of the near-well region in oil fields, and a core flood experiment of matrix acidization (Potdevin, et. al, 1992; Chen et. al, 1993). Except for being in environments of high acidity and sharp reaction fronts, these applications are very different from ARD prediction.

12.2.3 MPATH

MPATH is a multiple reaction path formulation of solute transport and mineral reaction. It uses advective transport in a single spatial dimension and the quasi-stationary state approximation (Lichtner, 1985) for solute concentration. The quasi-stationary state approximation specifies that the partial derivative of the concentration of any particular solute with respect to time at any given point is approximately zero, and thus concentration can be assumed to vary only as a function of distance along the flow path. The reaction of each unit of fluid is calculated as it traverses the path, the mineralogy at each point updated, and then the next unit is examined.

MPATH uses a moving grid to track narrow reaction fronts, a simple rate law for solids and a Debye-Hückel model for the activity coefficients for aqueous species. Equilibrium between all species in solution (including redox phases) are maintained. The porosity and permeability are assumed to be constant, but variation in surface area for each of the solids is calculated using a two-thirds power law. Temperature and pressure are also held constant.

Among other applications, MPATH has been applied to the supergene enrichment of a copper-iron sulphide ore body (Lichtner and Biino, 1992; Lichtner, 1994). In this application, the time scale is long compared to ARD problems, however the reaction fronts and pH shifts are similar to what would be expected in ARD.

12.2.4 1DREACT

1DREACT is a coupled chemical reaction, one-dimensional mass transport computer code for porous media, solved using a finite difference method (Steefel, 1993). 1DREACT can model both steady-state and transient phenomena, including any combination of advection, dispersive and diffusive

transport. A second important feature of the model is that reaction between the fluid and the minerals is controlled by rate laws, thus equilibrium between minerals and the fluid can be approached through the use of large rate constants.

Unlike other codes described, 1DREACT solves the coupled set of partial differential equations through the use of global implicit (one-step iterative) techniques to solve transport and reaction terms simultaneously. This results in a relatively large set of equations to solve for each iteration. The author believes that this method yields more rapid rates of convergence for many problem sets.

1DREACT can have fixed grid spacing or the grid can be allowed to adapt dynamically to resolve reaction fronts in detail. The time step is variable and also adapts to the appropriate scale for the process. Automatic basis switching, a complex kinetic rate law for all phases, Extended Debye-Hückel formulations for activity coefficients, and support for temperature gradients are supported by the program. Diffusion coefficients can be coupled to changes in porosity, and the quasi-stationary state approximation of Lichtner (1985) can be used if appropriate.

1DREACT is a relatively new geochemical model, and has only been used to examine a limited range of problems at this time. One reported application is leakage from a low-level nuclear waste repository in a marl - a possible prototype for a Swiss nuclear waste repository (Steefel and Lichtner, 1994). A two-dimensional version is being prepared.

12.2.5 FMT

The FMT (Fracture-Matrix Transport) code couples saturated porous media advection and diffusion with chemical models for speciation and mineral precipitation and dissolution in a two dimensional domain. FMT uses finite difference techniques to solve the transport equations (Novak, 1993a & b).

FMT has been developed using a dual porosity transport model in order to evaluate the effects of advection dominated flow through fractures, coupled to diffusion transport within the matrix. FMT uses a minimizing technique in Gibbs Free Energy to obtain the distribution of species between the various ion and complexes in solution, thus allowing the equilibrium precipitation and dissolution of solid phases, gas formation and ion exchange to be included and calculated.

FMT supports the Pitzer activity coefficient model, in addition to an Extended Debye-Hückel model, in order to calculate systems with a considerable change in fluid composition and density. FMT can model problems with large variations in fluid density (Novak, 1993a) and includes the effects of changing porosity and permeability. FMT does not currently support non-equilibrium reactions - all phases and species, if present, must be in equilibrium.

FMT is a relatively new code and is currently being tested and expanded. The primary application objective for FMT is to examine actinide solubility and retardation in a dual porosity environment with ground water compositions ranging from dilute to highly concentrated. FMT is based upon a 1D

modelling code called GEOFLOW, which was also used as the basis for KGEOFLOW (see below). The author reports plans to merge these two codes.

12.2.6 KGEOFLOW

KGEOFLOW is a one-dimensional coupled solute transport, mineral reaction program (Sevougian et. al, 1992). Conceptually, KGEOFLOW is very similar to 1DREACT, but uses a different solution method (time step splitting instead of a global implicit solution). KGEOFLOW uses explicit integration on both the transport and kinetic integration steps. It uses simple kinetic equations for non-equilibrium reactions and a free energy minimizing routine for the equilibrium reactions. It also includes provisions for ion exchange. KGEOFLOW uses the EQ3/6 database for thermodynamic properties of the aqueous species and complexes. KGEOFLOW has a interactive program to generate input files. Although it has primarily been used for advection dominated problems, it has options to include dispersion and diffusion.

KGEOFLOW was initially developed for applications in the oil industry and applied to matrix acidizing (Sevougian et al., 1992). Because of this background, KGEOFLOW includes a multiple injection option and the ability to have push/pull injection schemes. KGEOFLOW is currently being expanded to include two-dimensional problems and kinetically constrained redox equilibrium between the aqueous species and complexes in the fluid.

12.2.7 Unnamed (White et al.)

A coupled geochemical model which is currently under development has recently been presented by White et al. (1994). The model is being developed by calibration with column leach tests, and is therefore different than the models discussed above. Rather than use the convection and diffusion transport equations to solve for solute movement, this model divides the column into twenty continuous-stirred tank reactor's in series, with trickle flow between them. The geochemistry of the model is limited, as it only includes fourteen chemical species and five solids, based upon ten chemical equilibria. Reactions between the solids and the fluid are kinetically controlled, and are assumed to be a function only of temperature. The kinetic parameters have been calculated by examining the results from the experiments. Terms for bacteria-catalyzed oxidation have been included, as have shrinking core and coating precipitation terms for the solids.

The authors report good agreement between the experimental results and the model, and state that model development will continue to expand the model's capabilities.

12.2.8 PHREEQM

PHREEQM is designed to model geochemical reactions when combined with fluid flow and solute transport in one dimension (Appelo and Postma, 1993). It is based upon the equilibrium geochemical thermodynamics program PHREEQE (described previously). As is clear from its name, PHREEQM is an extension of PHREEQE, modified to include ion exchange and to use a mixing cell

approach to model the advection and dispersion of the solutes. Up to 10 layers, with each layer containing one or more cells up to a total of one hundred cells, are defined by the user. Each cell in each layer initially has the same mineralogy and fluid composition.

The rates of advection and dispersion between each cell are defined by the user in the data file, and can range between pure advection to pure dispersion by appropriate choice of the input parameters. PHREEQM initially makes a distribution of species calculation for each cell, and brings the fluid to total equilibrium by precipitating a new or existing phase, or by dissolving an existing phase. The degree of mixing between cells/layers is then calculated, the appropriate amount of fluid mixed, and the distribution of species calculation made again.

The approach used by PHREEQM has similarities to the approach used in MINTRAN (see below), and can be very good to address some classes of problems. Specifically, these problems must have advection and dispersion rates which are slow relative to mineral equilibrium. By the very nature of this approach, rate law information for the solid phases are not needed. Thus, information about the phases which form and then dissolve as each cell moves towards total equilibrium can not be obtained.

The approach used by PHREEQM has the advantage of simplicity, and needs much less computing resources than other approaches which involve reaction kinetics. If flow is relatively fast compared to the kinetics of the water-rock reactions, the model will most likely fail. A simple test to examine the validity of this approach for a real system is to analyze the fluid effluent and apply one of the equilibrium geochemical thermodynamic models discussed in a previous chapter. In many waste rock cases, the fluid is found to be significantly supersaturated with respect to many minerals. This suggests that the predictive use of the equilibrium-based method is limited, and that it can only be used as a scoping tool or to determine the ultimate equilibrium boundary conditions.

12.2.9 MINTRAN

MINTRAN is designed to simulate the coupled effects of complex geochemical reactions which occur during fluid flow and solute transport in ground water environments. MINTRAN is described by Frind and Molson (1994), and by Walter et al (1994a), and has been used to model the reactions which occur during the migration of acidic pore waters through aquifers underlying tailings impoundments (Walter et al 1994b; Blowes and Ptacek, 1994).

MINTRAN is based on an efficient two dimensional solute transport model, which calls the equilibrium geochemical thermodynamics code MINTEQA2 (described previously) to calculate the equilibrium between the fluid and the minerals. At each time step at each grid element, the fluid and minerals are brought back to equilibrium. Conceptually, MINTRAN is similar to PHREEQM, except that it calculates the flow and transport more rigorously than a simple mixing cell calculation.

The strongest point of MINTRAN is its handling of the fluid flow and solute transport. It can be used to model flow in complex geometries with heterogeneity in all initial properties (porosity,

permeability, composition, etc) and with a number of different boundary conditions. Both injection and drawdown wells can also be included.

The weakest point of MINTRAN is the assumption of total equilibrium between the fluid and the rock. As mentioned in the section on PHREEQM, this would not be appropriate for modelling a waste rock system. This equilibrium geochemical approach would have to be validated by field observation before it is used in a predictive mode, and might only be useful as a scoping tool to determine ultimate boundary conditions. Also, the simulation is chemically inaccurate where several minerals are dissolving and one is depleted before the others (Morin and Cherry, 1988). Current development of MINTRAN includes the coupling with a sulphide oxidation model.

12.3 **Discussion**

The ultimate geochemical model is a fully-coupled program which considers the effects of fluid flow, heat transport, solute transport and chemical reactions, in an environment which may contain several fluids, in three spacial dimensions and in time. The coupled geochemical mass transfer-flow models described above are presently the closest approximations of the ultimate model. However, each model in this category has important limitations and tends to specialize in specific problems. For most of the coupled geochemical mass transfer-flow models, the main emphasis has been to predict the flow path and the fate of conservative components, such as oil or dissolved contaminants. The need to predict complex reactions between formation mineralogy and fluids has been largely driven by geologists examining ore deposits or metamorphic rocks, or to a lesser extent, by the need to predict the fate of material in nuclear waste repositories over long times. It is only recently that modellers have addressed the prediction of complex geochemical reactions caused by industrial influence, which are typically of shorter time spans relative to geological times. Coupled geochemical-flow models are therefore generally still under development. Many of the assumptions, theories and numerical techniques that these models are based upon have yet to be proven. Programs may have to be modified for each class of problem and are not appropriate for non-specialist use unless a strong liaison with the developer is continuously maintained.

In the long term, it is foreseeable that coupled geochemical-flow models might evolve to the point where detailed predictive modelling of geochemical processes in waste rock will be possible. However, the current capabilities of these models are clearly insufficient for achieving even the most modest predictive goals in waste rock.

Model users generally expect the programs to have been verified and validated by the model developers. Many authors have argued that verification of any model representing natural processes is impossible. The most recent proponents of this view are Oreskes et. al (1994), who state that *"to say that a model is verified is to say that its truth has been demonstrated, which implies its reliability as a basis for decision-making"*. They then argue that verification is only possible for a closed system that can accurately be represented by mathematics. Since no natural system can be represented with total accuracy, what is typically labelled as "validation" is at best conformance with some set of observations, with all the limitations that this suggests.

Total validation and verification are clearly impossible; accurate predictions are therefore very difficult to obtain. Despite this, models are useful to elucidate discrepancies in preconceived notions. They are excellent for sensitivity analyses, thus providing comparative information and identifying data requirements and weaknesses. Well constrained models, based upon fundamental principles, are often the only available means to extrapolate into the future.

12.4 **Summary**

- Of the computer models discussed above, only the model of White et. al is designed specifically for acid rock piles. However, it is currently limited to column tests and is under early phases of development.

- PHREEQM and MINTRAN have been used to examine problems in acid mine tailings, but not on acid rock piles. There are limitations in the approach undertaken by these two models, as they assume local equilibrium between the minerals and the aqueous phase, which generally does not occur in waste rock piles.

- Of the models discussed above, none currently addresses both the physical and geochemical aspects in sufficient detail to model geochemical processes in waste rock piles.

13. SUPPORTING GEOCHEMICAL MODELS

13.1 Background

All geochemical modelling programs use thermodynamic data in one form or another. Data from the literature rarely seems to be in the appropriate format, and thus needs to be manipulated or extrapolated for different conditions of, for example, temperatures and pressures. Most modellers have a suite of programs that they use for thermodynamic manipulation, and any graduate courses in geochemistry have students write simple versions of these programs. For these reasons, only a few of the more common of these programs are discussed.

Another type of supporting geochemical programs are those that calculate intensive variable diagrams. Intensive variable diagram (a subset are more commonly known as log activity diagrams) plot the stability fields of minerals or the dominant aqueous species as a function of temperature, pressure, Eh or the log activity of a phase, aqueous species, gas or component. Water analyses can be plotted directly on these figures, which help identify the most stable minerals, the buffering assemblages and any alteration trends.

The third type included in this category are the codes that offer solutions to the "inverse" problem, which use the compositions of the water, minerals and the bulk composition of the rock to identify and quantify geochemical reactions using mass balance constraints. Their use is discussed is some detail in a series of papers by Plummer (Plummer, 1984; Plummer; 1992; Parkhurst and Plummer, 1993)

13.2 Specific Models

13.2.1 SUPCRIT92

SUPCRIT92 (Johnson et al, 1992) calculates the standard molal thermodynamic properties for minerals, gases, aqueous species and their reactions at up to 5 kilobars and 1000°C. SUPCRIT92 and its predecessor, SUPCRT, are arguably the most recognized software package of this nature in the geological community. It is distributed with a database containing approximately 550 minerals and aqueous species, including a considerable number of organic aqueous species and complexes.

13.2.2 BALANCE

BALANCE (Parkhurst et al, 1982) attempts to define and quantify the chemical reactions which occur between groundwater and minerals based upon the chemical compositions of the water before and after the event. There is no thermodynamic information or constraints used by the programs. Based upon personal insight, the user selects a set of phases which may have participated in the reaction, and the program calculates the amount of each which have been involved.

13.2.3 NETPATH

NETPATH (Plummer et al, 1991; 1992) is based upon the same concepts as BALANCE, but is much more general and sophisticated. NETPATH attempts to solve net geochemical mass-balance reactions between the initial, intermediate and final waters along a hydrologic flow path and model the evolution of various isotopes and the radiocarbon age of the groundwater. If more than one process is possible, the program reports it. If none are found, the program will determine if a model can be found by ignoring precipitation or dissolution constraints.

The processes potentially considered include dissolution and precipitation of solids (including incongruent reactions), ion exchange, oxidation and reduction degradation of organic compounds, mixing, evaporation and dilution, isotope fractionation and exchange. The user can place constraints on what processes are considered. NETPATH is coupled to a database-management program, DB, which facilitates the modelling exercise.

13.2.4 RXN

RXN is an interactive program (Bethke, 1992) which automatically balances chemical reactions among minerals, aqueous species and complexes, and gases. Optionally, it will calculate the log K's of reaction, subject to the temperatures and activities specified by the user. The equilibrium conditions for a reaction can also be calculated. It is fully-integrated with the databases used by other programs such as REACT. It is designed to be run on a UNIX workstation running Motif.

13.2.5 ACT2

ACT2 is an interactive program (Bethke, 1992) which calculates and plots log activity versus log activity diagrams, thus showing the stability of minerals and the predominance of aqueous species in chemical systems. Activities of various phases and species can be fixed, and predominance diagrams can be superimposed on top of activity diagrams. It is fully integrated with the databases used by other programs such as REACT. It can also plot data from from user specified databases. It is designed to be run on a UNIX workstation running Motif.

13.2.6 TACT

TACT (Bethke, 1992) is conceptually and practically identical to ACT2, except that it calculates and plots temperature versus log activity diagrams.

13.2.7 Ge0-Calc

Ge0-Calc (Brown et al, 1989) is an interactive personal computer program to calculate log activity versus log activity, log activity versus temperature and log activity versus pressure diagrams, where log activity generally refers to the log activity of an aqueous species or the charge neutral log activity ratio of a set of aqueous species (solids, gases, pe or components can also be specified).

Projection (fixed activities) from any species, phase or gas is also allowed. Ge0-Calc is general and calculates all possible reactions. An associated version of Ge0-Calc calculates pressure versus temperature versus $X(CO_2)$ diagrams. Ge0-Calc was derived from the PTXA software package (Perkins et al, 1986).

13.2.8 Ge0-Tab

Ge0-Tab (Brown et al, 1989) is an interactive PC-based program to calculate tables of thermodynamic properties for aqueous species, minerals, gases and their reactions. Ge0-Tab is part of the Ge0-Calc distribution and reads the Ge0-Calc database.

13.2.9 BOUNDS

BOUNDS (Connolly and Kerrick, 1987) calculates a wide range of diagrams, including axis variables of: log activity (or ratios) of species, gases or components, temperature, pressure, volume, entropy and mixing of two constituents. BOUNDS is different from the other activity diagram programs mentioned in that it uses free energy minimization for a fixed composition to calculate the diagram. This has the advantage that complex solid solution phases can be considered. It has the disadvantage that the entire figure is specific for only one bulk composition.

13.3 **Summary**

- Supporting geochemical models either calculate necessary thermodynamic constants for one of the many geochemical modelling programs, or they provide or calculate ancillary information which help interpret the numerical results or field observations.

- Supporting geochemical models are useful for constraining geochemical models, preparing thermodynamic data and analyzing results.

14. EMPIRICAL AND ENGINEERING MODELS

14.1 Background

The designation "engineering" was chosen to name one end-member of this class of geochemical models because of the recent interest (Schuiling, 1990) in recognizing the field of "engineering geochemistry". Most recently, Voronkevich (1994) has defined engineering geochemistry as consisting of four separate fields:

(i) developing theoretical ideas concerning the interrelation between changes in geochemical variables (e.g. pH, Eh, etc.) taking place in the geochemical environment and related changes in physico-mechanical properties such as stress distribution, thermal and moisture conditions and other physical conditions.

(ii) studying geochemical processes, such as hydrolysis, ion exchange, weathering and leaching, to forecast the uncontrollable development of hazardous engineering phenomena.

(iii) developing environmental technologies based on natural geochemical processes to remove contaminants from natural cycles.

(iv) developing physico-chemical methods to improve the conditions of the geological environment.

"Engineering" models are developed for a specific purpose which would fall under (i). Only specific geochemical processes are present in these models. The included geochemical processes are based on simplifying assumptions of which processes influence gross ARD changes over time. The geochemical processes are represented in the models by sophisticated kinetic rate laws for dissolution and precipitation of the solid phases of importance and assume homogeneous equilibria in the aqueous phase.

At the other extreme of the applied geochemical models lies the "empirical" model which treats the geochemistry and physics in the simplest terms. An example of this is the model of Morin and Hutt (1994a) which ignores many of the complexities of both the geochemical and physical processes and uses only five mass balance and time factors to predict seepage chemistry through time from mine rock piles.

Even though there is some disagreement on the exact details, a common methodology to examine the potential of acid generation is acid-base accounting. This technique has been included on a spreadsheet by at least one author (Ziemkiewicz, 1994), who cautions the user on the limitations of such an empirical model.

Some programs assume that the rate-limiting step to pyrite oxidation is the supply of oxygen. This observation has been used as a basis for a number of programs to evaluate the effects of heat production and resulting temperature gradients, gas diffusivities versus convection in the pile, air

permeability, inflow rates and the effects of geometry on acid production. Early work on this include Cathles and Apps (1975), who looked at the effects of convection, temperature and oxygen in heap leach operations. Jaynes et. al (1984) and Jaynes (1991) present a model simulating the oxidation of pyrite in coal spoils. Other recent studies include diffusion and particle size (Davis and Ritchie 1986, 1987; Davis, Doherty and Ritchie, 1986), gas convection and diffusion, and pile geometry (Bennett, Harries, Pantelis and Ritchie, 1990), gas convection, heat production and reaction rates (Pantelis and Ritchie, 1991a & b). Comparisons of intrinsic versus overall oxidation rates have also been made (Gibson, Pantelis and Ritchie, 1994). Although they address an important component of acid generation from waste rock piles, none of the oxygen-limited sulphide oxidation models are sufficient for ARD prediction, as they only take into account one of the reactions in the system. They do not take into account any other geochemical processes that follow sulphide oxidation and that control water chemistry.

Models that specifically address the geochemistry of acid drainage of rock piles in detail are rare. Other than those mentioned in Section 12, the engineering model ACIDROCK and the empirical model Q-ROCK are the only models specific for waste rock piles. These are discussed in the following section. RATAP and WATAIL are only discussed briefly since they were designed only for reactive tailings problems.

14.2 **Specific Models**

14.2.1 ACIDROCK (Scharer, et al., 1994b)

ACIDROCK is a model designed to evaluate acidic drainage in waste rock piles (Scharer et al., 1994b). The authors report that the model has been applied to several unpublished field cases and that they have used it to evaluate various decommissioning alternatives.

The conceptual basis for this model was the program RATAP (Senes Consultants, 1991; Scharer et al.,1994a), which was designed to assist in the prediction of acid generation caused by hydrological events and chemical reactions occurring in mine tailings sites. The transport, heat generation and oxygen flux portions of RATAP were replaced to reflect the difference in the chemical and physical environments between waste rock piles and reactive tailings sites. Scharer et al. (1994b) reported that the formulation of chemical equations used in RATAP were used for this model. The chemistry was expanded to include uranium and radium, including sorption on mineral solids and organic surfaces. The authors also report that the co-precipitation of radium with gypsum and that radioactive decay have been included. ACIDROCK uses measured fundamental rate laws for the dissolution of the sulphide minerals.

ACIDROCK simulates the waste rock pile as an equivalent rectangle of specified dimensions, which is divided into 20 layers, each interconnects to the other. Water flows downwards and exits as seepage at the base. Various parameters can be changed over a simulation to model the effects of different covers, re-profiling, changes in infiltration etc.

The model is currently limited in the chemical constituents (minerals, aqueous species and complexes) that it includes. The pH in the model is estimated using electroneutrality. Given the normal numerical precision limits on computers and the effects of errors in specification of the initial chemical conditions, divergence in the calculated pH would be expected to arise. Flow charts for this program (and for RATAP) do not indicate any coupling or iteration between the kinetics module, the pH module and the solids balance (precipitation and dissolution of secondary phases). Although this speeds up numerical computations enormously, it can yield incorrect results in solution compositions and mass of minerals produced or dissolved. This model is not a detailed geochemical model and can not make a detailed assessment of the reactions which occur between a fluid and solid phases. It is rather designed to examine implications of various containment options, using a simplified geochemical model with a restricted set of minerals and aqueous species.

14.2.2 Q-ROCK

Q-ROCK (Chapman et. al, 1994) is a PC-based model developed by SRK (Steffen, Robertson and Kirsten, Canada Ltd) which is used to examine acid rock drainage problems. The focus of this model is to integrate lab tests, field tests and observed field data into a framework which can be used as one component in a predictive program. The authors emphasize that it is only one component of a complete assessment of ARD and should not be undertaken without the appropriate experimental, field and engineering data.

Q-ROCK considers the rock pile in one to three dimensions, depending upon the details available, and simulates one of two idealized pile construction methods. The prediction of contaminant release is done using empirical equations fitted to data from laboratory column tests, while the neutralization potential rate constants are estimated empirically using laboratory data, and adjusted during model calibration to field data. Precipitation and subsequent dissolution reactions are also treated in a similar fashion. The bulk of the water is assumed to be present in a pseudo-steady state, unsaturated channel flow. Oxygen flux into the pile can be modelled either as a diffusive or a dispersive process. Fluid mixing is included.

Q-ROCK is the epitome of an engineering model and can only be used to assess various constraints on acid rock problems. All parameters are based upon fits to experimental data and are calibrated against field data. If necessary, the program can be modified to handle new functional forms and parameters. The strengths of this approach are obvious; there are very strong ties between the lab and field data. The geochemical weakness of this approach is that it assumes that short term experiments and field observations can be extrapolated to long time frames without any fundamental thermodynamic basis.

14.2.3 FIDHELM

FIDHELM (Pantelis, 1993) was developed to assess heap leaching in two dimensions, where the rock pile is modelled as a three phase system: a rigid porous medium, water and a gas phase. There is only one component dissolved in the water, the product of the solid reacting with the oxygen. The

output includes spatial values describing the oxygen density in the gas, the amount of reactant (sulphur density), temperature, air pressure and fluxes of air vertically and horizontally into or out of the pile. FIDHELM makes a number of simplifying assumptions: only oxygen is considered in the gas phase and is described by a mass fraction; the reactant in the solid phase is sulphur and is also described by a mass fraction; the rate of reaction of the solid is described by an intrinsic oxidation model, which includes provision for microorganisms and a modified shrinking core model for the solids. The typical assumptions that the pile is unsaturated but the base is fully saturated are also used.

FIDHELM can not be considered to be a geochemical model, however, it can be very useful to evaluate physical parameters such as oxygen supply which can then be used as input to other models.

14.2.4 WATAIL

WATAIL (Scharer et. al 1993) is a tailings basin model designed to evaluate various rehabilitation strategies, such as engineered covers, through the comparison of the loading rates of the major oxidation products. The tailings and surrounding area can be divided in to a maximum of ten regions, each of which can optionally have surface water and groundwater inflow or outflow. Precipitation, resulting in flow into a region, can also be included. Regions can represent either unsaturated tailings, ponded tailings or something in between. Diffusive and advective transport of oxygen control the rate of sulphide oxidation through a standard rate law, which includes biologic and non-biologic terms. Sulphide minerals are either pyrite, pyrrhotite or an intermediate combination. Only a limited number of components (calcium, iron, pH, sulphate and carbonate), and a limited number of solids (five) are included.

14.3 **Discussion**

The current waste rock engineering models ACIDROCK and FIDHELM are the state-of-the-art in geochemical modelling of waste rock piles. They are clearly insufficient to make detailed predictions of ARD chemistry, as their geochemical components are not complete enough. They can however be used for making relative comparisons and for data analysis. Even if they are currently evolving, these models cannot be expected to evolve to the point of including detailed geochemistry in the near future.

By comparison with engineering models, geochemical mass transfer-flow models (described in Section 12) are much more complex. This complexity arises not only from a more rigorous treatment of the geochemistry, but also from a detailed representation of the physical components of flow systems. Mass transport predictions from these models, performed on actual field cases, are generally mediocre. The accuracy of the predictions often depends on parameter fits and calibrations to field data. As for engineering models, their usefulness is more for making relative comparisons than for obtaining long-term predictions. Current complex models are therefore not more useful for prediction.

Furthermore, most applications of mass-transfer-flow models are on physical systems that are simpler than waste rock piles. Although this physical system has not been thoroughly defined, it is known to possess complex characteristics, as described at the beginning of this report. The waste rock prediction problem is further complicated by the fact that the required predictions have to be made close to the source, giving little time for water chemistry to equilibrate with solid mineral phases.

In view of the current limitations of complex mass transfer-flow models, the relatively simple empirical and engineering models have definite usefulness. Their development and application should be encouraged. Empirical and engineering model development should not be done in isolation, though, but with knowledge gained through geochemical studies of waste rock and applications of geochemical mass transfer models to well-defined field and laboratory systems.

14.4 **Summary**

- The empirical models used to predict ARD are derived from mass balance constraints. They contain few or no thermodynamic constraints. Predictions from these models are limited because they are mostly based on extrapolations of the effects of multiple undifferentiated short-term events.

- Engineering models are based on prior knowledge of the processes and only incorporate some subset of them. A weakness in the engineering models is that if the dominant process changes or is modified over time, the engineering model may be predicting the wrong process. Some engineering models are based on short term laboratory experiments which may not be representative of the long term processes in the pile.

- None of the current engineering models include adequate geochemical detail, for example the buffering and acid-generating effects of silicate minerals.

- Engineering models can be useful for understanding the potential magnitude of the ARD problem and the roles of various physical parameters in mitigating the impact of ARD.

- ACIDROCK is the only engineering model for rock piles which contains any significant component of geochemical calculations. However, it is currently insufficient. Modifications of this code may remove some of the geochemical limitations.

15. SUMMARY OF PART 2

1) Geochemical models were divided into five classes. The first class, **equilibrium thermodynamic models**, uses water analyses, temperature and pressure as input to solve for the distribution of mass among various dissolved aqueous species and complexes. The principal use of these programs is to calculate the saturation indices (SI) for possible minerals which are present or can form in a system, thus allowing the user to evaluate dissolution and precipitation of minerals. These models are usually flexible enough to allow users to modify water analyses, change temperature and pressure, evaporate the fluid, and, to a limited degree, react the fluid with one or more minerals.

2) Equilibrium thermodynamic modelling can be considered a mature technology. Thermodynamic models have been widely used for a variety of applications by a large body of users, and are actively maintained by their authors. Table 11 summarizes the review of equilibrium thermodynamic models by qualitatively assessing the capabilities of each model to simulate some of the most important processes identified in the review. Model features are also listed and rated.

3) The second class, **mass transfer models**, evaluates the evolution of solution chemistry in a fluid-rock system as the system progresses towards equilibrium. Some of the models also have various options for calculating the effects of other processes, such as evaporation.

   The input parameters to these programs are the initial fluid composition and a suite of minerals, with their initial masses and surface areas. When comparing the results of these programs with field observations, changes in field water chemistry over time are required. These programs have rarely been used in ARD research. More applications of mass-transfer models to ARD problems should be done.

   The mass-transfer models which should be most considered for application to ARD prediction problems are EQ6, for completeness, and PATHARC, for PC-based efficiency. These models also incorporate kinetic rate equations which are required to achieve prediction accuracy. Table 12 summarizes the capabilities of mass transfer models. The qualitative assessments in Table 12 are not to be related to those of Table 11 and are only placed to compare mass transfer models within their own class.

4) The third class of model, **coupled mass transfer-flow models**, evaluates reactions between fluid and rock in an open system. These models consider flow, solute transport and heat transport. In practice, the magnitude of the task and numerical difficulties result in a compromise. Some of these models focus on geochemistry, while others emphasize hydrology.

   Data requirements for these programs are detailed solution analyses describing the input composition as a function of time, initial mineralogy over the area being covered, flow rates into or out of the system, and temperature changes over time.

At this time, we do not recommend the use of this class of models for ARD applications because none of them currently addresses both the physical and the geochemical aspects of ARD in sufficient detail. Table 13 summarized the capabilities of the mass transfer-flow models.

5) The fourth class, **Supporting models,** calculates specialized geochemical functions or parameters such as free energies, log K's, and intensive variable diagrams. Mass balance programs that solve the inverse problem by using compositional constraints are also included.

6) The fifth class, **Empirical and Engineering Models,** aim at the prediction of acid generation and metal loadings under different containment conditions and physical structures. These models include several simplifying assumptions on the physics and the chemistry of the modelled systems. They can be useful for comparing various decommissioning options. They do not include detailed geochemistry, and thus have limited predictive capabilities. Table 14 presents a summary evaluation of the capabilities of the empirical and engineering models.

Table 11. Evaluation of capabilities of equilibrium thermodynamic models

	Summary	Dissol & ppt	Co-ppt	Redox	Buffer	Wet Dry Cycles	Rates	System	Dbase	Support	Graphics
EQ3	widely used - flexible input - five different thermodynamic databases - applied on waste rock	None	None	General	None	None	None	PC or Workstn	✓✓✓	✓✓✓	no
EQ3 (Pitzer)	lack of Pitzer coefficients	None	None	General	None	None	None	PC	✓	✓✓✓	no
SOLMINEQ PC/shell	user-friendly interface - includes many geochemical features	Limited	Limited	Limited	None	Limited	None	PC	✓✓	✓✓	yes
PHREEQE	widely used - widely tested on ARD and other problems - input program included	Limited	Limited	General	None	Limited	None	PC or Workstn	✓✓	✓✓	no
PHRQPITZ	lack of Pitzer coefficients	Limited	Limited	General	None	Limited	None	PC or Workstn	✓	✓✓	no
MINTEQA2	the most used - EPA-endorsed - greatest flexibility in modelling surface reactions - input program included	Limited	Limited	General	None	Limited	None	PC	✓✓	✓✓	no
WATEQ4F	several trace elements - input preparation program - some ARD applications	None	None	General	None	None	None	PC or Workstn	✓✓✓	✓✓	no
SOLVEQ	calculates partial heterogenous equilibria (not highly useful) - pre-processor included	Limited	Limited	General	None	Limited	None	PC	✓✓	✓✓	no

Table 12. Evaluation of capabilities of reaction path models

	Summary	Dissol& ppt	Co-ppt	Redox	Buffer	Wet Dry Cycles	Rates	System	Dbase	Support	Graphics
PATHARC	user-friendly - flexible restricted to iso-thermal processes - no solid solution mineral phases - cannot change internal convergence parameters.	General	Limited	General	General	Limited	Kinetic	PC	✓✓	✓✓	yes
EQ6	most widely used - can model solid solution - flexible - several running options - comprehensive - well tested - complex to use	General	Limited	General	General	Limited	Kinetic	Workstn	✓✓✓	✓✓✓	no
CHILLER	strongest for the handling of processes involving gases - plot program for graphics - needs user-specified "relative" rate laws and step size for reactions	General	Limited	General	General	Limited	Relative	PC	✓✓	✓✓	yes
REACT	can graphically output calculations	General	Limited	General	General	Limited	Kinetic	Workstn	✓✓	✓✓	yes
STEADYQL	specifically designed for soils - includes flux into and out ot the volume - number of reactions has to be defined by the user - assumes that all reactions will go to steady state	Limited	Limited	Limited	Limited	Limited	Kinetic	PC	✓	✓	no

Table 13. Evaluation of capabilities of mass-transfer/flow models

	Summary	Flow	Dissol& ppt	Co-ppt	Redox	Buffer	Wet Dry Cycles	Rates	System	Dbase	Support	Graphics
REACTRAN	simplified handling of reaction rates - well tested on natural systems	1D	General	Limited	General	General	Limited	Kinetic	workstn	✓	✓✓✓	yes
CIRF.A	comprehensive - input&support programs - well tested in oil industry on numerically difficult problems	2D	General	Limited	General	General	Limited	Kinetic	workstn	✓✓	✓✓✓	yes
MPATH	reaction path quasi steady state approximation - not widely tested	1D	General	None	General	General	None	Kinetic	workstn	✓✓	✓✓	no
IDREACT	finite difference may be more efficient for solving - not well tested	1D	General	None	General	General	None	Kinetic	workstn	✓	✓✓	no
FMT	finite difference - dual porosity - supports Pitzer coefficients - time-variable medium - assumes reactions go to equilibrium - not widely tested	2D	General	None	General	General	None	Kinetic	workstn	✓	✓✓	no
KGEOFLOW	has a interactive program to generate input files - finite difference may be more efficient for solving - tested in oil industry	1D	General	None	General	General	None	Kinetic	workstn	✓	✓✓	no
White et al.	developed by calibration with waste rock leach tests - limited number of reactions - includes lab-determined kinetic rate constants	1D	Limited	None	General	Limited	General	Kinetic	workstn	✓	✓✓	no
PHREEQM	simple equilibrium approach - assumptions limiting for cases where reaction kinetics are fast	1D	Limited	None	General	Limited	None	None	PC	✓✓	✓✓	no
MINTRAN	preliminary testing done in Acid drainage environments - versatile - limiting assumption of total equilibrium	2D	Limited	None	General	Limited	None	None	workstn	✓✓	✓✓	no

Table 14. Evaluation of geochemical capabilities of empirical and engineering models

	Summary	Dissol& ppt	Co-ppt	Redox	Buffer	Wet Dry Cycles	Rates	System	Dbase	Support	Graphics
RATAP		Limited	Limited	Limited	Limited	Limited	Limited	PC	✓	✓	yes
WATAIL	very simple model - can be used to evaluate various rehabilitation strategies - limited number of components and solids	Limited	Limited	Limited	Limited	Limited	Limited	PC	✓	✓	no
FIDHELM	applied on several waste rock piles - geochemical predictive capability limited by highly simplifying assumptions	None	None	None	None	Limited	Limited	PC		✓	no
QROCK	strongly integrates lab and field data - assumes that short term experiments and field observations can be extrapolated without any fundamental thermodynamic basis	Limited	None	Limited	Limited	Limited	Limited	PC	✓	✓	no
ACIDROCK	applied to several waste rock field cases - limited in the chemical constituents - inaccurate calculation of pH - limiting simplifying assumptions - good for comparing containment options	Limited	Limited	Limited	Limited	Limited	Limited	PC	✓	✓	no

7) Table 15 lists the input parameters required by each class of model. Engineering models, which simulate the most processes, require the most number of input parameters. However, mass transfer models, which address geochemistry in more detail, require more geochemical data.

8) Each class of geochemical models can be viewed as addressing a different type of ARD prediction objective such as described in the introduction of this report. In Table 16, relations between model class and prediction objective are presented. Equilibrium geochemical thermodynamic models address the identification of the soluble and mobile metal species and maximum metal concentrations. Mass transfer models more specifically address maximum metal concentrations and their evolution with time. Mass transfer-flow models address the prediction of concentration and load versus time. The engineering models are more directed towards examining decommissioning options. More developments are required in each model category to adequately achieve each prediction objective.

Table 15. Description of parameter requirements for ARD according to class of models

Model Input	**Class ----> Parameters**	**Equil.**	**M.T.**	**M.T./Flow**	**Emp/Eng**
Field Data	Water Chem.	+++	++	++	+
	Mineralogy	+	+++	++	+
	Surface Area	0	+++	+++	+
	Temperature	+	+	+	+
	Oxygen	+	++	++	++
	Water Balance	0	+	++	++
	Pile Structure	0	0	0	++
Lab Data	Column Test	0	0	0	+
	Humidity Cell	0	0	0	+
Database	Equil thermodynamic	+++	+++	+++	++
	Kinetic	0	+++	+++	+

Relative importance of input parameters
0 = none or not required
+ = required the least
++ = intermediate requirement
+++ = required with most accuracy

Table 16. Applicability of each class of models to different prediction objectives

Model	Class ---->	Equil.	M.T.	MT/Flow	Emp/Eng
Prediction Objective	I.D. Species	+++	++	+	0
	Max. Conc.	+	++	+	0
	Max. Loads	+	++	++	+
	Duration	0	++	+++	++
	Conc. - Time	0	+	++	+
	Decomm. Option	0	0	++	+++

Relative applicability of models
0 = none or not used
+ = the least
++ = intermediate
+++ = the most

16. RECOMMENDATIONS

Several recommendations have been formulated throughout this report. Following is a summary of the most important recommendations justified by this review for further development of geochemical models for the prediction of acidic drainage from waste rock piles.

- Recommendations on the study of geochemical processes and the determination of model input parameters:

  a) Waste rock datasets should be collected and interpreted to increase the understanding of geochemical processes. These should include field as well as column data, and should include complete water analyses and mineralogical determinations.

  b) Determinations of the reaction mechanisms and of the reactive surface area of sulphide minerals should be improved.

  c) Thermodynamic equilibrium constants for important minerals in ARD should be collected, in particular for hydroxide and sulphate secondary minerals. Current databases for Pitzer interaction coefficients should be improved.

  d) More research should be conducted to obtain kinetic rate data for precipitation, co-precipitation and dissolution reactions which can occur in waste rock; inhibitive and catalytic effects should be included in kinetic rate equations. Kinetic rate equations should address transitions between diffusion and surface-controlled reactions and redox disequilibrium in the aqueous phase.

- Recommendations on the use of existing geochemical models:

  e) Existing geochemical models should not be used with the objective of predicting water chemistry from waste rock piles. At best, they can be used for improving the understanding of the interactions between geochemical processes, and for performing comparisons between decommissioning scenarios.

  f) The application of existing mass transfer geochemical models such as EQ6 and PATHARC on well-defined oxidizing waste rock field or laboratory systems should be encouraged.

  g) Empirical models based on laboratory and field tests should be used and further developed to compensate for the limitations of presently available geochemical models.

- Recommendations on further model development:

  h) A model to predict water quality from waste rock piles should incorporate a geochemical component that takes into account reaction kinetics, and should be developed using knowledge gained from the applications described in f)

  i) Current developments of mass transfer-flow models should be closely followed. However, because of their current geochemical limitations and the lack of understanding of the physics of waste rock piles, a mass transfer-flow model for waste rock piles cannot be developed immediately from any current mass transfer-flow model.

  j) A thorough review of physical processes occurring in waste rock piles should be conducted.

ACKNOWLEDGEMENTS

This report incorporates contributions from the following individuals (in alphabetical order): B. Aubé (NTC), S. Knipe (UWO), and M. Li (NTC). Constructive comments were provided by reviewers S. Day (Norecol, Dames & Moore), B. Downing (Teck Corporation), R. Lett (MEMPR, BC), K. Morin (Morwijk Entreprises) and E. Yanful (University of Western Ontario). Discussions with B. Price (MEMPR, BC) and D. Boyle (GSC) are acknowledged, as well as guidance by M. Blanchette, scientific authority for MEND. K. Howard assisted in the editing and preparation of the final manuscript.

Funding for the study was provided under the Canada/Ontario Mineral Development Agreement.

APPENDIX A

AVAILABILITY OF THERMODYNAMIC AND KINETIC DATA

APPENDIX A - AVAILABILITY OF THERMODYNAMIC AND KINETIC DATA

MINERAL	COMPOSITION	THERMODYNAMIC PROPERTIES	DISSOLUTION KINETICS	PRECIPITATION KINETICS	REFERENCE NUMBER
		PRIMARY SILICATE MINERALS			
Plagioclase	$Na\ Al\ Si_3\ O_8$ - $Ca\ Al_2\ Si_2\ O_8$	yes	yes	no	1,2
Quartz	$Si\ O_2$	yes	yes	yes	1,3,4,5
K-feldspar	$K\ Al\ Si_3\ O_8$	yes	yes	no	1,2,6
Biotite	$K\ (Mg, Fe)_3\ Al\ Si_3\ O_{10}\ (OH)_2$	yes	yes	no	1,7,8
Muscovite	$K\ Al_3\ Si_3\ O_{10}\ (OH)2$	yes	yes	no	1,9,10
Hornblende	$Ca_2\ (Mg, Fe)_4\ Al_2\ Si_7\ O_{22}\ (OH)_2$	yes	no	no	1
Orthopyroxene	$(Mg, Fe)\ Si\ O_3$	yes	yes	no	1,11
Clinopyroxene	$Ca\ (Mg, Fe)\ Si_2\ O_6$	yes	yes	no	1,12
Talc	$Mg_3\ Si_4\ O_{10}\ (OH)_2$	yes	yes	no	1,8
Serpentine	$Mg_3\ Si_2\ O_5\ (OH)_4$	yes	yes	no	1,8,13
		CLAY MINERALS			
Gibbsite	$Al\ (OH)_3$	yes	yes	some	1,14,15
Illite	$K_{(2-x)}\ Al_4\ Si_{(6+x)}\ Al_{(2-x)}\ O_{20}\ (OH)_4$	yes	yes	no	1,16,17,18
Kaolinite	$Al_2\ Si_2\ O_5\ (OH)_4$	yes	yes	no	1,17,18, 19,20,38
Smectites	$(Na_2, K_2, Ca, Mg)\ Al_{14}\ Si_{22}\ O_{60}\ (OH)_{12}$	some	yes	no	21,17,18,20
		Fe-OXYHYDROXIDES			
Ferrihydrite	$Fe\ (OH)_3$	yes	yes	no	22,23,24
Goethite	$Fe\ O\ (OH)$	yes	yes	no	25,26,27
Hematite	$Fe_2\ O_3$	yes	yes	no	1,28,29,35
Magnetite	$Fe_3\ O_4$	yes	no	no	1
Schwertmannite	$Fe_8\ O_8\ (SO_4)\ (OH)_6$	no	no	no	
		CARBONATES			
Calcite	$Ca\ CO_3$	yes	yes	yes	1,30,31
Aragonite	$Ca\ CO_3$	yes	yes	yes	1,31
Dolomite	$Ca\ Mg\ (CO_3)_2$	yes	yes	no	1,32,33
Siderite	$Fe\ CO_3$	yes	no	no	25,34
		SULPHATES			
Gypsum	$Ca\ SO_4\ .\ 2H_2O$	yes	yes	yes	1,36,37
Anhydrite	$Ca\ SO_4$	yes	yes	no	1,3,6
Melanterite	$Fe\ SO_4\ .\ 7H_2O$	yes	no	no	
Rozenite	$Fe\ SO_4\ .\ H_2O$	no	no	no	
Szomolnokite	$Fe\ SO_4\ .\ H_2O$	no	no	no	
Copiapite	$Fe^2\ Fe^3_4\ (SO_4)_6\ .\ 20H_2O$	no	no	no	
Coquimbite	$Fe_2\ (SO_4)_3\ .\ 9H_2O$	no	no	no	
Rhomboclase	$H\ Fe\ (SO_4)_2\ .\ 4H_2O$	no	no	no	
		SULPHIDES			
Pyrite	$Fe\ S_2$	yes	yes	yes	1,39-52
Marcasite	$Fe\ S_2$	yes	yes	yes	1,55-57,60
Pyrrhotite	$Fe_{(1-x)}\ S$	yes	yes	yes	1,58-59,61
Arsenopyrite	$Fe\ As\ S$	yes	yes	no	62,58,59

references are listed on the following pages
full references are listed in the REFERENCE section

CROSS-REFERENCE LIST

No.	REFERENCE
1	Helgeson et al., 1978.
2	Busenberg and Clemency, 1976.
3	Van Lier et al., 1960.
4	Packter, 1979.
5	Rimstadt and Barnes, 1980.
6	Fogler et al., 1975.
7	Lin, 1981.
8	Lin and Clemency, 1981a.
9	Lin and Clemency, 1981b.
10	Huang et al., 1968.
11	Grandstaff, 1977.
12	Schott et al., 1981.
13	Luce et al., 1972.
14	Packter and Dhillon, 1972.
15	Packter and Dhillon, 1974.
16	Dayal, 1977.
17	Lerman et al., 1975.
18	Cabrera and Talibudeen, 1978.
19	Hydes, 1977.
20	Turner, 1964.
21	Nesbitt, 1977.
22	Langmuir, 1971.
23	Schwertmann et al., 1982.
24	Yates and Healy, 1975.
25	Nordstrom et al., 1990.
26	Surana and Warren, 1969.
27	Cornell et al., 1976.
28	Azuma and Kametani, 1964.
29	Gout et al., 1974.
30	Talman et al., 1990.
31	Busenberg and Plummer, 1986.
32	Sverdrup and Bjerle, 1982.
33	Busenberg and Plummer, 1982.
34	Bruno et al., 1992.
35	Bruno et al., 1992.
36	Barton and Wilde, 1971.
37	Nancollas et al., 1977.
38	Wieland and Stumm, 1992.
39	Lowson, Richard T., 1982.
40	Morse J.W., Millero F.J., Cornwell J.C. and Rickard D., 1987.
41	Sato M., 1992.
42	Bailey, L. K., Peters, E., 1976
43	Goldhaber, M.B., 1983.
44	Lalvani, S.B., DeNeve, B.A., Weston, A., 1991.
45	McKibben, M.A., Barnes, H.L., 1986.
46	Moses C.O., Nordstrom D.K., Herman J.S. and Mills A.L., 1987.
47	Mishra K.K., 1988.
48	Moses C.O. and Herman J.S., 1991.
49	Nicholson, R.V., Gillham, R.W., Reardon, E.J., 1990.
50	Nicholson, R.V., Gillham, R.W., Reardon, E.J., 1988.
51	Yelloji Rao., M.K., Natarajan, K.A., 1986.
52	Schoonen M.A.A. and Barnes H.L., 1991.
53	Tossell J.A., Vaughan D.J. and Burdett J.K., 1981.
54	Wiersma C.L. and Rimstidt J.D., 1984.
55	Buckley A.N., Hamilton I.C. and Woods R., 1985.
56	Sanchez V.M. and Hiskey J.B., 1988.
57	Steger H.F., 1977.
58	Papangelakis V.G. and Demopoulos G.P., 1990.
59	Richardson S. and Vaughan D.J., 1989.
60	Fleet M.E., 1978.
61	Lambert, J.M., Jr., Simkovich, G., Walker, P.L., Jr., 1980.
62	Heinrich and Eadington, 1986.

APPENDIX B

LITERATURE REVIEW OF GEOCHEMICAL PROCESSES AFFECTING SULPHIDES AND OXIDES

TABLE OF CONTENTS

Page #

LIST OF TABLES

LIST OF FIGURES

I. INTRODUCTION

This report contains a literature review of papers, and articles dealing with the kinetics of mineral reactions of fundamental importance to acid mine drainage (AMD). In particular, it concentrates on the minerals pyrite (FeS_2), pyrrhotite (Fe_7S_8), arsenopyrite (FeAsS), goethite (α-FeOOH), hematite (α-Fe_2O_3) and magnetite (Fe_3O_4). Literature searches were performed manually and using online databases; the search strategies are summarized in Appendix C. References dealing with kinetics of oxidation and/or dissolution of these minerals are given in each section. Specific information on the kinetics will be briefly reviewed in each section, but a detailed review of all kinetics studies is well beyond the scope of this literature survey. As well, this is not intended to be a critical review of the literature (see MORIN *et al.*, 1991), but inconsistencies will be brought to the attention of the reader. Once the appropriate kinetics and rate laws have been identified, the kinetics information will be used for modelling.

Reaction kinetics of the afore mentioned minerals will be dealt with in turn; the overlap of information with goethite and hematite is quite extensive. It was of particular interest to identify the reaction mechanisms for biological, chemical and electrochemical oxidation, surface reaction products and the precipitation of sulphide minerals. Dissolution of the iron oxides was reviewed in terms of nonreductive dissolution and reductive dissolution, as well as the effects of light and the presence of organic compounds such as humic acids. Lastly, the oxidation and reduction of sulphides and oxides by mixed potential processes was reviewed. Since many readers will have only passing familiarity with electrochemical kinetics and mixed potential theory, it will be presented in great detail.

II. METAL SULPHIDES

II.1 PYRITE

II.1.1 Oxidative Dissolution.

Biological.

There has been a considerable volume of literature written regarding the oxidation of sulphide minerals, in particular pyrite and chalcopyrite, with the focus on mineral processing technology (CUPP, 1984; SILVER, 1985; McCREADY and SANMUGASUNDERAM, 1985; and NATARAJAN, 1992) and environmental issues, like acid mine drainage (AMD) (see SINGER, and STUMM, 1970). Oxidation of sulphide minerals, cannot be classified as strictly biological oxidation, but oxidation by both biological and abiological (chemical/electrochemical) processes tend to occur together (see SILVERMAN, 1967; KELLER and MURR, 1982; LIZAMA and SUZUKI, 1989; and PALNENCIA *et al.*, 1991).

The kinetics of pyrite (massive and framboidal) and marcasite (FeS_2) oxidation will be discussed in terms of the following factors: 1) surface area, 2) morphology, 3) oxygen concentration. Treatments of the data (PUGH *et al.*,1984) were evaluated by regression analysis of the $\log_{10}[SO_4^{2-}]$ vs time as

$$\log_{10}[SO_4^{2-}] = \frac{kt}{2.303} + C \qquad (1)$$

where k is the rate constant, t is time in days, the $[SO_4^{2-}]$ is in ppm and C is a constant. The raw rate data can be found in Table 1.

Oxygen %	Slope	r^2	k	Relative rate
Massive Pyrite				
0	-0.006	0.32	-0.013	1.0
8	-0.018	0.98	0.087	10.0
20	0.048	0.97	0.111	12.1
Frambodial Pyrite				
0	0.007	0.26	0.017	3.0
8	0.054	0.97	0.125	13.8
20	0.069	0.96	0.158	17.1
Marcasite				
0	0.031	0.34	0.070	8.3
8	0.094	0.85	0.215	22.8
20	0.094	0.77	0.215	22.8

r=correlation coefficient
k=first-order rate constant for sulphate production (ppm/day).

Table 1: Influence of O_2 percent on the reaction rate of 250 - 70 μm fraction for iron sulphides.

PUGH *et al.* (1984) found that the rate of pyrite oxidation by *Thiobacillus ferrooxidans* was dependent on the partial pressure of oxygen. The rate of microbial production of sulphate was inhibited when the percentage of oxygen in the atmosphere dropped below 8%, and in addition no significant increase in the rate of sulphate production occurred when the percentage of oxygen in the atmosphere was increased to 20%. The rate of chemical/electrochemical (abiological) leaching of the pyrite was not affected by percentage of oxygen (< 20 %) in the atmosphere.

For massive pyrite samples, the rate of sulphate production was almost independent of particle size (50 to 2 μm), but a two-fold increase in sulphate production occurred when the same experiment was performed with framboidal pyrite. Rate constants and relative rates for the reaction of massive

pyrite, framboidal pyrite and marcasite are summarized in Table 1. The authors analyzed their kinetic data based on the reactions of SINGER and STUMM (1969):

Chemical Reaction

$$FeS_2 + 3½\ O_2 + H_2O \rightarrow Fe^{2+} + 2\ SO_4^{2-} + 2\ H^+ \quad (2)$$

Biological Reaction:

$$Fe^{2+} + ¼\ O_2 + H^+ + \textit{T. ferrooxidans} \rightarrow Fe^{3+} + 1/2\ H_2O \quad (3)$$

and do not assign a mechanism to their rate data.

LIZAMA and SUZUKI (1989) presented the most detailed study of pyrite oxidation kinetics, including rate equations and rate constants, found to date. Bioleaching is a complex process and there are at least three competing reactions to be considered: 1) direct bacterial oxidation of the mineral surface, 2) indirect oxidation by ferric iron, and 3) electrochemical interactions of the minerals (i.e., electrochemical corrosion). Electrochemical corrosion was not addressed in this article.

Ferric iron corrodes pyrite by the following reaction:

$$FeS_2 + 2\ Fe^{3+} \rightarrow 3\ Fe^{2+} + 2\ S^o \quad (4)$$

Their kinetic studies indicate that the oxidation of pyrite is catalyzed by ferric iron and that the rate determining step relies on the formation of an FeS_2-Fe^{3+} intermediate,

$$FeS_2 + Fe^{3+} \rightleftharpoons FeS_2\text{-}Fe^{3+} \rightarrow Fe^{2+}\ (\text{release}) \quad (5)$$

The rate law for this reaction is listed in Table 2 under indirect leaching.

The rate of pyrite oxidation by *Thiobacillus ferrooxidans (T. ferrooxidans)* was found to depend on the preparation of the pyrite. Pyrite that was washed prior to inoculation showed the standard Michaelis-Menton kinetics (see Table 2), while pyrite that was unwashed prior to inoculation showed kinetics indicative of an initial competitive-inhibition type mechanism. LIZAMA and SUZUKI (1989) proposed that the mechanisms differ for the washed and unwashed pyrite because of an initial rapid release of Fe^{2+} from the surface of the unwashed pyrite. The initial rapid rate of O_2 consumption can be attributed not only to the bacterial oxidation of the pyrite, but also the bacterial

oxidation of aqueous ferrous iron to ferric iron. In order to verify the hypothesis that ferrous iron can increase the rate of indirect leaching of the pyrite, they followed the rate of O_2 consumption of washed pyrite/*T. ferrooxidans* in a solution spiked with ferrous iron. In this experiment, they found that indeed the rate of O_2 oxygen consumption was initially quite rapid, and it was concluded that the bacteria could rapidly oxidize the ferrous iron as follows:

$$4\ Fe^{2+} + O_2 + 4\ H^+ + T.\ ferrooxidans \rightarrow 4\ Fe^{3+} + 2\ H_2C \qquad \textbf{(6)}$$

Reaction type	Rate Equation	Constants

Table 2: Rate laws for the biological oxidation of pyrite (LIZAMA and SUZUKI, 1989).

Spontaneous	Rate = $k[FeS_2]$	k = 3.5 / m	(7)
Indirect leaching	Rate = $\frac{k_3[Fe^{3+}][FeS_2]}{K_m + [FeS_2]}$	k_3 = 10 / min. K_m =	(8)
T. ferroxidans (washed FeS_2)	Rate = $\frac{k[cell][FeS_2]}{K_m + [FeS_2]}$	k = 90 / min. mg K_m =	(9)
T. ferroxidans (unwashed FeS_2)	Rate = $\frac{k[cell][FeS_2]}{K_m(1 + [cell]/K_i + [FeS_2]}$	k = ____ / min. K_i =	(10)
T. ferroxidans (Fe^{2+} oxidation)	Rate = $\frac{k[cell][FeS_2]}{K_m(1 + [cell]/K_i + [FeS_2]}$	k = ____ / mir K_i =	(11)

where: the Rate is defined as the rate of reaction, measured by the release of Fe^{2+} or the consumption of O_2.
$[FeS_2]$ is defined as the (wt pyrite in grams/volume of liquid (mL))x100%.
[cell] is defined as the weight of wet cells/volume in mg/mL

The rate law for pyrite oxidation with *T. ferrooxidans* in the presence of a large excess of Fe^{2+} is given in Table 2.

$$4\ Fe^{3+} + 3\ H_2O + T.\ ferrooxidans \rightarrow H_2SO_3 + 4\ Fe^{2+} + \cdot \quad \textbf{(12)}$$

They proposed that the rate of pyrite oxidation in the presence of bacteria and ferric iron could be due to the Fe^{3+}-sulphur oxidoreductase enzyme discovered in *T. ferrooxidans*; this enzyme has been shown by SUGIO *et al.* (1987, 1989) to oxidize sulphur (or sulphide) to sulphite by

PALENCIA *et al.* (1991) reported that the steady-state spontaneous oxidation of pyrite can be described by

$$4\ FeS_2 + 15\ O_2 + 2\ H_2O \rightarrow 2\ Fe_2(SO_4)_3 + 2\ H_2SO_4 \quad \textbf{(13)}$$

Pyrite can also be oxidized by an indirect mechanism (i.e., through chemical/electrochemical leaching) in the absence of bacteria. They reported that the pyrite surface, leached by ferric iron, was greatly enriched in sulphur with increasing oxidation time; these results are in contrast to those of PESIC and KIM (1990). The oxidation rate of the pyrite leached by ferric iron, in the presence of *T. ferrooxidans*, was found to be much greater than in the presence of ferric iron alone. PESIC and KIM (1990) concluded from their study of the leaching of pyrite with *T. ferrooxidans* that the rate of leaching was inhibited by both the high concentration of bacteria blocking the pyrite surface and the solid reaction products which create a passivated surface. Hence, they concluded that the rate of pyrite oxidation is limited by the rate pore diffusion.

Recently, MUSTIN *et al.* (1992) used electrochemical techniques and scanning electron microscopy to follow the oxidation of pyrite in the presence of *Thiobacillus ferroxidans*. They reported that oxidation of pyrite involved four stages. The first stage was called a lag phase and corresponded to the indirect mechanism as described above,

$$\begin{aligned} Fe^{3+} + 3\ e^- &\rightarrow Fe^{2+} \\ S^{2-} &\rightarrow SO_4^{2-} \end{aligned} \quad \textbf{(14)}$$

The second stage began about 1 day after the pyrite was exposed to the *Thiobacillus ferroxidans* and involved the incongruent dissolution of the mineral, in which sulphur was lost preferentially from the pyrite surface. This stage was indicative of the beginning of the bioleaching process. The third stage

began after an 18 day exposure of the pyrite to the inoculant and it was characterized by a very high concentration of Fe^{3+} in solution and a rapid drop in pH. The dominant reaction occurring in this stage is

$$FeS_2 + 8\ H_2O + 14\ Fe^{3+} \rightarrow 15\ Fe^{2+} + 2\ SO_4^{2-} + 16\ H^+ \qquad \textbf{(15)}$$

The fourth, and final stage of pyrite oxidation (at > 25 days exposure) involved the rapid bioleaching of the pyrite as in reaction **(15)**, except ferric sulphate was formed in solution and not ferrous sulphate. After 45 days of oxidation, the solution pH had dropped below 1.3 and it was felt by the authors that bacterial oxidation may be inhibited at these low pHs and the pyrite may be further corroded electrochemically/chemically. Some incongruent dissolution occurred at this stage, but now it was iron that was more rapidly lost from the pyrite surface. The pyrite surface was highly pitted or honeycombed, and the cells were concentrated at the bottom of the pits or channels. Oxidation was controlled by the mineral's crystalline structure.

For further reading on the oxidation of pyrite by bacteria see the following references: ARKESTEYN (1979, 1980); AHONEN and TUOVINEN (1992); BRUYNESTEYN and DUNCAN (1970); CHOI and TORMA (1989); EHRLICH (1990); EHRLICH and BRIERLEY (1990); KELLER and MURR (1980, 1982); LEES *et al.* (1969); MEHTA and MURR (1991); MORIN (1991); NATARAJAN (1988); OTWINOWSKI (1994); and PESIC *et al.* (1988).

Chemical/Electrochemical.

The rate of abiotic oxidation of pyrite was measured in aqueous solution as a function of pH (2-9), [Fe^{3+}] and aerobic and anaerobic conditions (MOSES *et al.*, 1987). Ion chromatography (IC) was used to follow the concentrations of oxysulphur species as a function of reaction time. It was reported that neither pH nor the presence of molecular oxygen could increase the reaction rate that was found with ferric iron alone.

The rate of pyrite oxidation in basic carbonate solution was studied by NICHOLSON *et al.* (1988) as a function of oxygen concentration (0.6-20%), pyrite particle size (54-215 μm), temperature (25-60°C) and pH (6.7-8.5); reaction rates were determined between 48 and 348 h of reaction time. The relation between reaction rate and the partial pressure of oxygen was in considerable controversy; the authors proposed an equilibrium adsorption-desorption rate-limiting decomposition of oxygen. The reaction rate was found to vary inversely with grain size diameter to

the first order. The "activation energy" (i.e., pseudo activation energy) was calculated to be 88 kJ mol^{-1}.

The rate of pyrite oxidation was followed in basic carbonate solutions (0.005 M $NaCHO_3$), by NICHOLSON (1990) and found to be an inverse function of grain size (75-250 μm) at short times (400 h) and approached an inverse square dependence at long times (8000 h). The shrinking core model was used to calculate a surface rate constant of 3.07×10^{-6} m h^{-1} ± 46% and a diffusion coefficient for oxygen through the surface oxide of 1.08×10^{-12} m^2 h^{-1} ± 30% (also see GUILINGER *et al.*, 1987).

LUTHER (1987) used molecular orbital theory to predict the interaction between the pyrite molecular orbitals and those of the oxidants Fe^{3+} and O_2, and the reductant Cr^{2+}. It was assumed that disulphide, S-S, bonds were stronger than the Fe-S bonds, and hence the disulphide ion remains intact (at least initially) and that the first electron transfer is between π^* orbital of S_2^{2-} to the π orbital of the oxidant. The predicted reaction intermediate in each case was FES_2-O. The proposed mechanism allows for facile oxidation of pyrite by Fe^{3+} but not O_2.

$$FeS_2 + 14\ Fe^{3+} + 8\ H_2O \rightarrow 15\ Fe^{2+} + 2\ SO_4^{2-} + 16\ H^+ \quad \textbf{(16)}$$

$$FeS_2 + 7/2\ O_2 + H_2O \rightarrow Fe^{2+} + 2\ SO_4^{2-} + 2\ H^+ \quad \textbf{(17)}$$

$$FeS_2 + 15/2\ H_2O_2 \rightarrow Fe^{3+} + 2\ SO_4^{2-} + H^+ + 7\ H_2O \quad \textbf{(18)}$$

The overall reactions for pyrite oxidation in the presence of ferric ion, dissolved oxygen and hydrogen peroxide at 30°C was reported by McKIBBEN and BARNES (1986) to occur by respectively. McKIBBEN and BARNES (1986), showed that the rate laws for pyrite oxidation are:

$$R_{Fe^{3+}} = -10^{-9.74}[Fe^{3+}]^{0.5}[H^+]^{-0.5} \quad \textbf{(19)}$$

$$R_{O_2} = -10^{-6.77}[O_2]^{0.5} \quad (20)$$

$$R_{H_2O_2} = -10^{-1.43}[H_2O_2] \quad (21)$$

where the rate, R, is in units of moles pyrite cm^{-2} min^{-1} and the concentration of dissolved species is mol L^{-1}. HPLC was used to follow the rates of the various oxidation experiments. They present the experimentally determined rate laws for pyrite oxidation by ferric iron and dissolved oxygen from a number of literature sources; these rate laws can be found in Table 3.

The effect of ferric iron, dissolved oxygen and surface area at near-neutral pH was studied by MOSES and HERMAN (1991). It was reported that the oxidation rate of pyrite is first order in the ratio of pyrite surface area to solution volume and that neither Fe^{3+} (aq) or dissolved O_2 directly attacked the pyrite surface. The rate of oxidation was dependent on the $[Fe^{2+}](aq)$; iron was cyclically oxidized and reduced, acting as a conduit for electrons from the pyrite surface to dissolved oxygen.

The above discussion is a cursory overview of the total literature regarding the chemical and electrochemical leaching (both oxidative and non-oxidative dissolution) of pyrite. The following references refer to the chemical leaching of pyrite: BARKER and PARKS (1986); BLOWES *et al.* (1992); DAVIS *et al.* (1986); DAVIS and RITCHIE (1986); de HAAN (1991); DUTRIZAC *et al.* (1970); GARRELS and THOMPSON (1960); GOLDHABER (1983); HWANG *et al.* (1987); JAMBOR *et al.* (1991); KING (1976); KING and PERLMUTTER (1977); KING and LEWIS (1980); LOWSON (1982); LUTHER (1982); MATHEWS and ROBINS (1972); MIZOGUCHI *et al.* (1983); MORIN (1991); MOSES *et al.* (1987); MOSES and HERMAN (1991); NORDSTROM (1982); PEARSE (1980); OTWINOWSKI (1994); TAYLOR and WHEELER (1984); THORPE *et al.* (1987); WADSWORTH (1984); and ZHENG *et al.*, (1986).

Rate Law	T/°C	pH Range	Ref.
Ferric iron			
$[Fe^{3+}]^{0.58}[H^+]^{-0.50}$	25-30	1-2	*a*
$[Fe^{3+}]$	25-50	2	*b*
$[Fe^{3+}]([Fe^{3+} + [Fe^{2+}])^{-1}\ [H^+]^{-0.44}$	30-70	0-1.5	*c*
$[Fe^{3+}]([Fe^{3+} + [Fe^{2+}])^{-1}$	30	0-2	*d*
Dissolved O_2			
$[O_2]^{0.49}$	20-40	2-4	*a*
$[O_2]^{0.81}$	30-70	-0.1-1.2	*c*
$[O_2]^{0.81}\ [H^+]^{0.81}$	20-35	2-10	*e*

a McKIBBEN and BARNES (1986); *b* WIERSMA and RIMSTIDT (1984); *c* MATHEWS and ROBINS (1972); *d* GARRELS and THOMPSON (1960); *e* SMITH and SHUMATE (1970)

Table 3: Experimentally-determined rate laws for the oxidation of pyrite by ferric iron and dissolved oxygen.

II.1.2 Corrosion Inhibitors.

Electrochemical polarization curves were recorded by LALVANI *et al.* (1991) on a variety of pyrite electrodes in 1 M sulphuric acid and compared to polarization curves recorded when a number of corrosion inhibitors were added to the electrolyte. Corrosion inhibitors tested were: acetyl acetone, methoxy triacetoxy silane, glycidoxy propyl trimethoxy silane, penyl triacetoxy silane, humic acid, lignin-NaOH solution, oxalic acid and benzene. It was reported that the corrosion rate of pyrite could be reduced by 98% with acetyl acetone and humic acid treatment.

LALVANI and SHAMI (1987) found that the addition of the cations: Fe^{3+}, Cu^{2+} and Ag^{+} changed the rate of oxidation of pyrite slurries. The rate of corrosion was enhanced with ferric iron, yet the particles are rendered electrochemically inactive by adding small quantities of Ag^{+} and Cu^{2+}. The surface is passivated not by the formation of Ag_2S or CuS, but the indirect formation of elemental sulphur as

$$\begin{aligned} FeS_2 + 4\ Ag^{+} &\rightarrow 2\ Ag_2S + Fe^{2+} \\ Ag_2S + 2\ Fe^{3+} &\rightarrow 2\ Ag^{+} + 2\ Fe^{2+} + S^{o} \end{aligned} \qquad \textbf{(22)}$$

The Ag^{+} is merely a catalyst in this process and that there is no net consumption of silver.

For further reading see: BUCKLEY *et al.* (1989); CHAPMAN *et al.* (1983); HISKEY *et al.* (1987); HISKEY and PRITZKER (1988); KORNICKER and MORSE (1991); PETERS and MAJIMA (1968); SATO (1960, 1992); and WARREN *et al.* (1984).

II.1.3 Surface Reactions.

Raman spectroscopy and X-ray photoelectron spectroscopy (XPS) were used to identify iron oxides, iron polysulphide and elemental sulphur on the surface of electrochemically oxidized pyrite electrodes (MYCROFT *et al.*, 1990). They propose that the oxidation of pyrite occurs through two parallel reaction paths: 1) the direct oxidation of pyrite to sulphate by

$$FeS_2 \rightarrow S_2O_3^{2-} \rightarrow SO_4^{2-} \qquad \textbf{(23)}$$

and 2) the oxidation of pyrite to polysulphides and elemental sulphur by

$$FeS_2 \rightarrow FeS_x + Fe^{2+}\ (Fe(OH)_3) \rightarrow S \qquad \textbf{(24)}$$

Raman spectroscopy was also used to follow the *in situ* electrochemical oxidation of chalcocite (Cu_2S), chalcopyrite ($FeCuS_2$), covellite (CuS), galena (PbS), pyrrhotite and pyrite electrodes (LI *et al.*, 1993). Pyrite was oxidized at 1.0 V in 0.5 M NaCl (pH=6.5) for periods up to 1500 s; polysulphide (460 cm^{-1}) and elemental sulphur were both detected on the surface. Pyrrhotite was oxidized under the same conditions and only elemental sulphur was detected.

BUCKLEY and WOODS (1987) compared XPS spectra of freshly fractured pyrite with samples that were exposed to air, air-saturated acidic and air-saturated alkaline aqueous solutions. The only oxidation products observed on the air-exposed surface were iron oxides (711 eV) and

sulphate (168.5 eV). The surface of the samples exposed to acidic solution showed no evidence of iron oxides or sulphates, but did show polysulphides. The fresh pyrite surface was virtually indistinguishable from the samples exposed to air-saturated basic solution.

The interaction of an $FeS_2(100)$ surface, cleaved in ultrahigh vacuum (UHV), with adsorbed H_2O as an electron donor and adsorbed Br_2 as an electron acceptor, was studied with low energy electron diffraction (LEED), low-energy ion scattering spectroscopy (LEIS), and XPS. The (100) cleavage plane was characterized as a c(2X2) or $p(\sqrt{2}X\sqrt{2})R45^\circ$ surface by LEED and was interpreted in terms of the unreconstructed FeS_2 surface. It should be brought to the attention of the reader that pyrite has very poor cleavage and that authors of this study were probably studying reactions on a (100) parting surface. The H_2O is molecularly adsorbed at low temperatures (100 K) and desorbs completely at room temperature. The LEIS-spectra taken at low coverages (<0.5 monolayer) suggest a preferential interaction with the iron sites with water molecules (PETTENKOFER *et al.*, 1991).

For further reading see: BRION (1980); BUCKLEY and WOODS (1984); BUCKLEY (1988); CECILE (1985); HOCHELLA *et al.* (1986); HOCHELLA (1988); KARTHE *et al.* (1993); LAI *et al.* (1990); MERNAGH and TRUDU (1993); MUIR and NESBITT (1994); WIESE *et al.* (1987); and WOODS (1992).

II.1.4 Electrochemistry.

HAMILTON and WOODS (1981) and BUCKLEY *et al.* (1988) used linear potential sweep voltammetry to study the redox reactions of pyrite and pyrrhotite in pHs = 4, 9.2 and 13 solutions. Through the use of Pourbaix diagrams, rotating disk studies and charge measurements, the authors were able to assign reactions to the various voltammetric peaks. In general, pyrite oxidizes to sulphur and sulphate, while the pyrrhotite surface is blocked by the formation of iron oxides. The voltammetric assignments of HAMILTON and WOODS (1981) were corroborated by the use of X-ray photoelectron spectroscopy. They concluded that sulphur species identified previously on pyrite were really a metal-deficient sulphide (polysulphide).

Electrochemical experiments, including cyclic voltammetry and rotating disk, were performed on ground pyrite (-120 + 75 and -75 + 40 μm) in pH = 11 $NaClO_4$ solution (AHLBERG *et al.*, 1990). The initial oxidation of pyrite produced hydrophobic sulphur and hydrophillic iron hydroxide species. In the presence of EDTA, pyrite could be rapidly floated.

Oxygen pressure leaching experiments on pyrite electrodes were performed by BAILEY and PETERS (1976) in order to determine whether the oxidation of pyrite was molecular or electrochemical in nature. Pyrite was reacted with isotopically enriched O_2^{18} and/or H_2O^{18}; sulphate was precipitated from the electrolyte and analyzed for its isotopic composition. Pyrite oxidation is electrochemical and not molecular in nature, i.e., the overall reaction was reported as

$$FeS_2 + 8\ H_2O \rightarrow Fe^{3+} + 2\ SO_4^{2-} + 16\ H^+ + 15\ e^- \qquad \textbf{(25)}$$

Anodic polarization curves and cyclic voltamograms were used to study the electrochemistry of pyrite as a function of pH and mineral-semiconductor type. The pyrite semiconductor type had no effect on the electrochemistry. A mechanism for the oxidation of pyrite was proposed, involving the direct transfer of oxygen from water to the sulphur atoms on the pyrite surface (BIEGLER and SWIFT, 1979).

Anodic polarization curves were reported for pyrite electrodes as a function of pH (0.3 - 5.5) and temperature (25 - 69°C). The activation energy for pyrite oxidation at 650 mV (SCE) was calculated to be 61.5 kJ mol^{-1}. The anodic Tafel slope varied from 80 - 95 mV $decade^{-1}$ for fractured samples and 90 - 110 mV $decade^{-1}$ for polished specimens; a plot of potential at constant current vs. pH measured from the linear Tafel region has a slope of 30 mV pH^{-1}. The kinetic data was summarized and a mechanism for the oxidation was proposed (MEYER, 1979). Again, the number of references dealing with the electrochemical oxidation and leaching of pyrite are far too many to review in detail. The following provides a cursory review of the literature: AHLBERG *et al.* (1990); ANDRIAMANANA and La MARCHE (1983); BAILEY (1977); BAUER and LeCLERC (1987); BIEGLER *et al.* (1975); BIEGLER (1976); BRICENO and CHANDER (1988); BUCKLEY *et al.* (1985); CHANDER and BRICENO (1988); CHANDER *et al.* (1988); CHANDER (1991); CHEN *et al.* (1991); DOWNES and BRUCE (1955); ENNAOUI *et al.* (1986); HAMILTON and WOODS (1984); JAGERMANN and TRIBUTSCH (1983); JANETSKI *et al.* (1977); KLEIN and SUEY (1978); LALVANI and SHAMI (1988); LALVANI *et al.* (1990, 1991); LeCLERC and BAUER

(1990); LIU *et al.* (1988); MICHELL and WOODS (1978); MISHRA and OSSEO-ASARE (1988, 1992); PANG *et al.* (1990); PETERS (1977); RADYUSHKINA (1986); RAMPRAKASHI *et al.* (1991); RAO and FINCH (1987); SALVADOR *et al.* (1991); SCHUBERT and TRIBUTSH (1990); SISENOV and TARASEVICH (1988); and ZHU *et al.* (1991).

II.1.5 Precipitation.

Pyrite, marcasite, pyrrhotite, and to a lesser extent, troilite (FeS) and mackinawite (FeS_{1-x}) precipitation on carbon steel electrodes, in the presence of H_2S (g), was studied by SHOESMITH *et al.* (1979). By applying an anodic current, the carbon steel electrode was oxidized producing ferrous iron and di- and polysulphides. Pyrite formed when the concentration of ferrous ions were greater than the concentration of polysulphide ions; marcasite formed when the reverse was true. It was proposed that the formation of these two minerals required the oxidation of sulphide ions to disulphide or polysulphide species at the electrode surface as

$$2\ H_2S \rightarrow S_2^{2-} + 4\ H^+ + 2\ e^- \qquad \textbf{(26)}$$

Depending upon the ferrous iron concentration, either pyrite or marcasite was precipitated by

$$Fe^{2+} + S_2^{2-} \rightarrow FeS_2(s) \qquad \textbf{(27)}$$

Pyrrhotite, like pyrite, tended to form when the $[Fe^{2+}] > [\text{sulphide}]$ and in addition pyrrhotite was much more predominant over pyrite as the reaction temperature increased. The precipitation of pyrrhotite occurs by

$$7\ Fe^{2+} + 8\ H_2S \rightarrow 8\ Fe_{0.875}S(s) + 16\ H^+ + 2\ e^- \qquad \textbf{(28)}$$

The soluble phases mackinawite and troilite were the precursors for the formation of pyrrhotite; the ferrous iron, in Equation **(28)**, may have been supplied by the dissolution of these two minerals. Similar observations were also reported by SCHOONEN and BARNES (1991 b).

The complete reaction scheme for the formation of all the iron sulphide minerals on carbon steel surface can be found in **Figure 1**.

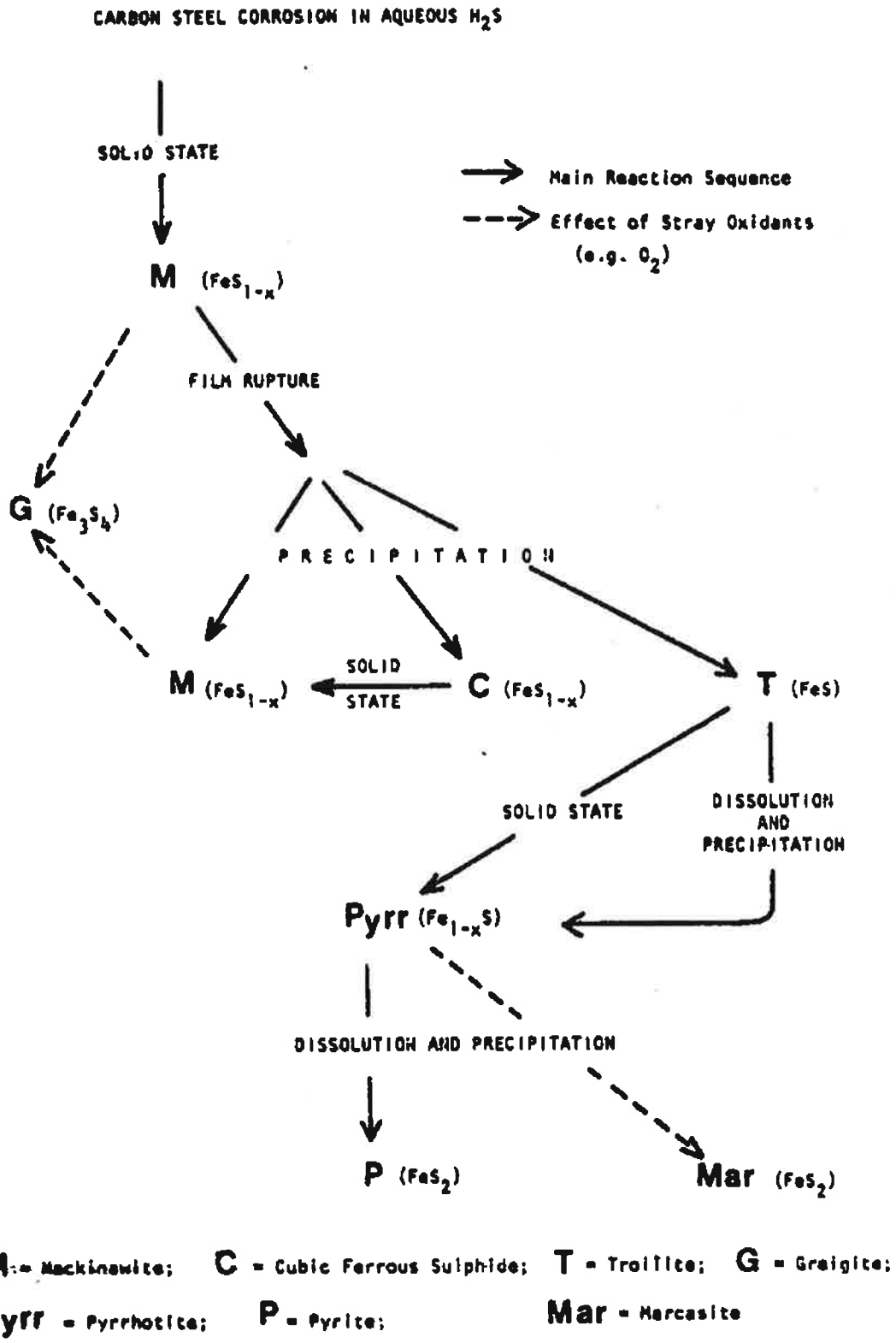

Figure 1: Corrosion scheme for carbon steel in aqueous H_2S. (Reproduced from SHOESMITH *et al.*, 1979, p 917.)

For further reading see: BERNER (1964, 1969, 1970, 1984); DAVISON (1980); FLEET (1978); HOWARTH (1979); LENNIE and VAUGHAN (1992); LAMBERT *et al.* (1980); MUROWCHICK and BARNES (1986); MORSE *et al.* (1987); RICKARD (1969, 1974, 1975) SCHOONEN and BARNES (1991 a, b); TAYLOR *et al.* (1979); WIKJORD *et al.* (1976).

II.2 PYRRHOTITE

II.2.1 Oxidative Dissolution.

Biological.

There is little published literature dealing specifically with the leaching of pyrrhotite by bacteria. Many of the published reports deal with either pyrite directly or mixed sulphides, as would be found in mine tailings. Recently, BHATTI *et al.* (1993) published the results of a study examining the solid phase oxidation products of pyrrhotite which had been leached in the presence of *Thiobacillus ferrooxidans*. They reported that the oxidation of the pyrrhotite began with the following oxidative and non-oxidative reactions:

$$Fe_{1-x}S + 2H^+ \rightarrow (1-3x)Fe^{2+} + 2x\ Fe^{3+} + H_2S \quad \textbf{(29)}$$

$$Fe_{1-x}S + O_2 + 4H^+ \rightarrow (2-6x)Fe^{2+} + 4x\ Fe^{3+} + 2\ H_2O + 2 \quad \textbf{(30)}$$

and, as with pyrite, the early stage of pyrrhotite oxidation began by chemical and/or electrochemical means, rather than as a result of biological oxidation of the mineral.

After approximately 5 days, the pH of the leach solution began to decrease, indicating that biological oxidation had begun. They identified the following solid products: sulphur, iron oxyhydroxides, K-jarosite ($KFe_3(SO_4)_2(OH)_6$ and Schwertmannite ($Fe_8O_8(OH)_6SO_4$) (see BIGHAM, 1994, p115). They proposed that the oxidation of elemental sulphur and ferrous iron were as a result of bacterial action by,

$$S^o + 1.5\ O_2 + H_2O \rightarrow SO_4^{2-} + 2\ H^+ \quad \textbf{(31)}$$

$$4\ Fe^{2+} + O_2 + 4\ H^+ \rightarrow 4\ Fe^{3+} + 2\ H_2O \quad \textbf{(32)}$$

while the K-jarosite and Schwertmannite precipitated from solution as the pH of the leachate increased. Bioleaching was significantly inhibited when the pH of the leachate exceeded four.

For further reading on the oxidation of pyrrhotite by bacteria see the following: AHONEN *et al.* (1986); MILLER and RISATTI (1988); ROSSI *et al.* (1983).

Chemical/Electrochemical.

The leaching of pyrrhotite was studied in aqueous solution using oxygen, ferric sulphate, ferric chloride, hydrochloric acid and in sulphuric acid. SUBRAMANIAN *et al.* (1972) reported that the best leaching results were obtained with sulphuric acid and molecular oxygen. Linear potential sweep voltammetry was used to study the redox reactions of pyrite and pyrrhotite at pHs = 4, 9.2 and 13. The voltammetric assignments were made in conjunction with X-ray photoelectron spectroscopic data. BUCKLEY *et al.* (1988) reported that the initial oxidation product for pyrrhotite was a metal-deficient sulphide rather than the previously believed sulphur phase.

HODGSON and AGAR (1984) studied the natural floatability of pyrrhotite using both single-crystal electrodes and particulate (packed-bed) electrodes. The major surface products were found to be $Fe(OH)_3$ and elemental sulphur. They reported that the oxidation of pyrrhotite was a two-stage process as follows:

Reaction 1:

$$FeS_{1.13} + H_2O = [Fe(OH)_a](S_2) + S_2^{2-}(aq) + H^+ + e^- \quad \textbf{(33)}$$

Reaction 2:

$$[Fe(OH)_a](S_2) + H_2O = [Fe(OH)_3] + S + H^+ + e^- \quad \textbf{(34)}$$

For further reading see the following: DOWNES and BRUCE (1955); GUO and LIU (1991); INGRAHAM *et al.* (1972); RADYUSHKINA *et al.* (1986) RAO and FINCH (1991); TOGURI (1975); SATO (1960, 1992); SUBRAMANIAN *et al.* (1972); VAN WEERT *et al.* (1974); and ZHENG and BAUTISTA (1984).

II.2.2 Surface Reactions.

FLEET (1978) used X-ray diffraction to study the alteration products of pyrrhotite. Using crystal structures it is shown that by removing one third of the iron from the pyrrhotite structure, contraction of the c-axis will allow the sulphur atoms to converge close enough to form disulphide groups and the marcasite structure.

STEGER (1978, 1982) has studied the air oxidation of pyrrhotite as a function of temperature, relative humidity (RH) and time. The progress of the oxidation of the mineral was monitored using a combination of spectral reflectance measurements and wet chemical methods. From the experimental results presented, STEGER (1982) concluded that the air oxidation of pyrrhotite proceeded by a sequence of reactions to give $FeSO_4$, $Fe(OH)(SO_4)\bullet nH_2O$, ferric oxide and elemental sulphur.

At low relativity humidities (RH = 37%), the oxidation of pyrrhotite proceeded by

$$Fe_7S_8 \rightarrow xFeS_2O_3 + (1-x)FeSO_4 \qquad \textbf{(35)}$$

without the formation of ferric hydroxide. Reaction **(35)** will continue in the presence of oxygen and/or water to form elemental sulphur, $FeSO_4$ and $Fe_2(SO_4)_3$. At high relative humidities (RH > 50%), the formation of ferric oxyhydroxide will occur according to

$$Fe(OH)(SO_4) + H_2O \rightarrow FeO(OH) + H_2SO_4 \qquad \textbf{(36)}$$

and the sulphuric acid in turn reacts with fresh pyrrhotite to form $FeSO_4$ and elemental sulphur or SO_2.

Fresh pyrrhotite ($Fe_{0.89}S$) surfaces were exposed to ambient conditions for periods of time varying from a few seconds to 86 days; the surfaces were analyzed by X-ray photoelectron spectroscopy (BUCKLEY and WOODS, 1985). It was reported that on a freshly fractured pyrrhotite surface, exposed to the air for no more than a few seconds, half of the iron in the first few layers had become bonded to oxygen. The alteration zone underlying the iron oxide zone was characterized by a sulphur-rich zone. BUCKLEY and WOODS (1985) found that the oxidation of the mineral was quite rapid and that after the first few seconds of air exposure, subsequent reaction was quite slow. Even after a 5 h exposure to air, iron bonded to sulphur could be detected within the depth analyzed

and that the altered thickness could have been no greater than 2 nm. When the spectra for the oxidation experiments lasting for 5 h and 86 days were compared, no substantial differences were observed.

BUCKLEY and WOODS (1985) concluded that during the first few seconds of oxidation iron diffuses to the surface to form, *via* iron(II) oxide, an iron(III) hydroxy-oxide which would leave an iron-deficient sulphide in the subsequent layer. The initial oxidation can be represented by

$$4\ Fe_{1-x}S + 3y\ O_2 + 2y\ H_2O \rightarrow 2y\ Fe_2O_3{\cdot}H_2O + 4\ Fe_{1-x-y}S \qquad \textbf{(37)}$$

with $y < (1-x)$

JONES *et al.* (1991) exposed ground pyrrhotite to (a) ambient conditions, (b) distilled water and (c) deoxygenated perchloric acid (0.05-1 M) and then the mineral surfaces were analyzed by X-ray photoelectron spectroscopy and X-ray diffraction. Surfaces exposed to air and water produced amorphous layers of iron oxyhydroxide, sulphates and iron-deficient sulphides. Pyrrhotite surfaces exposed to acidic solution were covered in a layer of crystalline Fe_2S_3.

PRATT *et al.* (1994 a) have published a detailed study of fractured pyrrhotite surfaces that were exposed to ambient conditions for 6.5 and 50 hours. Auger depth profiling was used to probe the change in atomic concentration of iron, sulphur and oxygen of the pyrrhotite-alteration zone as a function of depth. For the sample reacted for 6.5 hours, a 4 Å thick layer of iron(III) oxide (iron : oxygen = 1 : 1.5) lies on top of a sulphur-rich zone (iron : sulphur = 1 : 1.5). In this sulphur-rich zone, the sulphur to iron ratio drops almost linearly to the bulk iron to sulphur ratio of 1:1.15; this sulphur-rich zone was ≈ 24 Å thick. In the case of the pyrrhotite sample oxidized for 50 hours, a very similar iron-oxide layer, overlaying a sulphur-rich zone and the bulk pyrrhotite was observed. At the longer oxidation times, the iron oxide and sulphur-rich zones are about 30 - 50% thicker, and also, the sulphur-rich zone is richer in sulphur (iron : sulphur = 1 : 2) than in 6.5 hour case.

The mechanism of pyrrhotite oxidation, under ambient conditions, tentatively appears to be initiated by the reaction of oxygen and/or water molecules with the surface of the mineral. The oxyhydroxide species do not diffuse into the mineral, but iron diffuses from the bulk (near surface) to the mineral surface to form the iron-oxide layer. PRATT *et al.* (1994 a) proposed that the iron(III) sulphide is probably the most reactive species and provides the source of the iron. BUCKLEY and WOODS (1985 a) and JONES *et al.* (1992) and PRATT *et al.* (1994 a) all propose that the iron-oxyhydroxide layer partially blocks the pyrrhotite surface to further reaction. The sulphur-rich zone

(i.e., iron- depleted) forms as a result of the diffusion of iron to the surface. This sulphur-rich zone also contains minor quantities of polysulphide (see TERMES *et al.*, 1987), elemental sulphur and oxy-sulphur species (PRATT *et al.*, 1994 a).

PRATT *et al.* (1994 b) studied the oxidation of freshly fractured pyrrhotite surfaces which were reacted in a pH = 3.0 H_2SO_4 solution for an unspecified length of time. They found that the pyrrhotite surface was not homogeneously reacted; two distinct surface textures were observed. One surface was smooth and devoid of features, while the other was characterized by blocks separated by shrinkage cracks. It was also apparent that some of the blocks were in the process of spalling off the surface. The surface of the smooth area was reported to be approximately 100 Å thick. The outer most layer was 40 Å thick and composed of mainly iron oxyhydroxides with a small percentage of polysulphides. The next layer was also 40 Å thick and overlaid a layer of mixed iron oxyhydroxides and polysulphides. Under this layer was a 20 Å thick layer of iron sulphides, and the composition is transitional between the polysulphide and bulk pyrrhotite.

The blocky area was approximately 320 Å thick. The composition of this alteration zone was much more inhomogeneous than the smooth regions. Chemically, the blocky region was composed of iron oxyhydroxides and sulphur-rich zones.

PRATT *et al.* (1994 b) proposed that the smooth and blocky areas on the surface are related in time. The oxidation of fresh pyrrhotite placed in the acidic solution begins with the diffusion of ferrous ions from the mineral to the surface where the iron either dissolves into solution or is oxidized to form the ferric oxyhydroxide layer. Ferrous ions continue to diffuse through the surface film(s) as oxidative dissolution continues. Eventually, the surface oxidation product characterized by the blocky surface texture formed. The blocky layer becomes unstable and spalls from the surface leaving the underlying smooth texture. The process is repeated over and over as the mineral dissolves.

For further reading see: BUCKLEY AND WOODS (1985 b, 1988 b); CECILE (1985); HOCHELLA *et al.* (1986); HOCHELLA (1988); LAI *et al.* (1990); MERNAGH and TRUDU (1993); NOWOK and STENBERG (1988); WIESE *et al.* (1987); and WOODS (1992)

II.2.3 Precipitation.

The formation of pyrrhotite from ferrous iron and hydrogen sulphide has been discussed in some detail by SHOESMITH *et al.* (1979) and a summary of their findings was presented in the pyrite-precipitation section. The reaction kinetics iron monosulphide formation from iron oxyhydroxides and hydrogen sulphide, as would be found in sedimentary environments, has been reported by PYZIK and SOMMER (1981). They studied the principal reaction products for the reaction between goethite and dissolved sulphide ions and determined rate constants and rate expression(s) for reduction, dissolution and precipitation of iron monosulphides. The rate of reductive dissolution of FeOOH (see goethite reductive dissolution to follow) can be expressed as

$$)\rightarrow Fe(II)) = k[S]_t^{0.5}\ [H^+]^{0.5}\ A_{FeOOH} \qquad k = 0.017 \pm 0.002\ m \tag{38}$$

and in turn, the rate of formation of iron monosulphides can be expressed as

$$_{2}S) = k\ [S]_t\ [H^+]\ A_{FeOOH} \qquad k = 82 \pm 18\ mol^{-1}\ L^2 \tag{39}$$

where $[S]_t$ is the concentration of total dissolved sulphide, $[H^+]$ is the hydrogen ion activity, and A_{FeOOH} is the goethite specific surface area. It should be noted that this rate law is slightly different from that reported by RICKARD (1974); the reaction orders for $[S]_t$, $[H^+]$, and A_{FeOOH} are 1.5, 2 and 1, respectively.

Based on the rate laws for dissolution of FeOOH and precipitation of iron monosulphides, POHL (1954) and PYZIK and SOMMER (1981) proposed that the rate determining step is

$$(FeOH\cdot xH_2O)^+ + HS^- \rightarrow [Fe\cdot(x + 1)H_2O]SH \tag{40}$$

The entire mechanism for the formation of ferrous monosulphide is reproduced in **Figure 2**.

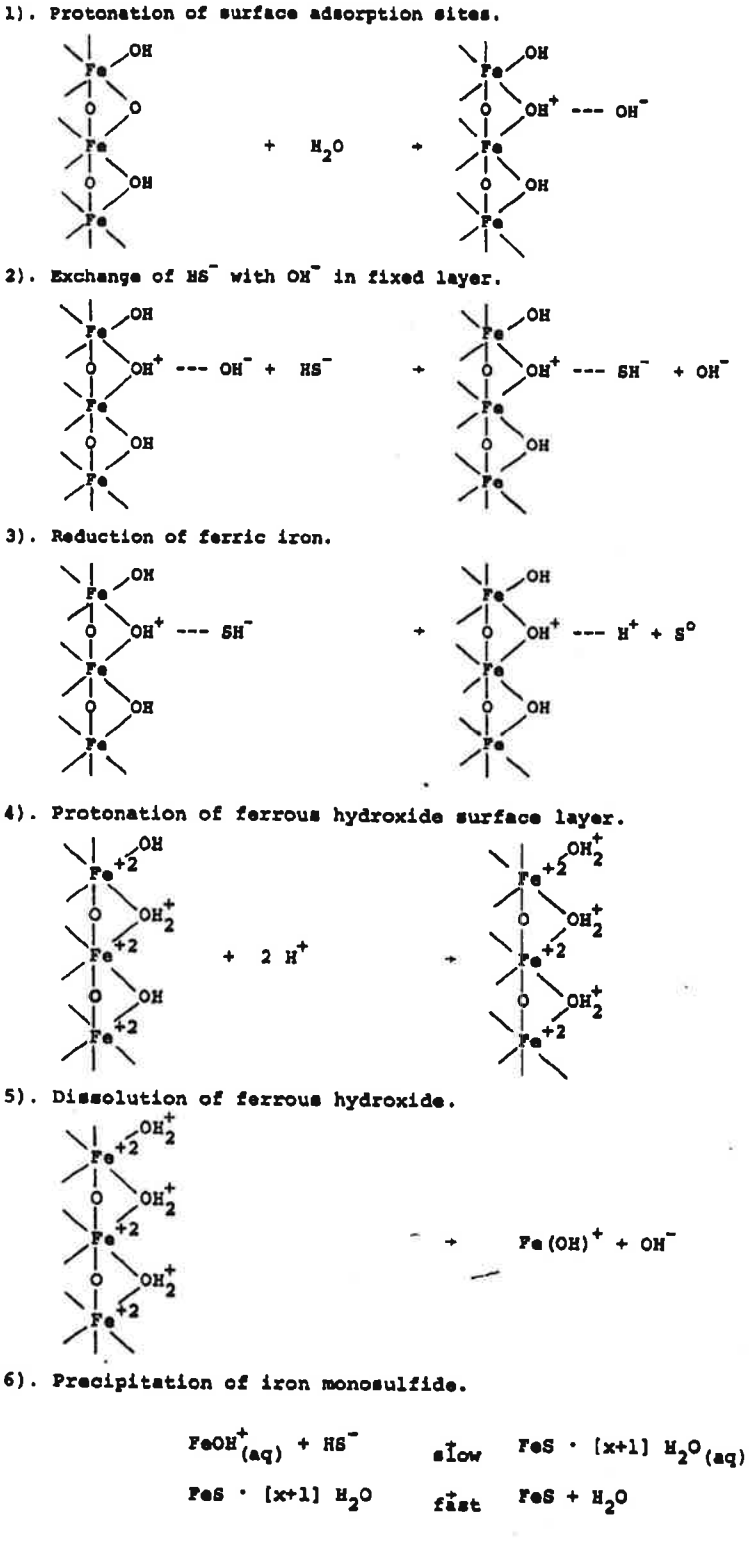

Figure 2: Postulated overall reaction mechanism for the formation of ferrous monosulphide. (PYZIK and SOMMER, 1981, page 696).

For further reading see: BERNER (1964, 1969, 1984); DAVISON (1980); HOWARTH (1979); LENNIE and VAUGHAN (1992); LAMBERT *et al.* (1980); MORSE *et al.* (1987); RICKARD (1969, 1974); SCHOONENE and BARNES (1991 a, b); TAYLOR *et al.* (1979); WIKJORD *et al.* (1976).

II.3 ARSENOPYRITE

II.3.1 Oxidative Dissolution.

Biological.

Even though the bioleaching of arsenopyrite is important in many industrial processes, little information has been reported in the literature; there are no detailed reports of the kinetics of the bioleaching of arsenopyrite. Recently, the General Mining Union Corporation in the Transvaal has used bioleaching to recover 90% of the gold from gold-bearing arsenopyrite at a lower capital cost than by floatation-roasting (CUPP, 1984; and HAINES, 1989). Similar technology has also been described by the Denison mines (WADDEN and GALLANT, 1985).

MANDL *et al.* (1992) reported that the bacterial oxidation of arsenopyrite occurs by the following reaction:

$$4\ FeAsS + 13\ O_2 + 6\ H_2O = 4\ H_3AsO_4 + 4\ FeSO_4 \qquad \textbf{(41)}$$

The ferrous iron can be oxidized by *T. ferrooxidans* to ferric iron ($Fe_2(SO_4)_3$) which can in turn oxidize arsenopyrite and arsenite by

$$S + Fe_2(SO_4)_3 + 6\ O_2 + 4\ H_2O = 2\ H_3AsO_4 + 4\ FeSO_4 + 2\ H_3AsO_4 + Fe_2(SO_4)_3 + 2\ FeAsO_4(s) + 3\ H_2SO_4 \qquad \textbf{(42)}$$

The oxidation of arsenopyrite to the As(III) or As(V) seems to be of some controversy and of great environmental importance. As(III) is much more toxic than As(V) and the formation of $FeAsO_4(s)$ provides a means of removal of arsenic from aqueous solution. NISHIMURA and TOZAWA (1988) reported that As(III) cannot be oxidized by oxygen and requires a stronger oxidizing agent, such as ozone. MANDL *et al.* (1992) reported that if the solution pH > 5, the As(III) will precipitate and/or be reduced. ILYALETDINOV and ABDRASHITOVA (1979) reported that the microbe *Pseudomonas arsentoxidans,* will oxidize As(III) to As(V) by

$$NaAsO_2 + H_2O \rightleftharpoons NaAsO_3 + 2\ H^+ + 2\ e^- \qquad \textbf{(43)}$$

in the pH range 6 < pH < 8.5 (see also TURNER, 1954).

For further reading on the oxidation of arsenopyrite by bacteria see the following: BARRETT (1993); BARRET *et al.* (1990); BRADDOCK *et al.* (1984); COLLINET and MORIN (1990); DOROFEEV *et al.* (1990); EHRLICH (1964); GOLDBLATT *et al.* (1983); KOSLIDES and CIMINELLI (1991); LIVESY-KOSTINA and CHERNYAK (1979); MILLER and HANSFORD (1992); OSBORNE and EHRLICH (1976); PHILLIPS and TAYLOR (1976); SEHLIN and LINDSTRÖM (1992); and TURNER (1949, 1954).

Chemical/Electrochemical.

PAPANGELAKIS and DEMOPOULOS (1990 a) reported that prior to their work, only incidental information had been reported on the oxidation of arsenopyrite and that most of it was derived from the literature on the oxidation of pyrite. From the present literature review it appears that little has improved in the understanding of FeAsS leaching under ambient conditions. PAPANGELAKIS and DEMOPOULOS (1990 a,b) and PAPANGELAKIS *et al.* (1990) studied the kinetics of pressure oxidation of arsenopyrite at high temperatures (120-180°C) and high oxygen pressures (2-20 atm O_2). This information may not be as pertinent to AMD situations as many of the leaching studies mentioned previously and, therefore, the work of PAPANGELAKIS will be briefly reviewed.

PAPANGELAKIS and DEMOPOULOS (1990 a) propose that the chemical reactions occurring during the pressure leaching of FeAsS in H_2SO_4 are:

$$\text{:) + 13 } O_2(aq) + 6\ H_2O \rightarrow 4\ H_3AsO_4(aq) + 4\ Fe^{2+}(aq) + \quad \textbf{(44)}$$

$$4\ FeAsS(s) + 7\ O_2(aq) + 8\ H^+ + 2\ H_2O \rightarrow 4\ H_3AsO_4(aq) + 4\ Fe^{2+}(aq) + 4\ S^\circ(l) \quad \textbf{(45)}$$

$$2\ Fe^{2+}(aq) + 1/2\ O_2(aq) + 2\ H^+(aq) \rightarrow 2\ Fe^{3+}(aq) + H_2O \quad \textbf{(46)}$$

$$\text{e}^{3+}(aq) + H_3AsO_4 + 2\ H_2O(aq) \rightarrow FeAsO_4 \cdot 2H_2O(s) + 3\ H \quad \textbf{(47)}$$

The authors point out that these reactions are based on stoichiometric considerations rather than measured speciation and these reactions are consistent with the principle reaction products found at the end of the leaching experiment, i.e., Fe(II), Fe(III), As(V) species, scorodite ($FeAsO_4 \cdot 2H_2O$) and elemental sulphur. No As(III) species were found. PAPANGELAKIS and DEMOPOULOS (1990 b) report that the oxidation of FeAsS occurs by two competing paths (reactions **(44)** and **(45)**). The kinetics data was modelled using the shrinking core model and it was assumed that the rate of FeAsS oxidation was controlled by either the surface reaction(s) or by diffusion processes through the product layer, or a combination of the two. Analysis of the reaction data showed that the rate controlling step involved a chemical reaction taking place at the surface of the mineral. Formation of elemental sulphur or $FeAsO_4 \cdot 2H_2O$ on the mineral surface did not hinder the rate of oxidation.

The rate of oxidation has been reported to follow the following rate law:

$$\text{Rate} = -49.527\ A\ \exp\left(\frac{-8672}{T}\right)\ P_{O_2} \qquad \textbf{(48)}$$

where the Rate is in the units of mol min^{-1}, T is the time (min.), A is the surface area in cm^{-2} and P_{O2} is the partial pressure of oxygen. From the rate data, they have determined that the activation energy calculated for the oxidation of monoclinic and triclinic FeAsS is 72.1 and 66.5 kJ mol^{-1}, respectively. They propose that the oxidation of FeAsS proceeds by the following electrochemical/surface reactions:

$$FeAsS(s) + 8\ H_2O \rightarrow Fe^{2+}(aq) + H_3AsO_4(aq) + SO_4^{2-}(aq) + 13\ H^+(aq) + 13\ e \qquad \textbf{(49)}$$

$$O_2(aq) + 4\ H^+ + 4\ e^- \rightarrow 2\ H_2O \qquad \textbf{(50)}$$

where the cathodic reaction **(50)** at the mineral surface was considered to be rate determining.

For further reading see the following: KOSLIDES and CIMINELLI (1991, 1992); PAPANGELAKIS *et al.* (1986, 1990); and PIRHONEN (1993).

Electrochemistry.

SANCHEZ and HISKEY (1988) studied the electrochemistry of arsenopyrite in basic solution (pH 8 - 12) using rest potential measurements, cyclic voltammetry and constant potential. They reported a two step oxidation sequence. The first step involved the oxidation of FeAsS to $Fe(OH)_3$ and $H_2AsO_3^-$ by

$$sS + 9\ H_2O \rightarrow FeOOH + H_2AsO_3^- + SO_4^{2-} + 15\ H^+ + 12 \qquad \textbf{(51)}$$

The second step involved the further oxidation (i.e., at higher oxidation potential) of arsenite with water to produce $HAsO_4^{2-}$ by

$$H_2AsO_3^- + H_2O \rightarrow HAsO_4^{2-} + 3\ H^+ + 2\ e^- \qquad \textbf{(52)}$$

BEATTIE and POLING (1987) studied the oxidation of FeAsS in basic solution by both electrochemical and surface analytical methods. They reported that the oxidation of FeAsS resulted in the formation of a thick iron oxide/arsenite layer; sulphur diffused from the surface as SO_4^{2-} into the electrolyte. They proposed that the dominant oxidation reaction was

$$FeAsS(s) + 11\ H_2O \rightarrow$$
$$s) + HAsO_4^{2-}(aq) + SO_4^{2-}(aq) + 18\ H^+(aq) + 14\ e^- \quad E^o \qquad \textbf{(53)}$$

They reported that the iron oxide film is of constant thickness and that the rate of diffusion through this barrier film is hindered. At temperatures above 45°C the morphology of the film changes and it becomes more porous. Even though the film thickness builds rapidly, the oxidation of the FeAsS continues.

The electrode potential (mixed potential, or rest potential) in the pH range of 3.8 to 11.2 obeys the relation

$$Eh\ (mV\ SHE) = 586\,mV - 48.2\ pH \qquad \textbf{(54)}$$

For further reading see the following: BUCKLEY and WALKER (1988); FENG and CHEN (1993); JAMBOR *et al.* (1991); KOSTINA and CHERNYAK (1977, 1979); SANCHEZ and HISKEY (1991); and WANG *et al.* (1992 b).

II.3.2 Surface Reactions.

RICHARDSON and VAUGHAN (1989) exposed arsenopyrite crystals to a variety of oxidizing conditions, including air (150°C), steam and the following aqueous solutions: ammonium hydroxide, hydrogen peroxide, and sulphuric acid. X-ray photoelectron spectroscopy and Auger electron spectroscopy were used to determine the surface chemistry after each treatment. They reported that arsenopyrite was stable in air and water, but oxidized rapidly in acidic or basic conditions. The oxidation reaction occurred only to a limited depth and the reaction appeared to be passivated. They reported that the major surface species are iron oxides, in particular magnetite (Fe_3O_4) and goethite (αFeOOH), arsenic oxides and sulphates.

BUCKLEY and WALKER (1988) used XPS to follow the oxidation of arsenopyrite which had been exposed to air, basic solution (pH = 11, ammonia) or acid solution (pH = 2.9, acetic acid). FeAsS which was exposed to air, oxidized rapidly with the arsenic being preferentially oxidized to both As(III) oxides and arsenic suboxides. The iron was also oxidized to Fe(III) oxides. With increasing exposure to air, the rate of oxidation slowed and As(V) oxides were produced. Sulphur showed no sign of oxidation, even after several days exposure to air. They propose that the air oxidation of FeAsS proceeds by

$$S + (3/4\ x + \tfrac{1}{2}\ by)\ O_2 \rightarrow \tfrac{1}{2}\ x\ Fe_2O_3 + y\ AsO_b + Fe_{1-x}A \qquad \textbf{(55)}$$

where $y > x$ and $b \leq 1.5$.

The oxidation of FeAsS in alkaline solution was more rapid than in air, but the oxidation products were virtually identical; no As(V) oxides were found. The oxidation of FeAsS in acidic solution produced a surface which became increasingly more enriched in sulphur; the arsenic and iron oxides had dissolved into solution. They determined that the sulphur-rich layer was not elemental sulphur, but rather a severely metal-deficient sulphide lattice (i.e., a polysulphide).

For further reading see the following: DRASKIC *et al.* (1984); FLEET *et al.* (1993); MERNAGH and TRUDU (1993); MUIR and NESBITT (1994); and WANG *et al.* (1992 a).

II.3.3 Precipitation.

No references were found dealing specifically with the kinetics of arsenopyrite precipitation.

II.4 CHALCOPYRITE/GALENA (etc.)

In the search for reference material, a number of particularly outstanding references dealing specifically with the leaching of sulphides were found. These references fell outside the scope of this study, but it was felt that they should be brought to the attention of AMD researchers. See the following references: AWAKURA *et al.* (1980); DUTRIZAC *et al.* (1970, 1992); DUTRIZAC and MacDONALD (1973, 1974 and 1978); DUTRIZAC (1989); EADINGTON (1973); LEI and CARNAHAN (1984); LIDDELL and BAUTISTA (1981); MAJIMA *et al.* (1985); MAJIMA (1988); MILLER and PORTILLO (1981); MORIN *et al.* (1985); MUNOZ *et al.* (1979); NIEDERKORN (1985); NUNEZ *et al.* (1990); PARKER *et al.* (1981); PAPANGELAKIS *et al.* (1986, 1990); SCOTT and NICOL (1977) SKEWES (1972); VAUGHAN (1982); WARREN *et al.* (1985); and ZHENG and BAUTISTA (1984).

III. IRON OXIDES

III.1 DISSOLUTION MECHANISMS

The kinetics and thermodynamics of the dissolution of goethite has been studied extensively, and is relatively well understood, (see HERING and STUMM, 1990; and WHITE, 1990). HERING and STUMM (1990) have listed approximately 150 references dealing with the dissolution of oxides, in particular goethite and hematite. They reviewed the basic models of dissolution and examined the effects of surface-controlled mineral dissolution, as well as the reductive and the oxidative dissolution of minerals.

The dissolution of many of the iron oxyhydroxide complexes can occur either directly without the change in oxidation state of the ferric iron, or by reduction of the iron to the soluble ferrous species. Nonreductive dissolution of the sparingly soluble ferric oxyhydroxides occurs in the presence of a complexing ligand.

CORNELL *et al.* (1974, 1976); MAJIMA *et al.* (1985, 1988); FLEER and JOHNSTON (1986); FURRER and STUMM (1986); ZINDER *et al.* (1986); MILLERO *et al.* (1987); TROLAND and TARDY (1987); and BRUNO *et al.* (1992) studied the rate of goethite and hematite oxidation in the presence of the inorganic ions: Cl^-, SO_4^{2-}, ClO_4^-, and/or in the presence of the complexing species: oxalate, humic acids, and fulvic acid. In general, the rate of reaction is limited by the rate of detachment of the iron centre from the oxide surface, as well as the surface concentration of the complexing ligand (FURRER and STUMM (1986) and the pH. The general rate law is

$$\text{Rate}_L = k_L\ (\text{Fe-L})_{sf}\ (C_H^s)^n \qquad \textbf{(56)}$$

where Fe is the metal centre and $(\text{Fe-L})_{sf}$ is the surface concentration of the ligand, k_L is the reaction constant and $(C_H^s)^n$ represents the surface concentration of H^+ to the power n. (i.e., n represents the number of protons required in weakening the Fe(III)-O bond).

III.2 GOETHITE

III.2.1 Dissolution.

Nonreductive Dissolution Of Goethite.

The following rate laws have been derived for the dissolution of goethite, under nonreductive conditions, in Cl^-, ClO_4^-, and oxalate solutions:

a) Cl^-/α-FeOOH

In dilute chloride solutions, the rate can be expressed as (CORNELL *et al.*, 1976), $1 >> K[Cl^-]$,

$$\text{Rate}=kK\ (\text{Fe-L})_{sf}\ [Cl^-]\ [H^+] \qquad \textbf{(57)}$$

In moderate concentrations of chloride i.e., $K[Cl^-] \approx 1$, where K is a constant which relates the surface concentration of the Fe-Cl on goethite and is related to the $[Cl^-]$ by the Langmuir relation

$$(\text{Fe-Cl})_{sf} = \frac{K[\text{number of surface sites}][Cl^-]}{1 + K[Cl^-]} \qquad \textbf{(58)}$$

In concentrated chloride solutions, the rate law is, i.e., $1 >> K[Cl^-]$

$$\text{Rate}=k\ (\text{Fe-L})_{sf}\ [H^+] \qquad \textbf{(59)}$$

A list of the rate data as a function of $[Cl^-]$ and $[H^+]$ can be found in Table 4.

$[H^+]$ mol L^{-1}	$[Cl^-]$ mol L^{-1}	Rate(g Fe)x10^4 released/g goethite/hr
0.1	0.1	0.012
0.1	0.5	0.018
0.5	0.1	0.050

Table 4: A comparison of the effect of anion and proton concentration on the rate of dissolution of goethite.

The average activation energy for goethite leaching in HCl solution was 23-24 kcal/mol.

b) ClO_4^-/α-FeOOH, (CORNELL *et al.*, 1976)

The rate of dissolution of goethite in perchlorate was reported to be

$$\text{Rate} = k[H^+] \qquad \textbf{(60)}$$

The activation energy for dissolution of goethite in $HClO_4$ was found to be only 1 kcal/mol less than that measured in identical experiments for HCl, as discussed above.

CORNELL *et al.* (1976) reported that, while the chloride ion has a role in the dissolution of goethite, it is not essential to the reaction; goethite dissolved in acid, for example $HClO_4$, even though no chloride ions were present. In the absence of protons, the chloride ion was unable to attack goethite. They reported that suspensions of goethite in NaCl at pH = 5.8 remained for months without showing release of ferric iron.

c) oxalate/α-FeOOH, (ZINDER *et al.*, 1986)

The rate law was reported to be

$$\text{Rate} = k(\text{oxalate})_{sf}(H^+)_{sf} \qquad \textbf{(61)}$$

where $(\text{oxalate})_{sf}$ is the surface concentration of the bidentate ferric oxalato complex. The value of the rate constant, k, was not reported.

Nonreductive Dissolution Mechanisms (General).

a) Cl^-/α-FeOOH

The mechanism of dissolution of goethite in chloride is

$$\begin{aligned} O\text{-}Fe\text{-}OH(sf) + Cl^- &\rightleftharpoons O\text{-}Fe\text{-}Cl(sf) + OH^- \\ OH^- + H^+ &\rightleftharpoons H_2O \end{aligned} \quad \textbf{(62)}$$

$$\begin{aligned} O\text{-}Fe\text{-}Cl(sf) + H^+ &\rightarrow Fe(OH)Cl^+(aq) \\ Fe(OH)Cl^+(aq) + H^+ &\rightarrow FeCl^{2+} + H_2O \end{aligned} \quad \textbf{(63)}$$

and the overall reaction is

$$FeOOH + 3\ HCl \rightarrow FeCl^{2+} + 2\ Cl^- + 2\ H_2O \quad \textbf{(64)}$$

as noted above, the chloride is not essential to the leaching mechanism, and therefore the mechanism changes with the chloride concentration.

b) ClO_4^-/α-FeOOH

The mechanism for the leaching of goethite in perchloric acid is:

$$OFe\text{-}OH(sf) + H^+ \rightleftharpoons OFe^+(sf) + H_2O \quad \textbf{(65)}$$

$$OFe^+(sf) + H^- \rightarrow Fe(OH)^{2+}(aq) \quad \textbf{(66)}$$

and then the following rapid reaction occurs:

$$Fe(OH)^{2+}(aq) + H^+ \rightleftharpoons Fe^{3+}(aq) + H_2O \quad \textbf{(67)}$$

c) oxalate/α-FeOOH, (ZINDER *et al.*, 1986; and HERING and STUMM, 1990)

The nonreductive dissolution mechanism for goethite and oxalate is complex involving many steps; the mechanism is given in **Figure 3**a.

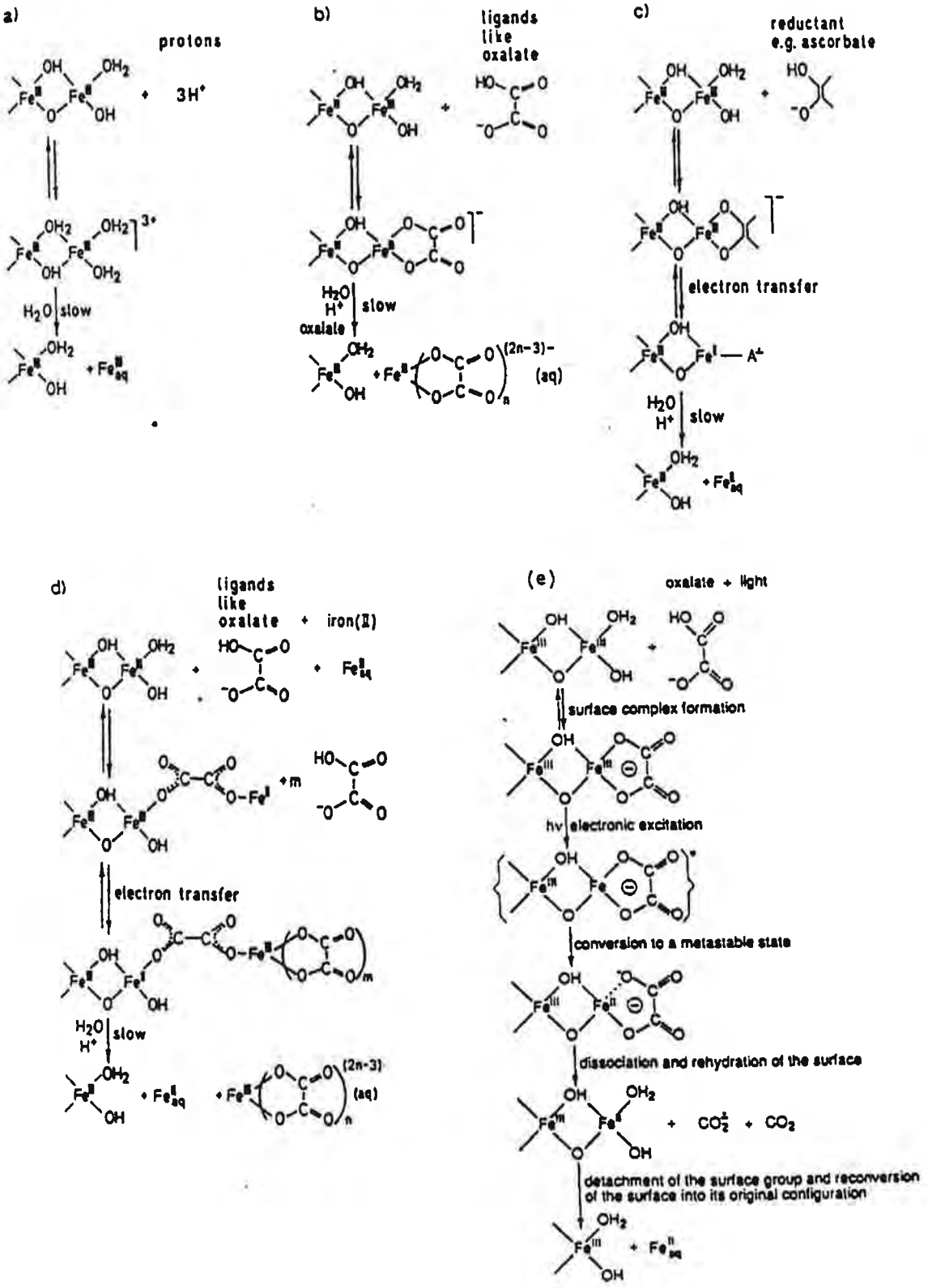

Figure 3: A schematic representation of the reaction modes for dissolution of iron oxyhydroxides. Reproduced from HERING and STUMM (1990 p. 441)

Reductive Dissolution Of Goethite.

Reductive dissolution can markedly enhance the rate of goethite dissolution. CHANG *et al.* (1983); CHANG and MATIJEVIĆ (1983); ZINDER *et al.* (1986); SULZBERGER *et al.* (1989); BANWART (1989); BANWART *et al.* (1989) HERING and STUMM (1990); RUEDA *et al.* (1992) and DENG and STUMM (1993) have all studied the reductive dissolution of iron oxyhydroxides, as well as other transition metal oxides. Ligands such as oxalate, humic acid, EDTA (ethylenediaminetetraacetic acid), ascorbate, citrate, phenols, sulphides, dithionite, bisulphite, hydroquinone and fulvic acid can complex with the iron centre at the oxide surface (ZINDER *et al.*, 1986; and HERING and STUMM, 1990) and participate in reductive dissolution (see **Figure 3**). Electron transfer from the reductant to the ferric-surface site precedes the detachment step. It should be noted that the reductive dissolution mechanism can be greatly enhanced under photochemical conditions (WAITE and MOREL, 1984; also see **Figure 3**e); and can be catalyzed by O_2, and transition metals (Fe^{2+}, Mn^{2+}, VO^{2+}) (FAUST and HOFFMANN, 1986; also see **Figure 3**d). The much more soluble ferrous species are released into the solution with or without complexation. This type of mechanism may be very important in the leaching of iron oxides in both mine tailings and soils.

Reductive dissolution of the ferric ion occurs "on" the surface of the iron oxide prior to the rate-determining reaction, i.e., the release of the ferrous ions is still rate determining. The general rate law involves the ligand and/or the H^+ ion. If the H^+ is involved in the rate law, this generally indicates that dissolution is proton promoted. For example, the reductive dissolution of α-FEOOH in the presence of H^+ and oxalate can either be proton promoted, Eqn.(**68**), or oxalate promoted, Eqn. (**69**), with the following rate laws,

$$\text{ate} = k(H^+)^3_{sf} \qquad k=\frac{-1.2\text{x}10^{-9}\ \text{mole}^{-2}\ \text{m}}{\text{h}} \qquad \textbf{(68)}$$

$$\text{Rate} = k(\text{Fe-oxalate})_{sf} \qquad k=8.9\text{x}10^{-2}\ \text{h}^{-} \tag{69}$$

The general rate law is

$$= k(\text{Fe-oxalate})_{sf}\ (H^{+})_{sf} \qquad k=\frac{3.8\text{x}10^{4}\ \text{mole}}{\text{h}} \tag{70}$$

The mechanism(s) for both oxalate and proton promoted reductive dissolution of goethite are given **Figure 3** b,c.

It should be noted that for non monodentate ligands (i.e., polydentate ligands like EDTA, oxalate, phosphate, etc..) the temperature of reaction is a very important parameter, since higher temperatures are required to release the reduced iron into solution. Also, DENG and STUMM (1994)

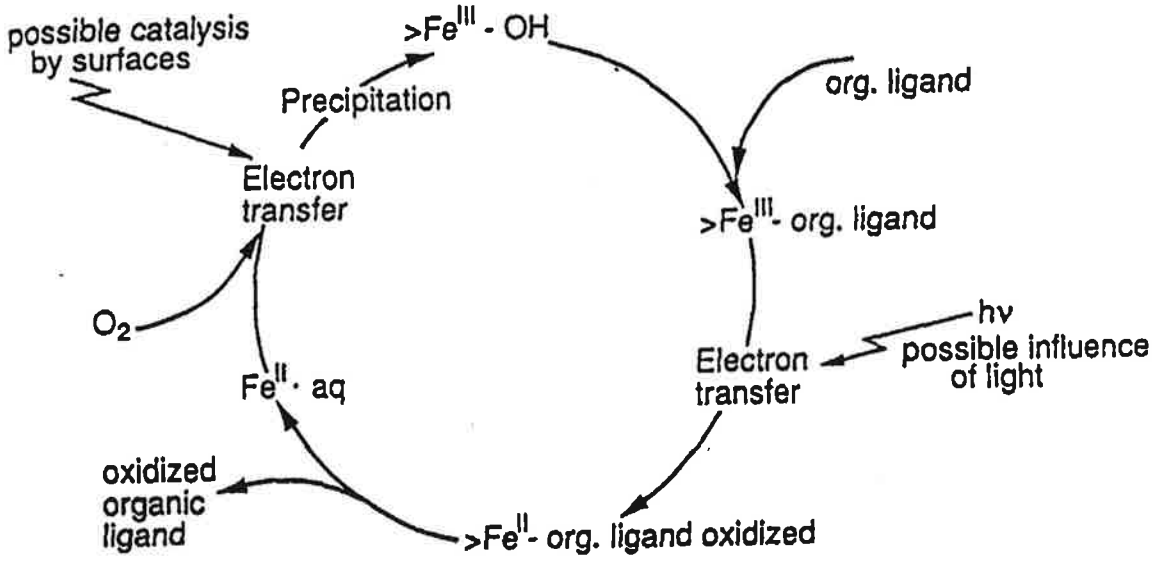

Figure 4: The dissolution of iron oxyhydroxides at the oxic-anoxic boundary. (reproduced from HERING and STUMM, 1990; page 457).

have reported that the rate of leaching of iron oxides is highly dependent on the ions present in

solution at the time of precipitation of the iron oxide. HERING AND STUMM (1990) have summarized the mechanisms for the dissolution of iron oxyhyrdroxides promoted by oxidizable organic ligands and subsequent reoxidation of ferrous iron by O_2 at the oxic-anoxic boundary. **Figure 4** depicts a schematic diagram showing the cycling of ferric and ferrous iron at the oxic-anoxic boundary.

III.2.2 Precipitation.

The mechanism of precipitation of goethite from aqueous solution has been reviewed by FERRON *et al.* (1991); BRYSON and TE RIELE (1986). Neither reference was available for review in time for the final report.

III.3 HEMATITE

Nonreductive Dissolution.

Acid	Activation Energy /kJ mol^{-1}
HCl	90.3, 95.7, 91.5, 77.5
H_2SO_4	76.1, 104
$HclO_4$	86.9, 80.3

Table 5: Activation energies for nonreductive dissolution of hematite by a number of mineral acids reported by MAJIMA *et al.*, (1985).

The theory given above applies to many of the iron (III) oxyhydroxides, including hematite and ferrihydrite, according to ZINDER *et al.* (1986). Much of the published literature refers to experiments performed on goethite, but some publications are specific to hematite and where the reaction mechanism(s) differs from that of goethite, it will be reviewed. MAJIMA *et al.* (1985) studied the nonreductive dissolution of hematite in the presence of the inorganic acids: HCl, $HClO_4$ and H_2SO_4. The activation energies of hematite are found in Table 5. They reported that the leaching

rate of hematite was first order in $[H^+]$ for HCl and $HClO_4$, as with goethite above, but half order in $[H^+]$ for H_2SO_4. They also studied the effect of mixing acids and salts (i.e., NaCl in H_2SO_4). From these experiments, they concluded the leaching rates of hematite were quite different in various acids having the same H^+ ion activity, and that this is indicative of the importance of anion adsorption at the hematite surface. For example, the rate of leaching of hematite in dilute sulphuric acid solutions was greater than that in hydrochloric acid. Calculations show that the concentration of sulphate ions, in the layer next to the hematite surface, is 200 times that of chloride ions.

BRUNO *et al.* (1992) studied the dissolution of hematite in bicarbonate solutions. The rate equation for the dissolution rate normalized to the specific area of the solid is

$$\text{Rate} = k[HCO_3^-]^{0.23} \qquad k = 1.42\text{x}10^{-7}\ \text{h}^{-1} \qquad \textbf{(71)}$$

The experimentally determined rate law for hematite dissolution in bicarbonate based on the concentration of the surface species is

$$\text{Rate} = k(\text{Fe-OH})_{sf} \qquad k=1.1\text{x}10^{-3}\ \text{h}^{-1} \qquad \textbf{(72)}$$

Based on the surface speciation studies of CO_2 (g), and the fact that the dissolution rate is first order with respect to the dominant surface species FeOH-HCO_3^-, they proposed that the mechanism, shown in **Figure 5**, accounts for the dissolution of hematite by bicarbonate.

They concluded that an increase in the partial pressure of CO_2 (g) in natural systems can mobilize Fe(III) and later precipitate the ferric iron if the partial pressure of CO_2 (g) drops.

For further reading see BALTZINGER and BARO (1973).

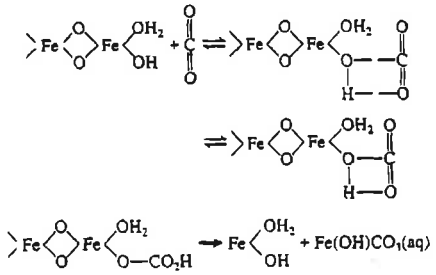

Figure 5: The mechanism of bicarbonate promoted dissolution of iron oxides (reproduced from BRUNO *et al.*, 1992, p-1145)

III.4 MAGNETITE

III.4.1 Dissolution.

The dissolution of magnetite $(Fe^{2+}, Fe^{3+}_2)O_4$ occurs in a similar manner to that of goethite and hematite, as discussed above, but the ferrous iron in the magnetite structure significantly complicates the dissolution mechanism. The dissolution of magnetite can occur by the following mechanisms:

1) leaching by inorganic acids (heterogeneous redox reactions),

2) reductive dissolution using organic ligands and transition metals and,

3) solid state electrochemical reactions and electron transfer.

Leaching and dissolution of magnetite by inorganic acids has been shown by GORICHEV *et al.* (1978), SIDHU *et al.* (1981), BRUYÈRE and BLESA (1985), WHITE (1990, p. 480), WHITE *et al.* (1994) to occur in a congruent manner in strong acids (0.5 N HCl, 0.5 - 2.0 N H_2SO_4) by

$$(Fe(II),Fe(III)_3)O_4 + 8\ H^+ \rightarrow 2\ Fe^{3+} + Fe^{2+} + 4\ H_2O \qquad \textbf{(73)}$$

GORICHEV *et al.* (1978) reported that the rate law is

$$\begin{aligned} \text{Rate} &= k[H^+]^{0.5}\ [Fe^{3+}]^{-0.5}\ [Fe^{2+}]^{0.5} \\ \text{Rate}' &= \text{Rate} + k'[Fe^{2+}];\quad \text{Rate}' = \text{rate when } [Fe^{2+}]=0 \end{aligned} \qquad \textbf{(74)}$$

and the activation energy is 71 kJ mol^{-1} (BRUYÈRE and BLESA, 1985). In more dilute acidic solutions, the concentration of ferrous iron increases with time, while the ferric iron concentration remains constant; hydrogen ions are incorporated into the magnetite structure. Again, the mechanism for dissolution involves the surface complexation of both protons and ligand ions.

BLESA (1984) reported that the reductive dissolution of magnetite by transition metals ligands, molecular oxygen and organic ligands have been documented in the literature, for example, ferrous iron can dissolve magnetite by,

$$I),Fe(III)_3)O_4 + 8\ H^+ + 2{*}Fe^{2+} \rightarrow 2{*}Fe^{3+} + 3\ Fe^{2+} + 4 \qquad \textbf{(75)}$$

The aqueous ferrous iron acts as an electron donor ($Fe^{2+} \rightleftharpoons Fe^{3+} + e^-$) and results in an increase in the release rate of the less strongly bound ferrous iron - i.e., it is autocatalytic (WHITE, 1990). Similarly, EDTA and oxalate will complex the ferrous iron on the surface of the magnetite and accelerate its dissolution rate.

The conductivity of magnetite (bandgap = 0.10 eV) is much higher than that of hematite (bandgap = 2.34 eV). Solid state electrochemical/chemical reactions can occur in/or on the magnetite surface; these reactions are driven by the potential at the solid/solution interface. For example, the oxidation of magnetite to maghematite (γFe_2O_3) by molecular oxygen in solution occurs *via*,

$$2\ (Fe^{2+},\ Fe_2^{3+})O_4\ +\ 1/2\ O_2 \rightarrow 3\ \gamma(Fe_2^{3+})O_3 \qquad \textbf{(76)}$$

Free oxygen is reduced at the surface by the oxidation ferrous iron to ferric iron. In order to balance the charge, 2 Fe^{3+} ions must be removed by solid state diffusion from the magnetite lattice for every 3 reduced oxygens; O_2 cannot diffuse into the magnetite lattice. The expelled ferric iron can either form maghematite or dissolve into solution (WHITE, 1990).

IV. MIXED POTENTIAL (BIMINERAL CORROSION)

WADSWORTH (1984) discusses the rate of corrosion of sulphide minerals or biminerallic reactions in both theoretical and practical terms. Mixed potential theory has been used for many years in corrosion engineering and has recently been recognized as model for the corrosion of sulphide minerals and sulphide mineral couples (PETERS and MAJIMA, 1968). Whenever metals, conductors and semiconductors are exposed to aqueous solutions, redox reactions will occur. In geologic systems, sulphides (except ZnS - which has a very low conductivity unless heavily doped, see MIZOGUCHI and HABASHI, 1983) in contact with oxides, other sulphides, and metals will set-up galvanic cells. The more liable mineral (i.e., the mineral with the more negative redox or open circuit potential) will tend to corrode, while the more noble mineral (more positive open circuit potential) will either be reduced (i.e., reductive dissolution, see Eqn. **(102)**) or reduce solution species. The theory and appropriate equations describing these processes will be presented in considerable detail in the next section.

IV.1 ELECTROCHEMICAL - THEORY

Electrochemical kinetic techniques have been well developed to study solid and aqueous reaction species. The following discussion will review general electrochemical kinetics and mixed potential theory.

IV.1.1 Electrochemical Kinetics.

Consider the following electrochemical reaction:

$$O + n\,e^- = R \tag{77}$$

in which an oxidized species O is reduced by n electrons to form the reduced species R. If this reaction occurs in an electrochemical cell at equilibrium, the potential of this reaction can be expressed by the Nernst equation:

$$E_e = E^o + \left(\frac{\ln(10)RT}{nF}\right)\log\frac{C_O^\infty}{C_R^\infty} \tag{78}$$

where E_e is the equilibrium cell potential, E° the standard potential, and C_O^∞ and C_R^∞ the bulk concentration of the oxidized and reduced species respectively (assuming activity coefficients = 1). At equilibrium no *net* current is flowing and the rate, or current, from the forward and backward reactions must be equal and opposite, such that:

$$I_o = I_a = -I_c \tag{79}$$

where I_o is called the exchange current. The subscripts a and c refer to anodic and cathodic direction, respectively. Now if the system is removed from equilibrium by applying an external potential, the current response can be described by:

$$-I_c + I_a = I \tag{80}$$

where I is the net current produced as a result of driving the reaction (**77**) in a positive or negative direction. The anodic and cathodic currents depend on: 1) the electrochemical rate constants; 2) the electrode area; and 3) the concentration of electroactive species at the electrode surface, C_O^σ and C_R^σ. These currents ($-I_c$, I_a) can be expressed as follows:

$$I_c = -nFAk_cC_O^\sigma \;;\; I_a = nFAk_aC_R^\sigma \tag{81}$$

where n is the number of electrons, F is the Faraday constant, A the electrode area and k_c and k_a the cathodic and anodic rate constants. Unlike classical chemical kinetics, not only can temperature affect

the rate constant, but also potential. The rate constants k_c and k_a can be expressed as a function of electrode potential, E:

$$k_c = k_{c,o} \exp\left(\frac{-\beta nFE}{RT} \right) \; ; \; k_a = k_{a,o} \exp\left(\frac{(1-\beta)nFE}{RT} \right) \qquad \textbf{(82)}$$

where β is the symmetry factor and $k_{c,o}$ and $k_{a,o}$ are the cathodic and anodic rate constants at $E = 0$.

Some digression is necessary at this point to discuss the symmetry factor β. The symmetry factor β represents the fraction of potential that drives the cathodic reaction in a single-electron, single-step charge transfer reaction (BOCKRIS and REDDY, 1970). The fraction of potential used to drive the anodic reaction is $1 - \beta$. In the case of multi-electron, multi-step reactions, the cathodic transfer coefficient, α_c, replaces the symmetry factor β. The transfer coefficient differs from the symmetry factor in that, in general, $\alpha_c \neq 1 - \alpha_a$ (BOCKRIS and REDDY, 1970).

The current can be related to the rate constant if k_c and k_a, from equation **(82)**, are substituted into equation **(81)** to give

$$= -nFC_0^{\sigma} k_{c,o} \exp\left(\frac{-\beta nF}{RT} \right) \; ; \; I_a = nFC_R^{\sigma} k_{a,o} \exp\left(\frac{(1-\beta)n}{RT} \right. \qquad \textbf{(83)}$$

If the currents I_a and I_c are in turn substituted into equation **(80)**, the net current can be expressed as:

$$I = F \left[k_{a,o} C_R^{\sigma} \exp\left(\frac{(1-\beta)F}{RT}\eta \right) - k_{c,o} C_O^{\sigma} \exp\left(\frac{-\beta F}{RT}\eta \right) \right] \qquad \textbf{(84)}$$

which is known as the Butler-Volmer equation. The exchange current,

$$I_o = FAk_{c,o} C_O^{\sigma} \exp\left(\frac{-\beta FE_e}{RT} \right) = FAk_{a,o} C_R^{\sigma} \exp\left(\frac{(1-\beta)FE_e}{RT} \right) \qquad \textbf{(85)}$$

can be substituted into equation **(84)** to give the more familiar form of the Butler-Volmer equation which relates the net current to the overpotential

$$I = I_o \left[\exp\left(\frac{(1 - \beta)F}{RT}\eta \right) - \exp\left(\frac{-\beta F}{RT}\eta \right) \right] \qquad \textbf{(86)}$$

The non-equilibrium interface potential E has been broken down into the equilibrium potential, E_e, and the overpotential, η, where the overpotential is defined as the difference between the equilibrium potential, E_e, and the applied potential E:

$$E = E_e + \eta \tag{87}$$

Strictly speaking, the Butler-Volmer equation has been derived for a one-electron single-step electrochemical reaction. Most reactions of electrochemical interest are not single-step, single-electron transfers. Fortunately, equation **(87)** can be generalized for more complex reactions. The symmetry factor, β, as defined above, must be replaced by the transfer coefficient α_c and the number of electrons n must also be included as follows:

$$I = I_o \left[\exp\left(\frac{\alpha_a nF}{RT} \eta \right) - \exp\left(\frac{-\alpha_c nF}{RT} \eta \right) \right] \tag{88}$$

IV.1.2 Mixed Potential Theory.

A mixed potential process occurs where a conducting or semiconducting electrode (mineral) is in contact with two or more oxidation-reduction systems; the mineral(s) can be <u>one</u> or, <u>both</u> members, of this redox pair. Thus,

$$O_1 + n_1 e^- \rightleftharpoons R_1 \tag{89}$$

$$O_2 + n_2 e^- \rightleftharpoons R_2 \tag{90}$$

Each of these two processes will reach a steady state with a compromised steady-state mixed potential. It is important to realize that this is not an equilibrium situation - a net overall reaction occurs. The three characteristics of a mixed potential system are:

1) Both redox reactions are removed from their equilibrium potential to a common mixed potential (E_{mp}). Therefore, each reaction will acquire its own overpotential (η_i, $i = 1, 2$):

$$\eta_1 = E_{mp} - E_{1,eq} \tag{91}$$

$$\eta_2 = E_{mp} - E_{2,eq} \quad \textbf{(92)}$$

2) Since both reactions occur at some overpotential, a net electrochemical reaction occurs;

3) Total cathodic ($i_c = I_c/A$) and anodic ($i_a = I_a/A$) current densities are equal:

$$i_o = i_{c,1} + i_{c,2} = i_{a,1} + i_{a,2} \quad \textbf{(93)}$$

where i_o (I_o/A) is the exchange current density (see Eqns **(85)**, **(86)** and **(88)**). When the mineral(s) potential departs from the steady-state potential E_{mp}, the total current is

$$i_{total} = (i_{c,1} + i_{c,2}) - (i_{a,1} + i_{a,2}) \quad \textbf{(94)}$$

At large departures from E_{mp}, the back reactions will occur at negligible rates and

$$i_{total} = i_{c,1} - i_{a,2} \quad \textbf{(95)}$$

Helpful reviews of mixed potential behaviour and Tafel relations can be found in FONTANA and GREENE (1978) and PAUNOVIC (1968). Three good reviews specific to hydrometallurgical conditions can be found in LI *et al.* (1992), WADSWORTH (1984), and RAND and WOODS (1984).

From the above discussion, it is clear that the individual electrode kinetics, mixed potentials must be known in order that the overall reaction kinetics can be understood. If the mixed potential (E_{mp}) or corrosion potential (E_{corr}), the exchange current (I_o), the electrode area A, and the stoichiometry of the corrosion reaction, the corrosion rate can be calculated using,

$$\text{Rate} = \left(\frac{M}{nF}\right)\frac{I_o}{A} \quad \textbf{(96)}$$

where M is the molecular weight of electroactive species, n is the number of electrons involved in the reaction, I_o is the exchange current, A is the electrode area and F is the Faraday. Equation **(96)** is defined for the plating of metals (PAUNOVIC, 1968), but can be used to calculate the rate of corrosion of minerals.

For example, consider if a mineral is placed in an aqueous solution it will set up an steady-state potential particular to that solution. RAO and NATARAJAN (1986) list the individual electrode

potentials before contact, the mixed potentials and galvanic or corrosion currents of many mineral pairs. The individual potentials of pyrite is 505 mV (SHE) and pyrrhotite is 355 mV (SHE). When the two minerals are place in contact, the mixed potential (E_{mp}, see equation **(88)**) is 418 mV (SHE) and the galvanic current (I_o) is -23.0 μA (see Table 6). At the mixed potential (E_{mp}), the potential of the pyrite electrode has shifted from its steady-state potential of 505 mV to a potential of 418 mV, or it is being reduced with an overpotential of 87 mV (i.e., 505 - 418 mV). Correspondingly, the pyrrhotite is being oxidized at an overpotential 63 mV (i.e., 418-355 mV). At the mixed potential (418 mV), the rate of pyrite reduction is EQUAL to the rate of pyrrhotite oxidation. Using equation **(96)**, and assuming that pyrrhotite is oxidized in a 2 e^- process (see Eqn.**(97)**), the overall rate of corrosion can be calculated from the galvanic current (assuming RAO and NATARAJAN, 1986 reported the electrode surface area, A, which they did not!).

The open circuit potentials for many minerals and mineral couples as well as corrosion (exchange current densities) have been published in the literature and the data is summarized in Table 6 .

Cathode	Anode	pH	Cathode	Anode mV (SHE)	E mV (SHE)	i mV (SHE)	I µA/cm	Rate µA	Rate mg/cm /year	Ref.
FeS_2	MoS_2	2		505	335	412		2.0‡		*a*
FeS_2	CuFeS	2		505	400	438		18.0‡		
FeS_2	FeS	2		505	355	418		23.0‡		
FeS_2	PbS	2		505	295	415		22.0‡		
MoS_2	CuFeS	2		335	410	375		18.0‡		
MoS_2	FeS	2		335	357	343		22.5‡		
MoS_2	PbS	2		335	295	315		23.0‡		
$CuFeS_2$	FeS	2		400	355	375		3.0‡		
$CuFeS_2$	PbS	2		400	295	355		7.5‡		
FeS_x	PbS	2		355	295	320		4.5‡		
FeS_2	PbS	2		575	305	357	---	---		*b*
FeS_2	PbS	3		530	270	266	---	---		
FeS_2	FeS	6.7	(N_2)	388	275	382-358		.149‡‡		*c*
FeS_2	FeS	"	(Air)	341	284	342-376		.153‡‡		
FeS_2	FeS	"	(O_2)	394	317	332-370		.358‡‡		
FeS_2	FeS	2	1	?	?	616	0.85		4.6x10	*d*
FeS_2	FeS	2	3	?	?	524*	0.32		1.7x10	
FeS_2	FeS	2	4	?	?	495*	0.07		3.8x10	
FeS_2	FeS	2	9	?	?	231*	0.63		3.4x10	
Fe_3O_4	Steel		8.5(N_2)	134	-186	-276	7		1.8x10	*e*
Fe_3O_4	Steel		8.5(Air)	134	-216	-376	42		0.11	
Fe_3O_4	Steel		8.5(O_2)	74	-326	-6	4.8		1.2x10	

† Reference potential not given; (Saturated Calomel Electrode assumed)
* Data not published; see MYCROFT Ph.D. thesis (1993).
‡ Electrode surface area was not given.
References: *a* RAO and NATARAJAN (1986); *b* SAKHAROVA and LOBACHEVA (1978); *c* NAKAZAWA and IWASAKI (1985); *d* MYCROFT Ph.D. (1993); and *e* NAKAZAWA and IWASAKI (1983)

Table 6: Open circuit data for individual sulphides and oxides as well as mixed potential corrosion data for mineral pairs.

The corrosion rate was calculated based on the oxidation of pyrrhotite, chalcopyrite, galena, pyrite and steel corrode at the mixed potential based on the following reactions (RAO and NATARAJAN, 1986; and NATARAJAN and IWASAKI, 1984):

1) Pyrrhotite

$$FeS \rightarrow Fe^{2+} + S + 2\ e^- \quad \textbf{(97)}$$

2) Chalcopyrite

$$CuFeS_2 \rightarrow Cu^{2+} + Fe^{2+} + 2\ S + 4\ e^- \quad \textbf{(98)}$$

3) Galena

$$PbS \rightarrow Pb^{2+} + S + 2\ e^- \quad \textbf{(99)}$$

4) Pyrite

$$FeS_2 \rightarrow Fe^{2+} + 2\ S + 2\ e^- \quad \textbf{(100)}$$

5) Steel

$$Fe \rightarrow Fe^{2+} + 2\ e^- \quad \textbf{(101)}$$

It should be noted that the potential of a pyrite electrode in contact with an aqueous solution is really a mixed potential (PETERS and MAJIMA, 1968); a second more noble mineral is not required for pyrite to under go galvanic corrosion. The anodic reaction is believed to proceed by reaction **(100)**, while the cathodic reaction occurs by

$$FeS_2 + 2\ H_3O^+ + 2\ e^- \rightarrow Fe^{2+} + 2\ HS^- + 2\ H_2O \quad \textbf{(102)}$$

RAO and NATARAJAN (1986) reported that, in pH = 2 sulphuric acid, the more noble to less noble (i.e., more easily oxidized) minerals are: pyrite > molybdenite > chalcopyrite > sphalerite > pyrrhotite > galena. Similarly, NATARAJAN and IWASAKI (1984) reported that in pH = 8.5 solution, the more noble to less noble are: magnetite > pyrrhotite > mild steel.

For further reading see the following references: ADAM *et al.* (1984); BAILEY and PETERS (1976); DONAHUE (1972); HOEY *et al.* (1975); HISKEY and WADSWORTH (1975); KWONG

(1993, page 27); MAJIMA (1969); MIZOGUCHI and HABASHI (1983); NAKAZAWA and IWASAKI (1986); NATARAJAN *et al.* (1983, 1984); NATARAJAN and IWASAKI (1972, 1973, 1974); NICOL (1988); HEPEL *et al.* (1988); PETERS and MAJIMA (1968); POZZO and IWASAKI (1987, 1989); and WADSWORTH (1984).

V. DATABASES AND KEYWORDS

Databases:

Chemical Abstracts CA - STN
Georef (CD ROLM)
MEDB (Mining Environmental Database) - Laurentian University
Science Citation Index (CD - ROLM, only the 1990's available)

Keywords:

	Registry Number †
pyrite	1309-36-0
pyrrhotite	131442-13-2
arsenopyrite	1303-18-0
marcasite	1317-66-4
hematite	1317-60-8
goethite	12181-28-1
magnetite	1309-38-2
oxidation	
leaching	
kinetics	
surface	
electrochemical	
electro...	
biological	
bacteria	
microb...	

†: Some databases allow searches to be done by registry number. Almost all elements, and common chemicals and minerals have a unique registry number. By searching by registry number, one avoids the possibility of missing a good reference because of too many keywords. Does one search for pyrite or iron disulphide or iron disulfide or iron sulphide or iron sulfide or FeS_2? One search by registry number would find all of the pyrite references regardless of the keyword used by the articles' author.

APPENDIX C

GEOCHEMICAL DATA SELECTION FOR MODELLING

C.1 Test Data Set 1: Mine Doyon Waste Rock Dump Waters

The first test case consists of several pore water/seepage water analyses from the saturated zone from the waste rock pile at Mine Doyon (Choquette et al., 1993). This data is used to test the equilibrium thermodynamic or equilibrium distribution of species models (Class 1 models). The output to be compared amongst the various models is the SI's of the minerals which can be calculated from the water analyses. The field data set for Mine Doyon is one of the most complete ARD data sets for eastern canadian waste rock. A detailed monitoring study of the Mine Doyon south waste rock dump has been recently reported in a series of 1994 MEND reports (Choquette et al. 1994). Consequently, this mine data set was reviewed as a possible candidate for geochemical modelling.

Five different types of data were collected at Mine Doyon. Six monitoring wells were placed in the waste rock pile and seven wells were placed around the dump. Leachate was collected at regular intervals from each well at two levels; at the contact between the bottom of the waste rock pile and the soil denoted "SOIL" and at the contact between soil and the underlying bedrock denoted "ROCK". In addition two groups of lysimeters were placed in the dump at three levels (approximately 1.5, 2.5 and 4 meters depth), and three weirs have been installed in a collecting ditch surrounding the dump. Drill core samples collected during drilling of the monitoring wells have been leached in the lab with distilled water to determine the water quality in the saturated and unsaturated zones of the dump. Mineralogical analyses have been completed on the solids of the drill core samples.

The only vadose zone waters are from the leached rock fragments of the drill core samples and the lysimeters. However only partial water analyses were done and are therefore of limited value for geochemical modelling. In addition the water analyses from the leached rock fragments are suspect because of dissolution of soluble minerals during leaching and poor knowledge of the water saturation. The only complete water analyses are from the collecting ditches and the monitoring wells. These water analyses were scrutinized in some detail using SOLMINEQ.88 pc/shell.

SOLMINEQ.88pc/shell runs were made on the water samples from the monitoring wells inside the waste rock pile and from the weirs in the collecting ditches taken on approximately April 24, 1991. These samples were chemically similar to earlier water samples, and later samples were not completely analyzed. In all 12 water samples were examined, including a SOIL and ROCK pair from the monitoring wells 01, 02, 03, 04 and 06 (only the ROCK sample was available from 06) from inside the waste rock pile and one sample from each of the weir collecting stations (i.e. 510, 511 and 512). The calculated charge balances (after the waters had been speciated) were all high on the positive side ranging from +10 to +60%. This could either be due to a missing element which has not been analyzed for or to an error in analysis (arising from too high a cation or too low an anion concentration). Elements missing in the analyses are inorganic carbon, chloride and sulphide. Compared to water analyses collected at other ARD sites, normally all three are low. TIC can be high if carbonates are present but in these acid waters, it would be present as dissolved CO_2 and in this form would not contribute to the charge balance. In addition, the calculated TDS (total dissolved solids) is also low compared to the measured values by more than 10% in every case examined except

one. This suggests to us that the total anion concentration is low. Since sulphate is the only anion analyzed, we would recommend its concentration value be increased to achieve a charge balance.

The Eh has been measured but it is consistently low with that calculated from the iron redox couple. Normally in high iron waters the platinum electrode potential will be controlled by the iron redox couple (Nordstrom et al., 1979a; Morin, 1991). If both the measurements were done correctly (e.g. including sample preservation for the Fe(II)/Fe(III) couple and the platinum electrode was not poisoned by foreign ions), then the Eh is not measuring the Fe(II)/Fe(III) couple as the two measurements differ. On the other hand, there could be an error in one or both of the measurements. There is insufficient information to decide which is correct. We have assumed that the iron analyses are correct and are controlling the measured redox potential. We used the activity ratio of Fe(II) to Fe(III) to calculate the Eh which can be used to calculate the concentration of other redox couples of interest. This is clearly in error if the waters are only in partial redox equilibrium. For those redox pairs in equilibrium with the Fe couple, the assumption is fine; for those out of equilibrium it is wrong.

The acidity was also measured by titrating with NaOH to pH 8.3. We suspect that it may be high but have not confirmed this by geochemical modelling. We recommend that it be done regularly as a check on the quality of the water analyses.

We chose to examine two waters from within the waste rock pile in detail. We chose one water analysis from the monitoring well BH-91-06-ROCK sampled on 24/4/91. This well consistently has the highest TDS (i.e. is a brine) and is also located near a high on the original soil surface before the dump was deposited. The other well, BH-91-01-SOIL has the lowest TDS (i.e. is brackish) and well down on the slope of the original soil surface. A sample was chosen from this well taken at the same date. These two samples represent two extremes of water chemistry as a result of leaching in an actively oxidizing waste rock dump. The different water chemistries may partly be due to the inhomogeneity of the dump mineralogically. The samples from the collection weirs were not considered further as they have probably undergone some mixing with the local groundwater.

C.2 Test Data Set 2: Stratmat Column Leach Tests

The second test is based on the laboratory column leaching data from the Heath Steele waste rock experiments (Yanful and Payant, 1993) and will be used to evaluate the mass transfer models (i.e. Class 2 models).

It was desirable to model waste rock waters from the vadose zone because the major change in the geochemical environment between mine tailings and waste rock is the large grain size and the large size of the vadose zone in waste rock piles. We know of no other vadose zone water analyses in waste rock besides those of Mine Doyon. The only vadose zone waters which are well characterized geochemically are those from tailings such as Waite Amulet, which we think could be used as a geochemical proxy for the vadose zone of waste rock, if the size of the vadose zone was geochemically scaled. However, these waters were not considered further since the data was not for a waste rock pile, and following recommendations by the reviewers. This limited us to examining waters beneath the waste rock pile or "toe" waters.

We decided to choose a new test data set for waste rock water drainage under a more controlled environment than at Mine Doyon, that of the laboratory. The recent lysimeter study on waste rock from the Heath Steele Mine property by Noranda Technology Centre (NTC) provided us with a good data set. Potentially acid-generating samples from the Stratmat site were used in outdoor and indoor lysimeter tests to evaluate cover strategies. Here we examine the data from the indoor control lysimeter leaching experiments for the control column leaching and for the limestone amendment. Each experiment was run in triplicate, and subjected to cycles of eight weeks of wet conditions and eight weeks of dry conditions for a period of approximately three years. The wet periods were physically simulated by doubling the average weekly rainfall (2 x 18.4 mm) for the year and adding this amount of distilled water weekly (650 ml) to the columns.

The average mineralogy of the waste rock (Table D1) used in the experiments is based on data provided by Centre de Recherches Minérales (CRM) and McGill University. In the limestone amendment either 1 or 3% of crushed limestone (<6 mm particle size) was added to the waste rock. For the 20°C laboratory experiments, 20 kilograms of waste rock of particle size between 2.5 and 5 cm were used having a cumulative volume of 6,220 cc in each experiment. Assuming spherical particles, the total exposed surface area is approximately 1 sq. meter per 20 kg of waste rock.

Table C1. Average mineralogy of Stratmat waste rock samples used in lysimeter tests

Minerals	S.G. (g/cc)	Weight %	Volume %
Quartz	2.65	35.0	40.07
Muscovite	2.82	30.0	32.27
Albite	2.63	5.0	5.77
Fe-Chlorite	3.3	6.0	5.51
Mg-Chlorite	2.6	3.0	3.50
Dolomite	2.86	0.2	0.21
Siderite	3.5	0.3	0.26
Rhodochrosite	3.7	0.1	0.08
Pyrite	5.00	20.	12.14
Sphalerite	4.1	0.1	0.07
Chalcopyrite	4.2	0.1	0.07
Galena	7.5	0.1	0.04
TOTALS	Av. SG=3.22	99.9	99.99

Note: Although siderite and rhodochrosite were not specifically identified, microprobe analyses by McGill University indicate the presence of ankerite and high amounts of manganese in the dolomite.

Assuming a pore space of 35%, one pore volume would be equivalent to 3,350 cc. The weekly addition of water during the wet season would only occupy 20% of the pore space and it would be expected to rapidly travel through the column (i.e. residence times of less than 1 hour for the bulk of the water). Probably less than 10% of the water would remain behind as surface coating of grains and forming pendular rings at grain to grain contacts. Thus even during the weekly water addition and flow through during the "wet season", voids would still exist in the pore space. For the purpose of modelling, as an end member case, it is assumed that the complete surfaces of the waste rock particles are "coated" with water and that the water/rock ratio is 1 to 31 by weight when the 650 ml of water is present in the column. Between water additions, rock surfaces remain coated with water but the water/rock ratio decreases dramatically to less than 1 to 300 if only 10% of the water remains behind and even lower if there is less residual water. In addition to the decrease in the water/rock ratio due to drainage, during the dry periods significant evaporative concentration will occur and ratios will exceed 1 to 1000.

One of the uncertainties from the Stratmat column experiments is whether the oxygen supply becomes depleted in the column between aqueous flushes. The fact that most of the pore space is occupied by air means that the water is buffered by atmospheric oxygen to some extent. For example, for the majority of the time, there is less than 60 ml of water (i.e. residual saturation) in the column compared to (3350-60) 3.3 litres of air. Normalizing to 1000 grams of water, this is equivalent to approximately 0.5 moles of oxygen (i.e. 2.5 moles of air) assuming no convection is taking place. For the purposes of modelling, we assumed that there is 1 pore volume flow of air (or 1 mole of oxygen available to react with the sulphide minerals) through the column between water additions.

Using this information, the mass transfer models can predict the change in water chemistry and mineralogy during these lysimeter tests and the results can be compared to the actual analyzed water chemistry and mineralogy. During the experiments, the acidity and pH of the aqueous effluents were monitored weekly. One set of complete chemical analyses were completed on the effluents at the beginning of the tests before pH lowering had occurred or appreciable acidity had accumulated by reaction with the waste rock. At this stage any acid generation was neutralized due to base buffering by dissolution of carbonate minerals. When the carbonate minerals were exhausted or armoured, acidity generation was unimpeded and reached an approximate steady state at a pH of 2 after approximately 20 weeks in the case of the control experiments. At this point, it is assumed that the bacteria (*Thiobacillus ferrooxidans*) had reached their optimum efficiency to catalyze the iron oxidation reaction. A check on this would be to monitor the changing bacterial activity by culturing the aqueous effluents from the columns.

The second set of water analyses which can be used as a control on the modelling was collected 26 months later. For the control experiments, the pHs had dropped below 3 and the acidities were in excess of 10,000 mg/L of $CaCO_3$. *The ability to history match this data would provide one test for the mass transfer models.* The complete chemical analyses of the three control experiments and the limestone addition experiments are presented in Table D.2 The 1% limestone addition reduces the acidity by more than a factor of 2 but the 3% limestone addition reduces the acidity by two orders of magnitude to acceptable values. This is a result of the dissolution of the calcite which can be monitored by the increase in dissolved calcium from 100 mg/L in the control experiments to 300 mg/L in the 1% addition limestone experiments to greater than 600 mg/L (see Table 5) in the 3% addition limestone experiments. The exact amount of calcite dissolution could have been calculated directly if TIC (total inorganic carbon) had been measured. A further test of the mass transfer models is to be able to model the neutralization effect caused by the dissolution of carbonate minerals.

Table 6. Leachate from NTC indoor ARD STRATMAT column leaching experiments, 29/09/93

A.R.D.	Ctrl#1	Ctrl#2	Ctrl#3	1%Cc#1	1%Cc#2	1%Cc#3	3%Cc#1	3%Cc#2	3%Cc#3	H2O#1	H2O#2	H2O#3
Specie	mg/L	mg/L	mg/L	mg/L	mg/L	mg/L	mg/L	mg/L	mg/L	mg/L	mg/L	mg/L
Na	6.1	6.1	6.1	6.4	6.0	7.6	7.2	7.6	8.2	7.0	6.7	7.1
K	<5.0	<5.0	<5.0	<5.0	<5.0	5.1	<5.0	<5.0	7.8	<5.0	<5.0	<5.0
Ca	105.	147.	138.	389.	333.	587.	672.	640.	683.	37.	37.	43.
Mg	456	597	532	203	205	64	111	84	136	11	9.1	7.8
Mn	36	59	41	33	30	12	27	12	29	7.3	7.9	6.4
Fe++	430	440	490	69	270	>.05	0.40	>.00	0.02	0.21	0.20	0.12
Fe+++	3370	3160	3510	703	1630	<.05	1.15	<.05	.11	0.64	0.37	0.30
Al	470	577	543	168	295	<.25	1.34	0.27	<.25	<.25	<.25	<.25
SiO2	86	97	110	68	74	12	25	16	20	11	11	10
Cu	7.4	10.9	11.8	8.0	6.7	0.08	0.34	0.03	0.09	<.03	<.03	<.03
Pb	<.25	<.25	<.25	<.25	<.25	<.25	<.25	<.25	<.25	<.25	<.25	<.25
Zn	81	339	66	100	80	10	64	18	40	1.2	2.3	2.3
As	17.5	19.5	26.8	1.93	5.44	<.25	<.25	<.25	<.25	<.25	<.25	<.25
Cd	0.33	0.82	0.43	0.17	0.19	<.03	0.13	0.03	0.10	<.03	0.04	<.03
Co	0.39	0.48	0.43	0.24	0.30	0.03	0.13	<.03	0.15	<.03	0.04	<.03
Cr	<.03	<.03	<.03	<.03	<.03	<.03	<.03	<.03	<.03	<.03	<.03	<.03
Ni	0.16	0.20	0.16	0.13	0.17	<.03	0.06	<.03	<0.06	0.03	<.03	<.03
Sb	2.67	2.60	2.47	0.79	1.22	<.25	<.25	<.25	0.31	<.25	<.25	<.25
Se	0.81	0.94	1.13	<.50	0.59	<.50	<.50	<.50	<.50	<.50	<.50	<.50
Te	0.60	0.58	0.64	<.50	<.50	<.50	<.50	<.50	<.50	<.50	<.50	<.50
Tl	<.25	<.25	<.25	<.25	0.25	<.25	<.25	<.25	<.25	<.25	<.25	<.25
SO4	13603	15251	15011	4584	8060	1520	1982	1720	2078	126	128	122
Cl	N/A	N/A	7.4	8.1	3.1	3.3	3.4	3.4	4.2	2.0	1.8	2.2
HPO4	N/A	N/A	<.10	<.10	<.10	<.10	<.10	<.10	<.10	<.10	<.10	<.10
NO3	N/A	N/A	<.05	<.05	<.05	<.05	<.05	<.05	<.05	<.05	<.05	<.05
^Chg	N/A	N/A	N/A	N/A	N/A	N/A	N/A	N/A	N/A	N/A	N/A	N/A
TDS	N/A	N/A	N/A	N/A	N/A	N/A	N/A	N/A	N/A	N/A	N/A	N/A
Acidty	10136	10558	10664	3180	5742	60	196	54	88	<15	<15	16
pH@25C	2.29	2.28	2.25	2.53	2.44	7.24	6.92	7.70	7.20	8.34	8.27	8.03
Eh	N/A	N/A	N/A	N/A	N/A	N/A	N/A	N/A	N/A	N/A	N/A	N/A

* N/A = not available

APPENDIX D — STATISTICAL ANALYSIS OF THERMODYNAMIC DATABASES OF EQUILIBRIUM GEOCHEMICAL MODELS

APPENDIX D — STATISTICAL ANALYSIS OF THERMODYNAMIC DATABASES OF EQUILIBRIUM GEOCHEMICAL MODELS

Tables 7, 8, 9, 10 of Chapter 11, calculated using the Equilibrium Thermodynamic Geochemical Models reviewed earlier, form the basis for the statistical analysis. Tables 7 and 8 list the calculated molality of the "free" ionic species for a brackish water and a brine collected through two piezometers from the base of the South Waste Dump at Mine Doyon. Tables 9 and 10 list the calculated saturation state (SIs) for a number of minerals for brackish water and the brine. The only additional piece of information used to calculate the SIs of the minerals is the thermodynamic equilibrium constants for the minerals.

The following approach was used to analyze the data from Tables 7 to 10. Simple statistics were first calculated on both the molalities of the individual "free" ionic species and the SI of each mineral, including number of observations (N), mean, range and standard deviation (STD). This identifies the ions or minerals having the greatest range or deviation. This analysis was followed by a standardizing procedure where the mean was set to zero and the standard deviation was set to 1 for each ion or mineral. Then each individual data point was analyzed to identify those which were outliers (i.e. arbitrarily defined here as greater or less than the value 1.5). As the standardization procedure sets all ions or minerals to have the same standard deviation, comparisons of this data between different ions or different minerals should not be done for the standardized data.

The simple statistics of the brackish water data from Table 7 are presented in Table D1. The standard deviation and range were normalized by dividing by the mean in order to evaluate the data on the same scale (this negates the effect of the ions having the largest concentrations normally tending to have the largest standard deviations and ranges). The major ions, Fe(II), Fe(III) and Al, and the minor ions Cu, Pb and Zn show both the largest deviations and ranges. The simple statistics of the brine from Table 8, presented in Table D2, show identical relationships although the uncertainties are larger. The standardized statistics for individual data points from the brackish water and the brine are presented in Tables D3 and D4. Only the "free" ionic species with the largest uncertainties, as identified from the simple statistical analysis, are discussed here. In the brackish water, outliers are present for Fe(II) and Fe(III) in SOLVEQ, Al in PATH.ARC, Cu in EQ3NR, Pb in EQ3 and Zn in PATH.ARC and EQ3NR. In the brine, outliers are present for Fe(III) in WATEQ4F, Al in PATH.ARC, Cu in EQ3NR and Zn in EQ3NR. No outliers are present for Fe(II) or Pb.

The simple statistics of the saturation states of minerals from the brackish water from Table 9, and the brine from Table 10, are presented in Tables D5 and D6. The simple statistics are not as easily interpreted as for the molality of the "free" ions. Firstly, the number of observations for each mineral varies, due to omissions of thermodynamic data for minerals in some of the databases. Secondly, the procedure of dividing the standard deviation and range by the mean could not be used here because the saturations can be positive or negative numbers (i.e. if the mean is close to zero, dividing by the mean will result in artificially large numbers). A procedure to correctly normalize SIs was briefly discussed in the main body of the report, where it was suggested to follow the normalizing

procedure suggested by Nordstrom (1994), by dividing the SI by the number of ionic units in the mineral formula. We followed Nordstrom's suggestion and normalized the standard deviations by dividing by the sum of the cations in the mineral formula in Tables D5 and D6. When this is done, the largest uncertainties are easily identifiable as belonging to the iron- and aluminous-minerals, melanterite, goethite, amorphous aluminum hydroxide and bohemite in both the brackish water and the brine. The standardized statistics for individual data points for the mineral saturations from the brackish water and the brine are presented in Tables D7 and D8. Only the mineral saturations with the largest uncertainties, as identified from the simple statistical analysis data, are analyzed. In the brackish water, outliers are present for melanterite and goethite in PATH.ARC, and for bohemite in SOLMINEQ. There are no outliers for amorphous aluminum hydroxide. In the brine, outlier saturation indices are found for melanterite in PATH.ARC and for bohemite in SOLMINEQ. No outliers were found for goethite or amorphous aluminum hydroxide.

The statistical analysis done here should only be used to point out where the largest differences exist between databases. If a cluster analysis is done on the data from Table 7, this conclusion becomes more apparent (see Figure D1). PHREEQE and WATEQ4F form the most tightly related clusters followed by SOLMINEQ and PATH.ARC. PHREEQE and WATEQ4F are supported by the U.S. Geological Survey while SOLMINEQ and PATH.ARC are supported by the Alberta Research Council (note that SOLMINEQ is jointly supported by ARC and the USGS). The other models (EQ3NR, SOLVEQ and MINTEQA2) only form part of a cluster at larger separation distances, exactly what was predicted.

Caution should be used in applying the statistical data presented above because the data from Tables 7 to 10 used for the analysis are not independent. For example, several of the geochemical codes may use literature data from the same source while another program uses data from a different source, which may appear as outliers in the statistical analysis. At this level of analysis, there is no reason to eliminate the outliers as they may be more correct than the other data.

Table D1: Simple statistical data for calculated "free" ionic species molalities of the brackish water from Mine Doyon
(T-1 Brackish Water Sample Concentration Analysis)

OBS	SPECIES	N	MIN	MAX	MEAN	STD	RANGE	STD/MEAN	RNG/MEAN
1	NA	7	0.0008610	0.0009230	0.0009023	0.0000285	0.0000620	0.03	0.07
2	K	7	0.0005030	0.0005210	0.0005080	0.0000064	0.0000180	0.01	0.04
3	CA	7	0.0041900	0.0049700	0.0044314	0.0002760	0.0007800	0.06	0.18
4	MG	7	0.0073100	0.0090300	0.0079571	0.0005563	0.0017200	0.07	0.22
5	MN	7	0.0002570	0.0002900	0.0002811	0.0000111	0.0000330	0.04	0.12
6	FE	7	0.0028900	0.0052200	0.0036986	0.0008961	0.0023300	0.24	0.63
7	FE	7	0.0000026	0.0000056	0.0000037	0.0000010	0.0000030	0.29	0.81
8	AL	7	0.0001080	0.0002050	0.0001501	0.0000332	0.0000970	0.22	0.65
9	SIO_2	7	0.0004330	0.0004330	0.0004330	0.0000000	0.0000000	0.00	0.00
10	CU	7	0.0000028	0.0000047	0.0000031	0.0000007	0.0000020	0.23	0.63
11	PB	7	0.0000005	0.0000013	0.0000007	0.0000004	0.0000008	0.56	1.20
12	ZN	7	0.0000012	0.0000153	0.0000086	0.0000041	0.0000141	0.48	1.64
13	COR_SO_4	7	0.0185000	0.0215000	0.0199000	0.0012583	0.0030000	0.06	0.15

Table D2: Simple statistical data for calculated "free" ionic species molalities of the brine from Mine Doyon
(T-2 Brine Sample Concentration Analysis)

OBS	SPECIES	N	MIN	MAX	MEAN	STD	RANGE	STD/MEAN	RNG/MEAN
1	NA	7	0.0004500	0.0007260	0.0006329	0.0001058	0.0002760	0.17	0.44
2	K	7	0.0000062	0.0000072	0.0000068	0.0000004	0.0000010	0.06	0.15
3	CA	7	0.0042000	0.0074200	0.0059971	0.0010014	0.0032200	0.17	0.54
4	MG	7	0.1040000	0.1640000	0.1317143	0.0252370	0.0600000	0.19	0.46
5	MN	7	0.0026500	0.0054300	0.0039414	0.0011279	0.0027800	0.29	0.71
6	FE	7	0.0980000	0.2340000	0.1640000	0.0552630	0.1360000	0.34	0.83
7	FE	7	0.0009000	0.0029300	0.0020614	0.0007534	0.0020300	0.37	0.98
8	AL	7	0.0061000	0.0522000	0.0258286	0.0152085	0.0461000	0.59	1.78
9	SIO_2	7	0.0036500	0.0036800	0.0036743	0.0000113	0.0000300	0.00	0.01
10	CU	7	0.0003460	0.0012600	0.0006664	0.0003040	0.0009140	0.46	1.37
11	PB	7	0.0000005	0.0000093	0.0000038	0.0000039	0.0000088	1.02	2.29
12	ZN	7	0.0000296	0.0007760	0.0003372	0.0002467	0.0007464	0.73	2.21
13	COR_SO_4	7	0.2150000	0.5370000	0.3428571	0.1002421	0.3220000	0.29	0.94

Table D3: Standarized statistical data for calculated "free" ionic species molalities of the brackish water from Mine Doyon
(T-3 Brackish Water Sample Concentration Analysis)

OBS	SPECIES	SOLMINEQ	WATEQ4F	PHREEQE	MINTEQA2	PATH.ARC	SOLVEQ	EQ3NRD
1	NA	-1.45	0.62	0.73	0.69	-1.45	0.59	0.27
2	K	-0.47	0.16	0.31	-0.47	2.05	-0.79	-0.79
3	CA	-0.01	-0.55	-0.48	-0.69	0.65	-0.87	1.95
4	MG	-0.08	0.15	0.22	1.93	-1.16	-0.14	-0.91
5	MN	0.80	0.62	0.08	0.26	0.44	-0.01	-2.17
6	FE	0.70	-0.71	-0.90	-0.79	0.58	1.70	-0.58
7	FE	0.25	0.29	-0.97	-0.99	0.23	1.86	-0.66
8	AL	0.51	-1.27	-0.16	0.06	1.65	0.33	-1.12
9	SIO_2	0.00	0.00	0.00	0.00	0.00	0.00	0.00
10	CU	-0.13	-0.41	-0.51	-0.44	-0.22	-0.54	2.24
11	PB	-0.54	-0.58	-0.57	-0.64	-0.59	1.44	1.49
12	ZN	0.36	-0.12	-0.00	-0.14	-1.79	0.07	1.62
13	COR_SO_4	-1.03	0.48	0.56	1.27	-1.11	-0.95	0.79

Table D4: Standarized statistical data for calculated "free" ionic species molalities of the brine from Mine Doyon
(T-4 Brine Sample Concentration Analysis)

OBS	SPECIES	SOLMINEQ	WATEQ4F	PHREEQE	MINTEQA2	PATH.ARC	SOLVEQ	EQ3NRD
1	NA	-1.05	0.88	0.82	0.58	-1.73	0.28	0.21
2	K	-0.73	1.11	1.11	0.73	-0.23	-1.44	-0.56
3	CA	1.42	0.02	-0.28	-0.37	0.33	-1.79	0.66
4	MG	1.28	0.61	0.09	1.00	-0.86	-1.02	-1.10
5	MN	0.83	-1.15	0.83	1.32	-0.08	-0.95	-0.81
6	FE	0.13	-1.19	0.71	1.27	-0.63	-1.14	0.87
7	FE	0.20	-1.54	0.73	1.15	-0.76	-0.64	0.86
8	AL	-0.32	-1.30	0.60	0.39	1.73	-0.76	-0.34
9	SIO_2	0.50	0.50	0.50	0.50	0.50	-0.38	-2.14
10	CU	0.14	-1.05	-0.02	0.27	-0.36	-0.93	1.95
11	PB	-0.10	-0.78	-0.84	-0.76	-0.34	1.42	1.41
12	ZN	0.47	-0.86	0.34	-0.02	-1.25	-0.45	1.78
13	COR_SO_4	-0.02	-0.59	-0.24	0.41	1.94	-1.28	-0.23

Table D5: Simple statistical data for calculated SIs of minerals in the brackish water of Mine Doyon
(T-5 Brackish Water Sample Saturation Analysis)

OBS	MINERAL	N	# of Cations	MIN	MAX	MEAN	STD	STD/# of ions	RANGE
1	GYPSUM	7	2	-0.39	0.02	-0.25	0.14	0.07	0.41
2	MELANTER	6	2	-2.79	-0.23	-2.21	0.99	0.45	2.56
3	EPSONITE	4	2	-2.59	-2.35	-2.47	0.11	0.05	0.24
4	ANGLESIT	8	2	-1.09	-0.52	-0.86	0.25	0.12	0.57
5	CHALCANT	5	2	-5.46	-5.17	-5.36	0.11	0.05	0.29
6	ZINCOSIT	3	2	-11.03	-10.58	-10.73	0.26	0.13	0.45
7	ALUNOGEN	0	-					-	
8	ALUNITE	7	12	6.21	10.30	8.55	1.44	0.12	4.09
9	JAROSITE	4	12	10.90	16.45	12.37	2.73	0.23	5.55
10	AMORP_FE	6	4	2.16	4.56	3.10	0.80	0.20	2.40
11	GOETHITE	6	2	7.27	9.68	8.21	1.01	0.50	2.41
12	AMORP_AL	3	4	-1.59	2.05	-0.27	2.02	0.50	3.64
13	BOEHMITE	7	2	-0.09	2.65	1.03	0.83	0.41	2.74
14	MAGHEMIT	3	2	9.16	9.54	9.29	0.22	0.11	0.38
15	AMORP_SI	7	1	-0.65	-0.34	-0.59	0.11	0.11	0.31
16	KAOLINIT	7	8	4.28	6.96	5.82	1.10	0.14	2.68
17	CHLORITE	6	18	-28.49	-22.29	-25.38	2.14	0.12	6.20
18	MUSCOVIT	7	11	5.14	8.35	6.91	1.02	0.09	3.21
19	ANORTHIT	6	5	-8.15	-6.11	-6.85	0.74	0.15	2.04

Table D6: Simple statistical data for calculated SIs of minerals in the brine from Mine Doyon
(T-6 Brine Sample Saturation Analysis)

OBS	MINERAL	N	# of Cations	MIN	MAX	MEAN	STD	STD/# of ions	RANGE
1	GYPSUM	7	2	-0.54	0.62	0.20	0.36	0.18	1.16
2	MELANTER	6	2	-1.72	1.71	-0.41	1.13	0.51	3.43
3	EPSONITE	4	2	-1.36	-0.65	-0.95	0.32	0.16	0.71
4	ANGLESIT	8	2	-0.95	0.84	0.03	0.59	0.29	1.79
5	CHALCANT	5	2	-3.40	-2.41	-2.80	0.37	0.18	0.99
6	ZINCOSIT	3	2	-8.94	-8.66	-8.78	0.14	0.07	0.28
7	ALUNOGEN	0	-						
8	ALUNITE	7	12	-5.18	0.32	-1.66	2.04	0.17	5.50
9	JAROSITE	4	12	3.67	9.10	5.23	2.59	0.22	5.43
10	AMORP_FE	6	4	-2.31	-0.37	-1.49	0.63	0.16	1.94
11	GOETHITE	6	2	2.78	4.76	3.64	0.93	0.46	1.98
12	AMORP_AL	3	4	-6.57	-3.32	-5.44	1.83	0.46	3.25
13	BOEHMITE	7	2	-5.55	-2.71	-4.39	0.94	0.47	2.84
14	MAGHEMIT	3	2	0.14	0.44	0.26	0.16	0.18	0.30
15	AMORP_SI	7	1	0.28	0.83	0.45	0.19	0.19	0.55
16	KAOLINIT	7	8	-4.23	-1.51	-2.52	1.11	0.14	2.72
17	CHLORITE	6	18	-55.53	-48.32	-50.88	2.76	0.15	7.21
18	MUSCOVIT	7	11	-12.77	-9.24	-10.11	1.32	0.12	3.53
19	ANORTHIT	6	5	-22.12	-19.13	-19.98	1.08	0.22	2.99

Table D7: Standarized statistical data for calculated SIs of minerals in the brackish water from Mine Doyon
(T-7 Brackish Water Sample Saturation Analysis)

OBS	MINERAL	SOLMINEQ	WATEQ4F	PHREEQE	MINTEQA2	PATH.ARC	SOLVEQ	EQ3NRD	EQ3NRP
1	GYPSUM	0.03	0.03	0.03	2.02		-1.00	-0.19	-0.93
2	MELANTER		-0.59	-0.58	-0.32	2.01		-0.41	-0.11
3	EPSONITE		0.59		1.05			-1.14	-0.50
4	ANGLESIT	-0.70	-0.58	-0.58	-0.81	-0.89	1.36	1.36	0.84
5	CHALCANT		-0.27		-0.18	-0.90		1.72	-0.36
6	ZINCOSIT	-1.15	0.58		0.58				
7	ALUNOGEN								
8	ALUNITE	0.90	-0.80	-0.14	-0.19		-1.62	0.63	1.22
9	JAROSITE		-0.54	-0.52	1.50			-0.44	
10	AMORP_FE	0.13	-0.27	-0.26	-0.27	1.84		-1.18	
11	GOETHITE	-0.72	0.55	0.57	-0.94	1.46		-0.93	
12	AMORP_AL	1.15	-0.65	-0.50					
13	BOEHMITE	1.96	-0.48		-0.08	-0.24	-1.34	-0.08	0.26
14	MAGHEMIT	1.15	-0.58		-0.58				
15	AMORP_SI	0.18	-0.44	-0.44	2.20	-0.44	-0.53	-0.53	
16	KAOLINIT	0.54	-1.40	-0.83	0.74	0.80	-0.89	1.03	
17	CHLORITE	0.46	-0.02	0.29		-0.72	-1.45	1.44	
18	MUSCOVIT	0.47	-0.73	0.20	-0.06	0.44	-1.73	1.42	
19	ANORTHIT	0.46	-0.57	0.29	0.58		-1.75	0.99	

Table D8: Standarized statistical data for calculated SIs of minerals in the brine from Mine Doyon
(T-8 Brine Sample Saturation Analysis)

OBS	MINERAL	SOLMINEQ	WATEQ4F	PHREEQE	MINTEQA2	PATH.ARC	SOLVEQ	EQ3NRD	EQ3NRP
1	GYPSUM	0.53	0.20	0.37	1.17		-0.29	0.04	-2.02
2	MELANTER		-0.20	-0.29	-0.15	1.87		-0.07	-1.16
3	EPSONITE		0.64		0.92			-0.27	-1.29
4	ANGLESIT	0.33	-1.10	-0.01	-0.03	0.04	1.37	1.05	-1.64
5	CHALCANT		0.46		-0.16	0.25		1.05	-1.61
6	ZINCOSIT	-1.10	0.86		0.23				
7	ALUNOGEN								
8	ALUNITE	0.92	0.18	0.44	0.20		-0.98	0.97	-1.73
9	JAROSITE		-0.47	-0.60	1.50			-0.42	
10	AMORP_FE	-0.04	0.01	-0.23	-0.22	1.79		-1.30	
11	GOETHITE	-0.92	0.83	0.67	-0.92	1.20		-0.86	
12	AMORP_AL	1.15	-0.62	-0.54					
13	BOEHMITE	1.79	0.05		0.14	0.13	-1.23	0.21	-1.09
14	MAGHEMIT	-0.76	1.13		-0.38				
15	AMORP_SI	0.37	-0.09	0.17	1.96	-0.70	-0.86	-0.86	
16	KAOLINIT	0.36	-0.91	-0.55	0.91	0.83	-1.55	0.91	
17	CHLORITE	0.46	0.40	0.63		-0.73	-1.68	0.93	
18	MUSCOVIT	0.29	0.22	0.66	0.33	0.51	-2.01		
19	ANORTHIT	0.19	0.20	0.25	0.78		-1.98	0.56	

Figure D1: Average linkage cluster analysis of Equilibrium Thermodynamic Geochemical Models
(T9 - Brackish Water Sample Concentration Analysis, Average Linkage Cluster Analysis)

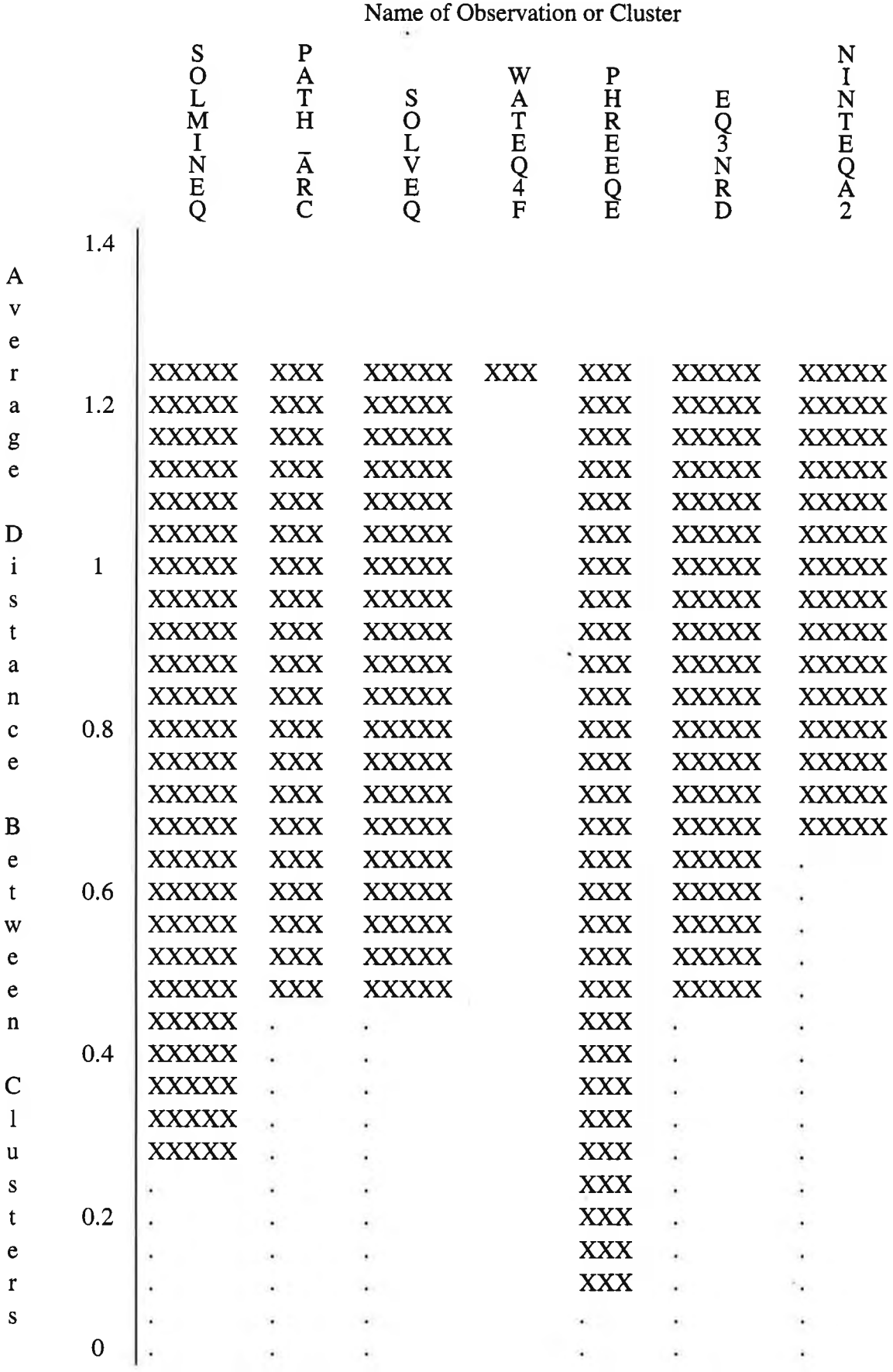

APPENDIX E

EQ6 OUTPUT

APPENDIX E

EQ6 OUTPUT

The following pages of output are typical for an EQ6 run. EQ6 is not distributed with a graphics package, and the output, which is quite complex, could not be shown as was the output for CHILLER and PATH.ARC.

The results shown are for a time of approximately 3.2 days. The conditions are appropriate for an acid rock pile, with an initial set of reactants of pyrite, galena, chalcopyrite, sphalerite, rhodochrosite, siderite, dolomite, clinochlore (7 angstrom spacing), chamosite (7 angstrom spacing), muscovite, albite and silica (in the form of amorphous silica). The initial fluid was typical of rainwater, and the oxygen fugacity is fixed. Of interest in the output is that the fluid has saturated with a clay mineral, a smectite which has been described by calcium, magnesium, potassium and sodium end-members of beidellite, montmorillonite and nontronite. The calculated amounts of each end-member of the clays have been presented. Other minerals which have precipitated include dolomite, kaolinite, pyrolusite and quartz, thus buffering the system.

EQ6 output

```
reaction progress        =  1.68704067826700E-01
log of reaction progress =      -0.7728744


time =  2.787E+05 sec
     =  3.226E+00 days
     =  8.831E-03 years

log sec =        5.445
log days =       0.509
log years =     -2.054

temperature    =     25.000 degrees c
total pressure =      1.013 bars

computing units remaining =      0.000
```

E2

step size is limited by the print requirement

--- reactant summary ---

reactant	moles	delta moles	grams	delta grams
galena	5.0000E-02	1.3923E-11	1.1963E+01	3.3314E-09
chalcopyrite	4.9998E-02	2.2802E-06	9.1758E+00	4.1847E-04
sphalerite	5.0000E-02	2.7917E-08	4.8728E+00	2.7207E-06
pyrite	4.6405E-02	3.5954E-03	5.5676E+00	4.3137E-01
rhodochrosite	0.0000E+00	5.0000E-02	0.0000E+00	5.7470E+00
siderite	0.0000E+00	5.0000E-02	0.0000E+00	5.7928E+00
dolomite	4.4757E-02	5.2426E-03	8.2533E+00	9.6674E-01
clinochlore-7a	5.0000E-02	2.7917E-08	2.7790E+01	1.5516E-05
chamosite-7a	5.0000E-02	2.7917E-08	1.7088E+01	9.5411E-06
muscovite	4.9141E-02	8.5947E-04	1.9573E+01	3.4234E-01
albite	1.3052E-02	3.6948E-02	3.4226E+00	9.6886E+00
sio2(am)	2.7944E-02	2.2056E-02	1.6790E+00	1.3252E+00

```
current total mass =  1.09386E+02 grams
delta total mass   =  2.42945E+01 grams
delta total volume =      7.91086 cc
```

EQ6 output

reactant	rel. rate mol/mol	rate mol/s	rate mol/s/cm2
galena	3.0337E-11	6.3291E-18	3.9121E-22
chalcopyrite	1.6575E-05	3.4580E-12	2.1374E-16
sphalerite	1.4755E-07	3.0783E-14	1.9028E-18
pyrite	6.1838E-02	1.2901E-08	7.9744E-13
rhodochrosite	0.0000E+00	0.0000E+00	0.0000E+00
siderite	0.0000E+00	0.0000E+00	0.0000E+00
dolomite	2.2457E-03	4.6851E-10	2.8959E-14
clinochlore-7a	1.4755E-07	3.0783E-14	1.9028E-18
chamosite-7a	1.4755E-07	3.0783E-14	1.9028E-18
muscovite	1.3107E-02	2.7345E-09	1.6903E-13
albite	5.9267E-01	1.2365E-07	7.6428E-12
sio2(am)	3.3013E-01	6.8873E-08	4.2572E-12

reactant	affinity kcal/mol	surface area mol/s/cm2
galena	176.6230	1.6178E+04
chalcopyrite	354.7491	1.6178E+04
sphalerite	176.9472	1.6178E+04
pyrite	327.9578	1.6178E+04
rhodochrosite	9.2111	1.6178E+04
siderite	20.8071	1.6178E+04
dolomite	0.0000	1.6178E+04
clinochlore-7a	33.3138	1.6178E+04
chamosite-7a	51.8496	1.6178E+04
muscovite	1.1756	1.6178E+04
albite	4.1710	1.6178E+04
sio2(am)	1.7541	1.6178E+04

reactant	rate constants, mol/s/cm2	
galena		
forward	2.0000E-04	
chalcopyrite		
forward	1.2589E-08	
sphalerite		
forward	5.7544E-08	
pyrite		
forward	1.2023E-05	6.3096E-09
rhodochrosite		
forward	3.1623E-04	
siderite		
forward	3.1623E-04	

EQ6 output

dolomite			
forward	8.1283E-04	2.9512E-08	
clinochlore-7a			
forward	5.7544E-08		
chamosite-7a			
forward	5.7544E-08		
muscovite			
forward	1.9953E-10	1.9953E-11	6.3096E-14
albite			
forward	1.8621E-09	3.1623E-12	2.5119E-15
sio2(am)			
forward	1.8621E-09	2.5119E-15	2.5119E-15

affinity of the overall irreversible reaction= 23.353 kcal
contributions from irreversible reactions
with no thermodynamic data are not included

--- element totals for the aqueous phase ---

element	mg/kg soln.	molal conc.	moles
o	8.863131E+05	5.578862E+01	5.571534E+01
al	3.128796E-05	1.167811E-09	1.166277E-09
ca	1.178080E+02	2.960266E-03	2.956378E-03
cl	3.524991E-07	1.001315E-11	1.000000E-11
cu	1.440669E-01	2.283169E-06	2.280171E-06
fe	8.037932E-08	1.449461E-12	1.447557E-12
h	1.111448E+05	1.110495E+02	1.109036E+02
c	1.301742E+03	1.091460E-01	1.090027E-01
k	2.173691E+01	5.598891E-04	5.591537E-04
mg	6.412618E+01	2.657063E-03	2.653573E-03
mn	9.877622E-07	1.810916E-11	1.808537E-11
na	8.043699E+02	3.523574E-02	3.518946E-02
pb	2.870482E-06	1.395170E-11	1.393338E-11
s	2.294060E+02	7.204802E-03	7.195339E-03
si	2.793879E+00	1.001815E-04	1.000499E-04
zn	1.815106E-03	2.795457E-08	2.791785E-08
co3--		1.091460E-01	1.090027E-01
so4--		7.204802E-03	7.195339E-03
s--		1.522232-138	1.520233-138

warning-- co3--, so4--, and s-- totals require that routine compl
have the names of non-carbonate carbon, sulfide sulfur,
and non-sulfate sulfur aqueous species

EQ6 output

single ion activities and activity coefficients are here defined
with respect to the modified nbs ph scale

	ph	eh	pe
modified nbs ph scale	5.8669	0.8672	1.4660E+01
rational ph scale	5.7930	0.8716	1.4734E+01

phcl = 16.9556

oxygen fugacity = 1.00000E-01
log oxygen fugacity = -1.00000

activity of water = 0.99732
log activity of water = -0.00116

ionic strength = 5.265613E-02 molal
sum of molalities = 0.1548266690976
osmotic coefficient = 0.96066

mass of solution = 1.005753 kg
mass of solutes = 0.007066 kg
conc of solutes = 0.702604 per cent (w/w)

moles of solvent h2o = 5.54355E+01
mass of solvent h2o = 9.98687E-01 kg

species	moles	grams	conc	log conc	log g	log act
h2o	5.54355E+01	9.98687E+02	9.97219E-01	-0.00121	0.00005	-0.00116
co2(aq)	7.64247E-02	3.36344E+00	7.65252E-02	-1.11620	0.00403	-1.11216
na+	3.36434E-02	7.73455E-01	3.36877E-02	-1.47253	-0.09422	-1.56675
hco3-	3.09088E-02	1.88597E+00	3.09495E-02	-1.50935	-0.08176	-1.59110
so4--	5.69990E-03	5.47552E-01	5.70739E-03	-2.24356	-0.34596	-2.58952
ca++	2.24022E-03	8.97837E-02	2.24317E-03	-2.64914	-0.33343	-2.98257
mg++	1.76550E-03	4.29105E-02	1.76782E-03	-2.75256	-0.30302	-3.05558
nahco3(aq)	9.90106E-04	8.31758E-02	9.91408E-04	-3.00375	0.00000	-3.00375
mgso4(aq)	5.83479E-04	7.02325E-02	5.84246E-04	-3.23340	0.00000	-3.23340
naso4-	5.55798E-04	6.61696E-02	5.56529E-04	-3.25451	-0.08176	-3.33627
k+	5.48884E-04	2.14604E-02	5.49606E-04	-3.25995	-0.09976	-3.35971
cahco3+	3.68705E-04	3.72743E-02	3.69190E-04	-3.43275	-0.09422	-3.52697

caso4(aq)	3.45495E-04	4.70363E-02	3.45950E-04	-3.46099	0.00000	-3.46099
mghco3+	3.03852E-04	2.59253E-02	3.04251E-04	-3.51677	-0.09422	-3.61098
o2(aq)	1.25054E-04	4.00158E-03	1.25219E-04	-3.90233	0.00403	-3.89830
sio2(aq)	1.00030E-04	6.01022E-03	1.00161E-04	-3.99930	0.00000	-3.99930
kso4-	1.02695E-05	1.38805E-03	1.02831E-05	-4.98788	-0.08176	-5.06963
caco3(aq)	1.95428E-06	1.95599E-04	1.95685E-06	-5.70844	0.00000	-5.70844
co3--	1.87352E-06	1.12429E-04	1.87599E-06	-5.72677	-0.32621	-6.05298
cuco3(aq)	1.78272E-06	2.20265E-04	1.78507E-06	-5.74834	0.00000	-5.74834
h+	1.60867E-06	1.62144E-06	1.61078E-06	-5.79296	-0.07396	-5.86693
mgco3(aq)	7.40919E-07	6.24700E-05	7.41893E-07	-6.12966	0.00000	-6.12966
cu++	4.81047E-07	3.05686E-05	4.81680E-07	-6.31724	-0.33343	-6.65067
hso4-	4.01640E-07	3.89878E-05	4.02168E-07	-6.39559	-0.08176	-6.47735
naco3-	9.45938E-08	7.85119E-06	9.47182E-08	-7.02357	-0.08176	-7.10532
zn++	2.00959E-08	1.31407E-06	2.01224E-08	-7.69632	-0.33343	-8.02975
cuoh+	1.05012E-08	8.45907E-07	1.05150E-08	-7.97819	-0.09422	-8.07241
hsio3-	9.88887E-09	7.62349E-07	9.90187E-09	-8.00428	-0.08176	-8.08604
nahsio3(aq)	9.88884E-09	9.89690E-07	9.90185E-09	-8.00428	0.00000	-8.00428
oh-	9.06552E-09	1.54180E-07	9.07744E-09	-8.04204	-0.08730	-8.12934
znhco3+	7.81260E-09	9.87569E-07	7.82288E-09	-8.10663	-0.09422	-8.20085
cu(co3)2--	5.89749E-09	1.08257E-06	5.90525E-09	-8.22876	-0.34596	-8.57472
al(oh)2+	4.76269E-10	2.90506E-08	4.76895E-10	-9.32158	-0.09422	-9.41579
al(oh)3(aq)	2.45922E-10	1.91828E-08	2.46245E-10	-9.60863	0.00000	-9.60863
mgh3sio4+	2.30018E-10	2.74669E-08	2.30321E-10	-9.63767	-0.09422	-9.73188
al(oh)4-	2.23005E-10	2.11879E-08	2.23298E-10	-9.65111	-0.08176	-9.73287
cah3sio4+	1.53031E-10	2.06875E-08	1.53232E-10	-9.81465	-0.09422	-9.90887
aloh++	1.46656E-10	6.45125E-09	1.46849E-10	-9.83313	-0.36073	-10.19386
caoh+	1.33919E-10	7.64482E-09	1.34095E-10	-9.87259	-0.09422	-9.96680
naoh(aq)	1.32845E-10	5.31342E-09	1.33020E-10	-9.87608	0.00000	-9.87608
al+++	3.95154E-11	1.06619E-09	3.95673E-11	-10.40266	-0.64556	-11.04822
also4+	2.92352E-11	3.59725E-09	2.92737E-11	-10.53352	-0.09422	-10.62774
pb++	1.39334E-11	2.88700E-09	1.39517E-11	-10.85537	-0.35113	-11.20650
mn++	1.29619E-11	7.12009E-10	1.29790E-11	-10.88676	-0.33343	-11.22019
cl-	9.95434E-12	3.52908E-10	9.96743E-12	-11.00142	-0.08730	-11.08872
khso4(aq)	9.92819E-12	1.35192E-09	9.94125E-12	-11.00256	0.00000	-11.00256
znoh+	9.32523E-12	7.68374E-10	9.33749E-12	-11.02977	-0.09422	-11.12399
al(so4)2-	5.67444E-12	1.24332E-09	5.68190E-12	-11.24551	-0.08176	-11.32726
mnso4(aq)	3.48835E-12	5.26721E-10	3.49294E-12	-11.45681	0.00000	-11.45681
mnhco3+	1.45867E-12	1.69130E-10	1.46059E-12	-11.83547	-0.09422	-11.92969
fe(oh)2+	1.21662E-12	1.09328E-10	1.21822E-12	-11.91427	-0.09422	-12.00849
koh(aq)	1.11040E-12	6.22997E-11	1.11186E-12	-11.95395	0.00000	-11.95395
fe(oh)3(aq)	2.25892E-13	2.41408E-11	2.26189E-13	-12.64553	0.00000	-12.64553
mnco3(aq)	1.76305E-13	2.02645E-11	1.76537E-13	-12.75316	0.00000	-12.75316
mgh2sio4(aq)	1.56484E-13	1.85284E-11	1.56690E-13	-12.80496	0.00000	-12.80496
mg(h3sio4)2(aq)	8.93806E-14	1.91738E-11	8.94982E-14	-13.04819	0.00000	-13.04819
nacl(aq)	3.68948E-14	2.15622E-12	3.69433E-14	-13.43246	0.00000	-13.43246
cuco3(oh)2--	1.81162E-14	2.85457E-12	1.81400E-14	-13.74136	-0.34596	-14.08732
cah2sio4(aq)	1.53988E-14	2.06617E-12	1.54191E-14	-13.81194	0.00000	-13.81194
mgcl+	6.52297E-15	3.89798E-13	6.53155E-15	-14.18498	-0.09422	-14.27920
ca(h3sio4)2(aq)	4.94607E-15	1.13904E-12	4.95258E-15	-14.30517	0.00000	-14.30517

feco3+	4.90519E-15	5.68296E-13	4.91164E-15	-14.30877	-0.09422	-14.40299
cacl+	2.12208E-15	1.60283E-13	2.12488E-15	-14.67267	-0.09422	-14.76688
h2sio4--	1.46559E-15	1.37911E-13	1.46752E-15	-14.83342	-0.34596	-15.17938
h2so4(aq)	4.52956E-16	4.44257E-14	4.53552E-16	-15.34337	0.00000	-15.34337
mnoh+	1.41000E-16	1.01433E-14	1.41186E-16	-15.85021	-0.09422	-15.94443
kcl(aq)	1.13867E-16	8.48893E-15	1.14017E-16	-15.94303	0.00000	-15.94303
fe(oh)4-	7.48545E-17	9.27270E-15	7.49530E-17	-16.12521	-0.08176	-16.20697
feoh++	5.94846E-17	4.33371E-15	5.95628E-17	-16.22502	-0.36073	-16.58575
al2(oh)2++++	1.96807E-17	1.73146E-15	1.97066E-17	-16.70539	-1.34972	-18.05511
cucl+	6.18385E-18	6.12193E-16	6.19199E-18	-17.20817	-0.09422	-17.30239
h6(h2sio4)4--	4.22990E-18	1.61770E-15	4.23547E-18	-17.37310	-0.34596	-17.71906
fe+++	3.75811E-18	2.09879E-16	3.76305E-18	-17.42446	-0.64556	-18.07001
hcl(aq)	2.36475E-18	8.62203E-17	2.36786E-18	-17.62564	0.00000	-17.62564
cu+	3.26228E-19	2.07305E-17	3.26657E-19	-18.48591	-0.09422	-18.58013
feso4+	2.29990E-19	3.49380E-17	2.30293E-19	-18.63772	-0.09422	-18.73194
mno4-	1.95357E-19	2.32335E-17	1.95614E-19	-18.70860	-0.08176	-18.79036
zncl+	1.49204E-19	1.50461E-17	1.49400E-19	-18.82565	-0.09422	-18.91987
fehco3+	6.81512E-20	7.96443E-18	6.82409E-20	-19.16596	-0.09422	-19.26017
fe++	4.10947E-20	2.29502E-18	4.11488E-20	-19.38564	-0.33343	-19.71907
fe(so4)2-	1.11129E-20	2.75571E-18	1.11275E-20	-19.95360	-0.08176	-20.03536
feso4(aq)	7.77744E-21	1.18148E-18	7.78767E-21	-20.10859	0.00000	-20.10859
pbcl+	1.72118E-21	4.17649E-19	1.72344E-21	-20.76360	-0.09422	-20.85782
feco3(aq)	9.06531E-22	1.05027E-19	9.07723E-22	-21.04205	0.00000	-21.04205
mn+++	4.37110E-22	2.40108E-20	4.37685E-22	-21.35884	-0.78339	-22.14223
al3(oh)4(5+)	3.06230E-22	4.56204E-20	3.06633E-22	-21.51338	-2.04853	-23.56191
mn(oh)2(aq)	2.04534E-22	1.81924E-20	2.04803E-22	-21.68866	0.00000	-21.68866
mncl+	1.21910E-22	1.10187E-20	1.22071E-22	-21.91339	-0.09422	-22.00761
cuo2--	5.13328E-23	4.90458E-21	5.14003E-23	-22.28903	-0.34596	-22.63499
mno4--	1.89529E-24	2.25404E-22	1.89779E-24	-23.72175	-0.34596	-24.06771
ho2-	4.96417E-25	1.63851E-23	4.97070E-25	-24.30358	-0.08176	-24.38534
fehso4++	2.36426E-25	3.61539E-23	2.36737E-25	-24.62573	-0.36073	-24.98646
cacl2(aq)	1.56974E-26	1.74215E-24	1.57180E-26	-25.80360	0.00000	-25.80360
mn2oh+++	4.44845E-27	5.64371E-25	4.45430E-27	-26.35122	-0.78339	-27.13461
hclo(aq)	3.64490E-27	1.91211E-25	3.64969E-27	-26.43774	0.00000	-26.43774
h4(h2sio4)4----	1.34729E-27	5.12545E-25	1.34906E-27	-26.86997	-1.41524	-28.28521
mg4(oh)4++++	6.91624E-28	1.14290E-25	6.92534E-28	-27.15956	-1.34972	-28.50928
hso5-	2.44927E-28	2.76941E-26	2.45249E-28	-27.61039	-0.08176	-27.69215
mn(oh)3-	1.70013E-28	1.80134E-26	1.70237E-28	-27.76895	-0.08176	-27.85070
clo-	8.74714E-29	4.50059E-27	8.75865E-29	-28.05756	-0.08176	-28.13932
fe(oh)2(aq)	2.58156E-29	2.31984E-27	2.58496E-29	-28.58755	0.00000	-28.58755
mn2(oh)3+	2.24159E-29	3.60636E-27	2.24454E-29	-28.64887	-0.09422	-28.74309
cucl2(aq)	2.13710E-29	2.87336E-27	2.13991E-29	-28.66961	0.00000	-28.66961
fecl++	2.45824E-30	2.24437E-28	2.46147E-30	-29.60880	-0.36073	-29.96953
zncl2(aq)	1.10394E-30	1.50462E-28	1.10539E-30	-29.95648	0.00000	-29.95648
fe2(oh)2++++	4.55037E-31	6.63029E-29	4.55636E-31	-30.34138	-1.34972	-31.69111
fecl+	1.33462E-31	1.21850E-29	1.33637E-31	-30.87407	-0.09422	-30.96829
pbcl2(aq)	4.15041E-32	1.15425E-29	4.15587E-32	-31.38134	0.00000	-31.38134
clo3-	7.65890E-35	6.39142E-33	7.66897E-35	-34.11526	-0.08176	-34.19702
clo4-	3.10679E-35	3.08972E-33	3.11088E-35	-34.50712	-0.08730	-34.59442

fe3(oh)4(5+)	1.00221E-35	2.36091E-33	1.00353E-35	-34.99847	-2.04853	-37.04700
fe(oh)3-	9.93573E-36	1.06182E-33	9.94880E-36	-35.00223	-0.08176	-35.08398
mn(oh)4--	1.94200E-36	2.38789E-34	1.94455E-36	-35.71118	-0.34596	-36.05714
cucl2-	1.39580E-36	1.87667E-34	1.39764E-36	-35.85461	-0.08176	-35.93636
pb++++	1.90793E-38	3.95323E-36	1.91044E-38	-37.71887	-1.34972	-39.06859
clo2-	9.68649E-39	6.53368E-37	9.69923E-39	-38.01326	-0.08176	-38.09502
fecl2+	9.46663E-39	1.19992E-36	9.47908E-39	-38.02323	-0.09422	-38.11745
hclo2(aq)	1.61245E-41	1.10387E-39	1.61457E-41	-40.79194	0.00000	-40.79194
s2o8--	9.65067E-42	1.85416E-39	9.66336E-42	-41.01487	-0.34596	-41.36083
zncl3-	5.82749E-42	1.00086E-39	5.83515E-42	-41.23395	-0.08176	-41.31570
formate	4.30410E-43	1.93761E-41	4.30976E-43	-42.36555	-0.08176	-42.44730
pbcl3-	1.97983E-43	6.20792E-41	1.98243E-43	-42.70280	-0.08176	-42.78456
h2(aq)	6.86648E-45	1.38420E-44	6.87551E-45	-44.16270	0.00403	-44.15866
fecl2(aq)	4.45474E-45	5.64649E-43	4.46060E-45	-44.35061	0.00000	-44.35061
formic acid(aq)	2.74222E-45	1.26212E-43	2.74582E-45	-44.56133	0.00000	-44.56133
mncl3-	1.82996E-45	2.95153E-43	1.83237E-45	-44.73699	-0.08176	-44.81874
hso3-	1.42869E-46	1.15827E-44	1.43057E-46	-45.84449	-0.08176	-45.92625
cucl3--	1.34279E-46	2.28146E-44	1.34456E-46	-45.87142	-0.34596	-46.21738
so3--	1.20411E-47	9.64063E-46	1.20570E-47	-46.91876	-0.34596	-47.26472
h2so3(aq)	1.63816E-50	1.34460E-48	1.64031E-50	-49.78507	0.00000	-49.78507
so2(aq)	1.16848E-50	7.48582E-49	1.17001E-50	-49.93181	0.00000	-49.93181
al13o4(oh)24(7+)	2.24580E-51	1.84814E-48	2.24875E-51	-50.64806	-3.99974	-54.64779
zncl4--	6.62624E-52	1.37296E-49	6.63496E-52	-51.17816	-0.34596	-51.52412
pbcl4--	1.88328E-54	6.57284E-52	1.88575E-54	-53.72452	-0.34596	-54.07047
cucl4--	5.91217E-56	1.21410E-53	5.91995E-56	-55.22768	-0.34596	-55.57364
fecl4-	7.35017E-64	1.45282E-61	7.35984E-64	-63.13313	-0.08176	-63.21489
fecl4--	2.35204E-66	4.64900E-64	2.35514E-66	-65.62798	-0.34596	-65.97394
s2o6--	9.18031E-67	1.47003E-64	9.19239E-67	-66.03657	-0.34596	-66.38253
s2o5--	4.74851E-97	6.84398E-95	4.75476E-97	-96.32287	-0.34596	-96.66883

--- summary of solid product phases---

product	log moles	moles	grams	volume, cc
dolomite-ord	-3.1300308	7.41258E-04	1.36689E-01	4.76925E-02
kaolinite	-1.8141884	1.53395E-02	3.96006E+00	1.52659E+00
pyrolusite	-1.3010300	5.00000E-02	4.34648E+00	8.30500E-01
quartz	-2.1978259	6.34124E-03	3.81009E-01	1.43870E-01
fix o2(g)	2.9999779	9.99949E+02	3.19972E+04	0.00000E+00
smectite-di	-1.5718569	2.68005E-02	1.13529E+01	3.50771E+00
beidellite-ca	-6.3337617	4.63701E-07	1.69975E-04	6.00632E-05
beidellite-k	-7.3458269	4.50996E-08	1.68155E-05	6.02982E-06
beidellite-mg	-6.2557248	5.54977E-07	2.01989E-04	6.83677E-05
beidellite-na	-6.5783156	2.64049E-07	9.70475E-05	3.44689E-05
montmor-ca	-7.0845535	8.23088E-08	3.01286E-05	1.09688E-05
montmor-k	-7.8832853	1.30832E-08	4.87131E-06	1.79805E-06

montmor-mg	-6.7956075	1.60100E-07	5.81870E-05	2.10127E-05
montmor-na	-7.1272892	7.45952E-08	2.73777E-05	1.00160E-05
nontronite-ca	-2.0285898	9.36290E-03	3.97261E+00	1.22748E+00
nontronite-k	-3.0409580	9.10001E-04	3.91831E-01	1.23096E-01
nontronite-mg	-1.9508559	1.11981E-02	4.72213E+00	1.45306E+00
nontronite-na	-2.2734467	5.32787E-03	2.26577E+00	7.03864E-01

--- grand summary of solid phases (e.s.+p.r.s.+reactants) ---

phase/end-member	log moles	moles	grams	volume, cc
albite	-1.8843151	1.30522E-02	3.42260E+00	1.30849E+00
chalcopyrite	-1.3010498	4.99977E-02	9.17583E+00	2.14140E+00
chamosite-7a	-1.3010302	5.00000E-02	1.70884E+01	5.31000E+00
clinochlore-7a	-1.3010302	5.00000E-02	2.77898E+01	1.05750E+01
dolomite	-1.3491352	4.47574E-02	8.25333E+00	2.88081E+00
dolomite-ord	-3.1300308	7.41258E-04	1.36689E-01	4.76925E-02
galena	-1.3010300	5.00000E-02	1.19633E+01	1.57450E+00
kaolinite	-1.8141884	1.53395E-02	3.96006E+00	1.52659E+00
muscovite	-1.3085602	4.91405E-02	1.95731E+01	6.91456E+00
pyrite	-1.3334387	4.64046E-02	5.56758E+00	1.11093E+00
pyrolusite	-1.3010300	5.00000E-02	4.34648E+00	8.30500E-01
quartz	-2.1978259	6.34124E-03	3.81009E-01	1.43870E-01
rhodochrosite	-999.0000000	0.00000E+00	0.00000E+00	0.00000E+00
sio2(am)	-1.5537190	2.79435E-02	1.67897E+00	8.10362E-01
siderite	-999.0000000	0.00000E+00	0.00000E+00	0.00000E+00
sphalerite	-1.3010302	5.00000E-02	4.87280E+00	1.19150E+00
fix o2(g)	2.9999779	9.99949E+02	3.19972E+04	0.00000E+00
smectite-di	-1.5718569	2.68005E-02		
beidellite-ca	-6.3337617	4.63701E-07	1.69975E-04	6.00632E-05
beidellite-k	-7.3458269	4.50996E-08	1.68155E-05	6.02982E-06
beidellite-mg	-6.2557248	5.54977E-07	2.01989E-04	6.83677E-05
beidellite-na	-6.5783156	2.64049E-07	9.70475E-05	3.44689E-05
montmor-ca	-7.0845535	8.23088E-08	3.01286E-05	1.09688E-05
montmor-k	-7.8832853	1.30832E-08	4.87131E-06	1.79805E-06
montmor-mg	-6.7956075	1.60100E-07	5.81870E-05	2.10127E-05
montmor-na	-7.1272892	7.45952E-08	2.73777E-05	1.00160E-05
nontronite-ca	-2.0285898	9.36290E-03	3.97261E+00	1.22748E+00
nontronite-k	-3.0409580	9.10001E-04	3.91831E-01	1.23096E-01
nontronite-mg	-1.9508559	1.11981E-02	4.72213E+00	1.45306E+00
nontronite-na	-2.2734467	5.32787E-03	2.26577E+00	7.03864E-01

	mass, grams	volume, cc

EQ6 output

created	3.201735E+04	6.056364E+00
destroyed	2.429451E+01	7.910859E+00
net	3.199306E+04	-1.854495E+00

warning-- these volume totals may be incomplete because
of missing partial molar volume data in the data base

--- mineral saturation state summary ---

mineral	affinity, kcal	state	mineral	affinity, kcal	state
albite	-4.1710		albite high	-5.9701	
albite low	-4.1710		alunite	-4.8798	
analcime	-4.1780		andalusite	-7.0026	
anglesite	-8.1084		anhydrite	-1.7268	
aragonite	-0.9548		bassanite	-2.6074	
beidellite-ca	-2.1439		beidellite-h	-2.8070	
beidellite-k	-2.5995		beidellite-mg	-2.1087	
beidellite-na	-2.2540		boehmite	-2.5665	
caso4:0.5h2o(beta)	-2.8367		calcite	-0.7578	
celadonite	-6.6394		cerussite	-5.0773	
chalcanthite	-9.0377		chalcedony	-0.3700	
chrysocolla	-7.0040		coesite	-1.1051	
corundum	-8.1196		cristobalite	-0.7510	
cristobalite-a	-0.7510		cristobalite-b	-1.3561	
dawsonite	-0.1355		delafossite	-9.2330	
diaspore	-1.4143		dioptase	-6.8156	
dolomite	0.0000		dolomite-dis	-2.1070	
dolomite-ord	0.0000	satd	enstatite	-9.0713	
epsomite	-5.0355		fe(oh)3	-8.3608	
ferrite-cu	-8.4258		gibbsite	-0.3376	
glauberite	-7.9485		goethite	-1.3726	
gypsum	-1.4900		hematite	-1.4333	
hexahydrite	-5.3552		huntite	-7.2949	
ice	-0.1905		illite	-3.1635	
jadeite	-6.3881		k-feldspar	-2.4700	
kalicinite	-7.1414		kalsilite	-6.8021	
kaolinite	0.0000	satd	kieserite	-7.3389	
kyanite	-6.6335		lansfordite	-4.9475	
laumontite	-8.3322		lawsonite	-9.0767	
magnesite	-1.4644		malachite	-4.4119	
manganite	-5.9745		maximum microcline	-2.4700	
mesolite	-3.0939		mirabilite	-6.2687	
mno2(gamma)	-2.0707		monohydrocalcite	-1.8968	
montmor-ca	-2.4819		montmor-k	-2.8415	
montmor-mg	-2.3518		montmor-na	-2.5011	

EQ6 output

mordenite	-5.4532		muscovite	-1.1756	
nahcolite	-4.1542		natrolite	-9.7006	
nepheline	-8.3152		nesquehonite	-5.1553	
nontronite-ca	-0.2056		nontronite-h	-0.8688	
nontronite-k	-0.6614		nontronite-mg	-0.1706	
nontronite-na	-0.3159		paragonite	-4.0997	
pentahydrite	-5.8169		pyrolusite	0.0000	satd
pyrophyllite	-2.2197		quartz	0.0000	satd
rhodochrosite	-9.2111		sanidine high	-4.1060	
scolecite	-5.8897		sio2(am)	-1.7541	
sillimanite	-7.4986		smithsonite	-5.7535	
starkeyite	-6.3437		stilbite	-3.6537	
syngenite	-9.9349		tenorite	-3.5116	
thenardite	-7.3861		tridymite	-0.2340	
fix o2(g)	0.0000	satd			

--- summary of solid solutions ---

mineral	aff. kcal/mol	mole frac.	lambda	state
biotite	-18.4119			
annite	-18.41185	0.9849E-14	0.9701E-28	
phlogopite	-18.41185	1.0000	1.0000	
carbonate-calcite	-0.6007			
calcite	-0.60066	0.7671	1.000	
magnesite	-0.60066	0.2328	1.000	
rhodochrosite	-0.60066	0.4883E-06	1.000	
siderite	-0.60066	0.1545E-14	1.000	
smithsonite	-0.60066	0.1671E-03	1.000	
chlorite-ss	-28.7117			
clinochlore-14a	-28.71166	1.0000	1.0000	
daphnite-14a	-28.71166	0.2128E-13	0.2050E-54	
clinoptilolite-hy-	-13.2559			
clinoptilolite-hy-ca	-13.25590	0.2000	1.000	
clinoptilolite-hy-ca	-13.25590	0.2000	1.000	
clinoptilolite-hy-ca	-13.25590	0.2000	1.000	
clinoptilolite-hy-ca	-13.25590	0.2000	1.000	
clinoptilolite-hy-ca	-13.25590	0.2000	1.000	
clinoptilolite-ss	-12.6902			
clinoptilolite-ca	-12.69023	0.4765	0.1614	
clinoptilolite-k	-12.69023	0.8796E-01	0.2529E-02	
clinoptilolite-na	-12.69023	0.4356	0.1295	
epidote-ss	-17.8534			

clinozoisite		-17.85339	0.3528E-02	1.000
epidote		-17.85339	0.9965	1.000
garnet-ss	-27.2749			
andradite		-27.27491	0.9632	0.9632
grossular		-27.27491	0.3685E-01	0.3685E-01
olivine	-19.7926			
fayalite		-19.79263	0.5154E-12	2.174
forsterite		-19.79263	1.0000	1.000
orthopyroxene	-9.0713			
enstatite		-9.07126	1.0000	1.000
ferrosilite		-9.07126	0.1646E-12	1.000
plagioclase	-5.9701			
albite high		-5.97010	1.0000	1.000
anorthite		-5.97010	0.2294E-06	1.000
sanidine-ss	-4.0811			
albite high		-4.08107	0.4125E-01	1.000
sanidine high		-4.08107	0.9588	1.000
saponite-tri	-14.8670			
saponite-ca		-14.86704	0.3452	2.039
saponite-h		-14.86704	0.1162E-01	19.79
saponite-k		-14.86704	0.3358E-01	9.718
saponite-mg		-14.86704	0.4132	1.808
saponite-na		-14.86704	0.1964	2.975
smectite-di	0.0000			saturated
beidellite-ca		0.00000	0.1730E-04	1551.
beidellite-k		0.00000	0.1683E-05	7389.
beidellite-mg		0.00000	0.2071E-04	1375.
beidellite-na		0.00000	0.9852E-05	2261.
montmor-ca		0.00000	0.3071E-05	4937.
montmor-k		0.00000	0.4882E-06	0.1693E+05
montmor-mg		0.00000	0.5974E-05	3162.
montmor-na		0.00000	0.2783E-05	5274.
nontronite-ca		0.00000	0.3494	2.023
nontronite-k		0.00000	0.3395E-01	9.645
nontronite-mg		0.00000	0.4178	1.794
nontronite-na		0.00000	0.1988	2.952

solid solution product phases

xbar	lambda	activity	log xbar	log lambda	log activity

EQ6 output

smectite-di
ideal solution

beidellite-ca					
0.1730E-04	1551.	0.2683E-01	-4.762	3.190	-1.571
beidellite-k					
0.1683E-05	7389.	0.1243E-01	-5.774	3.869	-1.905
beidellite-mg					
0.2071E-04	1375.	0.2847E-01	-4.684	3.138	-1.546
beidellite-na					
0.9852E-05	2261.	0.2228E-01	-5.006	3.354	-1.652
montmor-ca					
0.3071E-05	4937.	0.1516E-01	-5.513	3.694	-1.819
montmor-k					
0.4882E-06	0.1693E+05	0.8265E-02	-6.311	4.229	-2.083
montmor-mg					
0.5974E-05	3162.	0.1889E-01	-5.224	3.500	-1.724
montmor-na					
0.2783E-05	5274.	0.1468E-01	-5.555	3.722	-1.833
nontronite-ca					
0.3494	2.023	0.7068	-0.4567	0.3060	-0.1507
nontronite-k					
0.3395E-01	9.645	0.3275	-1.469	0.9843	-0.4848
nontronite-mg					
0.4178	1.794	0.7498	-0.3790	0.2539	-0.1251
nontronite-na					
0.1988	2.952	0.5868	-0.7016	0.4701	-0.2315

E13

--- summary of gas species ---

gas	log fugacity	fugacity	partial pressure
al(g)	-190.30229	4.98556-191	
c(g)	-185.33656	4.60719-186	
ch4(g)	-140.95349	1.11303-141	
co(g)	-44.20656	6.21493E-45	
co2(g)	0.35674	2.27372E+00	
ca(g)	-154.38428	4.12784-155	
cl2(g)	-38.85972	1.38126E-39	
cu(g)	-76.63628	2.31057E-77	
h2(g)	-41.05366	8.83764E-42	
h2o(g)	-1.58656	2.59081E-02	
h2s(g)	-136.86777	1.35590-137	
hcl(g)	-23.26404	5.44448E-24	
k(g)	-78.10597	7.83488E-79	
mg(g)	-131.62889	2.35020-132	
na(g)	-75.59550	2.53804E-76	
o2(g)	-1.00000	1.00000E-01	

EQ6 output

pb(g)	-73.13931	7.25581E-74
s2(g)	-217.27997	5.24845-218
so2(g)	-50.10181	7.91026E-51
si(g)	-220.05760	8.75790-221
zn(g)	-79.76756	1.70781E-80

APPENDIX F

SOURCES FOR PROGRAMS

APPENDIX F

SOURCES FOR PROGRAMS

All of the major models presented in this report are supported by their authors or an alternative group. The more complex models are under further development. Before using these models, it is recommended to contact the developers to obtain information on upgrade, support and future plans. Before using any computer modelling program, the user should examine the program documentation, and if possible, the program source code in detail. This should allow the user to determine if the model is appropriate for their application and expectations and if the fundamental assumptions in the model are reasonable for their problem.

The following contact people, postal addresses and e-mail adresses are the most current for the listed programs.

Model	Contact Person	Address	Other info
1DREACT	Dr. C. I Steefel	Battelle Pacific Northwest Laboratories Interfacial Geochemistry Group Mail Stop K3-61 P.O. Box 999 Richland, Washington 99352 USA	Available through negociated agreement
ACIDROCK	Dr. J.M. Scharer	SENES Consultants Limited 52 West Beaver Creek Road Unit No. 4 Richmond Hill, Ontario L4B 1L9	Not available for purchase used for consulting

Model	Contact Person	Address	Other info
BOUNDS	Dr. J.A.D. Connolly	Institut fur Mineralogie und Petrographie Eidgenossische Technische Hochschule CH-8092 Zurich, Switzerland	Support model
CHILLER SOLVEQ	Dr. M. Reed	Department of Geological Sciences University of Oregon Eugene, Oregon 97403 USA	Available for purchase as a package. Approximate cost $700
CIRF.A	Dr. P. Ortoleva	Department of Chemistry and Geological Sciences, Indiana University Bloomington, Indiana 47405 USA ortoleva@indiana.edu	Available for purchase through a negotiated agreement which includes training
EQ3 EQ6	Dr. T.J. Wolery	Requests to obtain the software should be addressed to: Technology Transfer Initiatives Program , L-795 Attn: Diana West Lawrence Livermore National Laboratory P.O. Box 808 Livermore, Ca 94550 USA Phone (510) 423-7678	Comments and questions concerning EQ3/6, contact: Dr. T.J. Wolery, L-219 Lawrence Livermore National Laboratory P.O. Box 808 Livermore, CA 94550 USA EQ3 and EQ6 are available for purchase as a single package. Approximate cost $700

Model	Contact Person	Address	Other info
GE0-CALC GE0-TAB	Dr. T.H. Brown	Dept. Geological Sciences University of British Columbia Vancouver, B.C. Canada	Dr. E.H. Perkins Alberta Research Council PO Box 8330 Edmonton, Alberta Canada T6H 5X2 *email*: perkins@arc.ab.ca Support model
ACT2 REACT RXN TACT	Dr. C. Bethke	Hydrogeology Program University of Illinois Urbana, Illinois USA *email*: bethke@aquifer.geology.uiuc.edu	Available as part of the "Geochemist's Workbench", a proprietary package, with participation in a consortium, at a cost of $20,000 per year
MINTEQA2		Center for Exposure Assessment Modeling (CEAM) US. Environmental Protection Agency Office of Research and Development 960 College Station Road Athens, GA 30605-2720 USA *email*: ceam@athens.ath.epa.gov Phone: (706) 546-3549	For those with internet access, the EPA maintains an FTP server. Contact earth1.epa.gov using anonymous ftp. The most current version of MINTEQ (for DOS) is in directory /pub/athens/DOS/MINTEQ Software is public domain

Model	Contact Person	Address	Other info
MINTRAN	Dr. E.O. Frind	Institute for Groundwater Research University of Waterloo Waterloo, Ontario Canada N2L 3G1	Not available for purchase
MPATH	Dr. P.C. Lichtner	Southwest Research Institute, Center for Nuclear Waste Regulatory Analyses 6220 Culebra Road San Antonio, Texas 78238-5155 *email*: lichtner@swri.edu	Available through negotiated agreement
PATHARC	Dr. E.H. Perkins	Alberta Research Council PO Box 8330 Edmonton, Alberta Canada T6H 5X2 *email*: perkins@arc.ab.ca	Available with participation to research consortium. Distribution currently under revision

Model	Contact Person	Address	Other info
NETPATH PHREEQE PHRQPITZ PHREEQM WATEQ4F	Ollie Holloway	National Water Information System United States Geological Survey 437 National Centre 12201 Sunrise Valley Dr. Reston VA 22092 (703) 648-5695	The most current versions of these programs are available via internet. The current copies of PHREEQE and related programs are maintained on an FTP server. Contact brrcrftp.cr.usgs.gov using anonymous ftp. The most current versions of PHREEQE, PHRQPITZ, NETPATH, BALNINP and WATEQ4F are in directories below /geochem/pc (DOS versions) and below /geochem/unix (Unix versions) for PHREEQM, PHREEQE, PHRQPITZ, NETPATH, BALNINP and WATEQ4F. Public domain, $40.00
Q-ROCK		Steffen, Robertson and Kirsten, Ltd Suite 800 - 580 Hornby Street Vancouver, B.C. Canada V6C 3B6	Not available for purchase. Used for consulting

Model	Contact Person	Address	Other info
RATAP	Dr. H. F. Steger	CANMET 555 Booth Street Ottawa, Ontario K1A 0G1 H.F. Steger (613) 992-4105 Henry.Steger@x400.emr.ca	Available for purchase Approximate price $10,000 Discount available for universities
REACTRAN	Dr. C.H. Moore	946 East Chambers Pibe Bloomington, Indiana 47408-97064 USA (812) 323-9138 *email*: crmoore@ucs.indiana.edu	Available for purchase. Approximate cost $100,000 US Includes 10 days of training
SOLMINEQ.88 PC/SHELL	Dr. E.H. Perkins	Alberta Research Council PO Box 8330 Edmonton, Alberta Canada T6H 5X2 *email*: perkins@arc.ab.ca	Purchasing status currently under revision
STEADYQL	Dr. J.C. Westall	Department of Chemistry Oregon Sate University Corvallis, Oregon 97331 USA	Available for purchase. Approximate cost $200

Model	Contact Person	Address	Other info
SUPCRIT92	Dr. H.C. Helgeson	Laboratory of Theoretical Geochemistry Department of Geology and Geophysics University of California, Berkeley, CA 94720 USA	Support model
Unnamed (White et al)	Dr. E.M. Trujillo	Department of Chemical and Fuels Engineering University of Utah Salt Lake City Utah, USA	Under development
WATAIL	Dr. R.V. Nicholson	Institute for Groundwater Research University of Waterloo Waterloo, Ontario Canada N2L 3G1 MEND rvnichol@sciborg.uwaterloo.ca	Also available through MEND Public domain

APPENDIX G

LIST OF REFERENCES

ADAM, K., NATARAJAN, K.A. and IWASAKI, I. (1984), Grinding media wear and its effect on the flotation of sulphide minerals. *Int. J. Miner. Process.* **12**, 39-54.

AGGARWAL, P.K., GUNTER, W.D. and KHARAKA, Y.K. (1990) Effect of Pressure on Aqueous Equilibria. Chapter 7 in Chemical Modelling of Aqueous Systems II, ACS Symposium Series 416, Eds: D.C. Melchior and R.L. Bassett, American Chemical Society, Washington, DC, 87-101.

AHLBERG, E., FORSSBERG, K.S.E. and WANG, X. (1990) The surface oxidation of pyrite in alkaline solution. *J. Appl. Electrochem.* **20**, 1033-1039.

AHMAD M.U. (1974) Coal mining and its effect on water quality. In Extraction of Minerals and Energy: Today's Dilemmas, R.A. Deju (ed.) Ann Arbor Science, Ann Arbor, MI, pp. 49-56.

AHONEN, L., HILTUNEN, P. and TUOVINEN, O.H. (1986) The role of pyrrhotite and pyrite in the bacterial leaching of chalcopyrite. In Fundamental And Applied Biohydrometallurgy. Elsvier, Amsterdam pp. 13-22.

AHONEN, L. and TUOVINEN, O.H. (1992) Bacterial oxidation of sulfide minerals in column leaching experiments at suboptimal temperatures. *Appl. Environ. Microbiol.* **58**, 600-606.

AHONEN, L. and TUOVINEN, O.H. (1993) Alterations in surface and textures of minerals during the bacterial leaching of a complex sulphide ore. *Geomicrobiol. J.* **10**, 207-217.

AL, T.A., BLOWES, D.W. and JAMBOR, J.L. (1994) A geochemical study of the main tailings impoundment at the Falconbridge Limited, Kidd Creek Division Metallurgical Site, Timmins, Ontario. Chap. 12 in Environmental Geochemistry of Sulphide Mine-Wastes, Eds: J.L. Jambor and D.W. Blowes, Short Course Handbook V.22, Min. Assoc. Canada, 133-161.

ALLER, R.C. and RUDE, P.D. (1988) Complete oxidation of solid phase sulphides by manganese and bacteria in anoxic marine sediments. *Geochim. Cosmochim. Acta* **52**, 751-765.

ALLISON, J.D., BROWN, D.S. and NOVO-GRADAC, K.J. (1991) MINTEQA2/PRODEFA2, A Geochemical Assessment Model for Environmental Systems: Version 3.0 User's Manual. Environmental Research Laboratory, Office of Research and Development, U.S. Environmental Protection Agency, EPA/600/3-91/021, Athens, Georgia, 30605, 93 pages.

ALPERS, C.N. and BRIMHALL, G.H. (1989) Paleohydrologic Evolution and Geochemical Dynamics of Cumulative Supergene Metal Enrichment at La Escondida, Atacama Desert, Northern Chile, V.84, 229-255.

ALPERS, C.N., BLOWES, D.W., NORDSTROM, D.K. and JAMBOR, J.L. (1994) Secondary minerals and acid mine-water chemistry. Chap. 9 in Environmental Geochemistry of Sulphide Mine-Wastes, Eds: J.L. Jambor and D.W. Blowes, Short Course Handbook, V.22, Min. Assoc. Canada, 247-270.

ALPERS, C.N. and NORDSTROM, D.K. (1991) Geochemical evolution of extremely acid waters at Iron mountain, California: Are there any lower limits to pH? Proceedings of the Second International Conference on the Abatement of Acidic Drainage, MEND, Sept. 16-18, Montreal, V.2, 321-342.

ALPERS, C.N. and NORDSTROM, D.K. (1995) Geochemical modelling of water-rock interaction in mining environments. In Environmental Geochemistry of Mineral Deposits, Eds: G.S. Plumlee and M.H. Logsdon, Reviews in Economic Geology, V.6, Society of Economic Geologists (under review)

AMHREIN, C. and SUAREZ, D.L. (1988) The use of a surface complexation model to describe the kinetics of ligand-promoted dissolution of anorthite. *Geochim. Cosmochim. Acta* **52**, 2785-2793.

ANBEEK, C. (1993) The effect of natural weathering on dissolution rates. *Geochim. Cosmochim. Acta* **57**, 4963-4975.

ANDRIAMANANA, A. and LAMACHE M. (1983) Étude electrochimique de la pyrite en milieu acide. *Electrochim. Acta* **28**, 177-183.

APPELO, C.A.J. and POSTMA, D. (1993) Geochemistry, Groundwater And Pollution. A.A. Balkema, Rotterdam, 536p. (Contains description of input for PHREEQM).

APPELO, C.A.J. and WILLEMSEN, A. (1987) Geochemical calculations and observations on salt water intrusions. I: A combined geochemical/mixing cell model. *J. Hydrology* **94**, 313-330.

APPELO, C.A.J. and WILLEMSEN, H.E. (1990) Geochemical calculations and observations on salt water intrusions. II: Validation of a geochemical transport model with column experiments. *J. Hydrology* **120**, 225-250.

ARKESTEYN G.J.M.W. (1979) Pyrite oxidation by *Thiobacillus ferrooxidans* with special reference to the sulphur moiety of the mineral. *Antonie van Laeurvenhoek (Microbiology)* **45**, 423-435.

ARKESTEYN G.J.M.W. (1980) Pyrite oxidation in acid sulphate soils: The role of microorganisms. *Plant and Soil* **54**, 119-134.

AWAKURA, Y., KAMEI, S. and MAJIMA, H. (1980) A kinetic study of nonoxidative dissolution of galena in aqueous acid solution. *Metall. Trans. B* **11B**, 377-381.

AZUMA, K. and KAMETANI, H. (1964) Kinetics of dissolution of ferric oxide. *Trans. Amer. Inst. Min. Engr.* **230**, 853-862.

BAILEY, L.K. (1977) Electrochemistry of pyrite and other sulfides in acid oxygen pressure leaching. [No pp. Given Avail.] National Library Canada, Ottawa, Ontario. From: Diss. Abstr. Int. B 1977, **38(5)**, 2318.

BAILEY, L.K. and PETERS, E. (1976) Decomposition of pyrite in acids by pressure leaching and anodization: The case for an electrochemical mechanism. *Can. Metall. Q.* **15**, 333-344.

BALL, J.W. and NORDSTROM, D.K. (1991) User's manual for WATEQ4F, with revised thermodynamic database and test cases for calculating speciation of major, trace and redox elements in natural waters. U.S. Geological Survey Open-File Report 91-183, 189p., (revised and reprinted August 1992).

BALTZINGER, C. and BARO, R. (1973) Anisotropy of dissolution of hematite by hydrochloric acid. *Bull. Soc. Fr. Mineral. Cristallogr.* **96**, 199-200.

BANWART, S. (1989) The reductive dissolution of hematite (α-Fe_2O_3) by ascorbate. Ph.D. dissertation. Swiss Federal Institute of Technology, Zürich, Switzerland.

BANWART, S., DAVIES, S. and STUMM, W. (1989) The role of oxalate in accelerating the reductive dissolution of hematite (α-Fe_2O_3) by ascorbate. *Coll. Surf.* **39**, 303-309.

BARKER, W.W. and PARKS, T.C. (1986) The thermodynamic properties of pyrrhotite and pyrite: A re-evaluation. *Geochim. Cosmochim. Acta* **50**, 2185-2194.

BARRETT, J., EWART, D.K., HUGHES, M.N., NOBAR, A.M. and POOLE, R.K. (1990) The oxidation of arsenic in arsenopyrite: The toxicity of As(III) to a moderately thermophilic mixed culture. In Biohydrometallurgy 1989, Salley, J., McCready, R.G.L. and Wichlacz, P.L. (eds) . CANMET, Ottawa, 49-57.

BARRETT, J., EWART, D.K., HUGHES, M.N. and POOLE, R.K. (1993) Chemical and biological pathways in the bacterial oxidation of arsenopyrite. *FEMS Microbiol. Rev.* **11**, 57-62.

BARTON, A.F.M. and WILDE, N.W. (1971) Dissolution rates of polycrystalline samples of gypsum and orthorhomic forms of calcium sulphate by a rotating disc method. *Trans. Faraday Soc.* **67**, 3590-3597.

BAUER, D. and LECLERC, O. (1987) Pulp electrolysis of pyrite in buffered media at pH 4.7 and 9.2. *C. R. Acad. Sci.,* Ser. 2, **305**(16), 1267-70.

BEATTIE, M.J.V. and POLING, G.W. (1987) A study of the surface oxidation of arsenopyrite using cyclic voltammetry. *Int. J. Miner. Process.* **20**, 87-108.

BENNETT, J.W., HARRIES, J.R., PANTELIS, G. and RITCHIE, A.I.M. (1989) Limitations on pyrite oxidation rates in dumps set by air transport mechanisms. Proceedings Internat.Symp. on Biohydrometallurgy. Eds: J. Salley, R.G.L. McCready and P.L. Wichlacz, CANMET report SP89-10, 551-561.

BERNER, R.A. (1964) Iron sulfides formed from aqueous solutions at low temperatures and pressures. *J. Geol.* **72**, 293-306.

BERNER, R.A. (1969) The synthesis of framboidal pyrites. *Econ. Geol.* **64**, 383-384.

BERNER, R.A. (1970) Sedimentary pyrite formations. *Amer. J. Sci.* **268**, 1-23.

BERNER, R.A. (1978) Rate control of mineral dissolution under earth surface conditions. *Amer. J. Sci.* **278**, 1235-1252.

BERNER, R.A. (1981) Kinetics of weathering and diagenesis. In Kinetics of geochemical processes, Lasaga, A.C. and Kirkpatrick, R.J. (eds.), *Min. Soc. Amer. Reviews in Mineralogy* **8**, 111-134.

BERNER, R.A. (1984) Sedimentary pyrite formation: An update. *Geochim. Cosmochim. Acta* **48**, 605-615.

BERNER, R.A. and HOLDREN, G.R. (1977) Mechanisms of feldspar weathering. Some observational evidence. *Geology* **5**, 369-372.

BERNER, R.A. and HOLDREN, G.R. (1979) Mechanisms of feldspar weathering -- II. Observations of feldspars from soils. *Geochim. Cosmochim. Acta* **43**, 1173-1186.

BERNER, R.A. and SCHOTT, J. (1982) Mechanism of pyroxene and amphibole weathering II. Observations of soil grains. *Amer. Jour. Sci.* **282**, 1214- 1231.

BETHKE, C. (1992) The Geochemist's Workbench: A users guide to Rxn, Act2, Tact, React and Gtplot. Copyright to University of Illinois, 174 pages.

BIEGLER, T. (1976) Oxygen reduction on sulfide minerals. Part II. Relation between activity and semiconducting properties of pyrite electrodes. *J. Electroanal. Chem. Interfacial Electrochem.* **70**, 265-275.

BIEGLER, T., RAND, D.A.J. and WOODS, R. (1975) Oxygen reduction on sulfide minerals. I. Kinetics and mechanism at rotated pyrite electrodes. *J. Electroanal. Chem. Interfacial Electrochem.* **60**, 151-162.

BIEGLER, T. and SWIFT, D.A. (1979) Anodic behaviour of pyrite in acid solutions. *Electrochim. Acta* **24**, 415-420.

BIGHAM, J.M. (1994) Mineralogy of ochre deposits formed by sulfide oxidation. In Mineralogical Association of Canada, Jambor, J.L. and Blowes, D.W. (eds). **23**, 103-132.

BLAKEMORE, R.P., SHORT, K.A. and BAZYLINSKI, D.A. (1985) Microareobic conditions are required for magnetite formation within aquaspirillum magnetotacticum. *Geomicrobiol. J.* **4**, 53-71.

BLESA, M.A., BORGHI, E.B., MARTO, A.J. and REGAZZONI, A.E. (1984) Absorption of EDTA and iron-EDTA complexes on magnetite and the mechanism of dissolution of magnetite by EDTA. *J. Colloid Interface Sci.* **98**, 295-300.

BLOWES, D.W. and CHERRY, J.A. (1987) Hydrogeochemical investigation of reactive tailings at the Waite-Amulet tailings site, Noranda, Quebec, Phase 2 - 1986 program. MEND, Project 1.17.1b.

BLOWES, D.W. and JAMBOR, J.L. (1990) The pore-water geochemistry and the mineralogy of the vadose zone of the sulphide tailings, Waite Amulet, Quebec, Canada. *Applied Geochemistry* **5**, 327-346.

BLOWES, D.W., JAMBOR, J.L., APPLEYAR, E.C., REARDON, E.J. and CHERRY, J.A. (1992) Temporal observations of the geochemistry and mineralogy of a sulphide-rich mine tailings impoundment, Heathe Steele Mines, New Brunswick. *Explor. Mining Geol.* **1**, 251-264.

BLOWES, D,W. and PTACEK, C.J. (1994) Acid-neutralization mechanisms in inactive mine tailings. Chap. 10 in Environmental Geochemistry of Sulphide Mine-Wastes, Eds: J.L. Jambor and D.W. Blowes, Short Course Handbook, V.22, Min. Assoc. Canada, 271-292.

BLOWES, D.W., PTACEK, C.J., FRIND, E.O., JOHNSON, R.H., ROBERTSON, W.D. and MOLSEN, J.W. (1994) Acid-neutralization in inactive mine tailings impoundments and their effects on the transport of dissolved metals. Proceedings of the 3rd International Conference on the Abatement of Acidic Drainage. U.S. Dept. Int. Bur. Mines Special Pub. SP 06A-94, V.1, 429-438.

BLUM, A.E and LASAGA, A.C. (1988) Role of surface speciation in the low-temperature dissolution of minerals. *Nature* **331**, 431-433.

BOCKRIS, J.O'M. and REDDY, A.K.N. (1970) Modern Electrochemistry. Vol 2, Plenum Press: New York, pp. 923-925, 991-1017.

BOORMAN, R.S. and WATSON, D.M. (1976) Chemical processes in abandoned tailings dumps and environmental implications for Northeastern New Brunswick. *Can. Inst. Mining Metall. Bull.* **69**, 86-96.

BOYLE, D.R. (1994) Oxidation of massive sulphide deposits in the Bathurst mining camp, New Brunswick: natural analogues for acid drainage in temperate climates. In Environmental Geochemistry of Sulphide Oxidation (eds., C.N. Alpers and D.W. Blowes). Amer. Chem. Soc. Symposium Series, 535-550.

BRADDOCK, J.F., LUONG, H.V. and BROWN, E.J. (1984) Growth kinetics of *Thiobacillus ferrooxidans* isolated from arsenic mine drainage. *Appl. Environ. Microbiol.* **48**, 48-55.

BRANTLY, S.L. (1992) Kinetics of dissolution and precipitation - Experimental and field results. Proceedings of the 7th Int. Symp. on Water-Rock Interaction. Ed: Kharaka, Y. and Maest, A., Balkema, Rotterdam, 3-6.

BRICENO, A. and CHANDER, S. (1988) An electrochemical characterization of pyrites from coal and ore sources. *Int. J. Miner. Process.* **24**, 73-80.

BRION, D. (1980) Étude par spectroscopie de photoelectrons de la degradation superficielle de FeS_2, $CuFeS_2$, ZnS et PbS à l'air et dans l'eau. *Appl. Surf. Sci.* **5**, 133-152.

BROUGHTON, L.M. and ROBERTSON, A. MacG. (1991) Modelling of leachate quality from acid generating waste rock dumps. Proceedings of the Second International Conference on the Abatement of Acidic Drainage, MEND, Sept. 16-18, Montreal, V.3, 341-361.

BROWN, T.H., BERMAN, R.G., PERKINS, E.H. (1989) A GeO-CALC Software package for the calculation and display of activity-temperature-pressure phase diagrams. *Amer. Mineral.* **74**, 485-487.

BRUNO, J., STUMM, W., WERSIN, P. and BRANDBERG, F. (1992) On the influence of carbonate in mineral dissolution : I. The thermodynamics and kinetics of hematite dissolution in bicarbonate solutions at T = 25 °C. *Geochim. Cosmochim. Acta* **56**, 1139-1147.

BRUNO, J., STUMM, W., WERSIN, P. and BRANDBERG, F. (1992) On the influence of carbonate in mineral dissolution II. The solubility of $FeCO_3$(s) at 25°C and 1 atm. total pressure. *Geochim. Cosmochim. Acta*, **56**, 1149-1156.

BRUYERE, V.I.E. and BLESA, M.A. (1985) Acid and reductive dissolution of magnetite in aqueous sulfuric acid: Site-binding model and experimental result. *J. Electroanal. Chem.* **182**, 141-156.

BRUYNESTEYN, A. and DUNCAN, D.W. (1970) Microbiological leaching of sulphide concentrates. *Can. Met. Q* **10**, 57-63.

BRYSON, A.W. and te RIELE, W.A.M. (1986) Factors that effect the kinetics of nucleation and growth and the purity of goethite precipitates produced from sulphate solutions. In *Iron Control Hydrometall.*, [Int. Symp.] (eds. J. E. Dutrizac and A. J. Monhemius), Horwood, 377-390.

BUCKLEY, A.N., HAMILTON, I.C. and WOODS, R. (1988) Studies of the Surface Oxidation of Pyrite and Pyrrhotite using X-ray Photoelectron Spectroscopy and Linear Sweep Voltammetry. *Electrochem. Soc., Proc.* **88-21**, (Proc. Int. Symp. Electrochem. Miner. Met. Process. 2, 1988) 234-246.

BUCKLEY, A.N., HAMILTON, I.C. and WOODS, R. (1985) Investigation of the surface oxidation of sulfide minerals by linear potential sweep voltammetry and x-ray photoelectron spectroscopy. *Dev. Miner. Process.* **6** (Flotation Sulphide Miner.), 41-60.

BUCKLEY, A.N. and WALKER, G.W. (1988) The surface composition of arsenopyrite exposed to oxidizing environments. *Appl. Surf. Sci.* **35**, 227-240.

BUCKLEY, A.N. and WOODS, R. (1984) An x-ray photoelectron spectroscopic investigation of the surface oxidation of sulfide minerals. *Proc. - Electrochem. Soc.* **84-10** (Proc. Int. Symp. Electrochem. Miner. Met. Process., 1984), 286-302.

BUCKLEY, A.N. and WOODS, R. (1985a) X-ray photoelectron spectroscopy of oxidized pyrrhotite surfaces. I. Exposure to air. *Appl. Surf. Sci.* **22/23**(1), 280-287.

BUCKLEY, A.N. and WOODS, R. (1985b) X-ray photoelectron spectroscopy of oxidized pyrrhotite surfaces. II. Exposure to aqueous solutions. *Appl. Surf. Sci.* **20**(1), 472-480.

BUCKLEY, A.N. and WOODS, R. (1987) The surface oxidation of pyrite. *Appl. Surf. Sci.* **27**, 437-452.

BUCKLEY, A.N. and WOODS, R. (1988) An X-ray photoelectron spectroscopic investigation of the surface oxidation of sulphide minerals. *Proc. - Electrochem. Soc.* **88-21**, 286-302.

BUCKLEY, A.N., WOODS, R. and WOUTERLOOD, H.J. (1988) The Deposition of sulfur on pyrite and chalcopyrite from sodium sulfide solutions. *Aust. J. Chem.* **41**, 1003-1011.

BUCKLEY, A.N., WOUTERLOOD, H.J., CARTWRIGHT, P.S. and GILLARD, R.D. (1988) Core electron binding energies of platinum and rhodium polysulfides. *Inorg. Chim. Acta* **143**, 77-80.

BUCKLEY, A.N., WOUTERLOOD, H.J. and WOODS, R. (1989) The interaction of pyrite with solutions containing silver ions. *J. Appl. Electrochem.* **19**, 744-751.

BUSENBERG, E. and CLEMENCY, C.V. (1976) The dissolution kinetics of feldspars at 25°C and 1 atm. CO_2 pressure. *Geochim. Cosmochim. Acta*, **40**, 41-49.

BUSENBERG, E. and PLUMMER, L.N. (1982) The kinetics of dissolution of dolomite in CO_2-H_2O systems at 1.5 to 65°C and 0 to 1 atm. P_{CO2}. *Amer. Jour Sci.* **282**, 45-78.

BUSENBERG, E. and PLUMMER, L.N. (1986) A comparative study of the dissolution and crystal growth kinetics of calcite and aragonite. In Studies in Diagenesis, F.A. Mumpton (ed.), *U.S. Geol. Surv. Bull.* **1578**, 139-168.

CABRERA, F. and TALIBUDEEN, O. (1978) The release of Al from aluminosilicate minerals - I. Kinetics. *Clays and Clay Minerals* **26**, 434-440.

CAROTHERS, W.W. and KHARAKA, Y.K. (1978) Aliphatic acid anions in oil field waters - Implications for origin of natural gas. *Amer. Ass. Petrol. Geol. Bull.* **62**, 2441-2453.

CASEY, W.H., WESTRICH, H.R. and ARNOLD, G.W. (1988) Surface of labradorite feldspar reated with aqueous solutions at pH = 2, 3, and 12. *Geochim. Cosmochim. Acta* **52**, 2795-2807.

CASEY, H.W., WESTRICH, H.R. and HOLDREN, G.R. (1991) Dissolution of plagioclase at pH = 2 and 3. *Amer. Miner.* **76**, 211-217.

CATHLES, L.M. and APPS, J.A. (1975) A model of the dump leaching process that incorporates oxygen balance, heat balance and air convection. *Metal. Trans.* **6B**, 617-624.

CATHLES, L.M. (1979) Predictive capabilities of a finite difference model of copper leaching in low grade industrial sulphide waste dumps. *Math. Geol.* **11**, 175-191.

CATHLES, L.M. (1994) Attempts to model the industrial scale leaching of copper-bearing mine waste. Chap. 10 in Environmental Geochemistry of Sulphide Oxidation. Eds: C.N. Alpers and D.W. Blowes, ACS Symposium Series 550, 122-131.

CECILE, J.L. (1985) Application of XPS in the study of sulphide mineral flotation-a review. *Dev. Min. Process.* **6**, 61-80.

CHANDER S. (1991) Electrochemistry of sulfide flotation: growth characteristics of surface coatings and their properties, with special reference to chalcopyrite and pyrite. *Int. J. Miner. Process.* **33**, 121-134.

CHANDER, S. and BRICENO, A. (1988) The rate of oxidation of pyrites from coal and ore sources - an a.c. impedance study. Inf. Circ. - U. S., Bur. Mines, IC 9183, Mine Drain. Surf. Mine Reclam., Vol. 1, 164-9.

CHANDER, S., PANG, J. and BRICENO, A. (1988) Some equivalent circuit models for a.c. impedance analysis of pyrite/solution interface. *Proc. - Electrochem. Soc.* **88-21** (Proc. Int. Symp. Electrochem. Miner. Met. Process. 2, 1988), 247-263.

CHANG, H., HEALY, T.W. and MATIJEVIĆ, E. (1983) Interactions of metal hydrous oxides with chelating agents III. Adsorption on spherical colloidal hematite particles. *J. Colloid Interface Sci.* **92(2)**, 469-478.

CHANG, H. and MATIJEVIĆ, E. (1983) Interactions of metal hydrous oxides with chelating agents IV. Dissolution of hematite. *J. Colloid Interface Sci.* **92(2)**, 478-488.

CHAPMAN, B.M., JONES, D.R. and JUNG, R.F. (1983) Processes controlling metal ion attenuation in acid mine drainage streams . *Geochim. Cosmochim. Acta* **47**, 1957-1973.

CHAPMAN, J.T., HOCKLEY, D.E., ROBERTSON, A. MACG. and BROUGHTON, L.M. (preprint). Rock Pile Water Quality Modelling - The Q-ROCK Mathematical Model (based upon a presentation at the Environmental Management for Mining Conference, Saskatoon, October 27-29, 1993).

CHEN, G., ZEN, J.M., FAN, F.R.F. and BARD, A.J. (1991) Electrochemical investigation of the energetics of irradiated FeS_2 (pyrite) particles. *J. Phys. Chem.* **95**, 3682-3687.

CHEN, Y., MU, J, CHEN, W., DAVIS, D. and ORTELEVA, P. (1993) Optimizing matrix acidizing for near-borehole remediation using the CIRF reaction transport simulator. SPE Gas Technology Symposium, Calgary, Alberta, SPE 26184, 471-476.

CHOI, W.K. and TORMA, A.E. (1989) Biotechnology in Minerals and Metal Processing, AIME, Littleton, CO, 17-24.

CHOQUETTE, M., GELINAS, P., and ISABEL, D. (1994) Monitoring of Acid Mine Drainage: Chemical data from La Mine Doyon-South Waste Rock Dump, MEND Report 1.14.2, 95p.

Coastech Research Inc. (1989) Investigation of Prediction Techniques for Acid Mine Drainage. Mend Report, project 1.16.1 250p.

COASTECK RESEARCH INC. (1989) Investigation of prediction techniques for acid mine drainage, final report. *Mine Environmental Neutral Drainage (MEND) Program.* Project 1.16.1a, 250p.

COLLINET, M.N. and MORIN, D. (1990) Characterization of arsenopyrite oxidizing *Thiobacillus*. Tolerance to arsenite, arsenate, ferrous and ferric ions. *Antonie van Leeuwenhoek* **57**, 237-244.

CONNOLLY, J.A.D. and KERRICK, D.M. (1987) An algorithm and computer program for calculating composition phase diagrams. CALPHAD, V.11, 1-55.

CORNELL, R.M., POSNER, A.M. and QUIRK, J.P. (1974) Dissolution of synthetic goethites. Early stage. *Soil Sci. Soc. Amer., Proc.* **38**, 377-378.

CORNELL, R.M., POSNER, A.M. and QUIRK, J.P. (1974) Crystal morphology and the dissolution of goethite. *J. Inorg. Nucl. Chem.* **36**, 1937-1946.

CORNELL, R.M., POSNER, A.M. and QUIRK, J.P. (1976) Kinetics and mechanisms of the acid dissolution of goethite (α-FeOOH). *J. Inorg. Nucl. Chem.* **38**, 563-567.

CRAMER J.J. and SMELLIE, J.A.T., (1994) Final Report of the AECL/SKB Cigar Lake Analog Study, Chap. 3.5, AECL Rpt-10851, AECL Research, Pinawa, Canada.

CUPP, C. R. (1985) After *Thiobacillus ferrooxidans* - What? *Can. Met. Q* **24**, 109-113.

DAVELER, S.A. and WOLERY, T.J. (1992) EQPT, A data file preprocessor for the EQ3/6 software package: User's guide and related documentation (Version 7.0) Lawrence Livermore National Laboratory UCRL-MA -110662 PT II, 89p.

DAVIS, G.B., DOHERTY, G. and RITCHIE, A.I.M. (1986) A model of oxidation in pyritic mine wastes: Part 2, Comparison of numerical and approximate solutions. *Appl. Math. Modelling* **10**, 323-329.

DAVIS, G.B. and RITCHIE, A.I.M. (1986) A model of oxidation in pyritic mine wastes: Part 1, Equations and approximate solutions. *Appl. Math. Modelling* **10**, 314-322.

DAVIS, G.B. and RITCHIE, A.I.M. (1986) A model of oxidation in pyritic mine wastes: Part 1 equations and approximate solution. *Appl. Math. Modelling* **10**, 314-322.

DAVIS, G.B. and RITCHIE, A.I.M. (1987) A model of oxidation in pyritic mine wastes: Part 3, Importance of particle size distribution. *Appl. Math. Modelling* **11**, 417-422.

DAVIS, J.A. and KENT, D.B. (1990) Surface complexation modeling in aqueous geochemistry. In Mineral-Water Interface Geochemistry, HOCHELLA, M.F. and WHITE, A.T. (eds.). *Min. Soc. Amer. Reviews in Mineralogy* **23**, 177-260.

DAVISON, W. (1980) A critical comparison of the measured solubilities of ferrous sulphide in natural waters. *Geochim. Cosmochim. Acta* **44**, 803-808.

DAY, S.J. and COWDERY, P.H. (1990) Prediction of oxidizable sulphide content and neutralization potential in acid generation studies at metal mines. In Acid Mine Drainage: Designing for Closure, GAC-MAC Annual Meeting, 141-150.

DAYAL, R. (1977) Kinetics of silica sorption and day dissolution reactions at 1 and 670 atm. *Geochim. Cosmochim. Acta* **41**, 135-141.

de HAAN, S.B. (1991) A review of the rate of pyrite oxidation in aqueous systems at low temperature. *Earth-Science Reviews* **31**, 1-10.

DEER, W.A., HOWIE, R.A. and ZUSSMAN, J. (1966) An Introduction to the Rock-forming Minerals. Longman, Harlow, 528p.

del VALLE HIDALGO, M., KATZ, N. E., MAROTO, A. J. G. and BLESA, M. A. (1988) The dissolution of magnetite by Nitrilotriacetoferrate(II). *J. Chem. Soc. Faraday Trans.* **84**, 9-18.

DELANEY, J.M., PUIGDOMENECH, I. and WOLERY, T.J. (1986) Precipitation kinetics option for the EQ6 geochemical reaction path code . Lawrence Livermore National Laboratory UCRL-53642, 44p.

DELANEY, J.M. and WOLERY, T.J. (1984) Fixed-fugacity option for the EQ6 geochemical reaction path code. Lawrence Livermore National Laboratory UCRL-53598, 20p.

DENG, Y. and STUMM, W (1993) Kinetics of redox cycling of iron coupled with fulvic acid. *Aquatic Sci.* **55**, 103-111.

DENG, Y. and STUMM, W. (1994) Reactivity of aquatic iron (III) oxyhydroxides—implications for redox cycling of iron in natural waters. *Applied Geochemistry* **9**, 23-36.

DENHOLM, E. and HALLAM, R. (1991) A review of acid generation research at the Samatosum Mine. Proceedings of the Second International Conference on the Abatement of Acidic Drainage, MEND, Sept. 16-18, Montreal, V.2, 561-578.

DEROOY, N.M. (1991) Mathematical simulation of biochemical processes in natural waters by the model CHARON. Delft Hydraulics, R1310-10, 144p.

DONAHUE, F.M. (1972) Interactions in mixed potential systems . *J. Electrochem. Soc., Electrochemical Science and Technology* **119**, 72-74.

DOROFEEV, A.G., PIVOVAROVA, T.A. and KARAVAIKO, G.I. (1990) Kinetics of ferrous iron oxidation by *Thiobacillus ferrooxidans*. Effect of arsenopyrite oxidation products and pH of the medium. *Mikrobiologiya* **59**, 205-212.

DOVE, P.M. and RIMSTIDT, J.D. (1985) The solubility and stability of scorodite, $FeAsO_4 \cdot 2H_2O$. *Amer. Mineral.* **70**, 838-844.

DOWNES, K.W. and BRUCE, R.W. (1955) The recovery of elemental sulphur from pyrite and pyrrhotite. *Can. Mining Metall. Bull.* 127-132.

DRASKIC, D., MANOJLOVIC-GIFING, M. and PAVLICA, M.J. (1984) Important surface modifications of pyrite and arsenopyrite in the presence of potassium permanganate in the depression of arsenopyrite. *Ind. Miner. Tech.* 468-474.

DUBROWSKY, N.M., MORIN, K.A., CHERRY, J.A. and SMYTH ,D.J.A. (1984) Uranium tailings acidification and subsurface contaminant in a sand aquifer. *Water. Pollut. Research J.* **19**, 55-89.

DUTRIZAC, J.E. (1989) Elemental sulphur formation during the ferric sulphate leaching of chalcopyrite. *Can. Met. Q.* **28**, 337-344.

DUTRIZAC, J.E. (1992) The leaching of sulphide minerals in chloride media. *Hydrometallurgy* **29**, 1-45.

DUTRIZAC, J.E., MACDONALD, R.J.C. and INGRAHAM T.R. (1970) Effect of pyrite, chalcopyrite and digenite on rate of bornite dissolution in acidic ferric sulphate solutions. *Can. Met. Q.* **10**, 3-7.

DUTRIZAC. J.E. and MACDONALD. R.J.C. (1973) The effect of some impurities on the rate of chalcopyrite dissolution. *Can. Met. Q* **12**, 409-420.

DUTRIZAC, J.E. and MACDONALD, R.J.C. (1974) Ferric ion as a leaching medium. *Minerals Sci. Engng* **6**, 59-100.

DUTRIZAC, J.E. and MACDONALD, R.J.C. (1978) The dissolution of sphalerite in ferric chloride solutions. *Metall. Trans. B* **9B**, 543-551.

EADINGTON, P. (1973) Leaching of illuminated lead sulphide with nitric acid as a function of the solid-state electronic properties. *Trans. Inst. Mining Metall.* **82**, C158-C161.

EHRLICH, H.L. (1964) Bacterial oxidation of arsenopyrite and enargite. *Econ. Geol.* **59**, 1306-1312.

EHRLICH, H.L. (1990) Geomicrobiology, 2nd ed. New York: Marcel Dekker, Inc.

EHRLICH, H.L. and BRIERLEY, C.L. (1990) Microbiol Mineral Recovery. New York: McGraw-Hill Publishing Co.

ENGESGAARD, P. and CHRISTENSEN, T. (1988) A review of chemical solute transport models. *Nordic Hydrol.* **19**, 183-216.

ENNAOUI, A., FIECHTER, S., JAEGERMANN, W. and TRIBUTSCH, H. (1986) Photoelectrochemistry of highly quantum efficient single-crystalline n-FeS2 (Pyrite). *J. Electrochem. Soc.* **133**, 97-106.

EPRI (1984) Geohydrochemical models for solute migration report no EA-3417, Battelle, Pacific Northwest Laboratories, Richland, Washington.

FAUST, B.C. and HOFFMANN, M.R. (1986) Photo-induced reductive dissolution of α-Fe_2O_3 by bisulfite. *Environ. Sci. Technol.* **20**, 943-948.

FAUST, B.C., HOFFMANN, M.R. and BAHNEWANN, D.W. (1989) Photocatalytic oxidation of sulphur dioxide in aqueous suspensions of α-Fe_2O_3. *J. Phys. Chem.* **93**, 6371-6381.

FENG, Q., XU, S. and CHEN, J. (1993) The study of pulp electrochemical flotation separation of pyrite and arsenopyrite. *Publ. Australas. Inst. Min. Metall.* **3**/93(XVIII International Mineral Processing Congress, 1993, Vol. 3), 767.

FERGUSON, K.D. (1986) Static and kinetic methods to predict acid mine drainage. In Fundamental and Applied Biohydrometallurgy, LAWRENCE, R.W., BRANON, R.M.R. and EBNER, H.G. (eds.), New York: Elsevier, 486-488.

FERRON, C.J., KWATENG, D.O. and DUBY, P.F. (1991) Kinetics of the precipitation of goethite from ferrous sulphate solutions using oxygen-sulfur dioxide mixtures. In *EPD Congr. 91, Proc. Symp. TMS Annu. Meet* (ed. D.R.M.M.M. GASKELL), 165-177. Soc.

FLEER, V.N. and JOHNSTON, R.M. 1986. A compilation of solubility and dissolution kinetics data on minerals in granitic and gabbroic systems. Atomic Energy of Canada Limited technical report **TR-328-2**, 170p.

FLEET, M.E. (1978) The pyrrhotite-marcasite phase transformation. *Can. Miner.* **16**, 31-35.

FLEET, M.E., CHRYSSOULIS, S.L., MACLEAN, P.J., DAVIDSON, R. and WEISENER, C.G. (1993) Arsenian pyrite from gold deposits: Au and As distribution investigated by SIMS and EMP, and color staining and surface oxidation by XPS and LIMS. *Can. Mineral.* **31**, 1-17.

FLEMING, G.W. and PLUMMER, L.N. (1983) PHRQINPT—an interactive computer program for constructing input data sets to the geochemical simulation program PHREEQE. U.S. Geological Survey Water-Resources Investigations Report 83-4236, 108p.

FOGLER, H.S., LUND, K. and McCUNE, C.C. (1975) Acidization III—The kinetics of the dissolution of sodium and potassium feldspar in HF/HCl acid mixtures. *Chem. Eng. Sci.* **30**, 1325-1332.

FONTANA, M.G. and GREENE, N.D. (1978) Corrosion Engineering, 2nd ed.. London: McGraw-Hill, 297-346.

FOSTER, M.D. (1950) The origin of high sodium bicarbonate waters in the Atlantic and Gulf Coastal Plains. *Geochim. Cosmochim. Acta* **1**, 33-48.

FRIND, E.O. and MOLSON, J.W. (1994) Modelling of mill-tailings impoundments. Chap. 2 in Environmental Geochemistry of Sulphide Mine-Wastes, Eds: J.L. Jambor and D.W. Blowes, Short Course Handbook V.22, Min. Assoc. Canada, 19-58.

FURRER, G., WESTALL, J.C. and SOLLINS, P. (1989) The study of soil chemistry through quasi-steady-state models: I. Mathematical definition of model. *Geochim. Cosmochim. Acta* **53**, 595-601.

FURRER, G., SOLLINS, P. and WESTALL, J.C. (1990) The study of soil chemistry through quasi-steady-state models: II Acidity of soil solutions. *Geochim. Cosmochim. Acta* **54**, 2363-2374.

GARRELS, R.M. and MACKENZIE, F.T. (1967) Origin of the chemical compositions of some springs and lakes. In Equilibrium Concepts in Natural Water Systems. Advances in Chemistry Series 67, American Chemical Society, Washington. D.C., 222-242.

GARRELS, R.M., THOMPSON, M.E. and SIEVER, R. (1960) Stability of some carbonates at 25°C and 1 atm. *Amer. J. Sci.* **258,** 402-418.

GARRELS, R.M. and THOMPSON, M.E. (1960) Oxidation of pyrite by iron sulphate solutions. *Amer. J. Sci.* **258A,** 57-67.

GARRELS, R.M. and THOMPSON, M.E. (1962) A Chemical Model for Seawater at 25°C and One Atmosphere Total Pressure. *American Journal of Science* **260**, 57-66.

GELINAS, P., CHOQUETTE, M., LEFEBVRE, R., ISABEL, D., LEROUEIL, S., LOCAT, J., BERUBE, M., THERIAULT, D. and MASSON, A. (1991) Evaluation du drainage minier acide et des barrières sèches pour les haldes de stériles: Étude du site de La Mine Doyon. Dépt. de Géologie, Univ. Laval, 147p.

GHILDYAL, B.P. and TRIPATHI, R.P. (1987) Soil Physics. NY: John Wiley & Sons, Inc.

GIBSON, D.K., PANTELIS, G. and RITCHIE, A.I.M. (1994) The relevance of the intrinsic oxidation rate to the evolution of polluted drainage from a pyritic waste rock dump. Proceedings of the 3rd International Conference on the Abatement of Acidic Drainage. U.S. Dept. Int. Bur. Mines Special Pub. SP 06A-94, V.2, 258-264.

GOLDHABER, M.B. (1983) Experimental study of metastable sulfur oxyanion formation during pyrite oxidation at pH 6-9 and 30°C. *Amer. J. Sci.* **283**, 193-217.

GORICHEV, I.G., MALOV, L.V. and DUKHANIN, V.S. (1978) Ratio of constants for the formation and dissolution of magnetite and hematite active centres in sulphuric acid. *Zh. Fiz. Khim.* **52**, 1195-1198.

GOUT, R., SOUBIES, F., BOULEAU, A. and LOURDE, C. (1974) Influence de la granulométrie et de la cristallinite sur la vitesse de dissolution de l'hématite dans l'acide chlorhydrique. *Can. ORSTOM, ser Pedol.* **XII** n°3/4, 289-295.

GRANDSTAFF, D.E. (1977) Some kinetics of bronzite orthopyroxene dissolution. *Geochim. Cosmochim. Acta* **41**, 1097-1103.

GROVE, D.B. and STOLLENWERK, K.G. (1987) Chemical reactions simulated by groundwater quality models. *Water Resour. Bull.* **23**, 601-15.

GUAY, R. (1994) Diversité microbiologique dans la production de drainage minier acide à la halde sud de la mine Doyon. MEND report 1.14.2, 72 pages

GUILINGER, T.R., SCHECHTER, R.S. and LAKE, L.W. (1987) Kinetics study of pyrite oxidation in basic carbonate solutions. *Ind. Eng. Chem. Res.* **26**, 824-830.

GUNTER, W.D., AGGARWAL, P.K. and BIRD, G.W. (1989) Modelling of Smectite Synthesis in Reservoir Sands: Comparison of PATH's Predictions to Autoclave Experiments, In Fourth

UNITAR/UNDP International Conference on Heavy Crude and Tar Sands Proceedings, R.F. Meyer and E.J. Wiggins (eds.), AOSTRA, Edmonton, Canada, Vol. 3, 383-398.

GUO, X. and LIU, C. (1991) Kinetics and mineralogical phase transformation of the nickel-bearing pyrrhotite oxidized with steam at elevated temperature. *Chin. J. Met. Sci. Technol.* **7**, 371-375.

HAINES, A.K. (1989) Two-stage oxidation of pyritic ores. (to General Mining Union Corp. Ltd., S. Afr.) Application: ZA 88-3546, 19 May 1988. Fr. Demande FR 2631635, issued 24 Nov 1989. (also FR Demande 89-6494, 18 May 1989), 9p.

HAMILTON, I.C. and WOODS, R. (1981) An investigation of surface oxidation of pyrite by linear potential sweep voltammetry. *J. Electroanal. Chem.* **118**, 327-343.

HAMILTON, I.C. and WOODS, R. (1984) A voltammetric study of the surface oxidation of sulfide minerals. In Proc. Electrochem. Soc: Electrochemistry in Mineral and Metal Processing (eds. P. E. RICHARDSON, S. SRINIVASAN and R. WOODS), Vol. 84-10, 259-285. The Electrochemical Society.

HARRIES, J.R. and RITCHIE, A.I.M. (1982) Pyrite oxidation in mine wastes: Its incidence, its impact on water quality and its control. In: Prediction in Water Quality: Proceedings of a Symposium on the Prediction in Water Quality. Eds: E.M. O'Loughin and P. Cullen. Australian Academy of Science and the Institute of Engineers, Canberra, Nov.30-Dec 2., 347-377.

HARRIES, J.R. and RITCHIE, A.I.M. (1983a) Runoff fraction and pollution levels in runoff from a waste rock dump undergoing pyritic oxidation. *Water, Air and Soil Pollution* **19**, 155-170.

HARRIES, J.R. and RITCHIE, A.I.M. (1983b) The microenvironment within waste rock dumps undergoing pyritic oxidation. In: Proceedings of an International Symposium on Biohydrometallurgy, Calgary, Canada, May 1-4.

HASKIN, H.K., HART, T.J., MARTIR, W.K. MOSS, R.M., DUDLEY, J. and MOORE, C. (1989) Modelling acid stimulation of the Halfway Formation, Canada using REACTRAN, a geochemical computer model. In Proceedings of the 6th Int. Symp. on Water-Rock Interaction. Ed: D.L. Miles, Balkema, Rotterdam, 289-292.

HEINRICH, C.A. and EADINGTON, P.J. (1986) Thermodynamic predictions of the hydrothermal chemistry of arsenic, and their significance for the paragenetic sequence of some cassiterite-arsenopyrite-base metal sulphide deposits. *Econ. Geol.* **81**, 511-529.

HELGESON, H.C. (1969) Thermodynamics of hydrothermal systems at elevated temperatures and pressures. *Am. J. Sci.* **167**, 729-804.

HELGESON H.C. (1970) Reaction rates in hydrothermal flow systems. *Econ. Geol.* **65**, 299-303.

HELGESON, H.C., BROWN, T.H., NIGRINI, A. and JONES, T.A. (1970) Calculation of mass transfer in geochemical processes involving aqueous solutions. *Geochim. Cosmochim. Acta* **34**, 569-592.

HELGESON, H.C., DELANY, J.M., NESBITT, H.W. and BIRD, D.K. (1978) Summary and critique of the thermodynamic properties of rock-forming minerals. *Amer. Jour. Sci.* **278A**, 1-229.

HELGESON, H.C., GARRELS, R.M. and MACKENZIE, F.T. (1969) Evaluation of irreversible reactions in geochemcial processes involving minerals and aqueous solutions. II. Applications. *Geochim. Cosmochim. Acta* **33**, 455-481.

HEPEL, T., HEPEL, M. and POMIANOWSKI, A. (1988) Effect of galvanic local cells on the oxidative leaching of metal sulphides. *Proc. - Electrochem. Soc.* **88-21**, 432-446.

HERING, J.G. and STUMM, W. (1990) Oxidative and reductive dissolution of minerals. In: Mineral-Water Interface Geochemistry. M.F. Hochella, Jr. and A.F. White (eds.) *Reviews in Mineral.* **23**, 427-465.

HISKEY, J.B., PHULE, P.P. and PRITZKER, M.D. (1987) Studies on the effect of addition of silver ions on the direct oxidation of pyrite. *Metall. Trans., B* **18**, 641-647.

HISKEY, J.B. and PRITZKER, M. D. (1988) Electrochemical behaviour of pyrite in sulfuric acid solutions containing silver ions. *J. Appl. Electrochem.* **18**, 484-490.

HISKEY, J.B. and SANCHEZ, V. (1988) An electrochemical study of the surface oxidation of arsenopyrite in alkaline media. In Arsenic Metall. Fundam. Appl., Proc. Symp (eds. R. G. REDDY, J.L. HENDRIX and P.B.M. QUENEAU), 59-75.

HISKEY, J.B. and WADSWORTH, M.E. (1975) Galvanic corrosion of chalcopyrite. *Met. Trans. B* **6B**, 183-190.

HOCHELLA, Jr,. M.F. (1988) Auger electron and X-ray photoelectron spectroscopes. In Spectroscopic Methods in Mineralogy and Geology, Vol. 18, Chap. 13, 573-637.

HOCHELLA, Jr., M.F., TURNER, A.M. and HARRIS, D.W. (1986) Scanning Auger microscopy as a high resolution technique for geologic materials. *Amer. Miner.* **71**, 1247-1257.

HODGSON, M. and AGAR, G.E. (1984) An electrochemical investigation into the natural floatability of pyrrhotite. *Proc. - Electrochem. Soc.* **84-10** (Proc. Int. Symp. Electrochem. Miner. Met. Process., 1984), 185-201.

HOEY, G.R., DINGLEY, W. and FREEMAN, C. (1975 Corrosion inhibitors reduce ball wear in grinding sulphide ore. *CIM Bull.* **68**, 120.

HOLDREN, G.R. and BERNER, R.A. (1979) Mechanisms of feldspar weathering—I. Experimental studies. *Geochim. Cosmochim. Acta* **43**, 1161-1171.

HOWARTH, R.W. (1979) Pyrite: Its rapid formation in salt marsh and its importance in ecosystem metabolism. *Science* **203**, 49-51.

HUANG, P.M., CROSSON, L.S. and RENNIE, D.A. (1968) Chemical dynamics of potassium release from potassium minerals common in soils. *Trans. Int. Congr. Soil Sci., Adelaide* **2**, 705-712.

HWANG, C.C., STREETER, R.C., YOUNG, R.K. and SHAH, Y.T. (1987) Kinetics of the ozonation of pyrite in aqueous suspension. *Fuel* **66**, 1574-1578.

HYDES, D.J. (1977) Dissolved Al concentration in seawater. *Nature* **268**, 136-137.

ILYALETDINOV, A.N. and ABDRASHITOVA, S.A. (1979) Autotrophic oxidation of arsenic by a culture of *Pseudomonas arsenitoxidans*. *Mikrobiologiya* **50**, 135-140.

INGRAHAM, T.R., PARSONS, H.W. and CABRI, L.J. (1972) Leaching of pyrrhotite with hydrochloride acid. *Can. Met. Q.* **11**, 407-411.

JAEGERMANN, W. and TRIBUTSCH, H. (1983) Photoelectrochemical reactions of FeS_2 (pyrite) with H_2O and reducing agents. *J. Appl. Electrochem.* **13**, 743-750.

JAMBOR, J.L. (1986) Detailed mineralogical examination of alteration products in core WA-20 from Waite Amulet tailings. *CANMET Division Report* ***MSL 86-137 (IR)***. Dept. Energy, Mines and Resources, Canada.

JAMBOR, J.L. (1987) Mineralogical and chemical investigation of cores from piezometric sites in Waite Amulet Tailings, Noranda, Quebec. CANMET Project 30.86.02. 28p.

JAMBOR, J.L. (1994) Mineralogy of sulfide-rich tailings and their oxidation products. Chap. 3 in Environmental Geochemistry of Sulphide Mine-Wastes, Eds: J.L. Jambor and D.W. Blowes, Short Course Handbook, V.22, Min. Assoc. Canada, 59-102.

JAMBOR, J.L., BLOWES, D.W. and OWENS, D.R. (1991) Mineralogy of tailings from Delnite Mines, a former gold producer near Timmins, Ontario. Prepared for CANMET, Department of Energy, Mines and Resources, Canada under MEND(NEDEM) Project No. 30.05.03.

JANETSKI, N.D., WOODBURN, S.I. and WOODS, R. (1977) An electrochemical investigation of pyrite flotation and depression. *J. Min. Proc.* **4**, 227-239.

JAYNES, D.B. (1991) Modelling acid mine drainage from reclaimed coal strip-mines. Proceedings of the 2nd International Conference on the Abatement of Acidic Drainage, Vol 2, 191-210.

JAYNES, D.B., ROGOWSKI, A.S and PIONKE, H.B. (1984) Acid mine drainage from reclaimed coal strip mines. I. Model Description. *Water Resources Research* **20**, 233-242.

JOHNSON, J.W., OELKERS, E.H. and HELGESON, H.C. (1992) SUPCRT92: A software package for calculating the standard molal thermodynamic properties of minerals, gases and aqueous species and reactions from 1 to 5000 bar and 0 to 1000°C. *Computers & Geosciences* **18**, 899-947.

JOHNSON, K.S. and PYTKOWICZ, R.M. (1979) Ion association and activity coefficients in multicomponent solutions. Chapter 1 in Activity Coefficients in Electrolyte Solutions, Vol. II, Ed. R.M. Pytkowicz, CRC Press, Inc., 1-62.

JONES, C.F., LECOUNT, S., SMART, R.S.C. and WHITE, T.J. (1992) Compositional and structural alteration of pyrrhotite surfaces in solution: XPS and XRD studies. *Appl. Surf. Sci.* **55**, 65-85.

KAGAWA, M., SHEEMAN, M.E. and NANCOLLAS, G.H. (1981) The crystal growth of gypsum in an an ammonical environment. *J. of Inorg. Nucl. Chem.* **43**, 917-920.

KAMNEV, A.A. and EZHOV, B.B. (1988) Kinetics of dissolution and crystallization of goethite (α-FeOOH) in alkali solutions. *Zh. Prikl. Khim. (Leningrad)* **61**, 1464-1468. (for translation see *J. Appl. Chem. USSR*).

KAMNEV, A.A., EZHOV, B.B., MALANDIN, O.G. and VASEV, A.V. (1986) Study of dissolution of goethite (α-FeOOH) in alkaline solutions. *Zh. Prikl. Khim. (Leningrad)* **59**, 1689-1693. (for translation see *J. Appl. Chem. USSR*).

KARTHE, S., SZARGAN, R. and SUONINEN, E. (1993) Oxidation of pyrite surfaces: a photoelectron spectroscopic study. *Appl. Surf. Sci.* **72**, 157-170.

KELLER, L. (1982) Acid-bacterial and ferric sulphate leaching of pyrite single crystals. *Biotechnol. and Bioeng.* **XXIV**, 83-96.

KELLER, L. and MURR, L.E. (1980) Lixiviant alteration by fungal absorption of iron during acid bacterial leaching of pure pyrite. *Metall. Trans. B* **11B**, 165-166.

KELLER, L. and MURR, L.E. (1982) Acid-bacterial and ferric sulphate leaching of pyrite single crystals. *Biotechnol. Bioeng.* **24**, 83-86.

KHARAKA, Y.K., GUNTER,W.D., AGGARWAL, P.K., HULL, R.W. and PERKINS, E.H. (1988) SOLMINEQ.88: A Computer Program Code for Geochemical Modelling of Water-Rock Interactions, U.S. Geological Survey Water Resources Investigations Report 88-4227, Menlo Park, California, 420p.

KING, Jr., W.E. (1976) Pyrite oxidation in aqueous ferric chloride: rate studies and reactor design. Thesis, Univ. Pennsylvania; Philadelphia, Pa., USA. (Avail. Xerox Univ. Microfilms, Ann Arbor, Mich., Order No. 76-22,716 From: Diss. Abstr. Int. B 1976, **37**(4), 1795).

KING, Jr., W.E. and LEWIS, J.A. (1980) Simultaneous effects of oxygen and ferric iron on pyrite oxidation in an aqueous slurry. *Ind. Eng. Chem. Process Des. Dev.* **19**, 719-722.

KING, Jr., W.E. and PERLMUTTER, D.D. (1977) Pyrite oxidation in aqueous ferric chloride. *AIChE J.* **23**, 679-685.

KINKAID, C.T., MORREY, J.R., ROGERS, J.E. (1984) Geohydrochemical Models for Solute Migration Volume I: Process Description and Computer Code Selection. EPRI EA-3417 Project 1619, 260p.

KINKAID, C.T., MORREY, J.R. (1984) Geohydrochemical Models for Solute Migration Volume II: Preliminary Evaluation of Selected Computer Codes. EPRI EA-3417 Project 2485-2, 1619-1, 335p.

KITTEL, C. (1956) Introduction to Solid State Physics. New York: John Wiley & Sons, Inc.

KLEIN, J.D. and SHUEY, R.T. (1978) Nonlinear impedance of mineral-electrolyte interfaces: Part I. Pyrite. *Geophysics* **43**, 1222-1234.

KORNICKER, W.A. and MORSE, J.W. (1991) Interactions of divalent cations with the surface of pyrite. *Geochim. Cosmochim. Acta* **55**, 2159-2171.

KOSLIDES, T. and CIMINELLI, V.S.T. (1991) Kinetics of oxidation of arsenopyrite and pyrite under pressure in a sodium hydroxide solution and characterization of solid reaction products. Congr. Anu. - Assoc. Bras. Met. 46th (Vol. 2), 463-483.

KOSLIDES, T. and CIMINELLI, V.S.T. (1992) Pressure oxidation of arsenopyrite and pyrite in alkaline solutions. *Hydrometallurgy* **30**, 87-106.

KOSTINA, G.M. and CHERNYAK, A.S. (1977) Coulometric study of the oxidation of arsenopyrite and pyrite in sodium hydroxide solutions. *Zh. Prikl. Khim. (Leningrad)* **50**, 2701-2705. (for English translation see *J. Appl. Chem. USSR* **50**(12), 2571.)

KOSTINA, G.M. and CHERNYAK, A.S. (1979) Study of the kinetics of the electrochemical oxidation of arsenopyrite and pyrite in sodium hydroxide solutions. *Zh. Prikl. Khim. (Leningrad)* **52**, 766-772. (for English translation see *J. Appl. Chem. USSR*)

KOSTINA, G.M. and CHERNYAK, A.S. (1979) Study of the mechanism of electrochemical oxidation of arsenopyrite and pyrite in caustic soda solutions. *Zh. Prikl. Khim. (Leningrad)* **52**, 1532-1535. (for English translation see *J. Appl. Chem. USSR* **57**, 1475.)

KURBATOV, G., DARQUE-CERETTI, E. and AUCOUTURIER, M. (1992) Characterization of hydroxylated oxide films on iron surfaces and its acid-base properties using XPS. *SIA, Surf. Interface Anal.* **18**, 811-820.

KWONG, Y.T.J. (1993) Prediction and prevention of acid rock drainage from a geological and mineralogical perspective. MEND Report 1.32.1, 47p.

LAI, R.W., DEIHL, J.R., HAMMACK, R.W. and KHAN, S.U.M. (1990) Comparative study of the surface properties and the reactivity of coal pyrite and mineral pyrite. *Minerals and Metallurgical Processing* (February), 43-48.

LALVANI, S.B. and SHAMI, M. (1987) Passivation of pyrite oxidation with metal cations. *J. Mater. Sci.* **22**, 3503-3507.

LALVANI, S.B. and SHAMI, M. (1988) Indirect electrooxidation of pyrite slurries: reaction rate studies. *Chem. Eng. Commun.* **70**, 215-25.

LALVANI, S.B., DENEVE, B.A. and WESTON, A. (1991) Prevention of Pyrite dissolution in Acidic Media. *Corrosion* **47**, 55-61.

LALVANI, S.B., WESTON, A. and MASDEN, J.T. (1990) Characterization of semiconducting properties of naturally occurring polycrystalline iron disulfide (pyrite). *J. Mater. Sci* . **25**, 107-112.

LAMBERT, Jr., J.M., SIMKOVICH, G. and WALKER, Jr., P.L. (1980) Production of pyrrhotites by pyrite reduction. *Fuel* **59**, 687-690.

LANGMUIR, D.E. (1971) Particle size effet on the reaction goethite-hematite + water. *Amer. J. Sci.* **271**, 147-156.

LASAGA, A.C. 1981. Rate laws of chemical reactions. Chapter 1. In A.C. Lasaga and R.J. Kirkpatrick (eds): Kinetics Of Geochemical Processes. Mineralogical Society of America's Reviews in Mineralogy v. 8, pp. 1-68.

LASAGA, A.C. 1984. Chemical kinetics of water-rock interaction. *J. Geophys. Research* **89**, 4009-4025.

LASAGA, A.C., SOLER, J.M., GANOR, J., BURCH, T.E. and NAGY, K.L. (1994) Chemical weathering rate laws and global geochemical cycles. *Geochem. Cosmochim.* **58**, 2361-2386.

LAXEN, D.P.H. and CHANDLER, I.M. (1982) Comparison of filtration techniques for size distribution in fresh water. *Analyt. Chem* **54**, 1350-1355.

LECLERC, O. and BAUER, D. (1990) Electrochemical study of the pyrite in aqueous medium at pH 4.7 and pH 9.2. *Analysis* **18**, 272-278.

LEES, H., KWOK, S.C. and SUZUKI, I. (1969) The thermodynamics of iron oxidation by the *ferrobacilli. Can J. Microbiol.* **15**, 43-46.

LEI, K.P.V. and CARNAHAN, T.G. (1984) Leaching sulfide minerals by oxidative electrolysis in membrane cells. *Proc. - Electrochem. Soc.* **84-10** (Proc. Int. Symp. Electrochem. Miner. Met. Process., 1984), 374-390.

LENNIE, A.R. and VAUGHAN, D.J. (1992) Kinetics of the marcasite-pyrite transformation: an infrared spectroscopic study. *Am. Mineral.* **77**, 1166-1171.

LERMAN, A., MACKENZIE, F.T. and BRICKER, O.P. (1975) Rates of dissolution of aluminosilicates in seawater. *Earth Planet. Sci. Letters* **25**, 82-88.

LI, J., ZHONG, T.K. and WADSWORTH, M.E. (1992) Application of Mixed Potential Theory in Metallurgy. *Hydrometallurgy.* **29**, 47-60.

LI, J., ZHU, X. and WADSWORTH, M.E. (1993) Raman spectroscopy of natural and oxidized metal sulfides. In: EPD Congr. 1993, Proc. Symp. TMS Annu. Meet. (Ed: Hager, John P. Miner. Met. Mater.) Soc., Warrendale, Pa., 229-244.

LICHTNER, P.C. (1985) Continuum model for simultaneous chemical reactions and mass transport in hydrothermal systems. *Geochim. Cosmochim. Acta* **49**, 779-800.

LICHTNER, P.C. (1994) Time-space continuum formulation of supergene enrichment and weathering of sulphide-bearing ore deposits. Chap. 12 in Environmental Geochemistry of Sulphide Oxidation. Eds: C.N. Alpers and D.W. Blowes, ACS Symposium Series 550, 1153-170.

LICHTNER, P.C. and BIINO, G.G. (1992) A first principles approach to supergene enrichment of a porphyry copper protore: I. Cu-Fe-S subsystem. *Geochim. Cosmochim. Acta* **56**, 3987-4013.

LIDDELL, K.C. and BAUTISTA, R.G. (1981) A partial equilibrium chemical model for the dump leaching of chalcopyrite. *Metall. Trans. B* **12B**, 627-637.

LIN, F.C. (1981) Dissolution kinetics of some phyllosilicate minerals. Ph.D. dissertation, SUNY-Buffalo, p. 142.

LIN, F.C. and CLEMENCY, C.V. (1981a) The dissolution kinetics of brucite, antigorite, talc and phlogopite at room temperature and pressure. *Amer. Mineral.* **66**, 801-806.

LIN, F.C. and CLEMENCY, C.V. (1981b) The kinetics of dissolution of muscovites at 25°C and 1 atm. CO_2 partial pressure. *Geochim. Cosmochim. Acta* **45**, 571-576.

LIU, C., PETTENKOFER, C. and TRIBUTSCH, H. (1988) Enhancement of photoactivity in pyrite (FeS_2) interfaces by photoelectrochemical processes. *Surf. Sci.* **204**, 537-554.

LIVESY-GOLDBLATT, E., NORMAN, P. and LIVESY-GOLDBLATT, D.R. (1983) Gold recovery from arsenopyrite/pyrite ore by bacteria leaching and cyanidation. In ROSSI G. and TORMA, A.E. (eds) Recent Progress In Biohydrometallurgy. Associazione Mineraria Sarda, Inglesias, 627-641.

LIZAMA, H.M. and ISAMU, I. (1989) Rate equations and kinetic parameters of the reactions involved in pyrite oxidation by *Thiobacillus ferrooxidans*. *Appl. Environ. Microbiol.* **55**, 2918-2923.

LORBACH, S.C., SHIVELY, J.M. and BUONFIGLIO, V. (1993) Kinetics of sulphur oxidation by *Thiobacillus ferrooxidans*. *Geomicrobiol. J.* **10**, 219-226.

LOWSON, R.T. (1982) Aqueous oxidation of pyrite by molecular oxygen. *Chem. Rev.* **82**, 461-497.

LU, Z. and MUIR, D.M. (1987) Dissolution of metal ferrites and iron oxides by hydrochloric acid under oxidizing and reducing conditions. *Symp. Ser. - Australas. Inst. Min. Metall.* **51**(Res. Dev. Extr. Metall.), 121-127.

LUCE, R.W., BARTLETT, R.W. and PARKS, G.A. (1972) Dissolution kinetics of magnesium silicates. *Geochim. Cosmochim. Acta* **36**, 35-50.

LUTHER, III, G.W. (1987) Pyrite oxidation and reduction: Molecular orbital theory considerations. *Geochim. Cosmochim. Acta* **51**(12), 3193-3199.

LUTHER, III, G.W., GIBLIN, A., HOWARTH, R. and RYANS, R. (1982) Pyrite and oxidized iron mineral phases formed from pyrite oxidation in salt marsh and estuarine sediments. *Geochim. Cosmochim. Acta* **46**, 2665-2669.

MAJIMA, H. (1969) How oxidation affects selective flotation of complex sulphide ore. *Can. Met. Q.* **8**, 269-273.

MAJIMA, H. (1988) Electrochemistry of the oxidative leaching of chalcopyrite. *Electrochem. Soc., Proc.* **88-21**, 303-324.

MAJIMA, H., AWAKURA, Y., HIRATO, T. and TANAKA, T. (1985) The leaching of chalcopyrite in ferric chloride and ferric sulphate solutions. *Can. Met. Q* **24**, 283-291.

MAJIMA, H., AWAKURA, Y. and KAWASAKI, Y. (1988) Analysis of dissolution rate of metal oxide in acidic chloride solution in terms of water activity. *Metall. Trans. B* **19B**, 505-507.

MAJIMA, H., AWAKURA, Y. and MISHIMA, T. (1985) The leaching of hematite in acid solutions. *Metall. Trans. B* **16B**, 23-30.

MANDL, M., MATULOVÁ, P. and DOČEKALOVÁ, H. (1992) Migration of arsenic(III) during bacterial oxidation of arsenopyrite in chalcopyrite concentrate by *Thiobacillus ferrooxidans*. *Appl. Microbiol. Biotechnol.* **38**, 429-431.

MANGOLD, D.C. and TSANG, C-F. (1991) A summary of subsurface hydrological and hydrochemical models. *Reviews of Geophysics* **29**, 51-79.

MATHEWS, C.T. and ROBINS, R.G. (1972) Oxidation of iron disulfide by ferric sulfat *Aust. Chem. Eng.* **13**, 21-25.

MCCREADY, R.G.L. and SANMUGASUNDERAM, V. (1985) The Noranda contract reports on the pre-feasibility study of in-place bacterial leaching: A Summation, Vol. 85-5E, Canadian Government Publishing Centre, 35p.

MCINTYRE, N.S. (1985) Surface analysis of geologic materials - A look at two complementary techniques. *Canadian Chemical News* **37**(5,May), 13-16.

MCKIBBEN, M.A. and BARNES, H.L. (1986) Oxidation of pyrite in low temperature acidic solutions: rate laws and surface textures. *Geochim. Cosmochim. Acta* **50**, 1509-1520.

MEHTA, A.P. and MURR, L.E. (1983) Fundamental studies of the contribution of galvanic interaction to acid-bacterial leaching of mixed metal sulphides. *Hydrometallur* **9**, 235-256.

MEND (1992) Proceedings, International workshop on waste rock modelling hosted by the Canadian MEND Program, edited by M.C. Blanchette.

MERNAGH, T.P. and TRUDU, A.G. (1993) A laser Raman microprobe study of some geologically important sulphide minerals. *Chem. Geol.* **103**, 113-127.

MEUNIER, A. and VELDE, B. (1976) Mineral reactions at grain contacts in early stages of granite weathering. *Clay Minerals* **11**, 235-240.

MEYER, R.E. (1979) Electrochemistry of FeS_2. *J. Electroanal. Chem.* **101**, 59-71.

MICHELL, D. and WOODS, R. (1978) Analysis of oxidized layers on pyrite surfaces by x-ray emission spectroscopy and cyclic voltammetry. *Aust. J. Chem.* **31**, 27-34.

MILLER, D.M. and HANSFORD, G.S. (1992) Batch biooxidation of a gold-bearing pyrite-arsenopyrite concentrate. *Miner. Eng.* **5**, 613-629.

MILLER, J. and PORTILLO, H.Q. (1981) Silver catalysis in ferric sulphate leaching of chalcopyrite. In Developments in Mineral Processing, Part A ed., Vol. 2. Elsevier Scientific Publishing Company.

MILLER, K.W. and RISATTI, J.B. (1988) Microbiol oxidation of pyrrhotites in coal chars. *Fuel* **67**, 1150-1154.

MISHRA, K.K. (1988) Dissolution and semiconductor electrochemistry of pyrite. Thesis, Pennsylvania State Univ., University Park, PA, USA. (Avail. Univ. Microfilms Int., Order No. DA8818031 From: Diss. Abstr. Int. B 1989, 49(7).

MISHRA, K.K. and OSSEO-ASARE, K. (1988a) Aspects of the interfacial electrochemistry of semiconductor pyrite (FeS_2). *J. Electrochem. Soc.* **135**, 2502-2509.

MISHRA, K.K. and OSSEO-ASARE, K. (1988b) Electrodeposition of H^+ on Oxide Layers at Pyrite (FeS_2) Surfaces. *J. Electrochem. Soc.* **135**, 1898-1901.

MISHRA, K.K. and OSSEO-ASARE, K. (1992) Electroreduction of Fe^{3+}, O_2, and $Fe(CN)_6^{3-}$ at the n-pyrite (FeS_2) surface. *J. Electrochem. Soc.* **139**, 3116-3120.

MIZOGUCHI, T. and HABASHI, F. (1983) Aqueous oxidation of zinc sulphide, pyrite and their mixtures in hydrochloric acid. *Trans. Institute of Mining and Metallurg* **92**, 14-19.

MORIN, K.A. (1987) Validity of redox measurements in hydrogeologic studies Proceedings of the Third Canadian Hydrogeological Conference. April 20-23, Saskatoon, 14-24.

MORIN, K.A. (1990a) A case study of data quality in routine chemical analyses of acid mine drainage. In Acid Mine Drainage: Design for Closure, Eds: J.W. Gadsby, J.A. Malick and S.J. Day, Geol. Assoc. Can./Min. Assoc. Can. Joint Annual Meeting, May 16-18, Vancouver, 415-425.

MORIN, K.A. (1990b) Problems and proposed solutions in predicting acid mine drainage with acid base accounting. In Acid Mine Drainage: Design for Closure. Eds: J.W. Gadsby, J.A. Malick and S.J. Day, Geol. Assoc. Can./Min. Assoc. Can. Joint Annual Meeting, May 16-18, Vancouver, 93-193.

MORIN, K.A. and CHERRY, J.A. (1988) Migration of acidic groundwater seepage from uranium-tailings impoundments, 3. Simulation of the conceptual model with application to seepage area. *A. Jour. Contam. Hydrology* **2**, 323-342.

MORIN, K.A., CHERRY, J.A., DAVE, N.K., LIM, T.P. and VIVYURKA, A.J. (1988) Migration of acidic groundwater seepage from uranium-tailings impoundments, 1. Field study and conceptual hydrogeochemical model. *Jour. Contam. Hydrology* **2**, 271-303.

MORIN, D., GAUNAND, A. and RENON, H. (1985) Representation of kinetics of leaching of galena by ferric chloride in concentrated sodium chloride solutions by a modified mixed kinetics model. *Metall. Trans. B* **16B**, 31-39.

MORIN, K.A., GERENCHER, E., JONES, C.E. and KONASEWICH, D.E. (1991) Critical literature review of acid drainage from waste rock. Prepared for CANMET, Department of Energy, Mines and Resources Canada under MEND(NEDEM) Project No. 1.11.1, 175p.

MORIN, K.A. and HUTT, N.M. (1994a) An empirical technique for predicting the chemistry of water seeping from mine-rock piles. Proceedings of the 3rd International Conference on the Abatement of Acidic Drainage. U.S. Dept. Int. Bur. Mines Special Pub. SP 06A-94, v.1, 12-19.

MORIN, K.A. and HUTT, N.M. (1994b) Observed preferential depletion of neutralization potential over sulphide minerals in kinetic tests: Site specific criteria for safe NP/AP ratios. Proceedings of the 3rd International Conference on the Abatement of Acidic Drainage. U.S. Dept. Int. Bur. Mines Special Pub. SP 06A-94, v.1, 148-156.

MORREY, J.R., KINCAID, C.T. and HOSTETLER, C.J. (1986) Geohydrochemical Models for Solute Migration Volume III: Evaluation of Selected Computer Codes. EPRI EA-3417 Project 2485-2, 270p.

MORSE, J.W. (1994) Release of toxic metals via oxidation of authigenic pyrite in resuspended sediments. Chap 20 in Environmental Geochemistry of Sulphide Oxidation. Eds: C.N. Alpers and D.W. Blowes, ACS Symposium Series 550, 289-297.

MORSE, J.W., MILLERO, F.J. CORNWELL, J.C. and RICKARD, D. (1987) The chemistry of the hydrogen sulfide and iron sulfide systems in natural waters. *Earth-Science Reviews* **24**, 1-24.

MOSES, C.O. and HERMAN, J.S. (1991) Pyrite oxidation at circumneutral pH. *Geochim. Cosmochim. Acta* **55**(2), 471-482.

MOSES, C.O., NORDSTROM, D.K., HERMAN, J.S. and MILLS, A.L. (1987) Aqueous pyrite oxidation by dissolved oxygen and by ferric iron. *Geochim. Cosmochim. Acta* **51**, 1561-1571.

MUIR, I.J., BANCROFT, G.M. and NESBITT, H.W. (1988) Characteristics of altered labradorite surfaces by SIMS and XPS. *Geochim. Cosmochim. Acta* **53**, 1235-1241.

MUIR, I.J., BANCROFT, G.M., SHOTYK, W. and NESBITT, H.W. (1990) A SIMS and XPS study of dissolving plagioclase. *Geochim. Cosmochim. Acta* **54**, 2247-2256.

MUIR, I.J. and NESBITT, H.W. (1991) Effects of aqueous cations on the dissolution of labradorite feldspars. *Geochim. Cosmochim. Acta* **53**, 1235-1241.

MUIR, I.J. and NESBITT, H.W. (1992) Controls on differential leaching of calcuim and aluminum from labradorite in dilute electrolyte solutions. *Geochim. Cosmochim. Acta* **56**, 3979-3985.

MUNOZ, P.B., MILLER, J.D. and WADSWORTH, M.E. (1979) Reaction mechanism for the acid ferric sulphate leaching of chalcopyrite. *Metall. Trans. B* **10B**, 149-158.

MUROWCHICK, J.B. and BARNES, H.L. (1986) Marcasite precipitation from hydrothermal solutions. *Geochim. Cosmochim. Acta* **50**, 2615-2629.

MURPHY, W.M. and HELGESON, H.C. (1987) Thermodynamic and kinetic constraints on reaction rates among minerals and aqueous solutions, III. Activated complexes and the pH-dependence of the rates of feldspar, pyroxene, wollastinite and olivine dissolution. *Geochim. Cosmochim. Acta* **51**, 3137-3153.

MUSTIN, C., BERTHELIN, J., MARION, P., DE DONATO, P. (1992) Corrosion and electrochemical oxidation of a pyrite by *Thiobacillus ferrooxidans*. *Appl. Environ. Microbiol.* **58**(4), 1175-1182.

MYCROFT, J.R., BANCROFT, G.M., MCINTYRE, N.S., LORIMER, J.W., HILL, I.R. (1990) Detection of sulphur and polysulphide on electrochemically oxidized pyrite surfaces by X-ray photoelectron spectroscopy and Raman spectroscopy. *J. Electroanal. Chem.* **292**, 139-152.

NAKAZAWA, H. and IWASAKI, I. (1985) Effect of pyrite-pyrrhotite contact on their floatabilities. *Miner. Metall. Process.* **2**(4), 206-211.

NAKAZAWA, H. and IWASAKI, I. (1986) Galvanic contact between nickel arsenide and pyrrhotite and its effect on flotation. *International Journal of Mineral Processing* **18**, 203-215.

NATARAJAN, K.A. (1988) Electrochemical aspects of bioleaching multisulfide minerals. *Miner. Metall. Process.* **5**, 61-65.

NATARAJAN, K.A. (1992) Electrobleaching of base metal sulphides. *Metall. Trans. B* **23B**, 5-11.

NATARAJAN, K.A. and IWASAKI, I. (1972) Eh-pH response of noble metal and sulphide mineral electrodes. *Trans. SME/AIME* **252**, 437.

NATARAJAN, K.A. and IWASAKI, I. (1973) Practical implications of Eh measurements in sulfide flotation circuits. *Trans. AIME* **254**, 323.

NATARAJAN, K.A. and IWASAK,I I. (1974) Eh measurements in hydrometallurgical systems. *Miner. Sci. Eng.* **6**, 35.

NATARAJAN, K.A. and IWASAKI, I. (1984) Electrochemical aspects of grinding media-mineral interactions in magnetite ore grinding. *Int. J. Miner. Process.* **13**, 53-71.

NATARAJAN, K.A., RIEMER, S.C. and IWASAKI, I. (1984) Influence of pyrrhotite on the corrosive wear of grinding balls in magnetite ore grinding. *J. Int. Miner. Process.* **13**, 73-81.

NESBITT, H.W. (1977) Estimation of the thermodynamic properties of Na- Ca- and Mg-beidellites. *Can. Mineral.* **15**, 22-30.

NESBITT, H.W. and CRAMER, J.J. (1993 Genesis and evolution of HCO_3-rich and SO_4-rich groundwaters of Quaternary sediments, Pinawa, Canada. *Geochim. Cosmochim. Acta* **57**, 4933-4946.

NESBITT, H.W., KETTLEWELL, D. and CRAMER, J.J. (1992) SPECIATE: A spreadsheet-based speciation program for aqueous radionuclides. Proceedings of the 7th Int. Symp. on Water-Rock Interaction. Ed: Kharaka, Y. and Maest, A., Balkema, Rotterdam, 237-238.

NESBITT, H.W., MACRAE, N.D. and SHOTYK, W. (1991) Congruent and incongruent dissolution of labradorite in dilute, acidic, salt solutions. *J. Geol* . **99**, 429-442.

NESBITT, H.W. and MUIR, I.J. (1994) X-ray photoelectron spectroscopic study of a pristine pyrite surface reacted with water vapour and air. *Geochim. Cosmochim. Acta* (in press).

NESBITT, H.W., MUIR, I.J. and PRATT, A.R. (1994) Elemental oxidation states and compositions of Arsenopyrite surfaces oxidized in air and air-saturated water. Prepared for CANMET, Department of Energy, Mines and Resources Canada under MEND(NEDEM) (Submitted Aug, 1993).

NESBITT, H.W. and PRATT, A.R (1994) Applications of Auger electron spectroscopy to geochemistry with emphasis on compostional depth profiles. *Can. Min.* Accepted Oct. 1993.

NICHOLSON, R.V. (1992) A Review of Models to Predict Acid Generation Rates in Sulphide Waste Rocks at Mine Sites. In: Proceedings, International Workshop on Waste Rock Modelling, Ed. M.C. Blanchette, MEND, Sept. 29-Oct. 1, Toronto, 12p.

NICHOLSON, R.V. (1994) Iron-sulphide oxidation mechanisms: Laboratory studies. Chap. 6 in Environmental Geochemistry of Sulphide Mine-Wastes, Eds: J.L. Jambor and D.W. Blowes, Short Course Handbook, V.22, Min. Assoc. Canada, 163-183.

NICHOLSON, R.V., GILLHAM R.W. and REARDON, E.J. (1988) Pyrite oxidation in carbonate-buffered solution: 1. Experimental kinetics. *Geochim. Cosmochim. Acta* **52**, 1077-1085.

NICHOLSON, R.V., GILLHAM, R.W. and REARDON, E.J. (1990) Pyrite oxidation in carbonate-buffered solutions: 2. Rate control by oxide coatings. *Geochim. Cosmochim. Acta* **54**, 395-402.

NICKEL, E.H., ALLCHURCH, P.D., MASON, M.G. and WILMSHURST, J.R. (1977) Supergene Alteration at the Perserverance Nickel Deposit, Agnew, Western Australia. *Econ. Geology* **72**, 184-203.

NICOL, M.J. (1988) An electrochemical study of the interaction of copper(II) ions with sulphide minerals. *Proc. - Electrochem. Soc.* **88-21**, 152-167.

NIEDERKORN, J.S. (1985) Kinetic study on catalytic leaching of sphalerite *J. Metals* 53-56.

NISHIMURA, T. and TOZAWA, K. (1988) Kinetics of oxidation of arsenic (III) by aqueous ozone. *Metall. Rev. MMIJ* **5**, 24-37.

NORDSTROM, D.K. (1982) Aqueous pyrite oxidation and the consequent formation of secondary iron minerals. Chap. 3 in Acid Sulphate Weathering. SSSA Special Publication #10, Madison, Wisconsin, 37-60.

NORDSTROM, D.K. (1990) Revised chemical equilibrium data for major water-mineral reactions and their limitations. In Chemical Modelling of Aqueous Systems II. D.C. Melchior and R.L. Bassett (eds.). *Amer. Chem. Soc.* Symposium Series 416, 398-413.

NORDSTROM, D.K. (1995) Fundamentals of aqueous geochemistry and trace element mobility. In Environmental Geochemistry of Mineral Deposits, Eds: G.S. Plumlee and M.H. Logsdon, *Reviews in Economic Geology*, V.6, Society of Economic Geologists (in review)

NORDSTROM, D.K., JENNE, E.A. and BALL, J.W. (1979a) Redox equilibria of iron in acid mine waters. Chap. 3 in Chemical Modelling in Aqueous Systems. ACS Symposium Series 93, Ed. E.A. Jenne, American Chemical Society, Washington, D.C., 50-79.

NORDSTROM, D.K., PLUMMER, L.N., LANGMUIR, D., BUSENBURG, E., MAY, H.M., JONES, B.F. and PARKHURST, D.L. (1990) Revised chemical data for major water-mineral reactions and their limitations. In Chemical Modelling of Aqueous Systems II, ACS Symposium Series 416, Eds: D.C. Melchior and R.L. Bassett, American Chemical Society, Washington, DC, 117-127.

NORDSTROM, D.K., PLUMMER, L.N., WIGLEY, T.M.L., WOLERY, T.J., BALL, J.W., JENNE, E.A., BASSETT, R.L., CRERAR, D.A., FLORENCE, T.M., FRITZ, B., HOFFMAN, M., HOLDREN, Jr., G.R., LAFON, G.M., MATTIGOLD, S.V., McDUFF, R.E., MOREL, F., REDDY, M.M., SPOSITO, G. and THRAILKILL, J. (1979b) A comparison of computerized chemical systems for equilibrium calculations in aqueous systems. Chapter 38 in Chemical Modelling in Aqueous Systems. ACS Symposium Series 93, Ed. E.A. Jenne, American Chemical Society, Washington, D.C., 857-892.

NORDSTROM, D.K., VALENTINE, S.D., BALL, J.W., PLUMMER, L.N. and JONES, B.F. (1984) Partial compilation and revision of basic data in the WATEQ programs. U.S. Geological Survey Water-Resources Investigation Report 84-4186, 39p.

NORECOL ENVIRONMENTAL CONSULTANTS (1988) Cinola Gold Project, Stage II report, Volume V: Environmental research and special studies. Report for City Resources Ltd.

NOVAK, C.F. (1993a) Modelling mineral dissolution and precipitation in dual-porosity fracture-matrix systems. *Jour. Contaminant Hydrology* **13**, 91-115.

NOVAK, C.F. (1993b) Development of the FMT chemical transport simulator: Advective transport sensitivity to aqueous density and mineral volume fraction coupled to phase compositions. Sandia National Lab., Preprint, SAND93-0429C, 22p.

NOWOK, J. and STENBERG, V.I. (1988) Iron(III) ESR-signal splitting in unoxidized and oxidized semimagnetic pyrrhotite, (Fe_7S_8). *Solid State Commun.* **66**, 835-840.

NUNEZ ,C., ESPIELL, F. and GARCIA-ZAYAS, J. (1988) Kinetics of nonoxidative leaching of galena in perchloric, hydrobromic; and hydrochloric acid solutions. *Metall. Trans. B* **19B**, 541-546.

NUNEZ, C., ESPIELL, F. and GARCIA-ZAYAS, J. (1990) Kinetics of galena leaching in hydrochloric acid-chloride solutions. *Metall. Trans. B* **21B**, 11-17.

ORESKES, N., SHRADER-FRECHETTE, K., and BELITZ, K. (1994) Verification, validation and the confirmation of numerical models in the earth sciences. *Science* **263**, 641-646.

ORTOLEVA, P., MERINO, E., MOORE, C. and CHADAM, J. (1987) Geochemical self-organization in reaction-transport feedbacks and modelling approach. *Amer. J. Science* **287**, 979-1007.

OSBORNE, F.H. and EHRLICH, H.L. (1976) Oxidation of arsenite by a soil isolate of *Alcaligenes faecalis. J. Appl. Bacteriol.* **41**, 295-305.

OTWINOWSKI, M. (1994) Quantitative analysis of chemical and biological kinetics for the acid mine drainage problem. Prepared for CANMET, Department of Energy, Mines and Resources Canada under MEND(NEDEM) Project No. (in review).

PACIOREK, K.J.L., KRATZER, R.H., KIMBLE, P.F., TOBEN, W.A. and VATASESCU, A.L. (1981) Degradation of massive pyrite: physical, chemical, and bacterial effects. *Geomicrobiol. J.* **2**, 363-374.

PACKTER, A. (1979) Kinetics of the heterogeneous reaction of quartz powders with aqueous sodium hydroxide solutions at 10° to 115°C. *Z. Phys. Chem.* **260**, 561-568.

PACKTER, A. and DHILLON, H.S. (1972) The heterogeneous reaction of recrystallized precipitated gibbsite powder with aqueous inorganic acid solutions, kinetics and mechanism . *Z. Phys. Chemie* **250**, 217- 229.

PACKTER, A. and DHILLON, H.S. (1974) Studies on recrystallized aluminium hydroxide precipitates, kinetics and mechanism of dissolution by sodium hydroxide solutions. *Colloid and Polymer Sci.* **252**, 249-256.

PALENCIA, I., WAN, R.Y. and MILLER, J.D. (1991) The electrochemical behaviour of a semiconducting natural pyrite in the presence of bacteria. *Metall. Trans. B* **22B**, 765-774.

PANG, J., BRICENO, A. and CHANDER, S. (1990) A study of pyrite/solution interface by impedance spectroscopy. *J. Electrochem. Soc.* **137**, 3447-3455.

PANTELIS, G. (1993) FIDHELM: Description of Model and Users Guide. Proprietry Report, Environmental Science Program of the Australian Nuclear Science and Techynology Organisation.

PANTELIS, G. and RITCHIE, A.I.M. (1991a) Rate controls on the oxidation of heaps of pyritic material imposed by upper temperature limits on the bacterially catalyzed process. FEMS *Microbiology Reviews* **11**, 183-190.

PANTELIS, G. and RITCHIE, A.I.M. (1991b) Macroscopic transport mechanisms as a rate controlling factor in dump leaching of pyritic ores. *Appl. Math. Modelling* **15**, 136-143.

PAPANGELAKIS, V.G., BERK, D. and DEMOPOULOS, G.P. (1986) Modelling and simulation of a batch reactor for an oxygen pressure leaching system. In Hydrometall. React. Des. Kinet., Proc. Symp (Eds. R.G. Bautista, R.J. Wesely and G.W.M. Warren), 209-225.

PAPANGELAKIS, V.G., BERK, D. and DEMOPOULOS, G.P. (1990) Mathematical modelling of an exothermic leaching reaction system: pressure oxidation of wide size arsenopyrite particulates. *Metall. Trans. B* **21B**, 827-837.

PAPANGELAKIS, V.G. and DEMOPOULOS, G.P. (1990a) Acid pressure oxidation of arsenopyrite: Part I. Reaction chemistry. *Can. Metall. Q.* **29**, 1-12.

PAPANGELAKIS, V.G. and DEMOPOULOS, G.P. (1990b) Acid pressure oxidation of arsenopyrite: Part II. Reaction kinetics. *Can. Metall. Q.* **29**(1), 13-20.

PARKER, A.J., PAUL, R.L. and POWER, G.P. (1981) Electrochemistry of the oxidative leaching of copper from chalcopyrite. *J. Electroanal. Chem.* **118**, 305-316.

PARKHURST, D.L. and PLUMMER, L.N. (1993) Geochemical models, Chapter 9 in Regional Ground-Water Quality. Ed.: W. Alley, Van Nostrand Reinhold, New York, 199-225.

PARKHURST, D.L., THORSTENSON, D.C. and PLUMMER, L.N. (1980) PHREEQE - A computer program for geochemical calculations: U.S. Geological Survey Water-Resources Investigations Report 80-96, 195p. (revised and reprinted 1990).

PARKHURST, D.L., PLUMMER, L.N. and THORSTENSON, D.C. (1982 BALANCE - A computer program for calculating mass transfer for geochemical reactions in groundwater. U.S. Geological Survey Water-Resources Investigations Report 82-14.

PAUNOVIC, M. (1968) Electrochemical aspects of electroless deposition of metals. *Plating* **55**, 1161-1166.

PEARSE, M.J. (1980) Chemical study of oxidation of sulfide concentrates. *Trans. -Inst. Min. Metall., Sect. C* **89**, 26-36.

PERKINS, E.H., BROWN, T.H. and BERMAN, R.G. (1986) PT-System, TX-System, PX-System: Three programs which calculate pressure-temperature-composition phase diagrams. *Computers and Geosciences* **12**, 749-755.

PERKINS, E.H. and GUNTER, W.D. (1989) Applications of SOLMINEQ/88 and SOLMINEQ.88 PC/SHELL to Thermally Enhanced Oil Recovery, in Fourth UNITAR/UNDP International Conference on Heavy Crude and Tar Sands Proceedings, Eds: R.F. Meyer and E.J. Wiggins, AOSTRA, Edmonton, Canada, Vol. 3, 413-422.

PERKINS, E.H., KHARAKA, Y.K., GUNTER, W.D. and DeBRAAL, J.D. (1990) Geochemical Modelling of Water-Rock interactions using SOLMINEQ.88, Chapter 9 in Chemical Modelling of Aqueous Systems II, ACS Symposium Series 416, Eds: D.C. Melchior and R.L. Bassett, American Chemical Society, Washington, DC, 117-127.

PESSIC, B. and KIM, I. (1990) EPD Congress '90, Ed.: D.R. Gaskell, TMS Anaheim, Ca, 136-160.

PETERS, E. (1977) The electrochemistry of sulphide minerals. In Trends in Electrochemistry Eds.: J.O'M. Bockris, D.A.J. Rand and B.J. Welch, Plenum Press, Fourth Australian Electrochemical Conference, 267-290.

PETERS, E. and MAJIMA, H. (1968) Electrochemical reactions of pyrite in acid perchlorate solutions. *Can. Metall. Q.* **7**, 111-117.

PETROVIĆ, R. (1976) Rate control in dissolution of alkali feldspars-I. Study of residual feldspar grains by X-ray photoelectron spectroscopy. *Geochim. Cosmochim. Acta* **40**, 537-548.

PETTENKOFER, C., JAEGERMANN, W. and BRONOLD, M. (1991) Site specific surface interaction of electron donors and acceptors on iron disulfide(100) cleavage planes. *Ber. Bunsen-Ges. Phys. Chem.* **95**(5), 560-565.

PHILLIPS, S.E. and TAYLOR, M.L. (1976) Oxidation of arsenite to arsenate by *Alcaligenes faecalis. Appl. Environ. Microbiol.* **32**, 392-399.

PINKA, J. (1991) Bacterial oxidation of pyrite and pyrrhotite. *Erzmetal l* **44**, 571-573.

PIRHONEN, V. (1993) Beforehand estimate of mass transfer in arsenoferrous gold mine tailing by means of minipilot plant process water analysis and geochemical simulations. *Appl. Geochem., Suppl.* **2**(Environmental Geochemistry), 291-293.

PITZER, K.S. (1979) Theory: Ion interaction approach. Chapter 7 in Activity Coefficients in Electrolyte Solutions. Vol. I, Ed.: R.M. Pytkowicz, CRC Press, Inc., 157-208.

PLUMMER, L.N. (1972) Rates of mineral-aqueous solution reactions. Unpublished Ph.D. Thesis, Northwestern Univ., Evanston, III.

PLUMMER, L.N. (1984) Geochemical modelling: A comparison of forward and inverse methods. In Proceedings First Canadian/American Conference on Hydrology - Practical Applications of Ground Water Geochemistry. Banff, Alberta, Eds: B. Hitchon and E.I. Wallick, National Water Well Association, 149-177.

PLUMMER, L.N. (1992) Geochemical modelling of water-rock interaction: Past, present, future. Proceedings of the 7th Int. Symp. on Water-Rock Interaction. Ed.: Y. Kharaka, and A. Maest, Balkema, Rotterdam, 23-33.

PLUMMER, L.N., BACK, W. (1980) The mass balance approach: Application to interpreting the chemical evolution of hydrologic systems. *Am. J. Sci.* **280**, 130-142.

PLUMMER, L.N., PARKHURST, D.L., FLEMING, G.W. and DUNKLE, S.A. (1988) A computer program incorporating Pitzer's equations for calculation of geochemical reactions in brines. U.S. Geological Survey Water-Resources Investigations Report 88-4153, 310p.

PLUMMER, L.N., PARKHURST, D.L. and THORSTENSON, D.C. (1983) Development of reaction models for groundwater systems. *Geochim. Cosmochim. Acta* **47**, 665-686.

PLUMMER, L.N., PRESTEMON, E.C. and PARKHURST, D.L. (1991) An interactive code (NETPATH) for modelling net geochemical reactions along a flow path. U.S. Geological Survey Water-Resources Investigations Report 91-4078.

PLUMMER, L.N., PRESTEMON, E.C. and PARKHURST, D.L. (1992) NETPATH: An interactive code for interpretating NET geochemical reactions from chemical and isotopic data along a flow PATH. In Proceedings of the 7th Int. Symp. on Water-Rock Interaction. Ed.: Y. Kharaka and A. Maest, Balkema, Rotterdam, 239-242.

POHL, H.A. (1954) The formation and dissolution of metal sulphides. *J. Am. Chem. Soc.* **76**, 2182-2184.

POTEDEVIN, J.L., CHEN, W., PARK, A., CHEN, Y. and ORTOLEVA, P. (1992) CIRF: A general reaction transport code: Mineralization fronts due to the infiltration of reactive fluids. Proceedings of the 7th Int. Symp. on Water-Rock Interaction. Ed: Y. Kharaka & A. Maest, Balkema, Rotterdam, 1047-1050.

POZZO, R.L. and IWASAKI, I. (1987) An electrochemical study of pyrrhotite-grinding media interaction under abrasive conditions. *Corrosion (Houston)* **43**, 159-164.

POZZO, R.L. and IWASAKI, I. (1989) Pyrite-pyrrhotite grinding media interactions and their effects on media wear and flotation. *J. Electrochem. Soc.* **136**, 1734-1740.

PRASAD, J., MURRAY, E. and KELBER, J.A. (1993) Site selective chemistry of S, Cl and H_2O at the iron oxide surface. *Surf. Sci.* **289**, 10-18.

PRATT, A.R., NESBITT, H.W. and MUIR, I.J. (1994a) X-ray photoelectron and AES electron spectroscopic studies of pyrrhotite and mechanism of air oxidation. *Geochim. Cosmochim. Acta* **58**, 827-841.

PRATT, A.R., NESBITT, H.W. and MUIR, I.J. (1994b) Generation of acids in mine waste waters: oxidative leaching of pyrrhotite in dilute H_2SO_4 solutions (pH 3.0). *Geochim. Cosmochim. Acta* **58**, (in press).

PTACEK, C.J. and BLOWES, D.W. (1994) Chap. 13 in Environmental Geochemistry of Sulphide Oxidation. Eds: C.N. Alpers and D.W. Blowes, ACS Symposium Series **550**, 172-189.

PUGH, C.E., HOSSNER, L.R. and DIXON, J.B. (1984) Oxidation rate of iron sulfides as affected by surface area, morphology, oxygen concentration, and autotrophic bacteria. *Soil Sci.* **137**, 309-314.

PYZIK, A. and SOMMER, S.E. (1981) Sedimentary iron monosulphides: kinetics and mechanism of formation. *Geochim. Cosmochim. Acta* **45**, 687-698.

RADYUSHKINA, K.A., VIGDERGAUZ, V.E., TARASEVICH, M.R. and CHANTURIYA, V.A. (1986) Electrochemistry of sulfide minerals. Electrochemical processes at pyrite and pyrrhotite surfaces in aqueous electrolyte solutions. *Elektrokhimiya (Sov. Electrochem.)* **22**, 1394-1398 (1311-1315).

RAMPRAKASH, Y., KOCH, D.F.A. and WOODS, R. (1991) The interaction of iron species with pyrite surfaces. *J. Appl. Electrochem.* **21**, 531-536.

RAND, D.A.J. and WOODS, R. (1984) Eh Measurements in Sulphide Mineral Slurries. *Int. J. Miner. Process.* **13**, 29-42.

RAO, S.R. and FINCH, J.A. (1987a) Electrochemical studies on the flotation of sulfide minerals with special reference to pyrite-sphalerite II. Flotation studies. *Can. Metall. Q.* **26**, 173-175.

RAO, S.R. and FINCH, J.A. (1987b) Electrochemical studies on the flotation of sulfide minerals with special reference to pyrite-sphalerite I. Cyclovoltammetry and pulp potential measurements. *Can. Metall. Q.* **26**, 167-172.

RAO, S.R. and FINCH, J.A. (1991) Adsorption of amyl xanthate at pyrrhotite in the presence of nitrogen and implications in flotation. *Can. Met. Q* **30**, 1-6.

REARDEN, E.J., and BECKIE, R.D. (1987) Modelling chemical equilibria of acid mine-drainage: The $FeSO_4$-H_2SO_4-H_2O system. *Geochim. Cosmochim. Acta* **51**, 2355-2368.

REED, M.H. (1982) Calculation of multicomponent chemical equilibria and reaction processes in systems involving minerals, gases and an aqueous phase. *Geochim. Cosmochim. Acta* **46**, 513-528.

REED, M.H. and SPYCHER, N.F. (1984) Calculation of pH and mineral equilibria in hydrothermal waters with application to geothermometry and studies of boiling and dilution. *Geochim. Cosmochim. Acta* **48**, 1479-1492.

REIMERS, G. W. and HJELMSTAD, K. E. (1987) Analysis of the oxidation of chalcopyrite, chalcocite, galena, pyrrhotite, marcasite, and arsenopyrite. *Bur. Mines, RI 9118*, Rep. Invest. - U.S., 20p.

RENICK, B.C. (1924) Base exchange in ground water by silicates as illustrated in Montana. U.S. Geol. Surv. Water-Supply Pap. 520-D, 63-72.

RIBBE, P.H. (1974) Sulphide mineralogy. *Mineral. Soc. Amer.* Short course notes Vol. **1**.

RICHARDSON, S. and VAUGHAN, D.J. (1989) Arsenopyrite: a spectroscopic investigation of altered surfaces. *Mineral. Mag.* **53**, 223-229.

RICKARD, D.T. (1969) The chemistry of iron sulfide formation at low temperatures. *Stockholm Contrib. Geol.* **20**, 67-69.

RICKARD, D.T. (1974) Kinetics and mechanism of the sulfidation of goethite at low temperatures. *Am. J. Sci.* **274**, 941-952.

RICKARD, D.T. (1975) Kinetics and mechanism of pyrite formation at low temperatures. *Am. J. Sci.* **275**, 636-652.

RIMSTIDT, J.D. and BARNES, H.L. (1980) The kinetics of silica-water reactions. *Geochim. Cosmochim. Acta* **44**, 1683-1699.

RIMSTIDT, J.D., CHERMAK, J.A. and GAGEN, P.M. (1994) Rates of reaction of galena, sphalerite, chalcopyrite and arsenopyrite with Fe(III) in acidic solutions. Chap. 1 in Environmental Geochemistry of Sulphide Oxidation. Eds: C.N. Alpers and D.W. Blowes, ACS Symposium Series **550**, 2-13.

RITCHIE, A.I.M. (1994a) Rates of mechanisms that govern pollutant generation from pyritic wastes. Chap. 9 in Environmental Geochemistry of Sulphide Oxidation. Eds: C.N. Alpers and D.W. Blowes, ACS Symposium Series **550**, 108-122.

RITCHIE, A.I.M. (1994b) The waste-rock environment. Chap. 5 in Environmental Geochemistry of Sulphide Mine-Wastes, Eds: J.L. Jambor and D.W. Blowes, Short Course Handbook V.22, Min. Assoc. Canada, 133-161.

RITCHIE, A.I.M. (1994c) Sulphide oxidation mechanisms: Controls and rates of sulphide oxidation. Chap. 8 in Environmental Geochemistry of Sulphide Mine-Wastes, Eds: J.L. Jambor and D.W. Blowes, Short Course Handbook V.22, Min. Assoc. Canada, 201-245.

ROBINSON, R.A. and STOKES, R.H. (1959) Electrolyte Solutions. Butterworths, London, 571p.

ROSSI, G., TORMA, A.E. and TROIS, P. (1983) Bacteria mediated copper recovery from a cuperiferous pyrrhotite ore: chalcopyrite/pyrrhotite interactions. In Recent Progress in Biohydrometallurgy Mineraria Sarada, Iglesis, Italy, 185-200.

RUEDA, E.H., BALLESTEROS, M.C., GRASSI, R.L. and BLESA, M.A. (1992) Dithionite as a dissolving reagent for goethite in the presence of EDTA and citrate. Application to soil analysis. *Clays Clay Miner.* **40**, 575-585.

SAKHAROVA, M.S. and LOBACHEVA, I.K. (1978) Microgalvanic systems involving sulphides and gold bearing solutions, and characteristics of gold deposition. *Geochem. Int.* **15**(6), 152-157.

SALVADOR, P., TAFALLA, D., TRIBUTSCH, H. and WETZE, H. (1991) Reaction mechanisms at the n-iron disulfide/iodine interface. An electrolyte electroreflectance study. *J. Electrochem. Soc.* **138**, 3361-3369.

SANCHEZ, V.M. and HISKEY, J.B. (1988a) Electrochemical behaviour of arsenopyrite in alkaline media. *Proc. - Electrochem. Soc.* **88-21** (Proc. Int. Symp. Electrochem. Miner. Met. Process. 2, 1988), 264-279.

SANCHEZ, V.M. and HISKEY, J.B. (1988b) An electrochemical study of the surface oxidation of arsenopyrite in alkaline media. *Metall. Trans. B* **19B**, 943-949.

SANCHEZ, V.M. and HISKEY, J.B. (1991) Electrochemical behaviour of arsenopyrite in alkaline media. *Miner. Metall. Process.* **8**, 1-6.

SATO, M. (1960) Oxidation of sulphide ore bodies, II. Oxidation mechanisms of sulphide minerals at 25°C. *Econ. Geol.* **55**, 1202-1234.

SATO, M. (1992) Persistency-field Eh-pH diagrams for sulfides and their application to supergene oxidation and enrichment of sulfide ore bodies. *Geochim. Cosmochim. Acta* **56**, 3133-3156.

SCHARER, J.M., ANNABLE, W.K., NICHOLSON, R.V. (1993) WATAIL 1.0 User's Manual, A tailings basin model to evaluate transient water quality of acid mine drainage. Instit. of Groundwater Research, University of Waterloo, 74p.

SCHARER, J.M., NICHOLSON, R.V., HALBERT, B. and SNODGRASS, W. (1994a) A computer program to assess acid generation in pyritic tailings. Chap. 11 in Environmental Geochemistry of Sulphide Oxidation. Eds: C.N. Alpers and D.W. Blowes, ACS Symposium Series **550**, 132-152.

SCHARER, J.M., PETTIT, C.M., CHAMBERS, D. and KWONG, E.C. (1994b) Mathematical simulation of a waste rock heap. Proceedings of the 3rd International Conference on the Abatement of Acidic Drainage. U.S. Dept. Int. Bur. Mines Special Pub. SP 06A-94, V.1, 30-39.

SCHINDLER, W.P. (1990) Co-adsorption of metal ions and organic ligands. Reviews in Mineralogy, Eds: M.F. Hochella and A.F. White, *Mineral. Soc. Amer.* **23**, 281-308.

SCHOONEN, M.A.A. and BARNES, H.L. (1991a) Reactions forming pyrite and marcasite from solution: I. Nucleation of FeS_2 below 100°C. *Geochim. Cosmochim. Acta* **55**, 1495-1504.

SCHOONEN, M.A.A. and BARNES, H.L. (1991b) Reactions forming pyrite and marcasite from solution: II. Via FeS precursors below 100°C. *Geochim. Cosmochim. Acta* **55**, 1504-1514.

SCHOTT, J., BERNER, R.A. and SJÖBERG, E.L. (1981) Mechanism of pyroxene and amphibole weathering - I. Experimental studies of iron-free minerals. *Geochim. Cosmochim. Acta* **45**, 2123-2135.

SCHUBERT, B. and TRIBUTSCH, H. (1990) Photoinduced electron transfer by coordination chemical pathways across pyrite/electrolyte interfaces. *Inorg. Chem.* **29**, 5041-5046.

SCHUILING, R.D. (1990) Geochemical engineering: Some thoughts on a new research field. *Appl. Geochem.* **5**, 251-262.

SCHWERTMANN, U.V. (1982) Identification of ferrihydrite in soils by dissolution kinetics, differential X-ray diffraction and Mössbauer spectroscopy . *Soil Sci. Amer. Jour.* **46**, 869-875.

SCOTT, P.D. and NICOL, M.H. (1977) The kinetics and mechanisms of the non-oxidative dissolution of metal sulphides. In Trends in Electrochemistry, Eds: J. O'M. BockriS, D.A.J. Rand and R. J. Welch. Plenum Press. Fourth Australian Electrochemistry Conference, 303-316.

SEDOV, V.M., KRUTIKOV, P.G., BELYAEV, M.B. and BYKOVA, E.M. (1981) Dissolution of hematite by solutions of organic acids and complexes. *Zh. Neorg. Khim.* **26**, 1490-1492.

SEHLIN, H.M. and LINDSTRÖM, E.B. (1992) Oxidation and reduction of arsenic by *Sulfolobus acidocaldarius* strain BC. *FEMS Microbiol Lett* **90**, 87-92.

SENES Consultants (1991) Reactive Acid Tailings Assessment Program (RATAP.BMT3), Richmond Hill, Ontario.

SEVOUGIAN, S.D., LAKE, L.W. and SCHECHTER, R.S. (1992) A new geochemical simulator to design more effective sandstone acidizing treatments. 67th Annual Technical Conference and Exhibition of the Soc. of Petrol. Engineers, Washington, D.C., SPE paper #24780, 161-175.

SHEWMON, P.G. (1963) Diffusion in Solids. New York: M^{c}Graw-Hill Book Company.

SHOESMITH, D.W., RUMMERY, T.E., BAILEY, M.G. and OWEN, D.G. (1979) Electrocrystallization of pyrite and marcasite on stainless steel surfaces. *J. Electrochem. Soc.* **126**, 911-919.

SHUEY, R.T. (1975) Arsenopyrite - FeAsS. In Developments in Economic Geology, 4: Semiconducting Ore Minerals, Chap. 8, Ed.: R. T. Shuey, Elsevier Scientific, 205-220.

SIDHU, P.S., GILKES, R.J., CORNELL, R.M., POSNER, A.M. and QUIRK, J.P. (1981) Dissolution of iron oxides and oxyhydroxides in hydrochloric and perchloric acids. *Clay Miner.* **29**, 269-276.

SILVER, M. (1985) Analytical techniques for research on the abatement of bacterial acid generation in pyritic tailings, Vol. 86-3E, Canadian Government Publishing Centre, 24p.

SILVER, M.P. (1967) Mechanism of bacterial pyrite oxidation. *J. Bacteriol.* **94**, 1046-1051.

SINGER, P.C. and STUMM, W. (1970) Acidic mine drainage: The rate-determining step. *Science*, **167**, 1121-1123.

SISENOV, G.K. and TARASEVICH, M.R. (1988) Redox transformations of pyrite and reduction of molecular oxygen in aqueous solutions of electrolytes. *Zh. Prikl. Khim. (Leningrad)* **61**, 1247-1252.

SKEWES, H.R. (1972) Electrowinning of lead directly from galena. *Proc. Aust. Inst. Min. Met.* **240** (December), 35-41.

SMITH, S.R. and SOBEK, A.A. (1978) Physical and chemical properties of overburdens, spoils, wastes and new soils. In Reclamation of Drastically Disturbed Lands, Eds: F.W. Schaller and P. Sutton, *Amer. Soc. Agron.* 192-208.

SOBEK, A.A., SCHULLER, W.A., FREEMAN, J.R. and SMITH, R.M. (1978) Field and laboratory methods applicable to overburden minesoils. *EPA* 600/2-78-054, 203p.

SPARKS, D.L. (1989) Kinetics of Soil Chemical Processes. San Diego: Academic Press, 210p.

SPOSITO, G. and MATTIGOLD, S.V. (1980) GEOCHEM: A computer program for calculation of chemical equilibria in soil solutions and other natural water systems. Kearny Foundation report, University of California.

SPYCHER, N.F. and REED, M.H. (1988) Fugacity coefficients of H_2, CO_2, CH_4, H_2O and of H_2O-CO_2-CH_4 mixtures: A virial equation treatment for moderate pressures applicable to calculations of hydrothermal boiling. *Geochim. Cosmochim. Acta* **52**, 739-749.

SPYCHER, N.F. and REED, M.H. (1990a) Users Guide for SOLVEQ: A Computer Program for Computing Aqueous-Mineral-Gas Equilibria. Department of Geological Sciences, University of Oregon, Eugene, Oregon, 947403, 37p.

SPYCHER, N.F. and REED, M.H. (1990b) Users Guide for CHILLER: A Program for Computing Water-Rock Reactions, Boiling, Mixing and other Reaction Processes in Aqueous-Mineral-Gas Systems. Department of Geological Sciences, University of Oregon, Eugene, Oregon, 947403, updates in 1992, 70p.

SRK CANADA INC. (1993) Rock pile water quality modelling phase 1 - final draft report. Prepared for B.C. Ministry of Energy Mines and Petroleum resources.

STEEFEL, C.I. (1993) 1DREACT: A one-dimensional reaction-transport model, Users manual and programmers guide. Battelle, Pacific Northwest Laboratories, Richland, Washington, 39p.

STEEFEL, C.I. and LICHTNER, P.C. (1993) Diffusion and reaction in rock matrix bordering a hyperalkaline fluid-filled fracture. Preprint, 74p.

STEGER, H.F. (1977) Oxidation of sulfide minerals. I. Determination of ferrous and ferric iron in samples of pyrrhotite, pyrite and chalcopyrite. *Talanta* **24**(4), 251-254.

STEGER, H.F. (1982) Oxidation of sulphide minerals VII. Effect of temperature and relative humidity on the oxidation of pyrrhotite. *Chem. Geol.* **35**, 281-295.

STEGER, H.F. and DESJARDINS, L.E. (1978) Oxidation of sulfide minerals. 4. Pyrite, chalcopyrite and pyrrhotite. *Chem. Geol.* **23**(3), 225-237.

STEINMANN, P., LICHTNER, P.C. and SHOTYK, W. (1994) Reaction path approach to mineral weathering reactions. *Clays and Clay Minerals* **42**, 197-206.

STILLINGS, L.L., BRANTLEY, S.L. and MACHESKY, M.L. (1992) Multi-site proton adsorption at the feldspar-water interface. *WRI-7* 69-72.

STRÖMBERG, B. and BANWART, S. (1994) Kinetic modelling of geochemical processes at the Aitik mining waste rock site in northern Sweden. *Applied Geochemistry* **9**, no. 5, 583-596.

STRÖMBERG, B., BANWART, S., BENNET, J.W. and RITCHIE, A.I.M. (1994) Mass balance assessment of initial weathering processes derived from oxygen consumption rates in waste sulphide ore. Proceedings of the 3rd International Conference on the Abatement of Acidic Drainage. U.S. Dept. Int. Bur. Mines Special Pub. SP 06A-94, V.1, 12-19.

STUMM, W. and MORGAN, J.J. (1981) Aquatic Geochemistry - An Introduction Emphasizing Chemical Equilibria in Natural Waters. New York: John Wiley & Sons, 780p.

STUMM, W. and WOLLAST, R. (1990) Coordination chemistry of weathering: Kinetics of the surface-controlled dissolution of oxide minerals. *Reviews of Geophysics* **28**, 53-69.

SUBRAMANIAN, K.N., STRATIGAKOS, E.S. and JENNINGS, P.H. (1972) Hydrometallurgical processing of pyrrhotite. *Can. Metall. Q.* **11**(2), 425-434.

SUGIO, T., KATAGIRI, T., INAGAKI, K. and TANO, T. (1987) Purification and some properties of sulfur:ferric ion oxidoreductase from *Thiobacillus ferrooxidans. J Bacteriol.* **169**, 4916-4922.

SUGIO, T., KATAGIRI, T., INAGAKI, K. and TANO, T. (1989) Actual substrate for elemental sulfur oxidation sulfur: ferric ion oxidoreductase purified from *Thiobacillus ferrooxidans. Biochim. Biophys. Acta* **973**, 250-256.

SULZBERGER, B., SUTER, D., SIFFERT, C., BANWART, S. and STUMM, W. (1989) Dissolution of iron(III) (hydr)oxides in natural waters; laboratory assessment on the kinetics controlled by surface coordination. *Mar. Chem.* **28**, 127-144.

SURANA, Y.S. and WARREN, I.H. (1969) The leaching of goethite. *Inst. Min. Metall. Trans., C* **78**, C133-139.

SVERDRUP, H.U. (1990) The Kinetics Of Base Cation Release Due to Chemical Weathering. Lund University Press, 245p.

SVERDRUP, H.U. and BJERLE, I. (1982) Dissolution of calcite and other related minerals in acidic aqueous solution in a pH-stat. *Vatten.* **38**, 59-73.

SVERDRUP, H.U. and WARFVINGE, P. (1988) Weathering of primary silicate minerals in the natural soil environment in relation to a chemical weathering model. *Water, Air, Soil Poll.* **38**, 387-408.

SVERDRUP, H.U. and WARFVINGE, P. (1993) Calculating field weathering rates using a mechanistic geochemical model PROFILE. *App. Geochem.* **8**, 273-284.

TALMAN, S.J. and NESBITT, H.W. (1988) Dissolution of populations of ultrafine grains with applications in feldspars. *Geochim. Cosmochim. Acta* **52**, 1467-1471.

TALMAN, S.J., WIWCHAR, B., GUNTER, W.D. and SCARFE, C.M. (1990) Dissolution kinetics of calcite in the H_2O-CO_2 system along the steam saturation curve to 210°C. In Fluid-Mineral Interactions: A Tribute to H.P. Eugster, Eds: R.J. Spencer and I-Ming Chou. *The Chem. Soc. Spec. Publ.* No. **2**, 41-55.

TASSÉ, N., GERMAIN, M.D. and BERGERON, M. (1993) Composition of interstitial gases in wood chips deposited on reactive mine tailings: consequences for their use as an oxygen barrier. Chap. 38 in Environmental Geochemistry of Sulphide Oxidation. Eds: C.N. Alpers and D.W. Blowes, ACS Symposium Series 550, 631-644.

TAYLOR, B.E. and WHEELER, M.C. (1984) Table isotope geochemistry of acid mine drainage: Experimental oxidation of pyrite. *Geochim. Cosmochim. Acta* **48**, 2669-2678.

TAYLOR, P. and OWEN, D.G. (1993) *[Rep.] AECL*, AECL-10821: Oxidation of magnetite in aerated aqueous media, Atomic Energy Can. Ltd., 34p.

TAYLOR, P., RUMMERY, T.E. and OWEN, D.G. (1979) On the conversion of mackinawite and greigite. *J. Inorg. Nucl. Chem.* **41**, 595-596.

TERMES, S.C., BUCKLEY, A.N. and GILLARD, R.D. (1987) 2p electron binding energies for the sulfur atoms in metal polysulfides. *Inorg. Chim. Acta* **126**, 79-82.

THORNBER, M.R. (1975a) Supergene alteration of sulphides: I. A chemical model based on massive nickel sulphide deposits at Kambalda, Western Australia. *Chem. Geol.* **15**(1), 1-14.

THORNBER, M.R. (1975b) Supergene alteration of sulphides: II. A chemicial study of the Kambalda nickel deposit. *Chem. Geol.* **15**(2), 117-144.

THORPE, A.N., SENFTLE, F.E., ALEXANDER, C., DULONG, F.T., LACOUNT, R.B. and FRIEDMAN, S. (1987) Oxidation of pyrite in an anoxic atmosphere. *Fuel* **66**, 147-153.

THORSTENSON, D.C. (1984) The concept of electron activity and its relation to redox potentials in aqueous geochemical systems. U.S. Geological Survey Open File Report 84-072, 45p.

TIPPING, E. (1994) WHAM - A chemical equilibrium model and computer code for waters, sediments, and soils incorporating a discrete site/electrostatic model of ion binding by humic substances. *Computers and Geosciences* **20**, 973-1023.

TOGURI, J.M. (1975) A review on the methods of treating nickel-bearing pyrrhotite; with special reference to the Sudbury area pyrrhotite. *Can. Met. Q* **14**, 323-338.

TORAN, L. and HARRIS, R.F. (1989) Interpretation of sulphur and oxygen isotopes in biological and abiological sulphide oxidation. *Geochim. Cosmochim. Acta* **53**, 2341-2348.

TORRENT, J., SCHWERTMANN, U. and BARRON, V. (1987) The reductive dissolution of synthetic goethite and hematite in dithionite. *Clay Miner.* **22**, 329-337.

TOSSELL, J.A., VAUGHAN, D.J. and BURDETT, J.K. (1981) Pyrite, marcasite and arsenopyrite type minerals: Crystal chemical and structural principles. *Phys. Chem. Minerals* **7**, 177-184.

TROLAND, F. and TARDY, Y. (1987) The stabilities of gibbsite, boehmite, aluminous goethites and aluminous hematites in bauxites, ferricretes and laterites as a function of water activity, temperature and particle size. *Geochim. Cosmochim. Acta* **51**, 945-957.

TURNER, A.W. (1949) Bacterial oxidation of arsenite. *Nature* **164**, 76-77.

TURNER, A.W. (1954) Bacterial oxidation of arsenite. I Description of bacteria isolated from arsenical cattle-dipping fluids. *Aust. J. Biol. Sci.* **7**, 452.

VAN LIER, J.A., de BRUYN, P.E. and OVERBEEK, J.T.G. (1960) The solubility of quartz. *J. Phys. Chem.* **64**, 1675-1682.

VAN WEERT, G., MAH, K. and PIRET, N. L. (1974) Hydrochloric acid leaching of nickeliferous pyrrhotites from the Sudbury District. *Hydrometallurgy* **LXXVII**, 63-69.

VAUGHAN, D.J. (1982) Electronic structures of sulfides and leaching behaviour. In *Proceeding of NATO Adv. Res. Inst*, pp. 23-39, Cambridge.

VAUGHAN, D.J. and CRAIG, J.R. (1978) Mineral Chemistry of Metal Sulphides. London: Cambridge University Press.

VAUGHAN, D.J. and TOSSELL, J.A. (1986) Interpretation of the Auger electron spectra (AES) of sulfide minerals. *Phys. Chem. Minerals* **13**, 347-350.

VORONKEVICH, S.D. (1994) Engineering geochemistry: problems and applications. *Appl. Geochem.* **9**, 553-559.

WADDEN, D. and GALLANT, A. (1985) The in-place leaching of uranium at Denison mines. *Can. Metall. Q.* **24**, 127-134.

WADSWORTH, M.E. (1984) Heterogeneous Rate Processes In Leaching Of Base Metal Sulfides. 6 vols. (Series Ed: G. Bautiston 10.) New York: Plenum Press, 41p.

WAITE, T.D. and MOREL, F.M.M. (1984) Photoreductive dissolution of colloidal iron oxides in natural waters. *Environ. Sci. Technol.* **18**, 860-868.

WAKO, N., KOYATSU, H., KOMAI, Y., SHIMOKAWARA, H., SAKURAI, Y. and SHIOTA, H. (1988) Microbial oxidation of arsenite and occurrence of arsenite-oxidizing bacteria in acid mine water from a sulphur-pyrite mine. *Geomicrobiol. J.* **6**, 11-24.

WALTER, A.L., FRIND, E.O., BLOWES, D.W., PTACEK, C.J. and MOLSON, J.W. (1994a) Modelling of multicomponent reactive transport in groundwater 1. Model development and evaluation. *Water Resources Research* **30**, 3137-3148.

WALTER, A.L., FRIND, E.O., BLOWES, D.W., PTACEK, C.J. and MOLSON, J.W. (1994b) Modelling of multicomponent reactive transport in groundwater 2. Metal mobility in aquifers impacted by acidic mine tailings discharge. *Water Resources Research* **30**, 3149-3158.

WANG, X.H., AHLBERG, E. and FORSSBERG, K.S.E. (1992a) Electrochemical study of surface oxidation and collectorless flotation of arsenopyrite. *J. Appl. Electrochem.* **22**, 1095-1103.

WANG, X.H., JIANG, C.L., XUAN, D. and FORSSBERG, E. (1992b) An electrochemical study of selective separation of copper(II)-activated pyrite and arsenopyrite. *Proc. - Electrochem. Soc.* **92-17** (Proc. Int. Symp. Electrochem. Miner. Met. Process. III, 3rd, 1992), 235-258.

WARREN, G.W., DROUVEN, B. and PRICE, D.W. (1984) Relationships between the Pourbaix Diagram for Ag-S-H_2O and Electrochemical Oxidation and reduction of Ag_2S. *Metall. Trans.* **15**, 235-242.

WARREN, G.W., HENEIN, H. and JIN, Z.-M. (1985) Reaction mechanism for ferric chloride leaching of sphalerite. *Metall. Trans. B* **16B**, 715-724.

WEERTMAN, J. and WEERTMAN, J. (1965) Elementary Dislocation Theory. New York: The McMillan Company.

WHITE, A.F. (1990) Heterogeneous electrochemical reactions associated with oxidation of ferrous oxide and silicate surfaces. In Mineral-Water Interface Geochemistry. Eds: M.F. Hochella, Jr. and A.F. White, *Reviews in Mineral.* **23**, 427-465.

WHITE, A.F. and PETERSON, M.L. (1990) Role of reactive-surface-area characterization in geochemical kinetic models. Chap. 35 in Chemical Modelling of Aqueous Systems II, ACS Symposium Series 416, Eds: D.C. Melchior and R.L. Bassett, American Chemical Society, Washington, DC, 461-475.

WHITE, A.F., PETERSON, M.L. and HOCHELLA, Jr., M.F. (1994) Electrochemistry and dissolution of magnetite and ilmenite. *Geochim. Cosmochim. Acta* **58**, 1859-1874.

WHITE, W.W., TRUJILLO, E.M. and LIN, C.K. (1994) Chemical predictive modelling of acid mine drainage from waste rock: Model development and comparison of modelled output to experimental data. Proceedings of the 3rd International Conference on the Abatement of Acidic Drainage. U.S. Dept. Int. Bur. Mines Special Pub. SP 06A-94, V.1, 157-166.

WHITFIELD, M. (1974) Thermodynamic limitations on the use of the platinum electrode in Eh measurements. *Limnology and Oceanography* **19**, 857-865.

WICKS, C.M. and GROVES, C.G. (1993) Acidic mine drainage in carbonate terrains: geochemical processes and rates of calcite dissolution. *Journal of Hydrology* **146**, 13-27.

WIELAND, E. and STUMM, W. (1992) Dissolution kinetics of kaolinite in acidic aqueous solutions at 25°C. *Geochim. Cosmochim. Acta.* **56**, 3339-3355.

WIERSMA, C.L. and RIMSTIDT, J.D. (1984) Rates of reaction of pyrite and marcasite with ferric iron at pH 2. *Geochim. Cosmochim. Acta* **48**, 85-92.

WIESE, Jr., R.G., POWELL, M.A. and FYFE, W.S. (1987) Spontaneous formation of hydrated iron sulphates on laboratory samples of pyrite- and marcasite-bearing coals. *Chem. Geol.* **63**, 29-38.

WIKJORD, A.G., RUMMERY, T.E. and DOERN, F.E. (1976) *Can. Mineral.* **14**, 571.

WILLIAMS-JONES, A.E, MOUNTAIN, B.W. and ALPERS, C. (1993) Geochemical modelling of effluent compositions: prevention and control of acid generation in waste rock. Appended to MEND Report 2.35.2 by YANFUL, E.K. and PAYANT, S.C. (1993) Evaluation of techniques for preventing acidic rock drainage: First milestone research report.

WOLERY, T.J. (1992a) EQ3/6, A software package for geochemical modelling of aqueous systems: Package overview and installation guide (Version 7.0). Lawrence Livermore National Laboratory UCRL-MA -110662 PT I, 66p.

WOLERY, T.J. (1992b) EQ3NR, A computer program for geochemical aqueous speciation-solubility calculations: Theoretical manual, User's guide, and related documentation (Version 7.0). Lawrence Livermore National Laboratory UCRL-MA -110662 PT III, 246p.

WOLERY, T.J., and DAVELER, S.A. (1992) EQ6, A computer program for reaction path modelling of aqueous geochemical systems: Theoretical manual, User's guide and related documentation (Version 7.0). Lawrence Livermore National Laboratory UCRL-MA -110662 PT IV, 338p.

WOLERY, T.J., JACKSON, K.J., BOURCIER, W.L., BRUTON, C.J., VIANI, B., KNAUSS, G. and DELANEY, J.M. (1990) Current status of the EQ3/6 software package for geochemical modelling. Chapter 8 in Chemical Modelling of Aqueous Systems II, ACS Symposium Series 416, Eds: D.C. Melchior and R.L. Bassett, American Chemical Society, Washington, DC, 104-116.

WOLLAST, R.and CHOU, L. (1984) Kinetic study of the dissolution of albite with a continuous flow-through reactor. In The Chemistry of Weathering, Ed.: J.I. Drever, Dordrecht: Reidel Publ. Co., 324p.

WOODS, R. (1992) Characterization of sulfide mineral surfaces. In Electrochemistry in Transition, Chap. 35, Ed.: O. J. Murphy, Plenum Press, 205-220.

YANFUL, E.K., NESBITT, H.W. and QUIGLEY, R.M. (1988) Heavy metal migration at a landfill site, Sarnia, Ontario, Canada - 1. Thermodynamic assessment and chemical interpretations. *Applied Geochemistry* 3, 523-533.

YANFUL, E.K. and PAYANT, S.C. (1993) Evaluation of techniques for preventing acidic rock drainage: First milestone research report. MEND Report 2.35.2, 82p.

YATES, D.E. and HEALY, T.W. (1975) Surface change and tritium exchange studies of Fe oxide (goethite) - solution interface. *Proc. Int. Conf. Colloid Surf.* **1**, 7-14.

YEH, G.T. and TRIPATHI, V.S. (1989) A critical evaluation of recent developments in hydrogeochemical transport models of reactive multichemical components. *Water Resources Research* **25**, 93-108.

ZHENG, C.Q., ALLEN, C.C. and BAUTISTA, R.G. (1986) Kinetic study of the oxidation of pyrite in aqueous ferric sulfate. *Ind. Eng. Chem. Process Des. Dev.* **25**, 308-317.

ZHENG, C.Q. and BAUTISTA, R.G. (1984) A kinetic study of the oxidation of complex nickeliferous sulfide ore in aqueous ferric sulfate. *Inst. Chem. Eng. Symp. Ser.* **87**(Chem. React. Eng.), 593-602.

ZHU, X., WADSWORTH, M. E., BODILY, D. M. and RILEY, A. M. (1991) Surface properties of mineral and coal pyrite after electrochemical alteration. *Coal Sci. Technol.* **18** (Process. Util. High-Sulfur Coals 4), 205-222.

ZIEMKIEWICZ, P.F. (1994) AMD-Time: A simple spreadsheet for predicting acid mine drainage. Proceedings of the 3rd International Conference on the Abatement of Acidic Drainage. U.S. Dept. Int. Bur. Mines Special Pub. SP 06A-94, V.2, 395-400.

ZINDER, B., FURRER, G. and STUMM, W. (1986) The coordination chemistry of weathering: II. Dissolution of iron(III) oxides. *Geochim. Cosmochim. Acta* **50**, 1861-1869.